

# **REPORT ON THE EFFECTS OF FIRE ON LNG CARRIER CONTAINMENT SYSTEMS**

**SIGTTO**



# **REPORT ON THE EFFECTS OF FIRE ON LNG CARRIER CONTAINMENT SYSTEMS**

**19<sup>th</sup> March 2009**



First Edition 2009

Copyright of SIGTTO, Bermuda

ISBN 978 1 905331 91 8

**British Library Cataloguing in Publication Data**

Society of International Gas Tanker & Terminal Operators Limited. Bermuda Guidelines for Hazard Analysis as an Aid to Management of Safe Operations

**Notice of Terms of Use**

While the recommendations and advice given in this guide have been based on information made available to the Society of International Gas Tanker & Terminal Operators (SIGTTO), no responsibility is accepted by SIGTTO or by any person, firm, corporation or organisation who or which has been in any way concerned with the furnishing of information or data, the compilation, publication or any translation, supply or sale of this guide for the accuracy of any information or advice given herein or for any omissions herefrom or for any consequences whatsoever resulting directly or indirectly from compliance with or adoption of any of the recommendations or guidance contained herein even if caused by a failure to exercise reasonable care.

Any queries or comments relating to these guidelines should be addressed to The General Manager, Society of International Gas Tanker & Terminal Operators Limited, 17 St. Helens Place, London EC3A 6DE.



Published in 2009 by  
**Witherby Seamanship International Ltd**  
4 Dunlop Square, Livingston  
Edinburgh, EH54 8SB  
Scotland, UK

Tel No: +44(0)1506 463 227

Fax No: +44(0)1506 468 999

Email: [info@emailws.com](mailto:info@emailws.com)

[www.witherbyseamanship.com](http://www.witherbyseamanship.com)

## EXECUTIVE SUMMARY

In 2004, SIGTTO was approached by Professor Havens of the University of Arkansas who expressed concern about the vulnerability of LNG carrier tanks that are insulated with non-fire-resistant materials such as polystyrenes or polyurethanes.

Current practice provides for pressure relief systems, designed with credit for the tank's insulation, to prevent LNG cargo pressurisation due to boil-off and fire (IMO IGC Code 8.5). However, it is uncertain to what extent any degradation of insulation, in a fire situation, is taken into account in the design of PRV systems. As foam plastic insulation materials are subject to possible melting, degradation and/or ignition at temperatures lower than might be achieved during such fire exposure, there is concern that the PRV systems may not be capable of relieving the vapour flows that would result from the increased boil-off due to partial or total insulation failure.

Following considerable dialogue between SIGTTO members, the LNGC containment system designers, the USCG and the major classification societies, at their April 2006 meeting the SIGTTO GPC sanctioned the formation of a working group to thoroughly investigate the subject and produce a detailed report on the possible effects and any mitigation measures that may be necessary.

During the progression of the working group studies, it became clear that, for this complex issue of how a large fire scenario may a) emit heat to a high sided vessel and b) affect the internal materials and structure of an LNG carrier, there were many areas of uncertainty. The studies presented above capture both steady state and time based calculations, the basis of which rely on knowledge of, or assumptions for, fire scenario conditions.

Given the uncertainty existing within the industry over large pool fire surface emissive powers, and how these are likely to impact a carrier structure, it was not possible to gain unanimous agreement in all respects. However, the vast majority came to agree with the conclusions and recommendations made in chapters 10 and 11.

Steady state conditions indicate that, in the extreme case of losing the entire insulation layer, then assuming that the factors included in the IGC Code for sizing the relief valves, the valves are capable of relieving the anticipated vapour albeit at raised tank pressures that can be withstood by the cargo tanks. Additionally, this relief valve capability can, as well as loss of insulation, also comfortably accommodate the further extreme case of complete loss of the weather cover of a Moss type LNG carrier.

For time based scenarios and studies, heat transfer and CFD calculations were performed, a review of previous studies on insulation tests was undertaken and further insulation heat tests were performed. A range of times for complete degradation of insulation were indicated through the various studies and tests such that definitive time could not be arrived at due to the conflicting evidence and, therefore, differing views of the working group members. For this reason, Recommendation 2 is made.

### Conclusions

1. IGC formula and methodology for LNG carrier relief valve sizing compares favourably and is consistent with similar codes such as API, CGA, EN, ISO and NFPA.
2. For the Moss design tank with polystyrene based foam insulation, assuming the worst case scenario of losing the entire insulation effect, the tank pressure will rise to a level that can be accommodated by the tank structure without failure. This is due to the capability of the LNG carrier relief valves to relieve far higher gas flow capacities with rising tank pressure, as indicated by calculations based on the methodology prescribed by the IGC code.
3. Further to 2 due to the capability of the relief valves to accommodate greater gas flows with rising tank pressures and assuming the worst case of cargo tank cover damage and loss of heat shielding due to the possibility of combustion of the insulation and degradation products causing over-pressures sufficient to fail the tank cover, the relief valve capacity is still sufficient to prevent over-pressure failure of the tank.
4. In addition to conclusions 2 and 3, where even if the entire insulation was lost and the tank cover was completely lost, the capacity of the relief valves can accommodate a further estimated 30% rise in heat flux from a surrounding fire above that contained in the codes referred to in 1.
5. The limit of relief valve capability is the 'choke point' at which no further increase of gas flow can be accommodated through the RV vent system. This is approximately at 4.3 barg.
6. The presence and use of the vapour header will provide further pressure relief via the assumed damaged (holed) cargo tank and the forward vent riser. However, this has not been relied upon for the protection of the cargo tank against over pressure in the points above. The extent to which the vapour header contributes to pressure relief will depend on the fire scenario.
7. The response of the insulation system to heat, with time, is unclear; a detailed understanding of rates of insulation degradation and recession was not available for the structural arrangement of an LNG carrier.  
One dimensional CFD/heat transfer calculations made by the working group indicate time periods of 10 minutes for a complete degradation to a depth of 30 cm. Conversely, other studies in this report result in a degradation time of

up to 29 minutes. Additionally, reports from physical tests carried out in the 1970s indicate time periods of greater than 2 hours, although in these tests the conditions did not entirely accurately reflect actual LNG carrier dimensions or heat source temperatures.

8. From the behaviour tests of polyurethane foam under heat in an N<sub>2</sub> inerted atmosphere, insulation properties and strength are retained such that the concern for complete failure by degradation under fire conditions is likely to be substantially less for polyurethane based materials.
9. Based on experience from earlier fire incidents and studies included in the report, the tank cover is not likely to collapse under fire loads. It should be noted that the ABS study did not take into account the effect of the water-spray system required under 11.3 of the IGC Code.

## Recommendations

1. If large scale LNG fire tests are carried out by Sandia, or others, that show significant conflict with existing values of heat flux used in the IGC Code and other industry codes and standards, the question of the current equations for determining fire-case pressure relief loads merit re-examination by the whole LNG industry and not just the shipping element.
2. Although the working group has determined that current polystyrene foam insulated Moss sphere LNG carriers are equipped with pressure relief valves that provide additional capacity to prevent failure by over-pressure of intact cargo tanks, a better understanding of the foam plastic insulation vulnerability to heating is required to adequately assess the hazards that could result from loss of insulation effectiveness with fire exposure. Given the comparatively short duration of LNG fires, as estimated by previous fire scenario studies, a much better understanding of the temporal response of foam plastic insulation materials is necessary to determine the worst case circumstances as referred to in the conclusions above. Further research, which should include physical insulation testing as well as a determination of the potential for additional damage due to combustion of the foam degradation products, is recommended.

# CONTENTS

<b>Introduction</b> .....	<b>1</b>
<b>1 Previous Incidents</b> .....	<b>5</b>
1.1 'Yuyo Maru' No.10.....	7
1.2 'Gaz Fountain' .....	8
1.3 25,000 dwt Single Hull Product Carrier .....	9
1.4 'Val Rosandra' Propylene Fire .....	9
<b>2 The Origins of the IGC-Code</b> .....	<b>11</b>
2.1 Introduction .....	13
2.2 Review of the IGC-Code Requirements.....	13
2.3 Relation between Volume Flow of Free Air and Heat Flux into the Tank.....	14
2.4 Origins of Section the 8.5 of the IGC-Code.....	14
2.5 Other Standards .....	16
2.6 Evaluating the Criteria.....	16
2.6.1 Heat flux $q$ from the fire.....	17
2.6.2 Affected tank area $A$ .....	17
2.6.3 Fire factor $F$ .....	17
2.6.4 Literature for this section .....	18
<b>3 Fire Scenarios</b> .....	<b>19</b>
3.1 Summary of Documentation Review.....	22
3.1.1 Guidance on risk analysis and safety implications of a large Liquefied Natural Gas (LNG) spill over water – Document No. 1 .....	22
3.1.2 Key results extracted .....	22
3.1.3 Cloud fire experiments.....	23
3.1.4 Pool fire experiments.....	23
3.1.5 Overall summary of results of experiments – pool fire & vapour cloud studies .....	24
3.1.6 Results of 40 m <sup>3</sup> LNG spills on water – Document No. 2.....	24
3.1.7 Consequence assessment methods for incidents involving releases from liquefied natural gas carriers – Document No. 4.....	24
3.1.8 Consequences of LNG marine incidents – Document No. 5 .....	25
3.1.9 Consequence modelling of LNG marine incidents – Document No. 6 .....	25
3.1.10 Potential for BLEVE associated with marine LNG vessel fires – Document No. 7.....	25
3.1.11 Input to modelling work of other members of the working group .....	25
3.1.12 Large hydrocarbon fuel pool fires: physical characteristics and thermal emission variations with height – Document No. 9.....	26
3.1.13 Large hydrocarbon fuel pool fires: physical characteristics and thermal emission variations with height – Document No. 11.....	26
3.1.14 LNG properties & hazards – understanding LNG rapid phase transitions (RPT) – Document No. 12 .....	26
3.1.15 LNG pool fire simulations – Document No. 14.....	26
3.1.16 LNG decisions making approaches compared – Document No. 13.....	27
3.1.17 Thermal response of gas carriers to hydrocarbon fires – Document No. 15.....	27
3.1.18 Maplin sands experiments 1980 – dispersion results from continuous releases of refrigerated liquid propane & LNG – Document No. 18.....	28
3.1.19 Maplin sands experiments 1980 – dispersion & combustion behaviour of gas clouds resulting from large spillages of LNG & LPG on the sea – Document No. 19 .....	28
3.2 Results.....	29
3.2.1 Results of documentation review .....	29
3.2.2 Summary .....	29

<b>4</b>	<b>LNG Carrier Pressure Relief Systems .....</b>	<b>31</b>
4.1	Functional Requirements .....	33
4.1.1	Cargo tanks to have an emergency over-pressure system which shall .....	33
4.1.2	Cargo tanks to have an emergency under-pressure system which shall .....	33
4.1.3	Cargo tanks to have a pressure control system .....	33
4.2	Design Requirements .....	33
4.2.1	Pressure Relief Valve (PRV) function .....	33
4.2.2	Pilot design .....	34
4.2	Pressure Settings .....	35
<b>5</b>	<b>Simplified Reapplication of the Code for Loss of Insulation .....</b>	<b>37</b>
5.1	Study 1 .....	39
5.1.1	IGC code Pressure Relief Valve (PRV) sizing .....	39
5.1.2	Moss rosenberg LNGC relief valve sizing considering pure methane conditions .....	39
5.1.3	IGC code PRV required capacity .....	41
5.1.4	Physical sizing of pilot-operated, Pressure Relief Valves (PRV) .....	41
5.1.5	Choked flow .....	42
5.1.6	Extrapolating fire conditions against PRV valve sizing .....	42
5.1.7	Total relieving capacity of cargo containment system .....	43
5.1.8	PRV capacity at maximum back pressure .....	45
5.1.9	Moss type LNG carrier – response to over-pressure conditions .....	46
5.2	Study 2 .....	47
5.2.1	Résumé .....	47
5.2.2	Selected relief valve .....	47
5.2.3	Cargo .....	48
5.2.4	Maximum cargo tank size .....	48
5.2.5	Over pressurization of cargo tank due to fire .....	49
5.2.6	Increase in relief valve capacity due to over pressurization .....	49
5.2.7	Existing ship .....	50
5.2.8	Results .....	50
<b>6</b>	<b>Heat Transfer Into the tank .....</b>	<b>53</b>
6.1	Fire Scenario .....	55
6.2	Limit for Heat Flux into LNG and Possibility of Tank Collapse .....	55
6.2.1	Heat flux into the weather cover .....	55
6.2.2	Possibility of film boiling .....	56
6.3	Burning of the Insulation or Explosion of Combustible Mixtures .....	57
6.3.1	Burning of insulation .....	57
6.3.2	Explosion within the cargo hold .....	57
6.4	CFD Evaluation of the Tank Fire Problem .....	58
6.4.1	CFD calculation .....	58
6.5	Heating up of the Weather Cover and the Insulation .....	60
6.6	Heat Transport into the Insulation .....	62
6.7	Relation of CFD Calculation Results to Pool Fire Burning Duration According SANDIA Report .....	63
6.7.1	Melting of insulation and leak size .....	63
6.7.2	Heating up of weather cover and leak size .....	64
6.8	Temperature in Skirt Area .....	65
6.9	Literature for this Section .....	67
<b>7</b>	<b>Time Based Heat Transfer .....</b>	<b>69</b>
7.1	One-Dimensional, Transient, Heat Transfer Analysis .....	71
7.1.1	Initial conditions .....	71
7.1.2	Boundary conditions .....	72
7.1.3	Results .....	72

7.2	Predicted Component Failure Commencement Times .....	74
7.2.1	Metal failure .....	74
7.2.2	Insulation failure .....	74
7.2.3	Insulation combustion .....	74
7.3	Update on Issues Remaining – Appropriate Values of the Environmental Factor $F_1$ to Account for Radiation Shielding by the Tank Cover .....	75
7.4	Critical Update on Issues Remaining – Thermal Degradation Properties of Polystyrene Foam: New Results for the Estimated Time for Insulation Failure .....	76
<b>8</b>	<b>Response of Insulation Materials to Heat .....</b>	<b>79</b>
8.1	Thermal Loads on Insulation .....	81
8.2	Thermal Effects on the Insulation .....	82
8.3	Outline of DNV Test Programme .....	83
8.3.1	Results .....	84
<b>9</b>	<b>Discussion .....</b>	<b>85</b>
9.1	Steady State Conditions .....	87
9.2	Time Based Conditions .....	87
9.3	Decisions and Agreement of the Working Group .....	87
<b>10</b>	<b>Conclusions .....</b>	<b>89</b>
<b>11</b>	<b>Recommendations .....</b>	<b>93</b>
	<b>Appendix 1 – Moss tank cover response to heat .....</b>	<b>95</b>
	<b>Appendix 2 – Thermodynamic boundary condition .....</b>	<b>133</b>
	<b>Appendix 3 – CFD Modelling of the heat input to an LNG tank .....</b>	<b>161</b>
	<b>Appendix 4 – JHM paper, Fire performance of LNG carriers insulated with polystyrene foam .....</b>	<b>177</b>
	<b>Appendix 5 – Thermodynamic boundary condition .....</b>	<b>187</b>
	<b>Appendix 6 – Insulation heating comparison .....</b>	<b>203</b>
	<b>Appendix 7 – Polyurethane heat tests .....</b>	<b>207</b>



# **INTRODUCTION**



In 2004, SIGTTO was approached by Professor Havens of the University of Arkansas who expressed concern about the vulnerability of LNG carrier tanks that are insulated with non-fire-resistant materials such as polystyrenes or polyurethanes.

Current practice provides for pressure relief systems, designed with credit for the tank's insulation, to prevent LNG cargo pressurization due to boil-off and fire (IMO IGC Code 8.5). However, it is uncertain to what extent any degradation of insulation, in a fire situation, is taken into account in the design of PRV systems. As foam plastic insulation materials are subject to possible melting, degradation and or ignition at temperatures lower than might be achieved during such fire exposure, there is concern that the PRV systems may not be capable of relieving the vapour flows that would result from the increased boil off due to partial or total insulation failure.

At their April 2006 meeting, the SIGTTO GPC sanctioned the formation of a working group to thoroughly investigate the subject and produce a detailed report on the possible effects and any mitigation measures that may be necessary.

The working group met six times between July 2006 and June 2008, under the chairmanship of Mark Hodgson of STASCo., with representatives of the following organisations participating in the work:-

STASCo.  
University of Arkansas  
University of New Brunswick  
Bureau Veritas  
American Bureau of Shipping  
GTT  
Hoegh Fleet Services  
BGT  
Golar LNG  
Germanischer Lloyd  
ExxonMobil  
Lloyd's Register  
Gaz de France  
Suez LNG  
Det Norske Veritas  
Moss Maritime  
SIGTTO

The working group (WG) was directed to investigate the response of LNGC cargo tanks exposed to a large enveloping pool fire that could possibly result from the spillage of LNG onto the sea and its subsequent ignition.

Full consideration was given to this question, making use of in-house documentation, government or industry publications and the experience of the WG members. The following activities were carried out by WG members working in four sub-groups, who were assigned specific tasks.

1. A review of reports and investigations related to a number of incidents involving liquefied gas carriers subjected to fire exposure.
2. A review of the methods allowed and used to size PRV systems on liquefied natural gas carriers. This determination included specific descriptions of current practices of allowing for insulation performance under severe thermal radiation (fire) exposure.
  - a. Review the origins of the empirical formulae used to determine the size of pressure relief valves in the IGC Code and other relevant industry codes.
  - b. A review of 22 documents covering a wide range of studies and actual LNG fire model tests and experiments conducted over the past 30 years.
3. An analysis of the increased boil-off of LNG that could occur if an un-breached LNG tank were subjected to an enveloping LNG pool fire burning on the water.

4. An estimation of the pressure development in the tank was made to judge suitability of PRV sizing and relieving characteristics.
5. Finite element analysis of buckling of the tank cover under fire exposure.
6. A time dependent CFD analysis of heat transfer into the tank under varying heat flux intensities from an enveloping pool fire.

This report and the attached appendices are the conclusions of this work.

## **PREVIOUS INCIDENTS**



To date there has been no incident involving uncontrolled loss of containment on an LNG carrier and the largest LNG pool fire tests carried out at Montoir and Maplin were only a maximum of 35 m diameter. Therefore, there is no experience to draw upon to estimate the effects of a release and subsequent ignition of a large quantity of LNG engulfing an LNG carrier.

There are however, numerous well documented incidents involving conventional tankers and LPG carriers and these can give us an insight into the effects of an engulfing fire on the structure of a ship and also the characteristics of fires involving large quantities of refrigerated liquefied gases in insulated tanks.

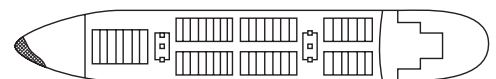
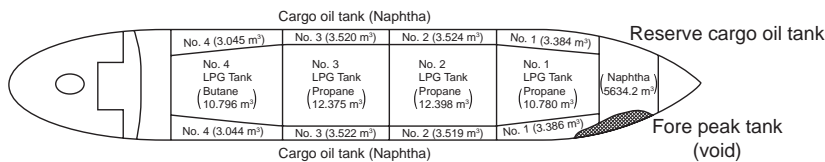
## 1.1 'Yuyo Maru' No.10

'Yuyo Maru' was of a design no longer permissible under the IGC Code (see diagram) whereby LPG was carried in the centre tanks and light naphtha in the wing tanks (MARPOL Regulation 13G, 1994, prohibits the carriage of petroleum products in tanks adjacent to the sea). In November 1974 the vessel was involved in a collision with a bulk carrier, resulting in a serious fire and the death of most of the crew of the bulk carrier and 5 members of the 'Yuyo Maru's' crew. The information below comes from the Japanese Maritime Safety Agency report.

Cargo of 'Yuyo Maru' No.10 and Damage to Both Vessels

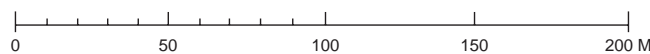
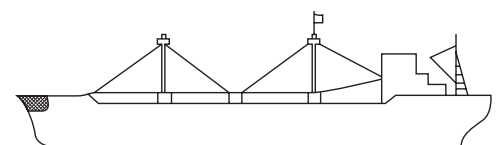
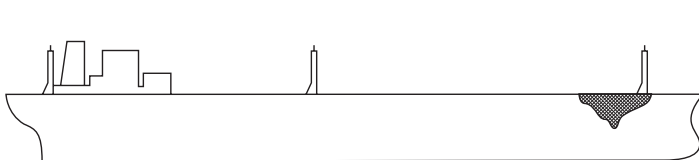
Yuyo maru. no.10  
 LOA : 227.10 metres  
 B : 35.80 metres  
 D : 20.75 metres

Pacific ares  
 LOA : 154.10 metres  
 B : 22.20 metres  
 D : 12.10 metres



Cargo	Total
Naphtha	32,378 m <sup>3</sup>
Propane	35,553 m <sup>3</sup>
Butane	10,796 m <sup>3</sup>
Bunker	2,800 Ton

Cargo  
 Steel material 14,836 Ton



The vessel burned for 10 days after which time it was boarded and a survey carried out to ascertain if it could be towed. It was estimated that approximately 25% of the naphtha and an unknown amount of propane and butane had been consumed in the fire. Most of the butterworth plates were missing on the wing tanks, but otherwise the deck was intact. The damage to the LPG tanks was "the safety valves and part of the hatch covers where the float gauges were installed" (sic). The vessel was towed out to sea, during which time the fire flared up again, and was eventually sunk by a combination of gun-fire, bombs and, eventually, a torpedo, 19 days after the collision.



## 1.2 'Gaz Fountain'

'Gaz Fountain' was a fully refrigerated LPG carrier with a cargo-carrying capacity of 40,232 m<sup>3</sup>. Her 3 free-standing prismatic cargo tanks were insulated with loose fill perlite. On 12 October 1984, during the height of the Iran-Iraq war and while carrying 6,300 tonnes of propane and 12,140 tonnes of butane from Ras Tanura to Fujairah, the ship was attacked by an Iranian aircraft and suffered three hits from air-to-ground, armour-piercing missiles. The crew shut down the propulsion and cargo refrigeration systems and abandoned ship. The following account describes how a salvage team quenched the fires and salvaged the vessel and over 93% of her cargo.

One missile exploded on deck above No 2 cargo tank, severely damaging much of the pipework in this area and setting off fires fuelled by escaping gas. The other two missiles hit the vessel's deck in the vicinity of No 3, or aftermost, tank. One of these penetrated the deck and blew a hole of several square metres in the roof of No 3 tank. A severe fire resulted, fed by the butane in No 3 tank. This quickly spread to the accommodation block, gutting it but, luckily, leaving the engine room relatively undamaged.



The following day a salvage tug approached 'Gaz Fountain' and started cooling the main fire areas. The salvors later experimented with dousing the torch fires using powerful water jets. This was an unconventional procedure, but one which was the only option as there was no means of isolating the ruptured tank and pipework.

The salvage crew used various combinations of wooden plugs, canvas patches, cement boxes and sandbags to stop the gas leaks in the damaged deck and pipework. However, it was impossible to plug the hole in No 3 tank and the hold space around the tank effectively became the cargo tank. A temporary gas vent was rigged to control tank pressures and the vessel, which by now had been anchored, was towed across the wind to aid the safe dispersal of gas.

A ship-to-ship transfer was started a month after the missile attack and 17,200 tonnes of cargo were successfully transferred over. On 12 December the operation, including the lengthy gas-freeing of No 3 hold, was concluded and the vessel was handed back to her owners.

Full details of this incident were presented at the Gastech 1985 conference in Nice, France, in a paper by Captain J A Carter entitled 'Salvage of Cargo from the War Damaged Gaz Fountain'.

## 1.3 25,000 dwt Single Hull Product Carrier

A single hull 25,000 dwt product carrier, owned and operated by a major oil company was involved in a collision in the southern North Sea. The vessel was carrying a full cargo of gasoline, which ignited and burned for over 24 hours before the fire was extinguished and the vessel boarded. Bronze butterworth plates and PV valves had melted in the intensity of the fire, and deck pipelines were badly buckled, but there was no serious buckling or distortion of the vessel's structure.



## 1.4 'Val Rosandra' Propylene Fire

On 28 April 1990 the 3,990 m<sup>3</sup> ethylene carrier 'Val Rosandra', laden with 2,250 tonnes of fully refrigerated propylene at minus 47degC, was discharging at Brindisi in Italy when a violent explosion occurred in the cargo compressor motor room.

### 'Val Rosandra' after initial explosion and fire



The motor room was so severely damaged that a switch panel was blown onto the deck and cargo pipework outside the room ruptured. In addition, the port and starboard domes of No 3 cargo tank also ruptured. As a result of the explosion the escaping propylene ignited and the fire continued to be fed by cargo evaporating from the damaged domes.

As local emergency services responded to the incident, the crew abandoned ship. The vessel was subsequently towed to the edge of the port limits where the fire was monitored from a safe distance. Although the fire showed no signs of escalation over a number of days, it was decided not to attempt to salvage the vessel or her cargo. Instead, charges were detonated around the domes of the remaining four tanks to allow the propylene cargo to escape gradually and burn off. It was agreed that once this had been accomplished, the vessel would be scuttled.

### 'Val Rosandra' after the tank domes were breached with charges



On 21 May 1990, over 3 weeks after the initial explosion and with the fire still burning at No 3 tank, the vessel was towed out to sea. The tank domes of the 4 undamaged tanks were breached with explosive charges. Although this resulted in some escalation of the fire, it was not to the extent the authorities had anticipated. The slow burn rate was attributed to the fact that the cargo was fully refrigerated and would only burn as fast as heat penetrated the insulated tank walls and domes and evaporated the propylene. On 8 June 1990, 41 days after the initial explosion and fire, a large quantity of explosive was detonated on 'Val Rosandra's' hull and, on this occasion, the ethylene carrier's demise was not long in coming.

# **THE ORIGINS OF THE IGC-CODE**



## 2.1 Introduction

In accordance with the Terms of Reference for the working group outlined in the introduction to this report, detailed determination was made of the methods allowed and used to size pressure relief valve systems on liquefied natural gas carriers. This review included the following;

A review of all working papers related to the requirements for cargo tank pressure relief valves generated between 1971 and 1974 at IMO Subcommittee on Design and Equipment. This included Sessions DE VII, VIII, IX and DE XII plus a number of intercessional meetings of the special working group that was established to develop the Gas Code, which was replaced in 1983 by the IGC-Code, (The International Code for the Construction and Equipment of Ships Carrying Liquefied Gases in Bulk). The final paper of DE IX contained the exact text of 8.5 of IGC as it exists today.

A review of the requirements for sizing of pressure relief valves contained in other standards and codes of practice in use today. This includes the CGA-S.1, API 521, API 2000 and NFPA 59-A as well as the requirements of the US Coast Guard.

A detailed review of work carried out by the National Academy of Sciences at the request of the USCG over a period of six(6) years as presented in the report 'Pressure-Relieving Systems for Marine Cargo Bulk Liquid Containers' 1973 (ISBN 0-309-02122-7) Ref-02.

## 2.2 Review of the IGC-Code Requirements

Section 8.2.1 of the IGC requires that each cargo tank with a volume exceeding 20 m<sup>3</sup> should be fitted with at least two pressure relief valves of approximately equal capacity, suitably designed and constructed for the prescribed service.

Section 8.5.2 IGC provides the following criteria for determining the combined minimum relieving capacity, under fire exposure, with not more than a 20% rise in cargo tank pressure above the maximum allowable relief valve setting.

$$(1) \quad Q = FGA^{0.82} (\text{m}^3/\text{s})$$

Where Q is the minimum required rate of discharge in cubic metres per second of air at standard conditions 0degC and 1.013 bar.

A is the external surface area of the tank in m<sup>2</sup>. This is a stronger requirement compared to the other regulations named that require the wetted surface of the tank to be used (comp. also below).

F is the fire exposure factor for different tank types and defined as follows:

F = 1.0 for tanks without insulation located on deck

F = 0.5 for tanks above the deck when insulation is approved by the Administration. (Approval will be based on the use of an approved fireproofing material, the thermal conductance of the insulation and its stability under fire exposure)

F = 0.5 for uninsulated independent tanks installed in holds

F = 0.2 for insulated independent tanks in holds (or uninsulated tanks in insulated holds)

F = 0.1 for insulated independent tanks in inerted holds (or uninsulated independent tanks in inerted, insulated holds)

F = 0.1 for membrane and semi-membrane tanks.

For independent tanks partly protruding through the open deck, the fire exposure factor should be determined on the basis of the surface areas above and below deck.

Equation (1) is equivalent to the equations which give a heat flux instead of a volume flow of free air (comp. eg NAS report). The relation to these expressions is given by the Gas factor G.

$$(2) \quad G = \frac{12.4}{LD} \sqrt{\frac{ZT}{M}}$$

Where L is the latent heat in kJ/kg, Z is the compressibility factor, M is the molecular weight of the cargo and D is a constant based on the relation of the specific heats of the cargo being vaporised. T is the temperature in degrees K at the relieving

conditions. Relieving conditions are 120% of the pressure at which the pressure relief valve is set. This pressure is the MARVS pressure (MARVS = Maximum Allowable Relief Valve Setting).

Prior to the 1993 Edition of IGC-Code, G was given as follows:  $G = 177/LC (ZT/M)^{1/2}$  with the latent heat L given in terms of Kcal/kg and Q given in  $m^3/min$  rather than  $m^3/s$ . For the 1993 edition of the IGC-Code the units have been changed to ISO standard units.

The current USCG regulations 46 CFR 54.15.2, are in full agreement with the requirements of 8.5 of IGC-Code. The only difference is in the wording, where the IGC-Code specifies approval by the Administration and the CFR substitutes the word 'Commandant', as is customary in US regulations incorporating IMO instruments.

As already indicated, a heat flux is hidden in the term for G. This heat flux  $\bar{q}$  is an assumed heat flux emanating from the fire, which we can call q.

In the IGC-Code, as in API 521, API-2000, NFPA 59A and CGA S.1, this heat flux is equal to 34500 BTU/(ft<sup>2</sup> h), which is equal to 108.83 kW/m<sup>2</sup>. Because the surface area A used by the IGC-Code is not in ft<sup>2</sup> but in m<sup>2</sup> and A is set to the power of 0.82 there is an additional factor included that is related to the unit transfer from US to ISO units. This factor leads to heat flux q in the IGC-Code, which is

$$q = 0.652 \bar{q}$$

$$q = 0.652 \times 108.83 = 70.96 \text{ kW/m}^2$$

This unit transfer related fact often leads to the misunderstanding that the IGC-Code uses a heat flux lower than the other regulation, which is not the case. Further explanation is given below and in the Annex.

The same value of q is used for all 32 cargos covered by IGC-Code.

## 2.3 Relation between Volume Flow of Free Air and Heat Flux into the Tank

It can be shown that the volume flow of free air, as given by the equation in IGC 8.5.2, is equivalent to the volume flow of gas that is evaporated by the heat flux of a fire.

The relation between the heat flux into a tank and the volume flow of free air, as given in 8.5 of the IGC Code, is in detail derived in the Article of Heller/Ref-01 on pages 129 to 132. He started with the general flow equation (Eq. 5 in/Ref-01, p. 129) and demonstrated that the volume flow of free air, as given in the IGC Code 8.5.2, resulted from the comparison of the flow of air at standard conditions to the flow of any gas through the same orifice of a safety valve.

The flow of the gas, which is LNG for the purpose of this report or any gas from the list of gases in the IGC Code, is calculated from the heat flux into the tank as explained in Section 2.4. With Eq. 14 (/Ref-01, p. 132), Heller gets the formula as given in the IGC, including the gas factor G.

## 2.4 Origins of Section the 8.5 of the IGC-Code

A detailed review of the database of IMO documents related to the requirements of 8.5 of IGC, submitted between 1971 and 1974 when subcommittee on Design and Equipment was drafting the Gas Code, as well as the DE reports to the Maritime Safety Committee (MSC), has provided the following insights:

1. The earliest version of the Gas Code criteria for sizing PRV appeared in paper DE 75 dated 7 June 1972. It was para 8.4 at that time.
2. The source of this criteria was not provided in the IMO documents reviewed, but it should be noted that, in accordance with the NAS report, it is exactly identical, including the fire factors, to the criteria that existed in the USCG regs 46, CFR 54-15-5(d) and 46 CFR 38.10-15 in 1968. This includes reference to ASME Section VIII, div 1, Appendix J, for values of 'D', the constant based on the relationship of the specific heats.
3. This same formula appeared in the ABS Rules and the BV Rules for gas carriers from 1965.
4. DE 75 proposed that  $F = 0.5$  for pressure vessel type tanks in a completely enclosed space below deck, and  $F = 0.2$  for non-pressure vessel type tanks in holds. By definitions 1.4.17 of DE/75, an independent pressure vessel tank

is what later became known as a Type C Independent Tank. By this definition a Type B tank, such as a Moss tank, where the stresses in the tank are primarily due to tank weight, product weight or sheer stresses, is a non-pressure vessel type independent tank and a factor of  $F = 0.2$  would apply as long as the tank was in a hold, regardless of insulation.

5. Japan paper DE/82, 20 November 1972, proposed that the ASME code should not be quoted in this regulation and defined pressure vessel type and non-pressure vessel type tanks for fire exposure factor as follows;
  - a. pressure vessel type – MAWP exceeding  $0.7 \text{ kg/cm}^2$ ,
  - b. non-pressure vessel type – MAWP not exceeding  $0.7 \text{ kg/cm}^2$
 By this definition Japan had proposed that a Moss type B tank is a non-pressure vessel type and the fire factor should be  $F = 0.2$  if it is installed in a cargo hold with no required insulation.
6. Norway's paper DE 83, 27 November 1972, states that the fire factor  $F$  will, to a large extent, depend on how the properties of the insulation is affected during the fire. They proposed that the Table should be completely reconsidered, the formulae for 'c' should be in the code, the factor 'A' should be reconsidered for different tank types. 'A' should be the area being exposed to heat during the fire.
7. UK paper DE/85, 27 November 1972, proposed modification to line 5/6. The maximum relieving pressure should not exceed 20% above the maximum working pressure and under conditions of external fire should not exceed the maximum test pressure of the tank.
8. DE-XII – 3 February 28 1974, contains an early consolidated version of the Gas Code. It reports about the results of the 'Ad Hoc Group' work, which met between 28 of January and 1 of February 1974 under the chairmanship of Robert Lakey (USA). At this time the NAS report (ISBN-0-309-02122-7) dated 1973 can be assumed to be known at least to the US participants. No details are given as to discussion of Chapter 8. Nevertheless, Chapter 8 was nearly in its final shape and the fire factors  $F$  given in annex II of the report are partly set into brackets to indicate that they are under discussion.
 

A closer look to the definitions indicated the following:

  - a. Reference to insulation is only given to tanks with fire resistant approved insulation on deck. This is in line with the example in the NAS report discussed below.
  - b. A footnote to  $F = 0.5$  for pressure vessels in hold spaces, regardless if insulated or not, gives the recommendation to look for the possibility for the reduction of  $F$  with regard to insulation. *This means that the proposed text itself does not look into the influence of tank insulation.*
  - c. No further direct reference is made to any influence of insulation. From the above it can be concluded that the fire factors in DE-XII-3 were defined mainly giving credit to the installation of the tanks in the ship and not to the insulation. This is in line with NAS report, which also sees the insulation as only one part to limit the heat flux into the tank.
  - d. An indirect relation to a credit in case of fire is the reduction of  $F$  from 0.2 to 0.1 for inerted holds. This gives credit to the fact that risk of fire in the hold has been reduced due to the lack of oxygen.
  - e. The nomenclature of the Section is given in the original US units and only partly in SI units.
  - f. The fire factors in brackets (or partly in brackets) are those for tanks installed below deck. Only the  $F = 1.0$  and the  $F = 0.5$  for tanks above deck seemed to be agreed on completely. These factors are the same in the IGC Code.
9. Germany submitted DE 110 on 9 May 1974, which presented the final version of the fire factors 'F' in then 8.4.1, which became 8.5 in Res. A 328 (IX) and is exactly as they exist today in the IGC.
10. Comparing DE XII -3, DE 110 and the IGC Code the following conclusions can be drawn:
  - a.  $F = 0.5$  was agreed to be valid for independent tanks without insulation and not only for pressure vessels (type C tanks) as proposed by DE-XII-3. In addition the effect of an insulation system was included by DE - 110 by proposing it for uninsulated tanks. This appears to give credit to the fact that these tanks are independent from the ship structure which is subjected to the fire.
  - b.  $F = 0.2$ , which was completely in brackets in DE-XII-3, was agreed to cover independent tanks with insulation. This appears to be the final conclusion on giving credit to tank insulation. It appears there was a decision not to limit this to insulation systems that are fireproof since the insulation is shielded by the cargo hold, the access to air is limited and, therefore, the duration of a fire will only affect small parts of the insulation so that a large heat increase is needed and melted parts of the insulation still remains on the tank surface.
  - c.  $F = 0.1$  for insulated independent tanks in inerted holds and for membrane tanks gives credit to the exclusion of any fire by lack of oxygen as already stated in DE-XII-3.
11. Norway submitted DE/144 on 2 July 1974 with the following proposals:
  - a. Where  $F = 0.5$ , add 'Foam plastics are not regarded as fire resistant materials'.
  - b. Where  $F = 0.5$ , delete the wording within the square brackets (Approval will be based on the use of an approved fire proofing material, the thermal conductance of the insulation, and its stability under fire exposure.)

- c. Delete all references to fire exposure factors lower than  $F = 0.5$ .
  - d. Delete footnote (shown at the bottom of page 58 of DE/75) and insert "In specific cases consideration should be given by the Administration to fire exposure factors less than specified above, based on a review of insulation and surrounding hull structure".
  - e. Delete present reference to external surface area of the tank (A) and insert  $A =$  external surface of the tank (sq metres). Delete the remainder of this sentence
  - f. Insert "In specific cases consideration should be given by the Administration to an  $A -$  value less than specified above where fire exposure is not liable to affect parts of the tank surface area.
12. Resolution. 328(IX) dated 17 December 1975 was the first version of IGC Code
- a. Included the equations as proposed in DE/75 with the value of F proposed by Germany in DE/110.
  - b. It would appear that none of the recommendations of DE/144 were adopted.
  - c. A metric as well as British version was provided.

In general the review indicated that the fire factors were defined in a well balanced engineering judgment process (as also claimed by NAS to be necessary even if more fire testing data is available). The review of papers submitted and reports from the working group meetings reflect that in the selection of the values of F consideration was given to the suitability of various insulation systems to fire exposure as well as the protection provided by the vessel's structure, including the tank cover.

## 2.5 Other Standards

It has been noted from the review of the other standards mentioned in item 2 that while the CGA standard, like the IGC Code, provides relief valve capacity requirements in terms of the equivalent air flow through the safety valve, the API codes and the NFPA 59A standard provide requirements for determining the total heat flow into the tank as follows:

$$H = 34,500 F A^{0.82} \text{ in US customary units}$$

$$H = 71,000 F A^{0.82} \text{ in SI units}$$

H is total heat flux (Btu/hr or watts) into the tank.

It should be noted that 34,500 Btu/hr ft<sup>2</sup> is numerically equal to 108.78 Kw/m<sup>2</sup> but, because of the 0.82 exponent on the area when the conversion is made from US customary to SI units, heat flux value becomes 70.93 Kw/m<sup>2</sup> (comp. above). The following unit conversion calculation can be applied:

$$Q = 34,500 \text{ Btu/hr ft}^2 \times F (A)^{0.82} \quad (1 \text{ Kwh} = 3412 \text{ BTU and } 1 \text{ ft}^2 = 0.09295 \text{ m}^2)$$

$$Q = \frac{34,500 \text{ Btu/hr ft}^2}{3412 \text{ Btu/kWh}} \times F (A)^{0.82}$$

$$Q = 10.1113 \text{ Kw/ft}^2 \times F (A)^{0.82}$$

$$Q = 10.1113 \text{ Kw/ft}^2 \times \frac{(0.09295)^{0.18} \times (0.09295)^{0.82}}{(0.09295) \text{ ft}^2/\text{m}^2} \text{ ft}^2/\text{m}^2 \times F (A)^{0.82}$$

$$Q = 108.78 \text{ Kw/m}^2 \times (0.09295)^{0.18} \times F (A \times (0.09295))^{0.82}$$

$$Q = 70.93 \text{ kw/m}^2 \times F (A)^{0.82}$$

## 2.6 Evaluating the Criteria

Since there appears to be no question as to the validity of the constant 'D' in Eq. (2) in 2.2, a review of the criteria for sizing pressure relief valves on vessels intended to carry liquefied gases in bulk then calls into question the following, which will be considered independently:

- the assumed heat flux q emanating from the fire
- the correct area A of the tank to consider
- finally, the selection of a fire factor F assumed.

## 2.6.1 Heat flux $q$ from the fire

There is considerable discussion in the NAS report regarding the proper heat flux to be used for sizing pressure relief valves for fire exposure. It is recognized in the NAS report that local heat fluxes from methane fire have been observed to be as high as 90,000 Btu/hr ft<sup>2</sup>. However, it is recommended that 34,500 Btu/hr ft<sup>2</sup> be used as a good approximation for the average heat flux over the entire wetted surface area exposed to fire. This exact same value is used in the CGA, API codes and NFPA codes as well as in the IGC-Code.

## 2.6.2 Affected tank area $A$

In the criteria for sizing pressure relief valves the API and NFPA codes use the wetted surface of the tank. The CGA and the IGC-Code use the full surface area. Considering that LNG is almost always transported in fully loaded tanks the difference is negligible.

The NAS report proposed that in sizing pressure relief valves consideration should be given to effects of supporting structures or other specially introduced features that may serve to confine the fire. It states:

*"In the calculation of heat transfer from fire to the cargo containment, special consideration should be given to the design features used to limit the portion of the tank surface directly exposed to the fire, such as bulkheads and weather shields".*

This precaution would serve to reduce substantially the effective safety device sizing requirements.

The NAS report proposed that a factor  $E$  be used, which is defined as the ratio between the tank area under fire  $A_e$  exposure and the total tank area  $A$  ( $E = A_e/A$ ; comp NAS Report page 20, Eq. 3). For this reason  $E$  is 1.0 as a maximum if the complete tank is subjected to the fire. So the product of  $E \times A$  represents the fraction of the wetted area  $A$  in direct contact with the fire. It is pointed out that, for marine installations, by taking credit for protective structure afforded by the ship's structure, the effective area will in almost all cases be less than which would be determined by using the tank area  $A$  raised to a power of 0.82.

It should be noted that the IGC-Code formula given can be derived from the NAS formula by applying  $A_e = A^{0.82}$ . This is demonstrated by a calculation provided in the annex.

Notwithstanding the recommendations of the NAS report, the CGA, API, NFPA codes as well as the IGC Code use the more conservative approach raising the surface area of the tank to the power 0.82, and use this figure as the part of the tank subjected to the fire ( $A_e$ ).

For a Moss tank, of approximately 36 m (125 ft) in diameter, using the IGC-Code criteria, the effective area of the tank considered to be exposed to the heat of the fire is approximately 15% of  $A$ .

It should be noted that while the API and NFPA codes use the value of  $A$  to the 0.82 factor, areas of the tank more than 9 m above the ground are completely excluded from the total area used to size pressure relief valves. It is stated that tests have shown that the effective heat flux from a pool fire at such elevations is negligible.

The API and NFPA codes also exclude areas of the tank that are protected from direct fire impingement, such as skirts and supporting structure on vertical tanks.

There is no reduction in effective area of the tank provided for in the IGC-Code, which consequently means that the IGC-Code is inherently more conservative in this respect for sizing of pressure relief valves.

## 2.6.3 Fire factor $F$

In accordance with the NAS report, if the insulation covers more than, say, 70% of the tank, the fire factor  $F$  can be determined by using the methods in Appendix G. The method of Appendix G is applicable for insulation systems that retain effectiveness at expected high temperatures. Under these conditions the  $F$  factor is determined as a direct function of the thermal conductivity of the insulation. For tanks that are 100% insulated Table G -2 shows  $F$  factors below 0.05.

The above is consistent with the API codes and NFPA 59A. API 521 would allow a value of  $F$  between 0.026 and 0.3 based on a thermal conductivity of 0.58W/mK.

The insulation system on an LNG carrier has a typical thermal conductivity of 0.038W/mK. However, for LNG carriers the value of  $F$  for insulated tanks is not lower than 0.1 and that is only applicable to insulated tanks inside an inerted cargo hold as per the above discussion.

Regarding the NAS report in Annex G, it should be noted, that the maximum insulation thickness assumed is 1 inch (25.6 mm). The insulation thickness of an LNG tank on an LNG carrier is at least 300 mm.

## 2.6.4 Literature for this section

Ref-01 Safety Relief Valve Sizing: API Versus CGA Requirements Plus a New Concept for Tank Cars; Frank J. Heller, API Proceedings 1983, Refining Department, Vol 62; API, W.D.C., p. 123-135

Ref-02 Pressure relief Systems for Marine Cargo Bulk Liquid Containers, National Academy of Science (NAS), W.D.C., 1973, ISBN-0-309-02122-7.

# **FIRE SCENARIOS**



The primary aim of this section is to:

- Focus on the particular elements in the allotted task, while not neglecting to bring to the other working group members issues that the subgroup considered influential or related to these elements for their consideration
- compile any reservations they had on the input information both to:
  - show they had considered these and possibly discounted them
  - or
  - they had prepared important reservations not discounted, if any, for consideration by the wider working group
- conclude - finally the subgroup concluded on the most representative scenario.

As was discussed during the first WG meeting, the Sandia report is widely taken as a seminal work on this subject. There are, however, other studies that were used that both reinforce the findings of the Sandia report or question its findings. This ensured that a considered analysis was made, as opposed to simply accepting the Sandia report without question, when it remains clear that there are concerns within the industry over some of its findings. These concerns revolve around quantification of the following points:

- Large fire scenarios are required to threaten significant parts of a cargo tanks
- large fires may occur if an LNG tank is ruptured and LNG dispersed to the sea
- the release rate determines both the size of the fire as well as the duration
- collision damage causing tank ruptures of, eg 1 m<sup>2</sup>, will fuel very large fires (dia > 300 m) but will have short duration (typically less than 15 min) due to the emptying of the tanks
- smaller releases can fuel fires of longer duration with the potential of threatening a large part of one side of the vessel
- these fires will have a very large flame height and may affect large part of the tanks above the main deck
- experimental data from large LNG fires on water does not exist and the effects of oxygen starvation and possible smoke screening are not known. A conservative approach would be to apply heat loads from large pool fires without smoke screening
- such fires will burn as pool fires with radiant heat loads 150 kW/m<sup>2</sup> and convective heat transfer from the combustion gases with temperatures 1000-1100 degC.

## Studies and Documentation Reviewed

Document No.	Title	Organisation	Date
1	Guidance on Risk Analysis and Safety Implications of a Large Liquefied Natural Gas (LNG) Spill Over Water	Sandia Report	2004
2	Results of 40 m <sup>3</sup> LNG spills on water	Lawrence Livermore National Laboratory	(circa 1983)
3	Spill tests of LNG and Refrigerated Liquid propane on the sea, Maplin Sands, UK, 1980	Shell Research Ltd.	1980
4	Consequence Assessment Methods for Incidents Involving Releases from Liquefied Natural Gas Carriers	ABS on behalf of FERC	May 13th 2004
5	Consequences of LNG Marine Incidents	DNV - CCPS Conference Orlando	June 29-July 1 2004
6	Consequence modelling of LNG Marine Incidents	DNV - Baik, Raghunathan, Witlox - American Society of Safety Engineers	March 18-22, 2005
7	Potential for BLEVE Associated with Marine LNG Vessel Fires	DNV - Dr. Robin Pitblado	August 2006
8	Model of Large Pool Fires	J.A. Fay - MIT	sept-05
9	Large Hydrocarbon fuel pool fires: Physical characteristics and thermal emission variations with height	Phani K. Raj - Technology & Management Systems	18th August 2006
10	Spread of Large LNG pools on the sea	J.A. Fay - MIT	October 2006
11	LNG Properties & Hazards - Understanding LNG Rapid Phase Transitions (RPT)	ioMosaic - G. Melhem, S. Saraf, H. Ozog	2006
12	Report on the Outline of Collision between Japanese tanker Yuyo Maru No. 10 & Liberia Freighter Pacific Ares	MSA - Japanese Government	March 1975
13	LNG Decisions Making Approaches Compared	Dr. R. Piblado, Dr. J. Baik, V. Raghunathan - DNV	2005

Document No.	Title	Organisation	Date
14	FDS LNG pool fire simulations : a preliminary study on the application of FDS to study potential marine tanker accidents	J E S Venart - University of New Brunswick	1st June 2006
15	Thermal Response of Gas Carriers to Hydrocarbon Fires	DNV For Shell International Marine Ltd.	26th November 1980
16	Public Safety Consequences of a terrorist attack on a tanker carrying LNG need clarification	US Government Accountability Office	February 2007
17	Department of Homeland security : LNG Tanker Security - Direct Testimony Dr. Phani K. Raj.	Dr. Phani K. Raj.- President - Technology & Management Systems, Inc.	
18	Maplin Sands experiments 1980 - Interpretations and modelling of Liquefied Gas Spills onto Sea	Shell Research B.V. & Shell Research Ltd.	1980 (Pub 1983)
19	Maplin Sands experiments 1980 - Dispersion results fro continuous releases of refrigerated liquid propane & LNG	Shell Research B.V. & Shell Research Ltd.	1980 (Pub 1984)
20	Maplin Sands experiments 1980 - Dispersion & combustion behaviour of gas clouds resulting from large spillages of LNG & LPG on the sea	Shell Research B.V. & Shell Research Ltd.	1980 (Pub 1982)
21	Maplin Sands experiments 1980 - Dispersion results from continuous releases of refrigerated liquid propane	Shell Research B.V. & Shell Research Ltd.	1980 (Pub 1982)
22	Review of published experimental results	Lloyd's Register of Shipping	Last ref. 1992

## 3.1 Summary of Documentation Review

Listed below are the salient points extracted from the documents submitted or researched that were reviewed by the subgroup. These points were those the group considered relevant to the terms of reference of the WG.

Those papers not referenced were considered not to have input directly related to the remit of the subgroup or the full WG.

### 3.1.1 Guidance on Risk Analysis and Safety Implications of a Large Liquefied Natural Gas (LNG) Spill Over Water – Document No. 1

The Sandia report is a compilation of previous work carried out in the field of LNG spills. The report summarises the different work and then performs various analyses with the assumption of certain inputs from the different input sources.

The report draws a number of conclusions, some of which are directly related to matters being discussed in this WG and within the remit of the work assigned to sub-group 'A'.

### 3.1.2 Key results extracted

- LNG cargo tank hole sizes for most credible threats range from two to twelve square metres, expected sizes for intentional threats are nominally five square metres
- the most significant impacts to public safety and property exist within approximately 500 m of a spill, due to thermal hazards from fires, with lower public health and safety impacts at distances beyond approximately 1600 m
- large, unignited LNG vapour releases are unlikely. If they do not ignite, vapour clouds could spread over distances greater than 1600 m from a spill. For nominal accidental spills, the resulting hazard ranges could extend up to 1700 m. For a nominal intentional spill, the hazard range could extend to 2500 m. The actual hazard distances will depend on breach and spill size, site-specific conditions, and environmental conditions
- cascading damage (multiple cargo tank failures) due to brittle fracture from exposure to cryogenic liquid or fire-induced damage to foam insulation was considered. Such releases were evaluated and, while possible under certain conditions, are not likely to involve more than two or three cargo tanks for any single incident. Cascading events were analysed and are not expected to greatly increase (not more than 20%-30%) the overall fire size or hazard ranges noted above, but will increase the expected fire duration.

### 3.1.3 Cloud fire experiments

Table 3.1 provides an overview of existing LNG spill testing data.

**Table 3.1: Largest Spill Volumes Tested to Date Giving Pool Radius and/or Distance to LFL**

Experiment	Spill Size (m <sup>3</sup> )	Spill Rate (m <sup>3</sup> /min)	Pool Radius (m)	Downwind Distance to LFL (m) (Max)
ESSO	0.8 – 10.8	9 – 17.5	7 – 14	400
U.S.C.G.	3 – 5.5	1.2 – 6.6	~7.5	Not measured
Maplin Sands (dispersion tests)	5 – 20	1.5 – 4	~10	190 ± 20 m
Maplin Sands (combustion tests)	10.35	4.7	~15	Not measured
Avocet (LLNL)	4.2 – 4.52	4	6.82 – 7.22	220
Burro (LLNL)	24 – 39	11.3 – 18.4	~5	420
Coyote (LLNL)	8 – 28	14 – 19	Not reported	310
Falcon (LLNL)	20.6 – 66.4	8.7 – 30.3	Not reported	380

### 3.1.4 Pool fire experiments

Liquid Pool Spreading

**Table 3.2: Largest Spill Volumes Tested to Date Giving Pool Radius and Max. Flux Rate**

Experiment	Volume Spilled (m <sup>3</sup> )	Pool Radius (m)	Mass Flux (kg/m <sup>2</sup> s)
Boyle and Kneebone (Shell)	0.02 – .085 Quiescent water surface (laboratory)	1.97 – 3.63	0.024 – 0.195 Increased with amount spilled & amount of heavy hydrocarbons
Burgess et al.	0.0055 – 0.36 (pond)	0.75 – 6.06	0.181
Feldbauer et al. (ESSO)	.8 – 10.8 (Matagorda Bay)	7 – 14	0.195
Maplin Sands	5 – 20 (300 m dyke around inlet)	~10	0.085
Koopman et al. (Avocet LLNL)	4.2 – 4.52 (pond)	6.82 – 7.22	Not reported

### 3.1.5 Overall summary of results of experiments – pool fire & vapour cloud studies

LNG pool and vapour cloud fire experiments and their results are summarised in Table 3.3. A detailed description of these experiments is provided in the following sections.

**Table 3.3: Large Scale LNG Fire Studies**

Study	Spill Terrain	Spill Vol. (m <sup>3</sup> )	Spill Rate (m <sup>3</sup> /min)	Pool DIA. (m)	Surface Emissive Power (kW/m <sup>2</sup> )		Burn Rate (10 <sup>4</sup> m/s) or kg/m <sup>2</sup> s	Flame Speed for Vapour Cloud Fires (m/s)
					Pool Fire	Vapor Cloud Fire		
U.S.C.G. China Lake Tests	Water	3 – 5.5	1.2 – 6.6	15 (max)	220 ± 50	220 ± 30	4 – 11 (measured) (.18 – .495)	8 – 17 (relative to cloud)
Maplin Sands	Water	5 – 20	3.2 – 5.6	30 (effective)	203 (avg) (178 – 248 range)	174 (avg) (137 – 225 range)	2.1 (calculated) (.0945)	5.2 – 6.0
Coyote	Water	14.6 – 28	13.5 – 7.1	Not measured	Not measured	150 – 340	Not measured	30 – 50 (near ignition sources – decayed rapidly with distance)
Maplin Sands	Land	No report	NA	20	153 (avg) 219 (max)	NA	2.37 (measured) (0.106)	NA
Montoir	Land	238	NA	35	290 – 320 (avg narrow angle) 257 – 273 (avg wide angle) 350 (max)	NA	3.1 (measured) (0.14)	NA

### 3.1.6 Results of 40 m<sup>3</sup> LNG spills on water – Document No. 2

Size of Spill – 25→40 m<sup>3</sup>  
 Outflow rate m<sup>3</sup>/minute – 10→20 m<sup>3</sup>  
 Varying wind speed  
 1 Metre depth of water  
 50 m diameter pool  
 Visible plume length – 50 metres  
 Not much input on specific values for heat flux, duration & distribution.

### 3.1.7 Consequence assessment methods for incidents involving releases from liquefied natural gas carriers – Document No. 4

Volume of spill – 12,500 m<sup>3</sup>  
 Duration – 33 mins  
 Heat Flux – 265 kW/m<sup>2</sup>  
 Flame Length (height) – (240→310 m)  
 Small size spills only as practical input  
 Summary results for pool fire calcs: Larger Pool size gives shorter fire duration and higher flame length.

**Table 3.4: Summary of Results for Example Pool Fire Calculations**

Hole Diameter	3.3 ft (1 m)	16 ft (5 m)
Initial Spill Rate	11,700 lb/s (5,300 kg/s)	290,000 lb/s (130,000 kg/s)
Total Spill Duration	33 min	1.3 min
Maximum Pool Radius	240 ft (74 m)	440 ft (130 m)
Total Fire Duration	33 min	6.9 min
Flame Length (Height)	910 ft (280 m)	1,400 ft (430 m)
Flame Tilt at Maximum Radius	35 deg	31 deg

### 3.1.8 Consequences of LNG marine incidents – Document No. 5

- Quote: The “effect of increased boil-off over water, will be to put more fuel into the same air space as over land without any mechanism for entraining more air.
  - This is likely to make the fire smokier and thus less luminous, with a greater fraction of the combustion energy going into heating the plume and less into thermal radiation.”
- “Overall, large pool fires have several areas of uncertainty.”
- “The large evaporating pool that is sustainable for dispersion is too thin to sustain combustion at the much higher rate of LNG consumption in a pool fire – LNG cannot flow from the source out to the periphery sufficiently quickly to replenish the material lost to combustion.”
- “Another uncertainty is associated with the degree of additional smoke associated with pool fires over water. The smaller diameter pool and the greater smoke generation would tend to reduce the thermal hazard range. This consequence area could benefit from large scale trials on water.”

**Table 3.5: Discharge Results – Various Holes Sizes and Locations**

Discharge Case	Above Waterline Release			Below Waterline Release		
	250	750	1500	250	750	1500
Hole Size (mm)	250	750	1500	250	750	1500
Initial Rate (kg/s)	226	2030	8130	200	1800	7220
Duration (hr)†	19	2.2	0.54	30+†	3+†	0.8+†
Total Release (%)	69%			100%		

† Durations are based on the average flowrate from the hole. For underwater cases this is an estimate only as the duration becomes complicated to estimate when the LNG driving force equalizes water back pressure.

### 3.1.9 Consequence modelling of LNG marine incidents – Document No. 6

Hole size: 250 mm→5000 mm  
 Discharge coefficient: 0.6→1.0  
 Burn Rate Range: 0.089→0.353 Kg/m<sup>2</sup>s  
 Pool Radius: 29 m→253 m  
 SEP: 178→265 Kw/m<sup>2</sup>

### 3.1.10 Potential for BLEVE associated with marine LNG vessel fires – Document No. 7

- A further protection is the limit on internal tank pressure to 0.28-0.30 barg. It will be shown later (in the paper) this is a major limitation on cargo flash and hence BLEVE potential
- this requires further investigation if it transpires that the safety valves are unable to accommodate the anticipated pressure rise.

### 3.1.11 Input to modelling work of other members of the working group

These papers did not provide any specific input to the work of the subgroup but were considered of possible use as input to the work of other members of the WG.

- Model of Large Pool Fires – J.A. Fay – MIT (Paper 8)
- Spread of Large LNG pools on the sea – J.A. Fay – MIT (Paper 10)

### 3.1.12 Large hydrocarbon fuel pool fires: physical characteristics and thermal emission variations with height – Document No. 9

- Variation of SEP depending on height

Statistics of Uncorrected NAR Data Apparent Surface Emissive Power (kW/m <sup>2</sup> )		
Data from	Mean	Std. Dev
Top of Fire	44.8	44.0
Mid Height of Fire	105.0	35.9
Bottom of Fire	230.2	10.2

- It was considered that further work might be required to ascertain the height of the flame, as clearly SEP impingement on the tank cover depends on height
- it was concluded that it might be necessary to commission work to further examine this.

### 3.1.13 Large hydrocarbon fuel pool fires: physical characteristics and thermal emission variations with height – Document No. 11

- Importance of pool size on SEP

Comparison of model predicted<sup>a</sup> SEP with experimental date

Fire Diameter (m)	Surface on which LNG Boils	Froude Number (Fc) (×10 <sup>-3</sup> )	Soot Mass Yield (y) <sup>b</sup> (%)	Soot Concentration (C <sub>i</sub> )(kg/m <sup>3</sup> )(×10 <sup>-4</sup> )	Fraction at Length of the 'Clean Burning Zone' (Ψ)	Soot Transmissivity (τ <sub>i</sub> ) (×10 <sup>-2</sup> )	Mean SEP Over the Visible Fire Plume Height (E <sub>max</sub> )		Remarks
							Current Model Tests Result (kW/m <sup>2</sup> )	From Field (kW/m <sup>2</sup> )	
15	Water	9.606	12.7	3.328	0.196	66.4	172	185–224	Raj, et al [8]. China Lake tests
20	Land	8.319	13.0	3.419	0.180	57.12	183	140–180	Mizner and Eyre [16]
35	Land	6.288	13.7	3.595	0.150	35.7	177	175±30	Malvos and Raj [14], Montoir tests
100	Land	3.720	14.9	3.926	0.093	4.0	113	–	Potential size of future pool fire tests
300	Water	2.148	16.2	4.272	0.033	0.0028	90	–	Estimated pool size due to 1/2 tank content spill (12,500 m <sup>3</sup> LNG) from an LNG ship

<sup>a</sup> Assured parameter values  $r = 17.17$  for CH<sub>4</sub>;  $\beta = 0.06$ ;  $k_m = 130$  m<sup>2</sup>/kg;  $E_{max} = 325$  kW/m<sup>2</sup>;  $T_a = 293$  K

<sup>b</sup> Notarianni et al. [17] correlation for smoke yield.

<sup>c</sup> Assumed optical depth at bottom of LNG fire = 13.8 m.

### 3.1.14 LNG properties & hazards – understanding LNG rapid phase transitions (RPT) – Document No. 12

- Rapid phase transitions are more likely to occur in LNG mixtures containing very high fractions of ethane and propane. LNG composition is a critical parameter
- the hazard potential of rapid phase transitions can be severe, but is highly localised within the spill area.

### 3.1.15 LNG pool fire simulations – Document No. 14

- The author had assumed that pressure valve settings were increased from 0.25 MARVS when at sea to 3 Bar
- the author had not accounted for the presence of inert gas surrounding the tank
- the author was not aware that pressure could be reduced by using gas boil-off in the propulsion and or steam dumping
- the author had not looked at the options for forced vaporising to reduce pressure
- the author was apparently not aware that Moss Tanks were design for emergency discharge under pressure
- no account of the heat reducing effect of water deluge systems, required by the IGC Code, had been accounted for

- the author had assumed that rate of the evaporation would be similar to the limited spill simulation Montoir Pool tests, where a small amount of LNG (pool) was ignited in a pit in the ground. We concluded that the heat influx would be less and so evaporation rate lower. However, in their calculation no consideration was given to the dispelling of oxygen due to a 600:1 ratio expansion and their modelling was of a fully mixed oxygen – methane cloud along one side of a vessel
- the author had assumed that a similar scenario to that of a Spanish LNG road tanker, that spilt LNG which then ignited. The tank was heated to the point of rupture and resulted in a BLEVE.

### 3.1.16 LNG decisions making approaches compared – Document No. 13

**Table 3.6: Proposed Baseline Cases for Models Used in LNG Marine Assessments**

<p>Validation scale: Use Burro 3,7,8,9, Coyote 5,6 and Maplin Sands 27, 29, 34, 35. Run models for dispersion only.</p> <p>Large Scale: Use an amalgam of current cases reported by many current LNG workers. Run these models for dispersion and pool fire results.</p> <ol style="list-style-type: none"> <li>Puncture case – leading to near instantaneous release of 500 m<sup>3</sup> LNG.</li> <li>Maximum credible event case (accidental release) – 750 mm hole above waterline releasing all the cargo that can flow from the single largest tank.</li> <li>Maximum credible event case (terrorism) – 1500 mm hole above waterline releasing all the cargo that can flow from the single largest tank.</li> <li>Maximum credible event case (jettison) – 10,000 m<sup>3</sup>/hr for 60 minutes.</li> <li>Worst case event (single tank) – 5000 mm hole above waterline releasing all the cargo that can flow from the single largest tank.</li> </ol> <p>Material – Pure liquid methane  Weather – Cases should be run for D 5 m/s and F 2 m/s  Surface roughness – Use 0.3 mm and 10 mm  Relative Humidity – 70%  Temperature – 20°C air and water  LFL – Base an latest data from AIChE DIPPR = 4.4% vol</p> <p>Outcomes:</p> <p>Source term – discharge rate duration and total amount, pool diameter and thickness (maximum and event average), boil-off rate (maximum and event average).</p> <p>Dispersion – distance to LFL.</p> <p>Fire – sustainable pool diameter for pool fire (maximum and event average), duration, and distance to thermal radiation predicted of 5 kW/m<sup>2</sup>.</p>
---

- ABS 2004a and Pitblado et al 2004 list example areas of LNG uncertainties that will probably require large scale experimental trials to resolve
- these will need to involve both the LNG vessel itself, its response to mechanical damages and to the physical consequences of large LNG spills onto water.

### 3.1.17 Thermal response of gas carriers to hydrocarbon fires – Document No. 15

- The principal contribution of this report was considered to be as a verification control
- it closely follows some of the work objectives of the WG and, as such, may be compared against work carried out at the behest of the WG
- an unknown mentioned previously is the effect of SEP based on height and location to any fire. This is proposed in the paper as:

## In Summarising the Results of Diagrams 1–9, We have for Condition with no Wind:

Surface	Flux in kW/m <sup>2</sup>		
	Location on Deck		
	Fire Side	Middle	Side Opposite Fire
Horizontal at deck level	150	40–150	16–150
Vertical at deck level	300	60–150	30–150
Horizontal at dome level	35–150		
Vertical at dome level	120–200		

### 3.1.18 Maplin sands experiments 1980 – dispersion results from continuous releases of refrigerated liquid propane & LNG – Document No. 18

- Measurements in this paper were taken from sensors mounted at a range of heights
- wind speed and direction was identified in being critical as this affects the flame shape, direction, heat transfer, exposure of any adjacent structure etc
- “Further analysis of the heat and water content of the plumes is necessary before heat transfer relations may be applied with confidence”.

### 3.1.19 Maplin sands experiments 1980 – dispersion & combustion behaviour of gas clouds resulting from large spillages of LNG & LPG on the sea – Document No. 19

- A maximum scaled volume of 25,000 m<sup>3</sup> was considered to be covered by tests using 20 m<sup>3</sup>
- “The two most prominent features of the dense gas spill are the gravity spreading of the gas (“Slumping”) and the inhibition of vertical mixing by the density gradients formed (“stratification”)
- Table 3.7 – Combustion Trials at Maplin.

**Table 3.7: Combustion Trials at Maplin**

Trial Number	Material and Spill Type	Volume (m <sup>3</sup> /min or m <sup>3</sup> )	Wind Speed* (m/s)	Comments
17	LNG Continuous	2.8	8	Flame failed
27	LNG Continuous	3.7	6	Cloud fire
38	LNG Continuous	5.8	5	Cloud fire
39	LNG Continuous	4.7	4	Cloud and pool fire
22	LNG Instantaneous	12	5	Cloud fire
23	LNG Instantaneous	8.5	5	Flame failed
24	LNG Instantaneous	12	5	Cloud fire
49	Propane Continuous	2.1	6	Cloud fire
50	Propane Continuous	4.3	7	Cloud and pool fire
51	Propane Continuous	5.6	7	Cloud and pool fire
68	Propane Instantaneous	5–10	6	Cloud fire

\*Wind speeds given are those relevant during the combustion studies.

**Table 3.8: Surface Emissive Powers**

Material	Surface Emissive Power (kW/m <sup>2</sup> )	
	Cloud Fire	Pool Fire
LNG	173 ± 26	203 ± 31
Refrigerated liquid propane	173 ± 20	43 ± 9

## 3.2 Results

### 3.2.1 Results of documentation review

The figures below should be considered as representative ballpark figures that were derived based on a summation of the overall review of available documentation.

There are undoubtedly contradictory values appearing in the work submitted for review, however those below were felt to provide a representation of the values proposed in the different works.

- Heat Flux
  - worst case direct flame impingement – 325 kW/m<sup>2</sup> (at source of flame hottest part)
  - this value is maximum at base of flame & reduces with height
  - applies to pool fire (not cloud fire)
- pool fire sizing v SEP

	Diameter	kW/m <sup>2</sup>
Small Pool Fire 	35 m 	220 
Large Pool Fire	300 m	90

- fire duration
  - release of 12,500 m<sup>3</sup> = 8.1 minutes
  - for 330 m (cloud fire) pool diameter ≈ 90 kW/m<sup>2</sup>
- fire height
  - not currently possible to define – not addressed by work to date
  - pool size 35→300 m diameter  
(Note: 35 m is considered to be unrealistically low due to probable structural failure)
- impingement
  - pool fire - worst case - side }  
• flame impingement }
- deck
  - cloud fire - 170 kW/m<sup>2</sup>
- gives a lower flame height
- cloud is advised to be max 10 m in height
  - BLEVE - Depends on a number of factors
- further consideration of this should be undertaken after modelling.

### 3.2.2 Summary

The result of the document review was that considerable uncertainty exists over the height of any LNG fire resulting from an accidental or deliberate release on water.

The height of the fire has a direct impact on the fire impingement and heat flux to which an LNG carrier would be subjected. The conclusion is that further definition of the flame height may only be achieved with appropriate modelling, for which the group would be in a position to provide a range of values for the different inputs required. It is only from such work or, alternatively, from full scale tests of larger LNG pool fires on water, that the consequential heat fluxes could then be derived.

The latter full scale tests would also perhaps confirm the shift in opinions over Surface Emissive Power, where current expert opinion is now in favour of incomplete combustion in an LNG pool fire on water, reducing the SEP as the size of any pool fire grows.

Further work by the subgroup is, therefore, pending completion of both modelling of an LNG pool fire on water (CFD and/or solid flame) for a range of values, and output from full scale testing of a large LNG pool fire on water. The latter is considered not to be the remit of this group but nonetheless is an important input for a conclusive output to the work of the WG.



# **LNG CARRIER PRESSURE RELIEF SYSTEMS**



## 4.1 Functional Requirements

LNG carrier cargo tanks shall be protected against harmful over-pressure and under pressure as follows:

### 4.1.1 Cargo tanks to have an emergency over-pressure system which shall

- Be independent of the vapour pressure control system
- shall be automatically activated and not dependent on the vessel's power supply for its operation
- provide for controlled venting, thus not relieve more of the cargo than necessary for limiting pressure rise
- in case of tanks with more than 20 m<sup>3</sup> volume, tolerate at least one valve failure without more than 50% loss of PRV capacity
- PRV valves should be so arranged that disabling of their function should not be readily possible
- PRV valves shall be constructed of materials suitable for the temperatures occurring
- the valves shall be so located that their function will not be disabled by ingress of liquid cargo with a ship's list of 15 deg and a trim of 0,015L or due to liquid expansion when heated
- the combined relieving capacity of the relief valves for each cargo tank shall be capable of discharging vapour at the rate required by the applied rules with not more than a 20% rise in cargo tank pressure above the relief valve set pressure.

### 4.1.2 Cargo tanks to have an emergency under-pressure system which shall

- Be automatically activated and not dependent on the vessel's power supply for its operation
- be independent of the vapour pressure control system.

### 4.1.3 Cargo tanks to have a pressure control system

- Cargo tanks to have a pressure control system keeping the vapour pressure within acceptable limits without venting cargo to the atmosphere during normal operation
- cargo tanks having a design pressure at least equal to the saturated vapour pressure of the cargo at maximum ambient temperature (45 Deg C) or, in case of ships intended for short voyages where pressure rise will not exceed the design pressure, a pressure control system need not be fitted.

## 4.2 Design Requirements

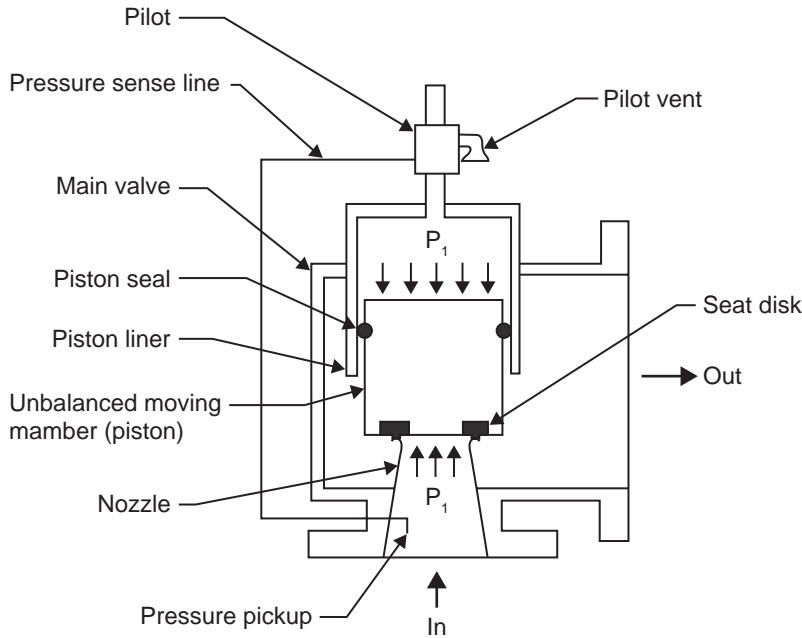
### 4.2.1 Pressure Relief Valve (PRV) function

In general, two types of PRVs exist. The oldest and most commonly used is the direct acting type. They are designed as direct acting because the force element keeping the valve closed is a weight or a spring or a combination of both. The other type of PRV is the pilot operated type. The primary difference between a pilot and direct acting type is that in the pilot type the process pressure is used to keep the valve closed instead of a weight or spring. PRVs on cargo tanks and hold spaces on LNG carriers are of the pilot operated type. Therefore, further explanations will focus on the pilot type only.

A pilot operated PRV consists of a main valve and a pilot. The basic principle is that the pilot controls the pressure on the top side of the unbalanced moving member (see fig 1). A seat is attached to the opposite side of the member.

- At pressures below set point, the pressure on the opposite sides of the moving member is equal
- when set pressure is reached, the pilot opens, depressurising the cavity on the top side and the unbalanced moving member strokes upward causing the main valve to relieve
- when the process pressure decreases, the pilot closes, the cavity on the top is re-pressurised, and the main valve closes.

**Figure 4.1: Basic Principles of a Pilot Operated PRV**



## 4.2.2 Pilot design

The design of the pilot for a pilot operated valve must be self actuated, ie it must be actuated by the process pressure. It must also be fail-safe in the open mode.

The most common type of pilot design is the no-flow, 'pop' action type (see fig 4.2a & 4.2b). A no-flow pilot is one designed to have no flow of the process gas when the main valve is open and relieving. A 'pop' action is one where the main valve rapidly opens at a set pressure to full lift and re-closes at some pressure below set point. The difference between opening pressure and reseal pressure is called blow down and is usually expressed as a percentage. For a set pressure of less than 100 mbar the blow down is to be 10-15% and over 100 mbar the blowdown is to be 3-7% (in accordance with SIGTTO 2.2 d).

The second most common type of pilot design is the no-flow 'modulating' action type (see fig 4.3a 4.3b & 4.3c). This pilot type produces a main valve opening characteristic that is proportional to the relieving capacity required to maintain a given pressure. In this sense, its performance is similar to a back pressure regulator. The pressure at which it opens and closes is approximately the same.

**Figure 4.2a: No-flow Pop Action Pilot, Dome Supply Position**

**Figure 4.2b: No-flow Pop Action Pilot, Dome Exhaust Position**

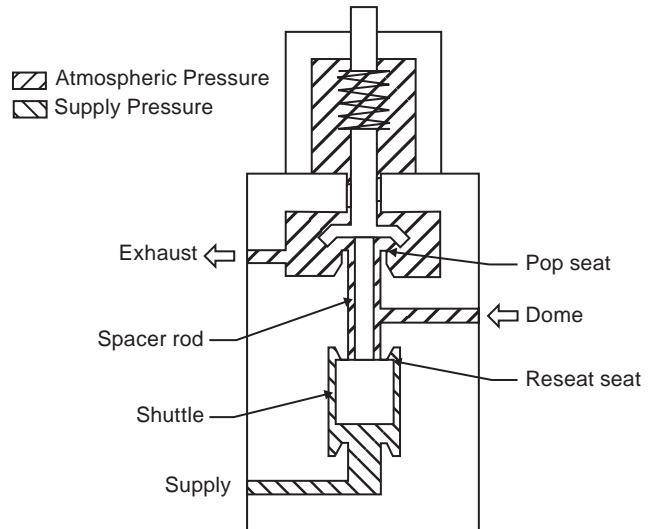
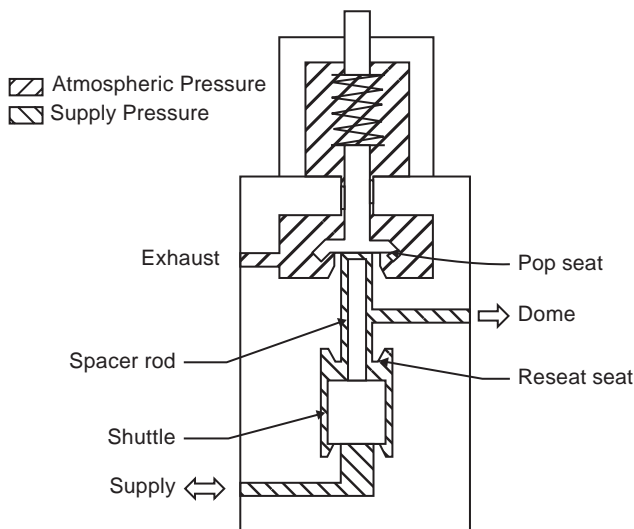


**Figure 4.3a: No-flow Modulation Action Pilot, Dome Supply Position.**

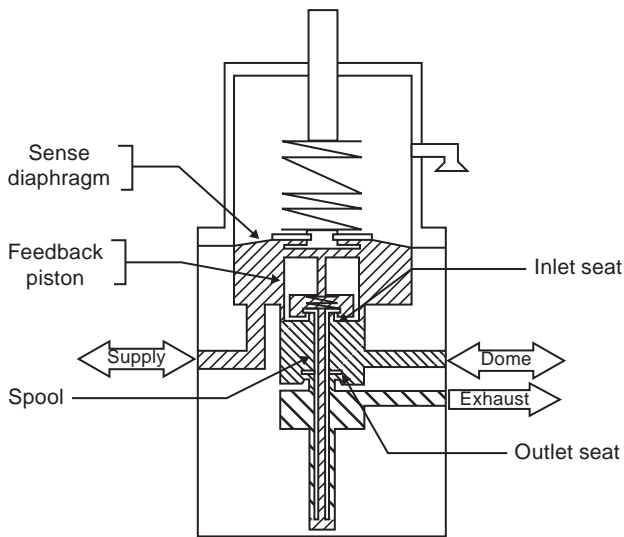


**Figure 4.3b: No-flow Modulation Action Pilot, Dome Vent Position.**

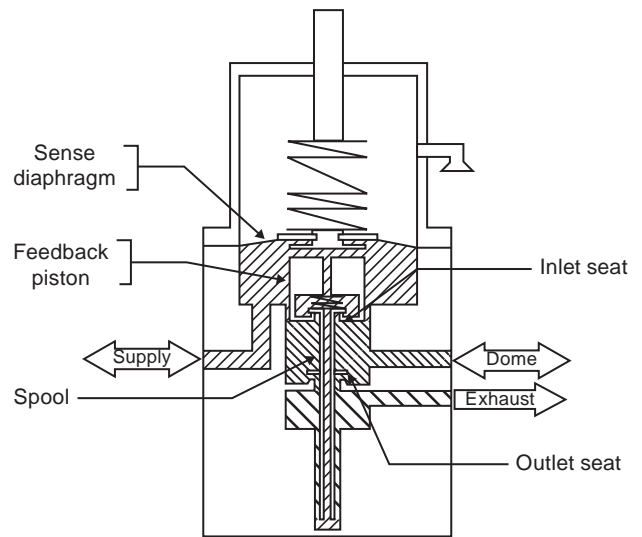
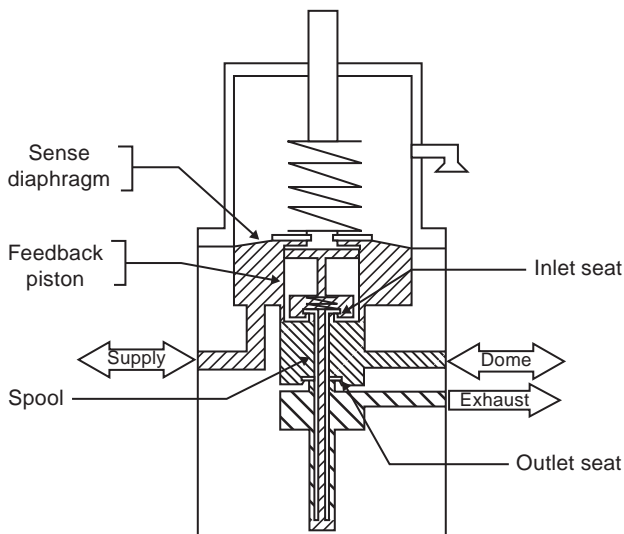


**Figure 4.3c: No-flow Modulation Action Pilot, Null Position.**



## 4.2 Pressure Settings

Typical pressure set points for a Moss type carrier PRVs would be:

High pressure alarm in tank:	220 mbarg
Opening of relief valve in tank:	250 mbarg
Low pressure alarm in tank:	10 mbarg*
High pressure alarm in hold:	120 mbarg
Opening of relief valve in hold:	150 mbarg
Low pressure alarm in hold:	-20 mbarg
Opening of relief valve in hold:	-50 mbarg

\*An automatic trip system for the gas compressors, the cargo and spray pumps, IGG, ESD valves and the spray inlet valves are activated when the pressure of any cargo tanks are equal to the atmosphere pressure.

A high differential pressure alarm is activated when hold space pressure exceeds the cargo tank's pressure by 30 mbarg. An automatic trip system for the gas compressors, the cargo and spray pumps dedicated to the tank in question, IGG, ESD valves and the spray inlet valves is activated at 40 mbarg of excess pressure in the hold space. In addition, a differential

pressure relief valve (for each hold) releases air in the hold space to the atmosphere at 50 mbarg of excess pressure in the hold space.

The cargo tanks PRV would also have possibilities for higher settings as well. The higher settings would be used in case of emergency pressure discharging of the tank.

For a typical Membrane type vessel, being Mk III, NO 96 or CS1, the corresponding MARVS (Maximum Allowable Relief Valve Setting) would be:

Opening of relief valve in tank:	250 mbarg
Opening of relief valve in tank:	-10 mbarg
Opening of relief valve in IBS*	300 mbarg (Mk III membrane system)
Opening of relief valve in IS**	350 mbarg (Mk III)
Opening of relief valve in IBS	120 mbarg (CS1 membrane system)
Opening of relief valve in IS	120 mbarg (CS1)
Opening of relief valve in IBS	100 mbarg (NO96 membrane system)
Opening of relief valve in IS	100 mbarg (NO96)

\*Inter Barrier Space

\*\*Insulation Space

As the membrane type insulation spaces are purged with nitrogen and are pressure controlled, the vessels are not equipped with any differential or low pressure relief valves in the insulation spaces.

**SIMPLIFIED REAPPLICATION OF THE CODE FOR  
LOSS OF INSULATION**



## 5.1 Study 1

### 5.1.1 IGC code Pressure Relief Valve (PRV) sizing

To comply with the requirements outlined in the International Code for the Construction and Equipment of Ships Carrying Liquefied Gases in Bulk (IGC Code), each cargo tank used for the carriage of LNG must be outfitted with a pressure relieving system providing protection from over-pressure scenarios.

Each tank shall be outfitted with pressure relieving valves, with a combined total capacity sufficient to ensure that the cargo tank vapour pressure does not increase more than 20% above the maximum allowable relief valve setting under fire conditions.

Typically, the relief valve setting pressure on LNG carriers is set at 250 mbar (gauge). Therefore, a 20% increase above this set pressure would result in a maximum allowable tank operating pressure of 300 mbar.

The procedure and formulae used when determining the correct capacity and size of the pressure relief valve(s) is stipulated in Chapter 8.5 of the IGC code. The output of the formula, equates to the amount of free air volume requiring release when the containment system is exposed to fire conditions.

The IGC code sizing formula is based on;

$$Q = FGA^{0.82}(\text{m}^3/\text{s})$$

Q = Equivalent air flow of free air, at 273 Kelvin, 1.013 bar absolute (Nm<sup>3</sup>/hr)

G = Gas factor

A = External surface area (m<sup>2</sup>)

F = Fire factor (as per definitions below)

1.0 = Tanks without insulation located on deck.

0.5 = Tanks above deck with insulation.

0.5 = Uninsulated independent tanks installed in holds.

0.2 = Insulated tanks in holds. **(Moss Rosenberg)**

0.1 = Insulated independent tanks in inerted holds.

0.1 = For membrane or semi membrane tanks. **(GTT Membrane)**

*Actual data from a sample 140,000 m<sup>3</sup> Moss Rosenberg LNG Carrier has been used to assist with generating realistic outputs from the formulas within this document. The design base is five spherical cargo tanks, externally insulated to restrict heat ingress, independently housed within a sealed hold space containing inert gas. The maximum liquid loading capacity would be 99.5% of the total volume, thereafter reducing by 0.15% per day of cargo carriage.*

### 5.1.2 Moss Rosenberg LNGC relief valve sizing considering pure methane conditions

A = external surface area.

$$A = 4\pi R^2$$

The surface area of a sphere can be equated from

Typical internal diameter of Moss Rosenberg cargo tank = 36 metres

Total wetted surface area (100%) = 4072.032 m<sup>2</sup>

This total calculated surface area is further reduced according to the amount of heat that is absorbed during exposure to fire conditions. Based on research conducted while developing and updating, among other standards, API 2000 recommended practices, compound curves relating to the amount of specific heat flow against external surface area where produced. This early research was used when producing the IGC code.

From these curves, the exponent of 0.82 is applied to the calculated total external surface area in an attempt to closely represent the actual exposure conditions experienced in fire engulfing scenarios.

Additionally, the vessel's hull further protects the lower hemisphere of the cargo tanks for the heat produced during fire scenarios and a steel weather cover gives protection to the upper hemisphere. The weather cover is additionally protected

# Simplified Reapplication of the Code for Loss of Insulation

by a salt-water deluge system that drenches the external surface area with a film of water, restricting the amount of radiant heat absorbed. The lower hemisphere is protected by the presence of the surrounding seawater up to the vessel's draft level, the vessel's side ballast tanks and the supporting skirt arrangement of each individual cargo tank.

Unlike non-refrigerated tanks, where a maximum amount of specific heat influx can be achieved and vapour generation stabilized, refrigerated tanks usually contain liquids close to their boiling point. As the cargo is at boiling point, any heat influx will continue to produce significant quantities of generated vapour until either the cargo tank becomes empty of liquid or the fire is extinguished.

From the above, the surface area exposed to fire conditions can be taken as:

$$A = 4072.032^{0.82} = 912.1 \text{ m}^2$$

**F** = Fire factor

Fire factors give allowance for the inherent protection offered by the vessel's structure and protection of the cargo tanks internal wetted surface areas from exposure to fire conditions. In this case, Moss Rosenberg type vessels can use the multiplier of 0.2 as their cargo tanks are carried in independents hold spaces and the exterior to the cargo tanks' surfaces are insulated to reduce heat gain into the stored cryogenic liquid.

It can be further debated whether this value should be reduced to 0.1 as the air space within the cargo tank hold (between outside of insulation material and inside of weather cover) is maintained in an inerted condition with nitrogen gas when the vessel is in active service.

In accordance with IGC Code for independent tanks partly protruding through the open deck, the fire exposure factor should be determined on the basis of the surface areas above and below the deck. In the case of a Moss type independent tank, the dome protrudes through the tank cover. This portion of the tank is protected by fire proofing insulation approved by the administration, so for this portion of the tank the correct fire exposure factor is 0.5. Accordingly, the overall fire exposure for the tank must be calculated as follows:

$$F_{\text{tank}} = 0.5 \times A_1 / (A_1 + A_2) + 0.2 \times A_2 / (A_1 + A_2)$$

Where  $A_1$  is the area of the dome and  $A_2$  is the tank area minus the dome area

However, it should be noted that  $A_1$  is less than 1% of  $A_2$ , so for the purpose of this study, the fire factor

**F** has been taken as: **0.2**

**G** = Gas factor

The Gas factor is calculated using a supporting formula within the IGC Code sizing section 8.5. This formula takes into account the physical characteristics of the vapour being released at actual relieving conditions. Also included within this formula is the specific heat flux that will be applied to the exposed surface area.

The IGC Code has adopted the empirical data used by both the American Petroleum Institute (API) and the Compressed Gas Association (CGA) with regards to maximum radiant heat generated when exposed to pool fires. The maximum specific heat flux value has been taken as 71 kW/m<sup>2</sup> when developing the below formula, this being the average value over exposure time over the entire tank area, rather than the peak value at a single location.

$$(1) \quad G = \frac{12.4}{LD} \sqrt{\frac{ZT}{M}}$$

As it is standard engineering practice to size pressure relief valves on worst case relieving conditions, pure methane has been used to represent the liquid being carried. However, actual operational conditions would involve carriage of a liquid with less vapour generating characteristics.

Pure Methane	L	D	Z	T	M	k	G
1.3 bar, -158.4 C	507	0.680	0.960	114.6	16.04	<b>1.372</b>	0.094

L = Latent heat of material being vaporised, (kJ/kg)

T = Temperature at relieving conditions, (Kelvin)

D = Constant based on specific heat ratio (k)

Z = Compressibility factor of gas being relieved

M = Molecular mass (kg/kmol)

G = 0.094

### 5.1.3 IGC code PRV required capacity

As per the IGC Code, pressure relief size when considering 'pure methane'

$$Q = 0.2 \times 0.094 \times 912.1$$

Total Air Equivalent Relief Capacity required = 17.15 Nm<sup>3</sup>/sec (79,922 kg/hr)

(Density of air at relieving conditions 1.293 kg/m<sup>3</sup>)

The pressure relieving system must provide adequate capacity to relieve the above calculated value and take into account the physical layout of the discharge piping systems and any back pressure, superimposed or build up, which may affect the relieving capacity of the pressure relief valves.

It has become standard practice on LNG carriers to install pilot-operated, pressure relief valves for this duty, which sense the internal tank pressure and are less affected by 'superimposed' back-pressure, and its associated effects of valve lift and chatter, than conventional spring types. Superimposed back pressure is the pressure on the outlet side of the valve before operation.

However, 'build up' back-pressure resulting from friction or sonic flow, is applicable and must be considered and accounted for.

### 5.1.4 Physical sizing of pilot-operated, Pressure Relief Valves (PRV)

Using the sizing formula from a typical PRV manufacture (Fukui Seisakusho Co.), that is based on formulas and guidance taken from applicable API standards, it is possible to calculate the mass flow of free air at the relieving condition stipulated by the IGC Code, ie air at STP.

Additionally, the IGC value represents the combined total capacity of the installed pressure relief system on each cargo tank and gives allowance for the capacity to be covered by two PRV valves sized to 50% of this total capacity.

$$Q = 548 K A P_1 \sqrt{\left\{ \left( \frac{k}{k-1} \right) \left( \frac{P_2^{\frac{2}{k}}}{P_1} - \frac{P_2^{\frac{k+1}{k}}}{P_1} \right) \left( \frac{M}{ZT} \right) \right\}}$$

Q = Relieving capacity (kg/hr)

A = Orifice area of PRV (cm<sup>2</sup>) (inlet orifice 759.644 cm<sup>2</sup>)

K = Coefficient of discharge (manufacturer supplied data)

P<sub>1</sub> = Relieving set point pressure (P<sub>atm</sub> + (P<sub>set</sub>+20%)) (bar a)

P<sub>2</sub> = Back pressure (bar a) (Limited to 50% of set pressure)

k = Ratio of specific heat

T = Flowing (relieving) temperature (Kelvin)

M = Molecular Weight (kg/kmol)

Z = Compressibility Factor

P<sub>set</sub> = Set Pressure (barg)

P<sub>acc</sub>' = Accumulation pressure allowance = P<sub>set</sub> + 20%

B = Ratio of P<sub>2</sub>/P<sub>1</sub>

Air density at relieving conditions (1.293 kg/m<sup>3</sup>)

# Simplified Reapplication of the Code for Loss of Insulation

The below tabulated figures form the basis of the IGC code PRV relief requirement.

Vapour	B	K	P <sub>1</sub>	P <sub>2</sub>	P <sub>atm</sub>	P <sub>set</sub>	Z	T	M	k
Air @ STP	0.8858	0.7869	1.313	1.138	1.013	0.250	1.0	273	29	1.4

When sizing PRV valves the effects of back pressure on capacity should be assessed. Back pressure is the summation of both 'superimposed' and 'build up' back pressures caused by the discharge header conditions of length and pressure.

Superimposed back pressure is the pressure present downstream of the PRV before operation. The PRV valves used on LNG vessels are of the pilot operated type, which are less affected by any downstream pressure as their activation is independent of the valve's outlet pressure.

Build up back pressure is a summation of frictional, sonic and turbulent flows in the PRV discharge piping system. Following guidance in IMO standards, it is advised that the build up back pressure in the downstream piping should not rise above 50% of the PRV setting pressure. Therefore, for LNG service using 0.250 bar as the set pressure, 50% would give 0.125 bar + atmospheric pressure of 1.013 bar would give a maximum build up pressure of 1.138 bar a.

Using the manufacturer's sizing equation, the above values and the maximum allowable back pressure of 1.138 bar, the mass flow rate per valve equals

Q = 47,500 kg/hr (for a 300 mm inlet and 400 mm outlet PRV)

The installation of two 300 mm inlet PRV on the 36 metre diameter spherical cargo tank would provide the required over-pressure protection as stipulated by the IGC code during exposure to fire conditions at worst case back pressure levels when considering a set pressure of 0.25 bar.

Required Q<sub>IGC</sub> = 79,922 kg/hr, available Q<sub>PRV</sub> = (2 × 47,500) = 95,000 kg/hr

## 5.1.5 Choked flow

A further check is needed to ensure this mass flow remains below the choked flow of the outlet system. For a single phase flow choking occurs where the velocity of the gas is equal to the sonic velocity. The flow rate is absolutely independent of the discharge pressure provided this pressure remains below the choked pressure.

To calculate the choked flow the following critical flow formula can be applied,

$$P_{Critical} = P_1 \left( \frac{2}{k+1} \right)^{\frac{k}{k-1}}$$

P<sub>1</sub> = Inlet or upstream pressure, in this case 0.250 bar + 20% accumulation allowance + atmospheric pressure = 1.313 bar a

k = Isentropic exponents at valve inlet, for air at STP conditions, k = 1.400

From the standard formula for critical pressure, the critical pressure value would be 0.694 bar, corresponding to an inlet pressure of 1.313 bar and specific heat ratio of 1.4.

Therefore P<sub>1</sub> can only be 1.89 times (1.313/0.694 = 1.89) greater than the pressure in the discharge header. If P<sub>1</sub> is more than 1.89, critical flow would occur.

It is important to note that, although the gas velocity reaches a maximum and becomes choked, the mass flow rate is not choked. The mass flow rate can still be increased if the upstream source pressure (P<sub>1</sub>) is increased.

## 5.1.6 Extrapolating fire conditions against PRV valve sizing

The IGC Code PRV sizing formula allows reductions in the anticipated fire exposure due to differing levels of protection offered by varying design of cargo containment systems and the type of cargo tank involved.

The previous calculations were based on a fire factor of 0.2, this representing an insulated cargo tank installed within a hold space exposed to the radiant heat of an adjacent fire.

To assess the amount of additional vapour generated if the external cargo tank insulation was lost or became degraded, the fire factor can be increased to 0.5 to represent this scenario. However, it must be noted that it is extremely unlikely that

# Simplified Reapplication of the Code for Loss of Insulation

total loss of the cargo tank insulation would occur as the damage would be restricted to a relatively small area due to the protection of the hull steelwork, ballast and hold spaces, particularly at the lower portions of the cargo tank.

Therefore, using a fire factor of 0.5 for the entire surface area of the cargo tank must be considered as an absolute extreme case.

Using the original IGC sizing formula to predict the increase in capacity required

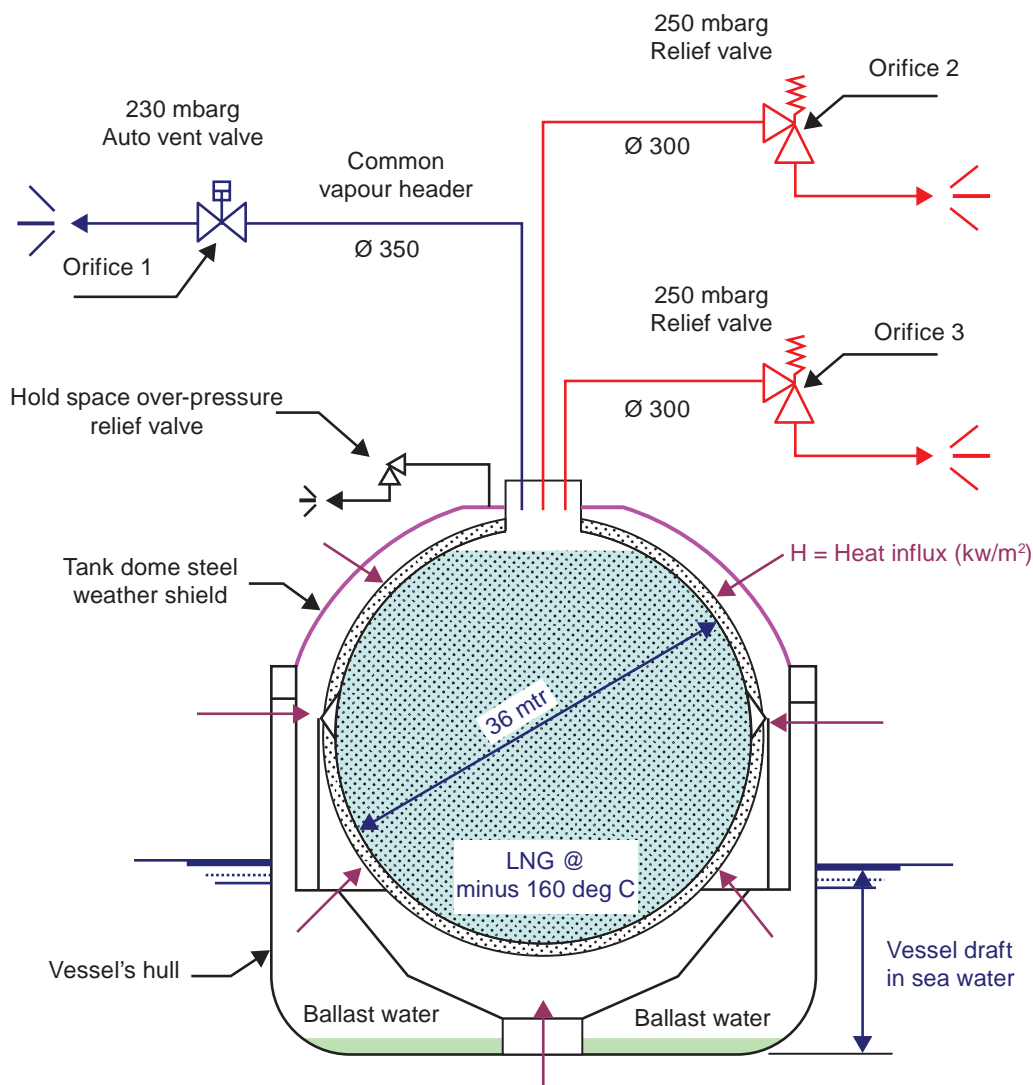
$$Q = 0.5 \times 0.094 \times 912.1$$

$$\text{New capacity} = 42.87 \text{ Nm}^3/\text{s} \text{ (199,550 kg/hr)}$$

## 5.1.7 Total relieving capacity of cargo containment system

From figure 5.1 it can be seen that three over pressure relieving options are available and applicable on Moss Rosenberg type LNG Carriers.

**Figure 5.1: Cross Sectional View of Spherical, Moss Rosenberg Cargo Tank**



Therefore, the overall relieving capacity of a single tank is dictated by the maximum release capacity of the tank pressure control valve (orifice area 1) situated in the common vapour header and the combined capacity of the two pressure relieving valves (orifice area 1 and 2).

The capacity of each of the 300 mm or 12" diameter pressure relief valves, when operating at the maximum allowable tank pressure of 300 mbar g (P set +20% accu') and maximum allowable back pressure of 1.138 bar has been calculated as being 47,500 kg/hr per valve. (Orifice 2 & 3).

# Simplified Reapplication of the Code for Loss of Insulation

The relieving capacity of the attached 350 mm or 14" diameter common vapour header (Orifice area 1) can be calculated using the same manufacturer's sizing formula with  $P_1$  of 1.313 bar and  $P_2$  of 1.138 bar. This outlet allows for a further discharge rate of 60,200 kg/hr.

	PRV Size	Orifice Area	Flow Capacity
Orifice 1 (Vapour header pressure control)	350 mm 14"	962.11 cm <sup>2</sup>	60,200 kg/hr
Orifice 2 (No 1 Relief Valve)	300 mm 12"	759.64 cm <sup>2</sup>	47,500 kg/hr
Orifice 3 (No 2 Relief Valve)	300 mm 12"	759.64 cm <sup>2</sup>	47,500 kg/hr
	Totals	2481.39 cm <sup>2</sup>	155,200 kg/hr

When considering a single 36 m diameter Moss Rosenberg cargo tank layout, the total relieving capacity available while remaining within the MAWP stipulated by the IGC Code would equate to:

$$47,500 + 47,500 + 60,200 = 155,200 \text{ kg/hr}$$

This available capacity is almost double the requirement stipulated by the IGC Code under exposure to fire conditions represented by a 0.2 fire factor, which required a release capacity of 79,922 kg/hr.

However, when using an extreme fire factor of 0.5 the required release capacity of 199,550 kg/hr is needed, this being in excess of the capacity available at the maximum allowable working pressures stipulated by the IGC code.

To achieve the required capacity, the inlet pressure to the PRV valves needs to increase, which in turn gives a higher back pressure allowance and a greater relief capacity.

The following cases represent the increase in cargo tank pressure required to achieve the increased capacity imposed by using a fire factor of 0.5.

Vapour	B	K	$P_1$	$P_2$	$P_{atm}$	$P_{set}$	Z	T	M	k
Air @ STP	0.8304	0.7869	1.533	1.273	1.013	0.520	1.0	273	29	1.4

**Case 1** – tank pressure increased to 1.533 bar absolute (0.520 barg)

Vapour header outlet (orifice area 1)	=	77,450 kg/hr
PRV 1 (Orifice area 2)	=	61,150 kg/hr
PRV 2 (Orifice area 3)	=	61,150 kg/hr
Total		199,750 kg/hr

$MAWP_{IGC} = 300 \text{ mbar}$ , above condition requires 220 mbar additional tank pressure

Case 1 used all three relief possibilities, Case 2 assess the increase in tank pressure required to achieve sufficient capacity using the PRV valves only.

Vapour	B	K	$P_1$	$P_2$	$P_{atm}$	$P_{set}$	Z	T	M	k
Air @ STP	0.7342	0.7869	2.163	1.588	1.013	1.150	1.0	273	29	1.4

**Case 2** – tank pressure increased to 2.163 bar a (1.15 barg) (PRV valves only)

PRV 1 (Orifice area 2)	=	101,000 kg/hr
PRV 2 (Orifice area 3)	=	101,000 kg/hr
Total		202,000 kg/hr

$MAWP_{IGC} = 300 \text{ mbar}$ , above condition requires 850 mbar additional tank pressure

The cargo tank over pressures calculated above remains well within the maximum pressure capabilities of the cargo tank structure.

# Simplified Reapplication of the Code for Loss of Insulation

To ensure both of the above conditions do not cause choked flow to occur in the PRV discharge header system, the following equation can be used to determine if critical flow conditions exist. If the pressure ratio across the PRV is less than, or equal to, the ratio of the specific heat, critical flow will occur representing the maximum velocity of flow.

$$\frac{P_2}{P_1} \leq \left( \frac{2}{k+1} \right)^{\frac{k}{k-1}}$$

$$\frac{1.273}{1.533} \leq \left( \frac{2}{1.4+1} \right)^{\frac{1.4}{1.4-1}}$$

## Case 1

The calculated critical pressure ratio for case 1 equates as 0.830. As this figure is greater than the specific heat ratio of 0.528, choked or critical flow will not occur.

$$0.830 < 0.528$$

## Case 2

$$\frac{2.163}{1.588} \leq \left( \frac{2}{1.4+1} \right)^{\frac{1.4}{1.4-1}}$$

$$0.734 < 0.528$$

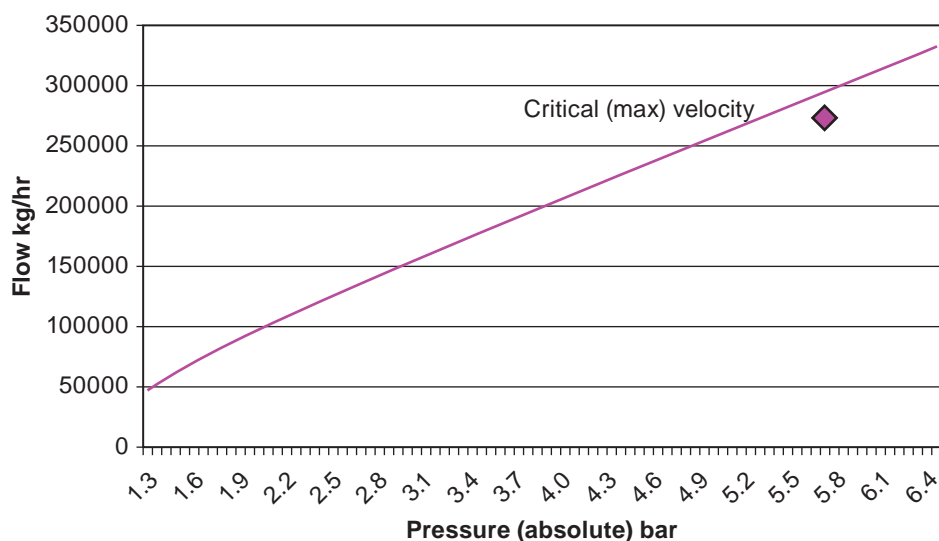
The calculated critical pressure ratio for case 2 equates as 0.734. As this figure is greater than the specific heat ratio of 0.528, choked or critical flow will not occur.

### 5.1.8 PRV capacity at maximum back pressure

The graphical representation below plots a theoretical increase in cargo tank pressure ( $P_1$ ) against the maximum allowable back pressure ( $P_2$ ) and records the calculated mass flow rate of a single PRV.

It can be seen from the chart that increasing the internal tank pressure to 2.163 bar, as required in case 2, is well within the relieving capacity of the valve.

Single 12" PRV peak flow at max back pressure (50% ser pressure)



To be noted is the inlet pressure required to reach choked flow, this representing a pressure in the region of 5.3 bar absolute (4.3 bar Gauge).

**Figure 5.2: Positioning of PRVs on Cargo Tank Dome**



### 5.1.9 Moss type LNG carrier – response to over-pressure conditions

With reference to Figure 5.3 – Cargo Piping Layout, it can be seen that all of the LNG cargo tanks are interconnected via a common vapour header. Each tank is individually connected to this common header via a manually operated, full-bore, butterfly valve, which remains in the fully open position while the vessel is in normal service conditions.

Having all cargo tank vapour spaces interconnected allows a common vapour pressure control strategy to be maintained throughout the cargo tanks, assisting with the vessel's standard operations and its ability to burn boiled off gas (BOG) in its main propulsion, dual fuel fired, steam generating boilers or diesel engines.

Any upset witnessed to the vessel's cargo tank vapour pressure becomes evident with a rise in vapour header pressure. The primary way of controlling any increases in tank pressure is via the vessel's inherent ability to burn the generated BOG in the main propulsion boilers. (Some LNG carriers have the ability to reliquify the BOG and return it back to the cargo tanks, this would be considered their primary BOG control system, with a back up provided by a gas combustion unit that safely burns excess BOG).

In low steam load conditions, the vessel's steam plant has the ability to artificially increase the steam demand, allowing excess BOG to be consumed, generating the maximum possible quantity of steam, then dumping this steam to a seawater cooled condenser where it is cooled back into a liquid state and returned to the feed system.

If in the unusual case that the vessel's boilers were unable to consume the generated BOG, the common vapour header pressure would continue to increase over an extended time period. This header pressure is continuously monitored by the vessel's safety systems and used as a set point for the tank pressure safety control valve, situated at the forward end of vapour header.

This automated control valve is set to fully open when the header pressure increases above 230 mbarg, and remains in this open position until the combined cargo tank pressure, and hence the vapour header pressure, has decreased to 210 mbarg.

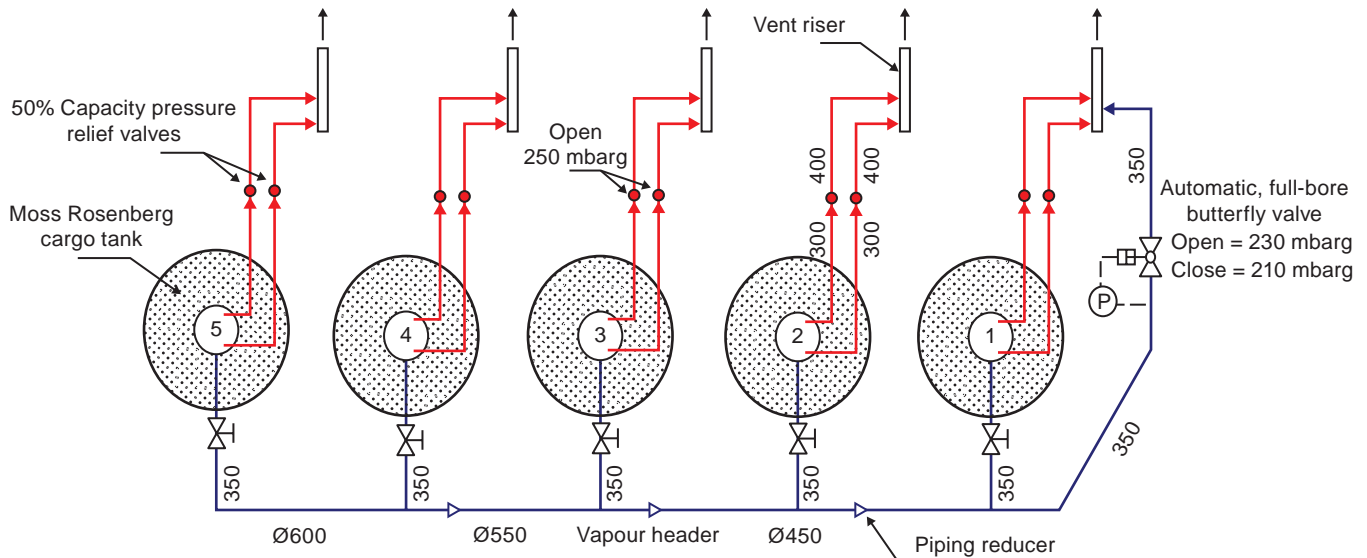
In the event of the cargo tank pressure continuing to rise, possibly due to the vessel being unable to burn the quantity of BOG being generated, the combined tank vapour pressure would continue to rise until the pressure relieving valves, as defined in the IGC code, became active. It is an extremely rare event if an LNG carrier's pressure relief valves are activated and it should not be considered as standard operational practice.

Depending on the scenario, the effected tank pressure would increase reaching a maximum allowable value of 250 mbarg, when the pilot operated relief valves would fully open, releasing the over pressure to atmosphere via a specifically designed, individual vent mast until the pressure has reduced to 230 mbarg, when the valve would reset.

# Simplified Reapplication of the Code for Loss of Insulation

It should be noted and considered that the cargo tanks remain physically interconnected via the common vapour header throughout all scenarios. Therefore, any scenario causing a rapidly increasing pressure would cause all, in this case ten, relief valves to open simultaneously, effecting an equally rapid reduction in pressure.

**Figure 5.3: Moss Rosenberg Cargo Piping Layout**



## 5.2 Study 2

### 5.2.1 Résumé

During discussion at working group meetings, the task ‘Simplified reapplication of the IGC Code formula for loss of insulation’ was requested to be considered. The requirements of the IGC Code have been applied with regard to the installation of a standard design relief valve of the size that would normally be fitted to a Moss design LNG gas carrier.

The results obtained have been to:

- Determine the maximum size of cargo tank that the relief valve can protect at the standard set pressure of 250 mbar, plus 20% rise, in accordance with Chapter 8 of the IGC Code
- determine the actual relief valve flow rate at the maximum size cargo tanks allowable over-pressure of 2 barg. Use this additional capacity to recalculate the fire exposure factor
- by utilising an actual Moss LNG gas carrier, fitted with the same design and size of relief valves, determine the capacity at the allowable over-pressure of 2 barg. Again, use this capacity to recalculate the fire exposure factor.

The common vapour header, which is in use during normal operation and so interconnects all cargo tanks, has been considered for both venting through the control valve into the forward vent mast and allowing equalization between tanks when one tank is subject to a heat flux from a fire load. The results show that the constrictive inlet pipe to the forward vent mast would restrict the flow due to choke pressure (sonic flow) occurring. The connection between each cargo tank and the common vapour header would be the element restricting other cargo tank relief valves from operating at their maximum capacity.

### 5.2.2 Selected relief valve

The relief valve selected is a Fukui Seisakusho Co., Ltd (FKI), Type PSL-MD13-131-NS1, with a 12" inlet size and 16" outlet size. The orifice area of the valve is 759.6 cm<sup>2</sup>. The supply to the pilot valve is taken directly from the cargo tanks and not from the inlet flange of the valve.

This design of relief valve has been approved by UV, NKK, DNV, BV, GL, RINA and LR. Further details of the relief valve are shown in the FKI brochure, which forms appendix one.

In accordance with the IGC Code, a minimum of two relief valves, each sized at 50% of the required capacity, has been considered.

## 5.2.3 Cargo

It is proposed that the worst-case cargo needs to be considered and so pure methane has been taken as the referenced cargo. While most LNG cargoes have a methane content between 90% and 95%, it should be noted that the constituents of Alaskan LNG is 99.5% methane, 0.4% nitrogen and 0.1% ethane.

## 5.2.4 Maximum cargo tank size

Using the formula provided by FKI, the maximum flow rate of the relief valve was calculated. With the valve having a set pressure of 0.25 barg, including the allowable 20% rise in operating pressure the capacity was calculated at 1.31325 bar a. The value obtained for air for two relief valves being: 31.506 m<sup>3</sup>/s.

$$W = \frac{A \times C \times K_d \times P_1 \times \sqrt{M \times K_b}}{\sqrt{T} \times Z}$$

W = Valve capacity (kg/h)  
 A = Valve orifice area (cm<sup>2</sup>)  
 K<sub>d</sub> = Coefficient of discharge  
 M = Molecular weight  
 Z = Compressibility factor

$$C = 387 \times \sqrt{k \times \left(\frac{2}{k+1}\right)^{\frac{k+1}{k-1}}}$$

k = Ratio of specific heats  
 C = Coefficient determined by specific heats

$$K_b = \frac{548}{C} \times \sqrt{\frac{k}{k-1} \times \left( \left[ \frac{P_2}{P_1} \right]^{\frac{2}{k}} - \left[ \frac{P_2}{P_1} \right]^{\frac{k+1}{k}} \right)}$$

K<sub>b</sub> = Correction factor - constant back press  
 P<sub>1</sub> = Actual relieving pressure (bar a)  
 P<sub>2</sub> = Back pressure - ambient pressure (bar a)

This value was the design flow rate through the valve but did not take into consideration the effects of the pressure losses due to the inlet (upstream) pipework to the valve and the pressure loss in the discharge (downstream) lines through to the vent mast and out to atmosphere. Using standard designs of inlet pipework and commoned discharge headers, the actual maximum flow rate for air was then calculated. The value obtained for two relief valves being: 28.146 m<sup>3</sup>/s.

Using the above value of 28.146 m<sup>3</sup>/s and the formula provide in Section 8.5 of Chapter 8 of the IGC Code, the maximum tank area and diameter was determined using a gas factor for pure methane. The values obtained being; area of 7,419 m<sup>2</sup>, which equates to a diameter of 48.6 m.

$$G = \frac{12.4}{LD} \times \sqrt{\frac{ZT}{M}}$$

G = Gas factor for cargo at relieving conditions  
 L = Latent heat of cargo at relieving pressure  
 D = Constant based on relation of specific heats  
 Z = Compressibility of gas at relieving pressure  
 T = Absolute temperature at relieving pressure  
 M = Molecular mass of product

$$A = \left[ \frac{Q}{FG} \right]^{0.82}$$

A = External surface area of tank (m<sup>2</sup>)

Q = Minimum required discharge of air (m<sup>3</sup>/s)

F = Fire exposure factor (see list below)

G = Gas factor

## 5.2.5 Over pressurization of cargo tank due to fire

Using the maximum cargo tank the effects of over pressurization of the cargo tank were considered. Guidance was obtained from Moss Maritime on the actual over-pressure that the cargo tank could be subject to at design conditions.

The details provided were:

Design allowable vapour pressure	2.0 barg
Over-pressure before deformation	3.5 barg
Over-pressure before yield point	5 – 6 barg
Over-pressure before tensile failure	8 – 9 barg

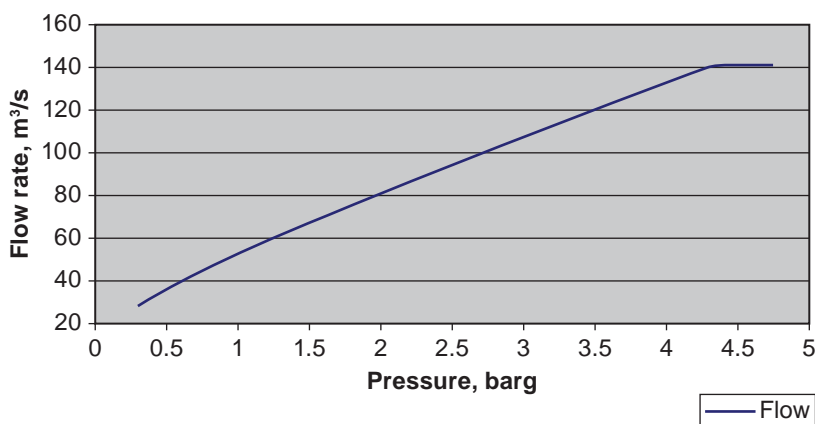
It was confirmed that the above pressures would be applicable to any size of cargo tank as the scantlings of the shell plate are sized for the tank's actual diameter.

## 5.2.6 Increase in relief valve capacity due to over pressurization

Having now fixed the maximum size of cargo tank at 48.6 m, the effect of over pressurization and the subsequent increase in relief valve capacity was considered.

The increase in relief valve capacity was recalculated in 0.1 bar increments until choke pressure (sonic velocity) on the downstream (discharge) line occurred. The results are shown in the graph that forms Figure 5.4. Choke pressure occurred at a relieving pressure of 4.38 barg.

**Figure 5:4 Relief value capacity**



In addition to the design maximum allowable vapour pressure of 2 barg, which is applicable with the vessel not subjected to the heavy seas that would cause dynamic loads and sloshing, it is considered realistic for the tank to be able to accept an over-pressure up to the point before deformation, this equating to 3.5 barg. Therefore, these two specific pressures have been used to determine the additional capacity of the relief valves. These values in turn have been used to determine the oversizing factor of the relief valves. This factor has been determined by recalculation of the fire exposure figure using the increase in capacity.

Relief valve flow at allowable over-pressure in accordance with the IGC Code's of 0.3 barg.

Relief valve flow = 28.146 m<sup>3</sup>/s.

At design allowable over-pressure of 2.0 barg. Relief valve flow 80.80 m<sup>3</sup>/s.

At deformation over-pressure of 3.5 barg. Relief valve flow 120.07 m<sup>3</sup>/s.

At discharge vent line choke pressure of 4.33 barg. Relief valve flow 140.93 m<sup>3</sup>/s.

Tank diameter fixed at 48.6 m and area of 7,419 m<sup>2</sup>. 'G' changes and depends on pressure within the cargo tank.

$$A = \left[ \frac{Q}{FG} \right]^{0.82}$$

At the IGC Code's allowable over-pressure of 0.3 barg:

Q = 28.146 m<sup>3</sup>/s      G = 0.0943      Fire factor = 0.2

At design allowable over-pressure of 2.0 barg:

Q = 80.80 m<sup>3</sup>/s      G = 0.1008      Fire factor = 0.537 (2.69)

At deformation over-pressure of 3.5 barg:

Q = 120.07 m<sup>3</sup>/s      G = 0.1049      Fire factor = 0.767 (3.84)

At discharge vent line choke pressure of 4.33 barg:

Q = 140.93 m<sup>3</sup>/s      G = 0.107      Fire factor = 0.883 (4.42)

## 5.2.7 Existing ship

An existing ship, using the above relief valves, was then considered. This ship (name not given because of confidentiality requirements) has a tank diameter of 40.46 m, which equates to an area of 5,131 m<sup>2</sup>. All other aspects with regard to inlet pipework and discharge arrangement are as before.

Tank diameter fixed at 40.46 m and area of 5,131 m<sup>2</sup>. As previously, 'G' changes and depends on pressure within the cargo tank.

$$A = \left[ \frac{Q}{FG} \right]^{0.82}$$

At IGC Code's allowable over-pressure of 0.3 barg:

Q = 28.146 m<sup>3</sup>/s      G = 0.0943      Fire factor = 0.271 (1.35)

At design allowable over-pressure of 2.0 barg:

Q = 80.80 m<sup>3</sup>/s      G = 0.1008      Fire factor = 0.727 (3.64)

At deformation over-pressure of 3.5 barg:

Q = 120.07 m<sup>3</sup>/s      G = 0.1049      Fire factor = 1.038 (5.19)

At discharge vent line choke pressure of 4.33 barg:

Q = 140.93 m<sup>3</sup>/s      G = 0.107      Fire factor = 1.195 (5.97)

## 5.2.8 Results

For an existing ship using the subject relief valve, the system has an over capacity at the maximum design pressure of 2 barg of 364%. At the deformation over-pressure of 3.5 barg the over capacity of 519%.

It is important to note that the above figures are intended only to demonstrate the overcapacity of the relief valves using the IGC criteria but do not take any credit for the additional relieving capacity provided by the vapour header.

Under fire conditions the relief valves on the other tanks will also be able to operate up to the choke pressure of the flow through the common header tank outlet (normally 350 mm diameter). This also increases the flow.

# **HEAT TRANSFER INTO THE TANK**



The following summary is based on the results of two studies related to the heat transfer into an LNG cargo tank undertaken in 2007 and 2008 Ref. 01 & Ref. 02. The content of an article published in The Journal of Hazardous materials in February 2008 Ref. 03 has also been considered. The first study dated 2007-11-07 is related to the thermodynamic boundary conditions of the fire case and was undertaken by the Helmut Schmidt University Hamburg and Germanischer Lloyd Hamburg. The second study is based on these first findings and is related to transient (time dependent) modelling of the heat transfer into the tank by the use of Computational Fluid Dynamics (CFD). This study was the subject of a Master's thesis undertaken at the University of Rostock

All studies are related to a pool fire engulfing a Moss Type LNG tank. Source Ref. 01, Ref. 03 are attached as an Appendix to this report. For the CFD modelling Ref. 02 only the Powerpoint presentation at the University of Rostock on 2008-07-17 is attached. The major findings and conclusions are given as follows.

## 6.1 Fire Scenario

Considerable uncertainties exist about the flow behaviour of an engulfing fire and the realistic modelling of the heat flux to the tank or, in the given case, to the ship structure above the waterline and the weather cover of the LNG Moss type tank under consideration. The fire itself has not been modelled. Instead simplified scenarios are used.

Heat fluxes known from pool fire experiments are generally measured at the visible outer boundary of the fire. At this location the access of air to the fuel is much better compared to the access of air to unburned fuel within the fire ball formed by the pool fire. For this reason the combustion in a large fire ball is incomplete and the flame temperature lower compared to the complete combustion at the boundary between fire ball and ambient air. Therefore, the heat flux from the fire is lower in the fire ball than at the surface of the fire ball. According to GDF comments and a video presented to the WG, maximum values measured at the Montoir fire test were about 300 kW/m<sup>2</sup>. This is also reported in Ref. 03 by stating "... local surface emissive heat fluxes have been measured in test LNG fires as high as 300 kW/m<sup>2</sup>,..." (p.3).

The experiments that form the bases of all regulations related to the sizing of safety valves for the fire case (comp. Sec 4) give maximum values of 108 kW/m<sup>2</sup> as a baseline for safety valve design (comp. Sec 4 source cite-01, cite-02). This heat flux is assumed to be uniform at all parts of the tank that is subjected to the fire. In reality the heat flux will have large variations depending on the smoke within the fire ball and on the completeness of the combustion. For this reason the value used by the regulations covers much higher maximum heat fluxes because it is an average value.

For the reasons stated above, the maximum average value of a realistic fire scenario is accepted to be 108 kW/m<sup>2</sup>. Nevertheless, this study has included evaluation of much higher values; up to 300 kW/m<sup>2</sup> for the sake of completeness of the evaluation since these values were suggested as plausible by at least one WG member.

For the purpose of the studies a constant flame temperature corresponding to the assumed initial heat flux into the tank has been assumed to be present at the complete surface above the waterline.

## 6.2 Limit for Heat Flux into LNG and Possibility of Tank Collapse

The following is an evaluation of the possibility that the tank can theoretically fail in the wetted surface area (comp-01)

If the insulation is not present and the weather cover is at very high temperatures, the LNG in the tank starts boiling. Until the boiling reaches 'film boiling' the tank wall is kept nearly at LNG temperature. If a transition to film boiling occurs the tank wall is no longer protected by the liquid LNG because a film of methane vapour is separating the tank wall from the LNG. If this situation occurs the tank wall can overheat and collapse. This case has been evaluated in Ref. 01.

As explained below, film boiling will not occur even under extreme theoretical assumptions. Therefore, overheating of wetted surface area of the tank and the possibility of tank collapse for this reason can be excluded from further consideration.

### 6.2.1 Heat flux into the weather cover

The following results are from Ref. 01, which assumes stationary conditions without time dependency. Most of the heat from the fire is transferred into the steel structure by radiation and not by convection. Without convection the flame temperature can be calculated from the basic equation for radiation:

$$T_0 = \left[ \frac{\bar{q}}{\sigma} + T_1^4 \right]^{\frac{1}{4}} = 1517 \text{ K}$$

An initial heat flux of  $q = 300 \text{ kW/m}^2$  corresponds to a flame temperature of approx 1500 K, which is very close to the highest flame temperatures measured in large LNG fire tests. The relevant heat flux for the tank is the heat flux that comes from the inner surface of the weather cover, and it heats up the air gap under the weather cover and also the insulation system itself. The time dependent CFD calculations demonstrate that the convective heat transfer in the insulation space is only contributing to a small extent to the overall heat transfer. Using radiation only, a flame temperature of 1500 K and a maximum cover temperature of 1273 K, the heat flux to the weather cover from the fire is

$$\bar{q} = \sigma \cdot [T_0^4 - T_1^4] = 151 \text{ kW/m}^2$$

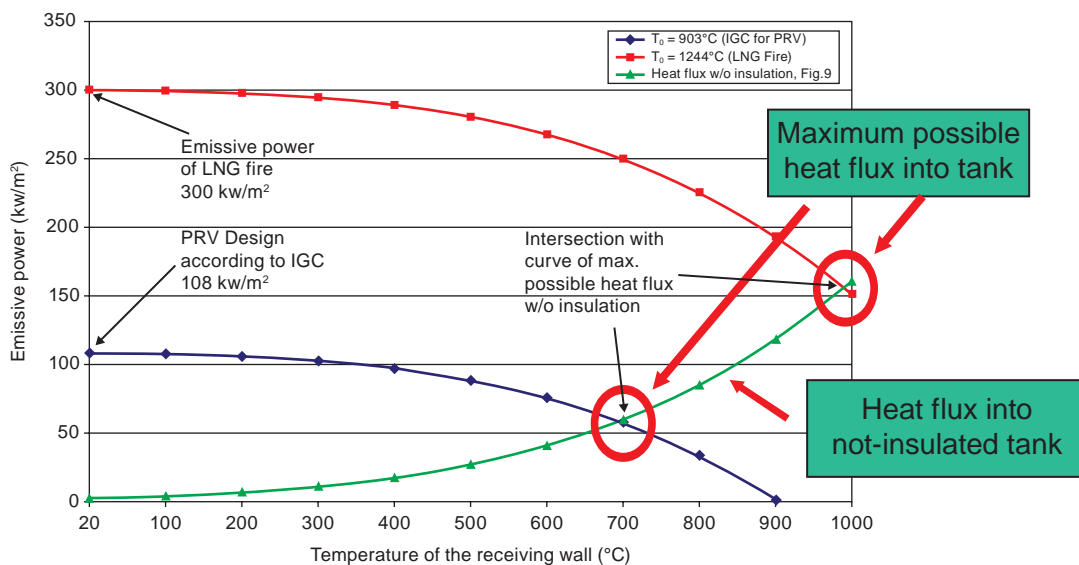
As is demonstrated in Fig. 6.1, even with a maximum initial heat flux of the fire at  $300 \text{ kW/m}^2$  it is not possible to heat up the tank cover above  $1000^\circ\text{C}$  if at the same time the insulation is assumed to be completely destroyed (comp below). For this reason it has been agreed in the WG that temperatures of the (complete) weather cover of more than  $1273^\circ\text{K}$  can be excluded, even in theoretical evaluations. At the same time the maximum heat flux into a complete bare tank is limited to  $150 \text{ kW/m}^2$ .

## 6.2.2 Possibility of film boiling

The x-axis of Fig. 6.1 shows the temperature of the weather cover. The y-axis gives the heat flux that is received from the fire by the weather cover. For a fire of  $300 \text{ kW/m}^2$  initial heat flux the flame temperature is about 1500 K (red curve). For a fire with  $108 \text{ kW/m}^2$  the flame temperature of the fire is about 1180 K (blue curve). The heat flux received is decreasing with increasing steel temperature, as explained above.

The green line in Fig. 6.1 shows the heat flux to wetted surface of the bare tank. At the beginning with the weather cover at  $20^\circ\text{C}$  the heat flux to the tank wall, which is at minus  $163^\circ\text{C}$ , is relatively low (approx.  $2.2 \text{ kW/m}^2$ ). With increasing weather cover temperature the heat flux into the tank is increasing. The maximum value is reached at the intersection of the curves. A higher value is not possible because the radiation from the tank is starting to cool the weather cover instead of the weather cover heating up the tank.

**Figure 6.1: Maximum Heat Flux into the Tank**



From Fig. 6.1 it can be concluded that heat fluxes into the tank, and therefore energy available to evaporate the LNG of more than  $150 \text{ kW/m}^2$  for the most extreme conditions and of more than  $60 \text{ kW/m}^2$  for the PRV sizing criteria of the IGC-Code, are not possible. Again this extreme case assumed that all the insulation has been removed or is otherwise ineffective, a scenario considered in detail below.

As can be seen from Fig 3 in the 1-D study Ref. 01, film boiling does not occur at these heat fluxes. Therefore, overheating of the tank wall in the wetted surface area, which would create the possibility of tank collapse, is excluded from further consideration.

## 6.3 Burning of the Insulation or Explosion of Combustible Mixtures

### 6.3.1 Burning of insulation

In Ref. 01 the possibility of insulation burning was evaluated by calculating the amount of insulation that can be burned by the available oxygen in the insulation space (cargo hold) assuming that the hold is filled with ambient air. It was established that in many cases the hold is at least partly filled with nitrogen. The insulation system itself under the aluminium sheet covering is always filled with nitrogen as this atmosphere is constantly monitored as part of the gas detection system required by the IGC-Code.

As described in detail in Ref. 01 page 19, the air in the cargo hold is only able to supply oxygen for burning of 21 m<sup>2</sup> of styrene. If the insulation burning was uniform this would be equal to 5 mm insulation thickness. It must be noted that this calculation assumes that all air reacted with the insulation. In reality this will be not the case because combustion needs minimum oxygen content in the air. A more realistic value will be the burning of less than 10 m<sup>2</sup> of insulation, even if the atmosphere in the cargo hold has 21% oxygen (ambient air oxygen content) at the beginning of the burning event.

### 6.3.2 Explosion within the cargo hold

During the WG deliberations the possibility of formation of explosive mixtures of oxygen and vaporized insulation was discussed. According to the time dependent CFD calculations done in Ref. 02, the time for reaching the melting temperature of styrene of about 500 K is between 170 s for 300 kW/m<sup>2</sup> initial heat flux to 420 s for 88 kW/m<sup>2</sup> initial heat flux (comp below). According Ref. 03 p. 6, the melting rate of the insulation may be up to 30 mm per min, which gives 0.5 mm per s or 2 s per mm. Also according Ref. 03 p. 6, only 1 mm is needed to reach the lower explosion limit of an air styrene mixture, which is about 1%vol. The upper limit is in the range of about 6% vol (source: data for styrene monomer from the internet). The only ignition source is the hot weather cover.

The CFD calculations explained below Ref. 02 give a time range for reaching the self ignition temperature of styrene (according Ref. 03 p. 6 of about 760 K) that is between 132 s (for 300 kW/m<sup>2</sup> initial heat flux) to 480 s (88 kW/m<sup>2</sup> initial heat flux). This means that the weather cover reaches the auto ignition temperature of styrene 38 s before melting occurs (300 kW/m<sup>2</sup>) and up to 60 s after melting occurs (88 kW/m<sup>2</sup>).

Using the assumption of a homogeneous mixture, without mixing time as a first step to judge the problem, it was concluded that for the high heat fluxes of 300 or 200 kW/m<sup>2</sup> the flammable gas content in the hold would be too high to allow burning or explosion because, according Ref. 03, 6% vol is reached 12s after the melting point temperature is reached at the insulation surface. Only at lower heat fluxes would the weather cover be hot enough to ignite styrene vapour and burning or explosion be theoretically possible because the insulation reaches melting temperature 20s to 60 s after the weather cover reaches auto ignition temperature.

The question considered was; is it even theoretically likely that the ignition of styrene will be able to damage the weather cover in a way that causes it to lose its effectiveness as a radiation shield for the insulation system? (ie, is it possible to blow-off the cover?). Such an event is not supported by any reported historical gas carrier incident. Nevertheless, it was addressed because the likelihood of creating explosive mixtures increases with decreasing heat flux into the insulation, as explained above.

The view was expressed by members of the WG that, based on their individual engineering experiences, it appears more likely that there would be local insulation melting in a random process even if the complete tank is under fire. The vapour would tend to mix with air and reach the hot weather cover after travelling with the turbulent convection flow (result of CFD calculations in Ref. 02). It may ignite if within the flammable range and randomly driven combustion would last until the very limited amount of air was consumed.

There appeared to be no technical basis to expect that vaporized styrene would mix with air into a stoichiometric mixture, needed for a violent explosion, and be ignited by the hot weather cover at the same time across the tank of 41 m diameter.

It appeared far more likely that small amounts of combustible mixtures at the hot surface of the cover may cause small explosions, but these events were not considered likely to result in a dangerous pressure increase. The amount of combustible mixtures reacting at a given time will be small compared to the large volume of the hold space.

*Note: Beside the subject of this report it should be noted that care must be taken to the presence of combustible mixtures after a fire that may have lead to melting of insulation material because styrene is much heavier than air and may accumulate in the lower hold space parts after the fire. During the fire this can be excluded because of the convection flow, which will keep the combustible mixtures in the upper part of the tank (result of CFD calculations Ref. 02).*

## 6.4 CFD Evaluation of the Tank Fire Problem

The 1-D stationary calculations performed in the first study in 2007, Ref. 01, left the questions of real time dependent behaviour of a theoretical catastrophic fire event open. Particularly, the influence of the convective flow that occurs between the upper and lower part of the tank (the part protected by water ballast tanks and the sea water below the water line) could not be judged. Furthermore, the real time dependent heat transfer through the insulation was an open question.

Time dependent calculations of the heat transfer into the tank were the COMSOL calculations that were documented by Ref. 03. These gave results but no information that would allow the re-calculation of the results.

In addition, questions that came from the findings of the 1-D study undertaken by Helmut Schmidt University and GL Ref. 01, had been left open. Also the finite element buckling evaluation done by ABS, Ref. 06, left questions open. On the other hand it was obvious that the theoretical scenario under discussion would last only a very limited time (between 3.4 and 40 min Ref. 05) and therefore a detailed evaluation of the theoretical fire scenario agreed by the WG was necessary.

Related to this background it was obvious that only time dependent CFD calculations could give needed insight to allow judgement on the very severe theoretical fire scenario that was set up as a basis of the WG terms of reference.

For this reason GL decided to work together with the Institute of Fluid Dynamics at the University of Rostock to contribute to the work of the WG on the scale of a Master thesis. The calculations were performed under advice of GL Hamburg and in close co-operation with ANSYS Company, who license the CFX software to GL. Input was provided by the ABS WG member regarding the model and parameters used in the ABS buckling evaluation, Ref. 06, and from the Moss Maritime WG member with regard to the details of Moss Type LNG cargo tank system.

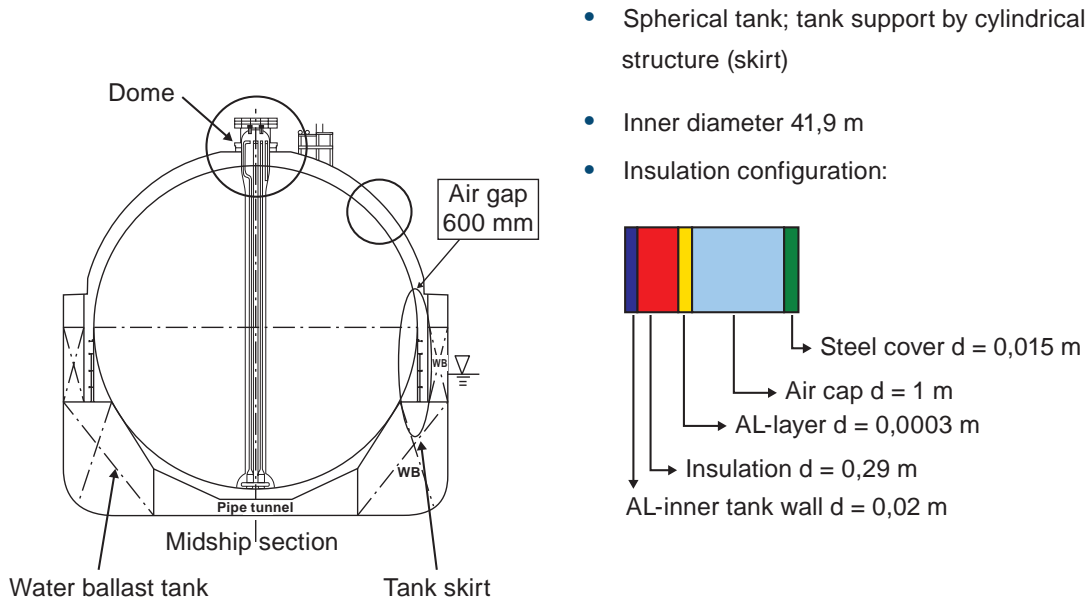
### 6.4.1 CFD calculation

As a simple check on potential buckling of the tank cover, under the influence of a fire, ABS performed a finite element thermal stress analysis to determine the time from the initiation of the fire to the point where structural damage starts to occur, Ref. 06. ABS assumed values for a constant heat flux from the fire into the tank cover of 88, 108 and 200 kW/m<sup>2</sup>. The tank cover to deck connection was held at 100°C so there was conductive heat flow to the hull structure but no radiant heat flowing from the tank cover to the insulation system.

According to the more realistic behaviour of decreasing heat flux into the weather cover with increasing weather cover temperature, the time dependent CFD calculations were carried out by assuming a temperature relation between fire and the heat transfer from the weather cover into the hold space and finally into the tank.

The configuration for the CFD modelling is shown in Fig. 6.2.

**Figure 6.2: Configuration for CFD Model**

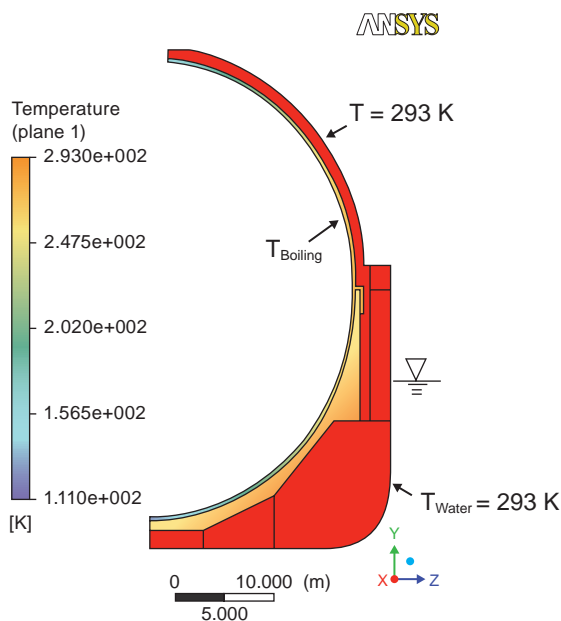


Transient heat transfer calculations were undertaken for the combined heat transfer of radiation, convection and conduction. The model was extensively validated, including reference calculations of temperature distributions under normal operation conditions that were compared to data supplied by Moss Maritime, time step and mesh validation. In addition, the results of ABS buckling calculations were reproduced by independent calculation using only the ABS input data. Detailed results are given in Ref. 02.

Fig. 6.3 shows an image of the CFD model for the reference calculation under normal operation temperature conditions.

### Consideration of radiation, convection and conduction

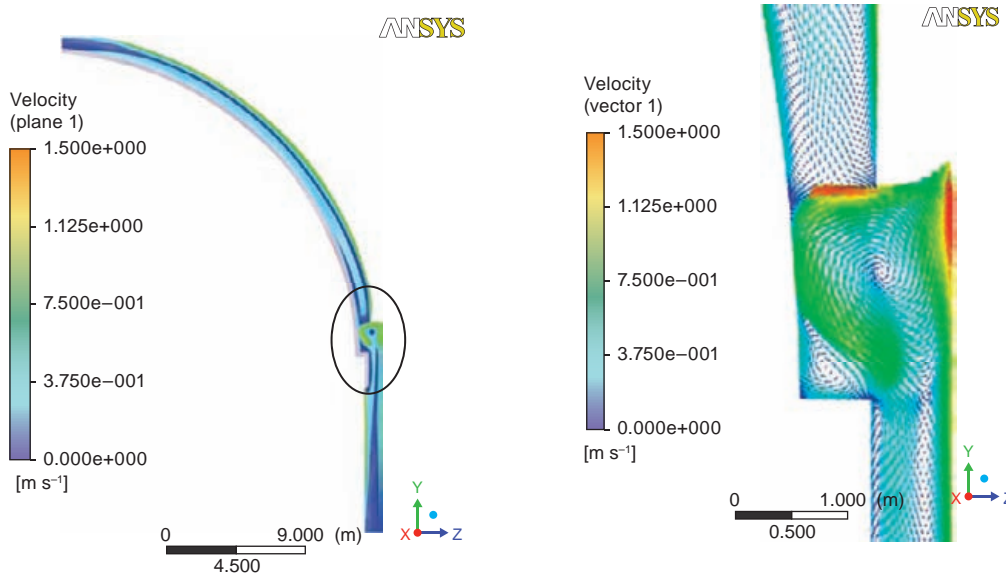
**Figure 6.3: Reference Calculation for Normal Ambient Conditions**



All calculations for fire conditions were set up with the normal operational conditions present until the fire started.

Transient calculations were necessary because the natural convection especially, in the area of the skirt, fluctuated and could not be calculated with sufficient stability using stationary assumptions. Fig. 6.4 shows the flow field in the tank at 148 s after the start of the fire.

**Figure 6.4: Flow Field After 148 s of Fire Start up**



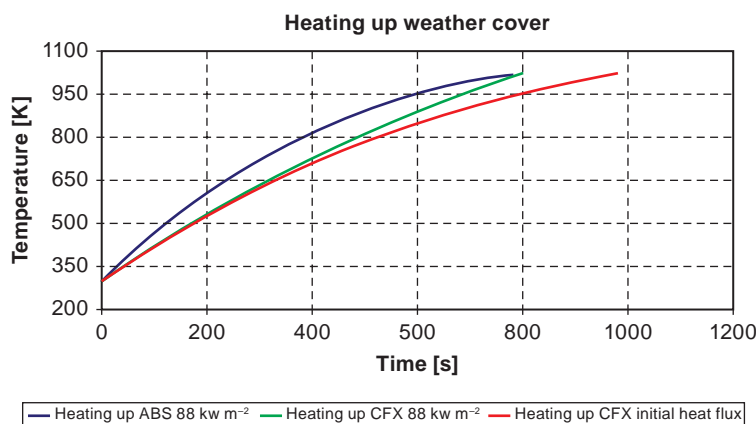
## 6.5 Heating up of the Weather Cover and the Insulation

The heat flux into the weather cover was calculated for initial heat fluxes of 88, 108, 200 and 300 kW/m<sup>2</sup>. The ABS calculation used a constant heat flux over time. The CFD calculation used a time dependent temperature heat flux, which is related to the weather cover temperature as already described above. The heat flux is calculated for each time step by:

$$\bar{q} = \sigma \cdot (T_{Fire}^4 - T_{Cover}^4)$$

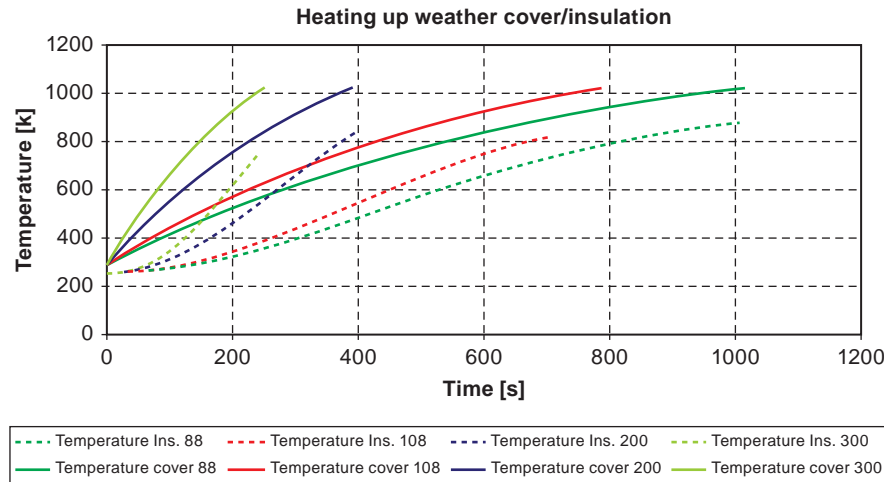
Fig. 6.5 shows the comparison of the original ABS data for heating up the weather cover with 88 kW/m<sup>2</sup> (blue line), the CFD calculation using a constant heat flux as used by ABS (green line) and the temperature difference between fire and cover related heat flux as given above (red line). It can be seen that the ABS and GL CFD calculation results are very close for the same boundary conditions and that the more realistic temperature difference dependent heat flux leads to longer times for heating up the weather cover.

**Figure 6.5: Weather Cover: Comparison of CFD Results with ABS Buckling Calculation Data**



The summary of results for temperature increase of the weather cover and the insulation are shown in Fig. 6.6.

**Figure 6.6: Summary of Results for Time Dependence of Weather Cover and Insulation Temperature. (88, 108, 200 and 300 kW/m<sup>2</sup> Initial Heat Flux)**



Melting of insulation was assumed to start between 473 and 573 K. Initial damage of the weather cover started at about 1023 K according to the ABS report. This is based on an abrupt drop in the Young's modulus of the A-32 steel cover, which predicted very local deformation of the cover plate at the joint to the top girder.

The time needed to reach an insulation temperature of 573 K (melting) and a cover temperature of 1023 K (start of damages) is given in Fig. 6.7. The related values from CFD calculations are given in Table 6.1.

**Figure 6.7: Heat Flux Dependent Cover and Insulation Temperature**

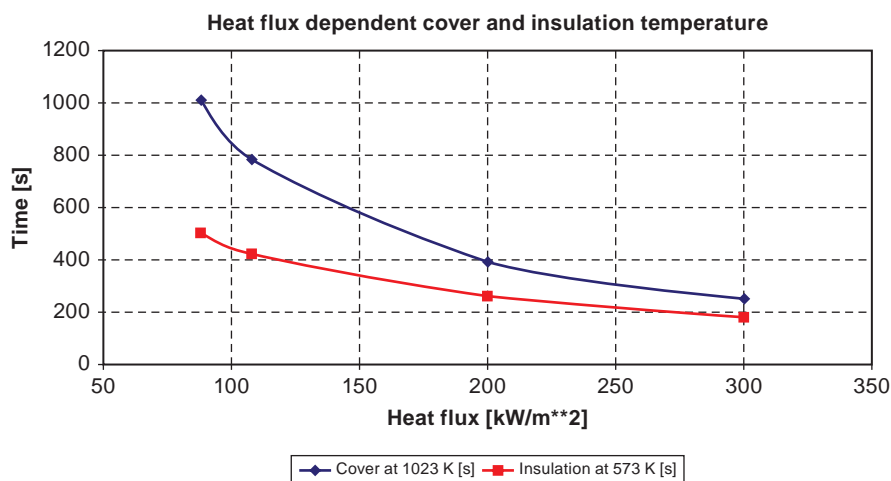


**Table 6.1: Time to Reach Limits for Cover and Insulation Temperature**

kW/m <sup>2</sup>	Cover at: 1023 K [s]	Insulation at 573 K [s]
88	1013	500
108	784	420
200	391	260
300	250	180

The figures indicate the necessary time to heat up the weather cover and insulation to temperature values where any damage may start to develop. It should be noted again that the assumption is a fire that completely engulfs the tank above waterline and has a uniform heat flux into the complete tank structure in the fire. The heat flux was assumed to strike the cover in a radial direction, (ie there was no reduction in heat flux for the upper parts of the tank cover due to a low thermal

radiation view factor.) This would effectively mean that the flames were higher than the tank cover, more than 40 m above the water and on all sides. This is again important because the first structural deformation of the cover is predicted at the upper most part of the hemisphere, as is shown in Fig. 6.11.

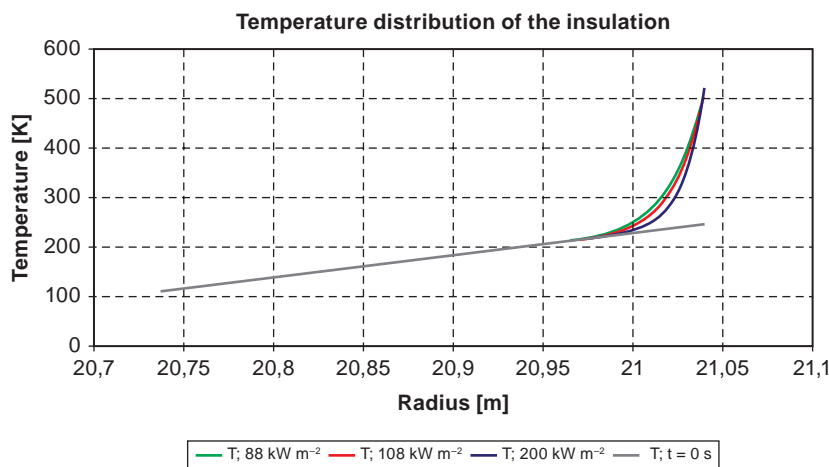
Depending on the assumed heat flux the minimum time to heat up the weather cover to temperatures where damage starts is 1013 to 250 s (approx. 17 min to 4 min).

Depending on the assumed heat flux the minimum time to heat up the insulation surface to a temperature where first damages by melting occur is 500 to 180 s (approx. 8 to 3 min)

## 6.6 Heat Transport into the Insulation

The transient heat transport into the insulation could not be modelled with 1-D stationary evaluations. The CFD analysis allowed the detailed modelling of the temperature distribution and as a result the determination of the heat transport into the insulation. Fig. 6.8 shows the temperature distribution in a profile of the insulation at the time when the melting temperature is reached at the surface. It was calculated that approximately 4 cm of insulation thickness (see Fig. 6.8) would be affected by the increased heat flux caused by the fire. It is not possible to heat up the rest of the insulation during the short time until the surface of the insulation reaches its melting temperature. This effect is independent of the assumed value of the heat flux.

**Figure 6.8: Temperature Distribution in a Profile of the Insulation for an Initial Heat Flux of 88, 108, 200 kW/m<sup>2</sup> when the Melting Temperature is Reached**



The extremely low heat transfer characteristics of the insulation system on an LNG carrier are chosen to reduce the boil-off rate to less than 0.15% per day. Consequently, it is obvious that the LNG in the tank will have no increased heat flux under fire exposure until the insulation is almost completely destroyed. Therefore, the pressure increase in the tank will only start at this point.

In Ref. 03 a melting rate of 30 mm/min is stipulated. This melting rate did not consider the necessary heat which is needed to heat up the insulation itself. As can be seen from the recalculation undertaken with the data given in Ref. 03, the 30 mm/min is based on the energy needed for melting only. Considering the fact that the insulation must be heated up to the melting point leads to additional time required to do so. This is demonstrated by the calculation enclosed in the Appendix 6 (Insulation -Heating Comparison). Using the heat flux into the insulation of 1500 W per m<sup>2</sup> as given in Ref. 03 leads to an additional time of 970 to 1240 s (for 473 and 573 melting temperature respectively). This is 1.8 to 3.0 times the values assumed in Ref. 03. The corresponding melting rate will, therefore, be smaller than 30 mm/min. Using the data above a value of 17 mm/min to 10 mm/min will be more realistic.

Therefore, the melting of the insulation will be in the range of 17 to 29 min, not 10 min as was assumed in Ref. 03.

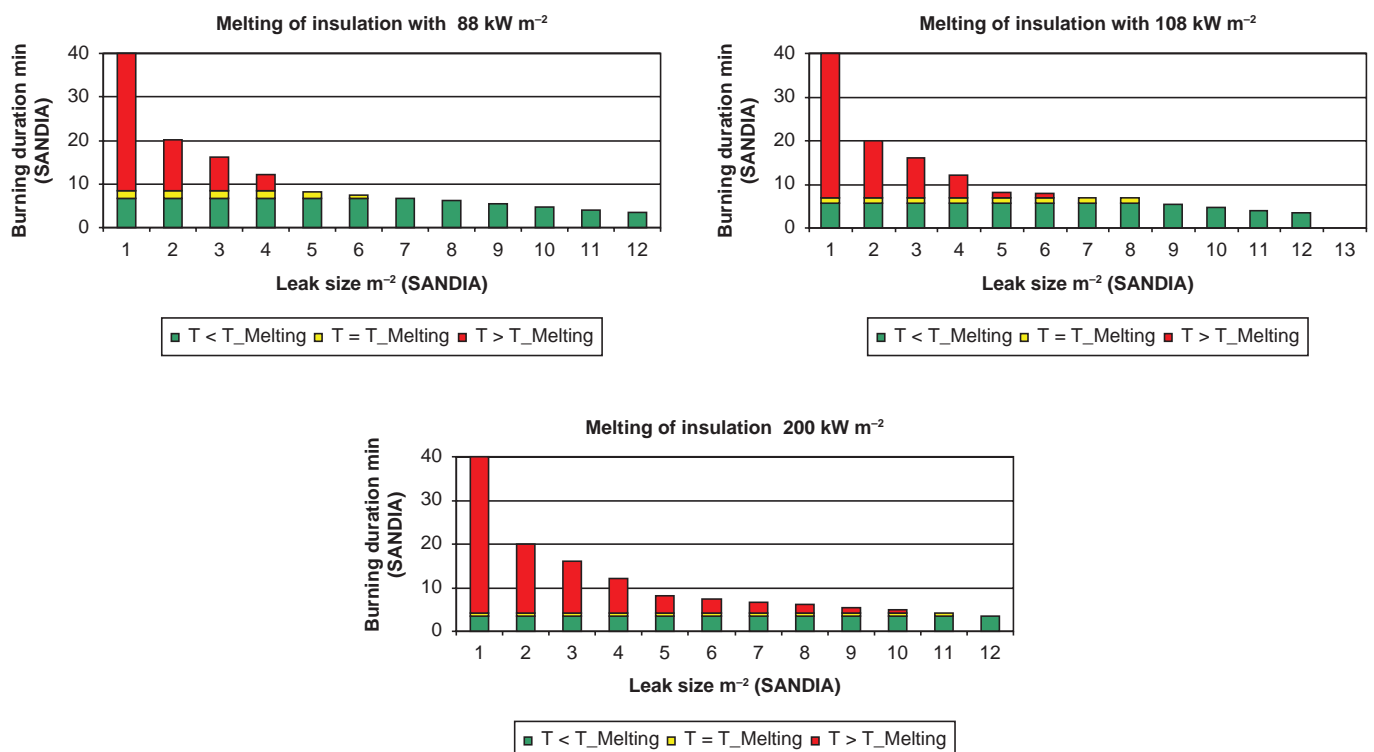
## 6.7 Relation of CFD Calculation Results to Pool Fire Burning Duration According SANDIA Report

As a final result the durations calculated within the CFD evaluation were related to the burning durations and leak sizes as given in the SANDIA report Ref. 05.

### 6.7.1 Melting of insulation and leak size

In Fig. 6.9 and Fig. 6.10 the fire durations are given on the y-axis and the leak sizes are given on the x-axis. Fig. 6.9 illustrates the minimum time related to the leak sizes until the melting of the insulation may start and begin to destroy the insulation. It gives these relations for the initial heat fluxes of 88, 108 and 200 kW/m<sup>2</sup>.

**Figure 6.9: Start of Insulation Melting: Relation between CFD Calculation Results and SANDIA Report Results**



The green bar indicates the time required to reach the lower assumed melting temperature of 473 K. The yellow bar indicates the time needed to heat up the insulation from 473 to 573 K, which is the upper value of the melting range assumed. The red bar indicates the time which is available to destroy the insulation until the fire is out according SANDIA results, ie only for holes with a red bar will the insulation be effected.

The smallest fire, with 1 m<sup>2</sup> equivalent hole, will last about 40 min. The largest, with 12 m<sup>2</sup> equivalent hole, will last 3.4 min and the reference fire agreed in the WG with 5 m<sup>2</sup> equivalent hole will last 8.2 min. No evaluation has been undertaken to determine which size will result in the ship being enveloped by the pool fire, but the CFD calculations assume an enveloping pool fire for even a 1 m<sup>2</sup> hole. According to the Sandia report, a pool fire from a 1 m<sup>2</sup> hole would have a diameter of 1.48 m, about half the length of the vessel.

For the 5 m<sup>2</sup> hole no melting starts for the 88 kW/m<sup>2</sup> fire, 1.42 min are available for the 108 kW/m<sup>2</sup> fire and 3.85 min are available for the 200 kW/m<sup>2</sup> fire. There is no figure for the 300 kW/m<sup>2</sup> assumed by Ref. 03 as the most severe case, but from Table 9.1 it can be concluded that the time available to destroy the insulation is 5.1 min (8.1 min fire duration minus 3 min to heat up to 573 K). According to Ref. 03, 153 mm of insulation may be destroyed, but it can be assumed that less insulation will be destroyed because the time to heat up the insulation to melting temperature has to be added (comp. above). If 17 additional minutes are added the 300 kW/m<sup>2</sup> initial heat flux fire has to last 30 min to theoretically destroy all the insulation. This time is needed by 3 min to heat up to melting temperature, 10 min to melt the insulation according Ref. 03 and an additional 17 min, as a minimum, to heat up the insulation. This is the burning time for a hole of less than 2 m<sup>2</sup> hole size according SANDIA.

Using 17 min to heat up the insulation and 10 min to melt the insulation leads to required burning times of 31.25 min for 200 kW/m<sup>2</sup>, 34 min for 108 kW/m<sup>2</sup> and 35.33 min for 88 kW/m<sup>2</sup>.

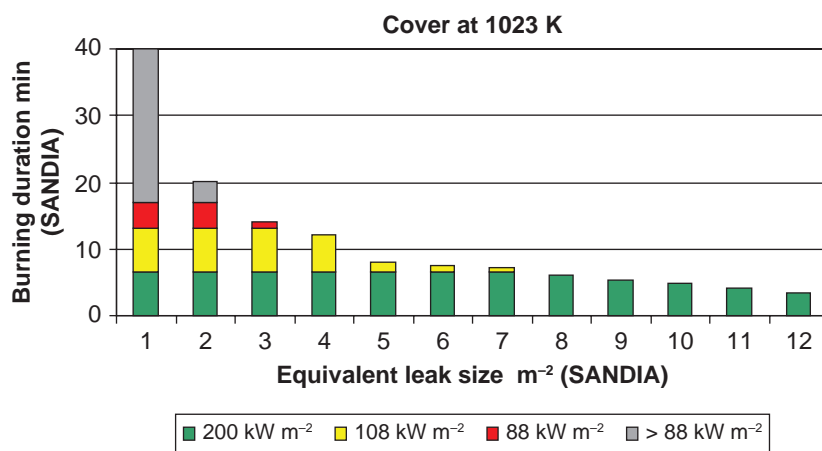
Therefore, according to the SANDIA report assumptions, it can be concluded that the insulation will not be completely destroyed by a fire resulting from the outflow from a 5 m<sup>2</sup> hole because the theoretical time available for the fire duration must be 30 min or more. This limits the size of hole to a maximum of 2m<sup>2</sup> even for 300 kW/m<sup>2</sup> initial heat flux. According to the Sandia report, a 2 m<sup>2</sup> hole could lead to a pool with diameter up to approximately 209 m, in the order of 2/3 the length of the vessel. According to DOE/Sandia briefing to NARUC Staff Subcommittee on Gas July 15, 2007 Ref. 08, "large fires, (D > 100 m) generally break up into 'mass fires', characterized by low L/D ratios (< 0.5)". Therefore it is unlikely that such a hole will create an enveloping fire with a heat flux of 300 kW/m<sup>2</sup> at an elevation above that of the tank.

## 6.7.2 Heating up of weather cover and leak size

The same evaluation used for the melting of the insulation can also be used for the weather cover that is protecting the insulation. Fig. 6.10 relates the temperature from which the weather cover starts to become damaged to the leak sizes and fire durations given by SANDIA report.

The green bar indicates the time needed for a 200 kW/m<sup>2</sup> fire to reach 1023 K (6.51 min). The yellow bar indicates the additional time (6.59 min) needed if the fire is 108 kW/m<sup>2</sup> (6.51 min + 6.59=13.1 min). The red bar indicates the additional 3.5 min needed to reach the 1023 K for a fire with initial heat flux of 88 kW/m<sup>2</sup> (6.51+6.59+3.5=16.6 min). The grey bar indicates the remaining time until the fire is off according SANDIA report. The 300 kW/m<sup>2</sup> case can again be included by using the figures from Table 6.1 (4.16 min to reach 1023 K).

**Figure 6.10: Start of Cover Damage: Relation between CFD Calculation Results and SANDIA Report Results**



The time available to heat the weather cover above 1023 K for a fire caused by a 5 m<sup>2</sup> hole is about 4.03 min for a 300 kW/m<sup>2</sup> initial heat flux and only 1.59 min for a 200 kW/m<sup>2</sup> initial heat flux. Lower heat fluxes will not be able to heat up the weather cover to 1023 K in case of a 5 m<sup>2</sup> hole because the fire is out before this temperature is reached. In other words: the more realistic cases of 88 and 108 kW/m<sup>2</sup> will not be able to heat up the weather cover to a temperature where the uppermost part of the cover may start to show local deformation, Fig. 6.11, if a 5 m<sup>2</sup> or greater leak in the damaged tank is assumed.

**Figure 6.11: Predicted Local Deformation at the Attachment of the Upper Hemispherical Part of Tank Cover to Ring Girder and Top Plat from ABS Buckling Analysis**

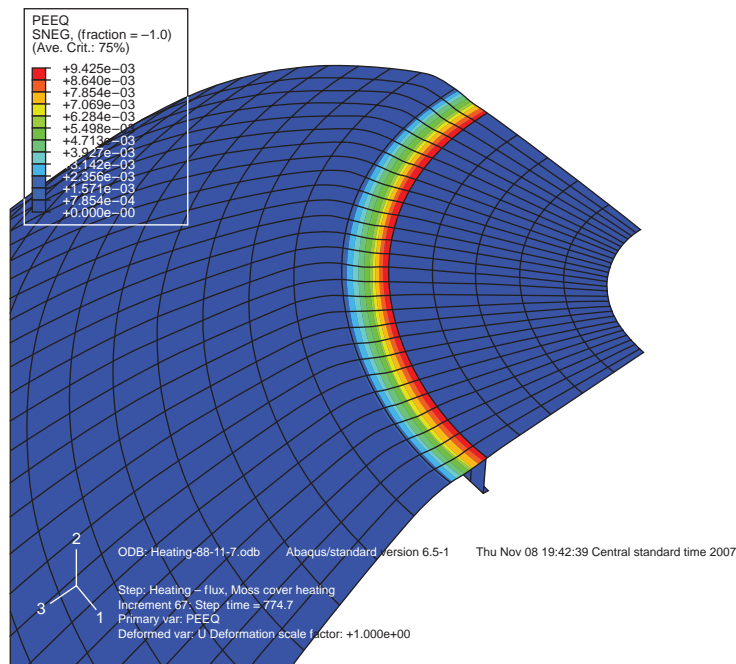


Fig. 6.11 predicted local deformation at the attachment of the upper hemispherical part of tank cover to ring girder and top plate from ABS Buckling Analysis.

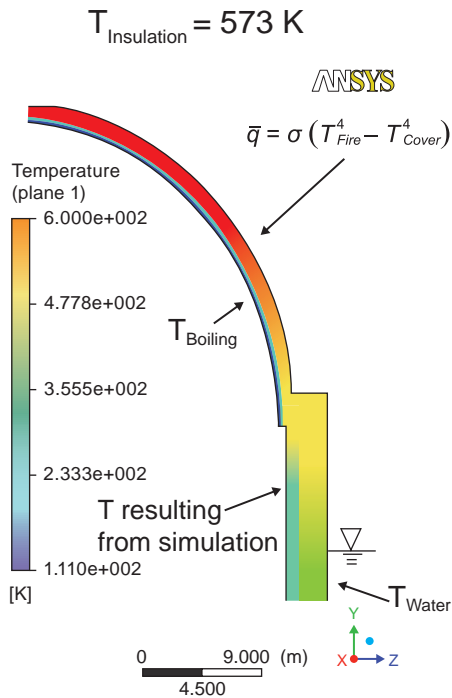
With  $108 \text{ kW/m}^2$  the maximum hole size, which will lead to a temperature of approx  $1023 \text{ K}$  at the weather cover, is  $3 \text{ m}^2$ . For  $88 \text{ kW/m}^2$  the hole size is even smaller.

It should be noted and repeated from above that the maximum flame temperature related to the  $300 \text{ kW/m}^2$  case is approx.  $1500 \text{ K}$ . It can be assumed that the weather cover will keep its function to protect the insulation even if parts of the cover are reaching the temperature corresponding to this heat flux.

## 6.8 Temperature in Skirt Area

The skirt is protected by ballast tanks. In the calculation the ballast tanks have been assumed to be empty which would be the case in a fully laden vessel. As can be seen from Fig. 6.12 the skirt area does not reach high temperatures. All calculations indicate that the skirt area will not be heated to critical temperatures for structural integrity. Failure of the support structure can be excluded from further consideration, even for very high heat fluxes into the cover ( $300 \text{ kW/m}^2$ ).

Figure 6.12: Temperature in Skirt Area is Limited to Low Values



## Conclusions

1. The maximum value of a realistic fire scenario is regarded to be  $108 \text{ kW/m}^2$ . Evaluating higher values up to  $300 \text{ kW/m}^2$  has only been done for sake of completeness since these values had been raised during deliberations at WG meetings. (comp. Sec 9.1).
2. The maximum possible emissive power of a LNG fire reaches the maximum value (eg  $300 \text{ kW/m}^2$ ) only initially and decreases with receiving wall temperature increase (comp. Sec. 9.2).
3. If a complete loss of insulation is assumed the theoretical maximum temperature of the weather cover is limited to  $1000^\circ\text{C}$  with  $300 \text{ kW/m}^2$  initial heat flux and to  $700^\circ\text{C}$  with  $108 \text{ kW/m}^2$  initial heat flux. At the same time the heat flux into the bare tank would be limited to  $150 \text{ kW/m}^2$  and to  $60 \text{ kW/m}^2$  respectively (comp. Sec. 9.2).
4. Film boiling will not occur even under extreme theoretical assumptions. Therefore overheating of the wetted surface area of the tank, and the possibility of tank collapse for this reason, can be excluded from further consideration (Sec. 9.2).
5. There is no possibility of a large scale burning of insulation material due to the lack of oxygen. The amount of air in the hold space only allows burning of a volume of insulation equal to the top 5 mm (p.19) (comp. Sec 9.3).
6. Large explosion events that could damage the weather cover to the extent that it would no longer be effective at providing heat shielding to at least most portions of the tank can be excluded from further consideration (comp Sec. 9.3).
7. Depending on the assumed heat flux, the minimum time to heat up the weather cover to temperatures where first deformation is predicted is 1013 to 250 s (approx 17 min to 4 min) (comp. Sec. 9.5).
8. Depending on the assumed heat flux, the minimum time to heat up the insulation surface to a temperature where damages by melting begins to occur is 500 to 180 s (approx. 8 to 3 min) (comp Sec.9.5).
9. The melting rate of  $30 \text{ mm/min}$  given in Ref. 03 only considers the energy of melting and does not consider the heating up of insulation material to melting conditions. A simple calculation based on the model also used by Ref. 03 demonstrates that the melting time will be more likely in the range of 17 to 29 min than the 10 min assumed in Ref. 03 (comp. calculation attached in Ref. 07.) (comp. Sec. 9.6).
10. Very little additional heat will go into the LNG until at least 80% of the insulation is destroyed (about 24 cm). Pressure built up will therefore start only after this point is reached. (comp. Sec. 9.6) Even in the case of a fire with an initial heat flux of  $300 \text{ kW/m}^2$ , this will be more than 25 min after fire initiation.
11. It can be concluded that the insulation will not be completely destroyed by a fire caused by a  $5 \text{ m}^2$  hole according SANDIA report assumptions. The theoretical time available for the fire must be 30 min or more. This limits the hole

size to holes below 2 m<sup>2</sup> even for 300 kW/m<sup>2</sup> initial heat flux. It is considered unlikely that such a hole will create an enveloping fire (comp. Sec. 9.7).

12. The more realistic cases of fires with initial heat flux of 88 and 108 kW/m<sup>2</sup> will not be able to heat up the weather cover to a temperature where the cover may sustain local deformation if a 5 m<sup>2</sup> or greater leak in the damaged tank is assumed. The heat fluxes must be 200 kW/m<sup>2</sup> or greater to have this effect. With 108 kW/m<sup>2</sup>, the maximum hole size which will lead to a temperature of approx 1023 K at the weather cover is 3 m<sup>2</sup>. For 88 kW/m<sup>2</sup> the hole size is even smaller (comp. Sec 9.7). It is not considered likely that such fires will be able to envelope the tank.
13. Failure of the support structure (skirt) can be excluded from further consideration even for very high heat fluxes into the cover (300 kW/m<sup>2</sup>) (comp. Sec 9.8).
14. The actual time dependent heat flux of an LNG fire is crucial for a complete understanding of the effect of fire on the containment system. While there is a high level of confidence in the analytical work that has been carried out in this review, this can only be determined by a pool fire test. The tests should determine:
  - the actual heat flux of the LNG fire
  - the actual emissivity during the phases of the test
  - the melting rate, melting behaviour, and properties of melting insulation material.

One such test agenda was proposed to the WG and was regarded to be adequate to address these unknown factors. However, it was considered that conducting or overseeing such testing was beyond the scope of the WG..

## 6.9 Literature for this Section

Ref. 01 Prof.-Dr. Stephan Kabelac, Dr. Gerd Würsig, Dipl.-Ing. Malte Freund; Thermodynamic Boundary Conditions, Report, Helmut Schmidt University Hamburg, Germanischer Lloyd Hamburg, Hamburg 2007-11-07

Ref. 02 Benjamin Scholz, CFD Modelling of the Heat Flux into an LNG Ship Tank, Master Thesis, University of Rostock, Institute for Fluid Dynamiks, Rostock June 2008 (German language)

Ref. 03 Prof Jerry Havens, Prof. James Venart; Fire Performance of LNG Carriers Insulated with Polystyrene Foam; Journal of Hazardous Materials; electronically published February 2008, HAZMAT-7824, 7 pages

Ref. 04 SIGTTO Working Group on LNG Fire: Thermodynamic Boundary Conditions; presentation at 4<sup>th</sup> WG meeting in New Jersey, 2007-11-13/14<sup>th</sup>, Gerd Würsig

Ref. 05 Sandia National Laboratories; Guidance on Risk Analysis and Safety Implications of a Large Liquefied Natural Gas (LNG) Spill Over Water, Printed December 2004

Ref. 06 ABS Technical Report TR-2007 -020 Coupled Thermal-Stress Analysis on Cover Dome in Moss-Type LNG Carrier.

Ref. 07 Calculation of heat absorption of the insulation: Recalculation of Havens, Venart assumptions and additional heat up of styrene to melting temperature, GL internal note, Gerd Würsig, Benjamin Scholz, July 2008

Ref.08 DOE/Sandia National Laboratories Coordinated Approach for LNG Safety and Security Research – Briefing to NARUC Staff Subcommittee on Gas July 15, 2007.



# **TIME BASED HEAT TRANSFER**



## 7.1 One-Dimensional, Transient, Heat Transfer Analysis

A transient heat transfer analysis<sup>1</sup> was made to estimate the time at which complete melting to the tank wall of the insulation could occur, and the potential for fire and or explosion of the vapour/air mixtures formed under the Moss sphere's steel weather cover following the melting/degradation process were considered.

This report expands on earlier work on heat transfer analysis, particularly the following:

1. Consideration of the credit that should be allowed for limitation of the heat flux to the insulation foam surface, and ultimately to the cargo, by the presence of the steel weather cover.
2. Provision of additional information obtained from the peer-reviewed literature and our own continuing research on the thermal degradation properties of polystyrene foam required to more accurately estimate the expected PS foam surface recession rate as a function of incident heat flux; and new COMSOL calculations of the total time required to completely fail 30 cm of polystyrene foam insulation following exposure of an undamaged Moss sphere to the LNG fire scenario under consideration by the working group.

The COMSOL Multiphysics® Heat Transfer Module and Moving Mesh Modules<sup>2</sup> were used to perform a one-dimensional analysis of the thermal response of a unit area section of a Moss sphere (assumed flat) in which fire (R1) is contacting the steel weather cover (R2), followed by serial resistances representing the air gap (R3) between the cover and the aluminium foil covering the insulation, the aluminium foil (R4) covering the insulation, the insulation (R5), and the inner aluminium tank wall (R6), which is in contact with LNG (R7).

Table 7.1 specifies the properties of the resistances R2-R6 assumed for the analysis.

**Table 7.1: Specifications and Thermodynamic Properties of System Components**

Zone	Thickness (m)	Density (kg/m <sup>3</sup> )	Heat Capacity (J/kg °K)	Thermal Conductivity (W/m °K)	Emissivity	Failure Temperature (°K)
R2	0.015	7850	475	44.5	0.85	810
R3	1.0	COMSOL®	COMSOL®	COMSOL®	NA	NA
R4	0.0003	2700	900	70	0.1, 0.5	873
R5	0.30	26.5	1045	0.038	NA	510
R6	0.02	2700	904	70	NA	873

The following sections describe the initial conditions assumed for the analysis and the boundary conditions interconnecting the resistances specified in Table 1 as well as the boundary conditions connecting the fire (R1) to the steel cover (R2) and the aluminium tank wall (R6) to the LNG (R7).

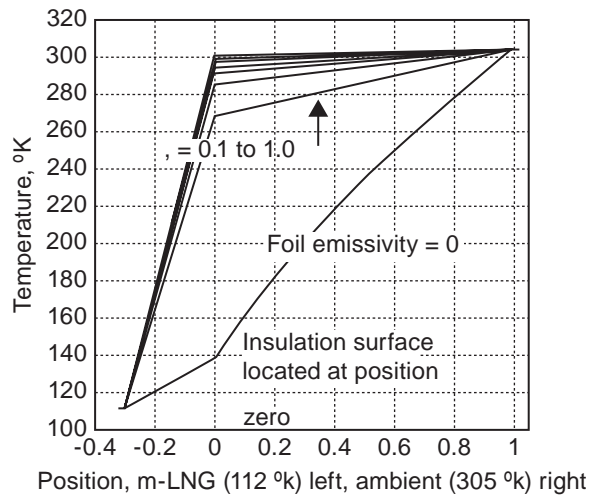
### 7.1.1 Initial conditions

The initial-condition temperature profile for the one-dimensional system was calculated with a steady-state COMSOL® analysis assuming an ambient air temperature of 305°K. Figure 7.1 shows the temperature profile through the system with aluminium foil emissivity specified as a parameter, illustrating the sensitivity of the heat transfer calculations to the emissivity of the aluminium foil covering the insulation. Figure 7.2 shows the heat flux into the cargo with the foil emissivity as a parameter. For an emissivity of 0.1 (assumed appropriate for a new, clean system) the heat flux into the cargo is approximately 20 W/m<sup>2</sup>. For a 36 m diameter Moss sphere, this heat flux to the cargo at ambient conditions (305°K) would result in a boil-off rate of ~ 0.12% of the cargo per day. This result, which is in good agreement with typical specifications for operating Moss-design carriers, provides a useful check on the propriety of the heat transfer calculation methods utilised in the analysis.

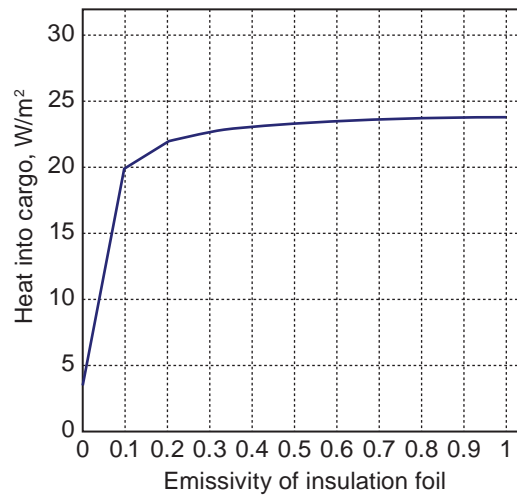
<sup>1</sup> Havens, J. and J. Venart, "Fire performance of LNG carriers insulated with polystyrene foam," Journal of Hazardous Materials; electronically published February 2008, HAZMAT 7824, 7 pages.

<sup>2</sup> The COMSOL Multiphysics Heat Transfer Module solves partial differential equation systems representing combinations of conduction, convection, and radiation heat transfer. WWW.COMSOL.COM.

**Figure 7.1: Initial Temperature Profile Figure**



**7.2: Operating Heat Flux into Cargo**



### 7.1.2 Boundary conditions

Radiative heat transfer (assuming grey body properties) and convective heat transfer ( $h = 28 \text{ W/m}^2 \text{ }^\circ\text{K}^3$ ) from the flame to the weather cover were accounted for. Radiative heat transfer and conductive heat transfer were accounted for in the air space under the weather cover; convective heat transfer in that space was neglected. The temperature profiles at the interfaces R4/R5, R5/R6, and R6/R7 assumed continuity (infinite heat transfer coefficient assumed from the tank wall to the LNG). Calculations were made for flame temperatures of 1300, 1400, and 1500°K, corresponding to calculated initial (maximum) total (black-body radiative and convection) heat fluxes from flame to the steel weather cover (with emissivity = 1.0) of 188, 245, and 315 kW/m<sup>2</sup> respectively; values that bracket the range of experimental SEP obtained in LNG pool fires.

### 7.1.3 Results

The time-varying temperatures and heat fluxes throughout the system were calculated with the properties specified in Table 1 for flame temperatures of 1300, 1400, and 1500°K and aluminium foil emissivities of 0.1 and 0.5, the latter representing the range of emissivities that might be expected for new clean aluminium foil and dirty aged aluminium foil respectively. All initial calculations assume that the materials (including the insulation) remain in place and function with the properties specified above. The primary purpose of these initial calculations was to estimate the times at which the components of the tank system would reach temperatures sufficient to cause failure and to facilitate estimation of the time period expected for complete failure of the insulation. These calculation results are not applicable for greater times.

It was assumed for the purposes of this analysis that failure of the steel and aluminium components of the system would begin once the designated failure temperature had been reached, and initially it was assumed that the minimum rate at which the polystyrene insulation would fail would be determined by its melting rate, which would in turn be determined by the heat flux into the foam at the time at which the foam reached its melting temperature.

Figures 7.3 – 7.5 show, as a function of time for 600 seconds of fire exposure, temperatures of the steel weather cover (wc) surface (contacting flame with,  $\epsilon = 0.85$ ) and the (hot-side) insulation (ins) surface, as well as the heat flux into the insulation surface, for aluminium foil emissivities of 0.1 and 0.5, for flame temperatures of 1300, 1400, and 1500°K.

<sup>3</sup> Welker, J.R., and C.M. Sliepcevich, Heat Transfer by Direct Flame Contact Fire Tests – Phase I. Prepared for the National Academy of Sciences by University Engineers, Inc., Norman, Oklahoma, 1971.

Figure 7.3: Temperature and Heat Flux – wc Solid, ins Dashed –  $T_{fire} = 1300 \text{ }^\circ\text{K}$

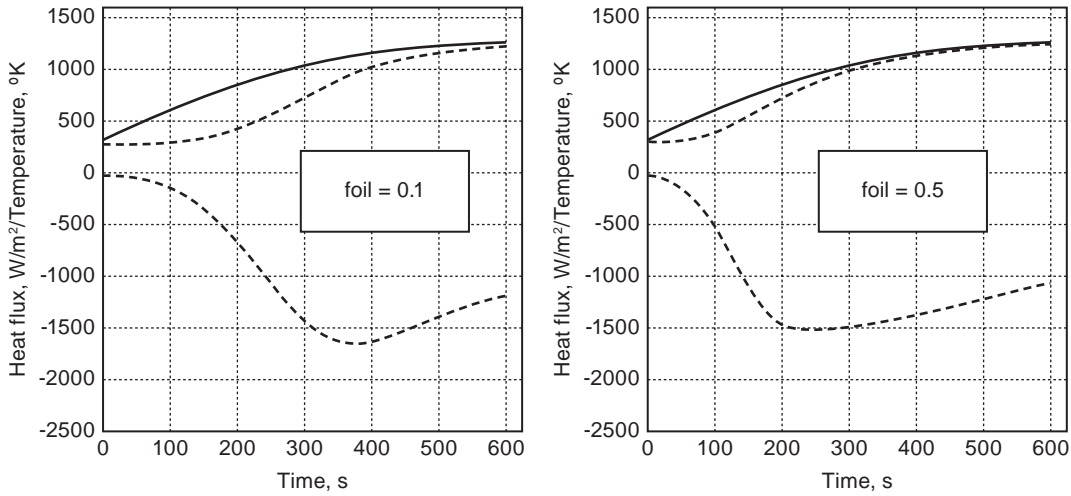


Figure 7.4: Temperature and Heat Flux – wc Solid, ins Dashed –  $T_{fire} = 1400 \text{ }^\circ\text{K}$

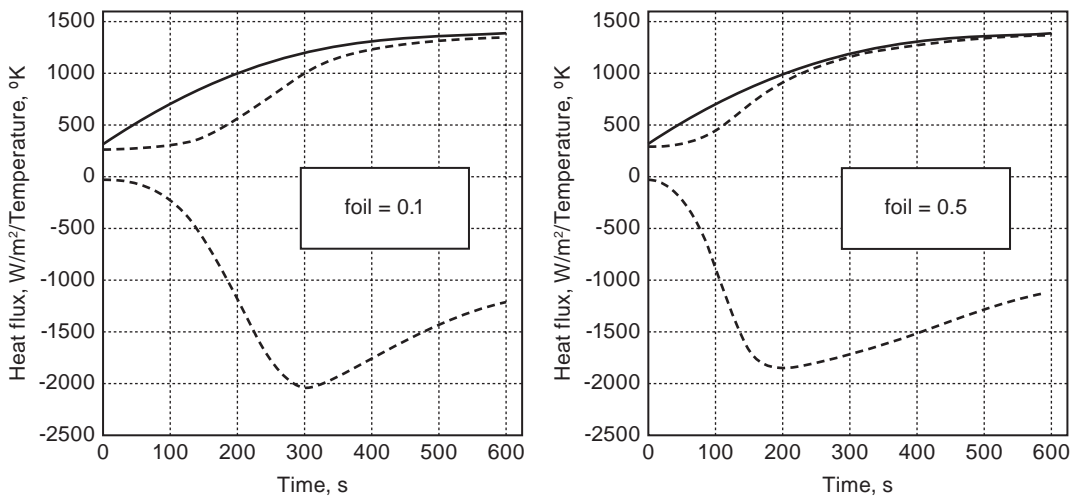
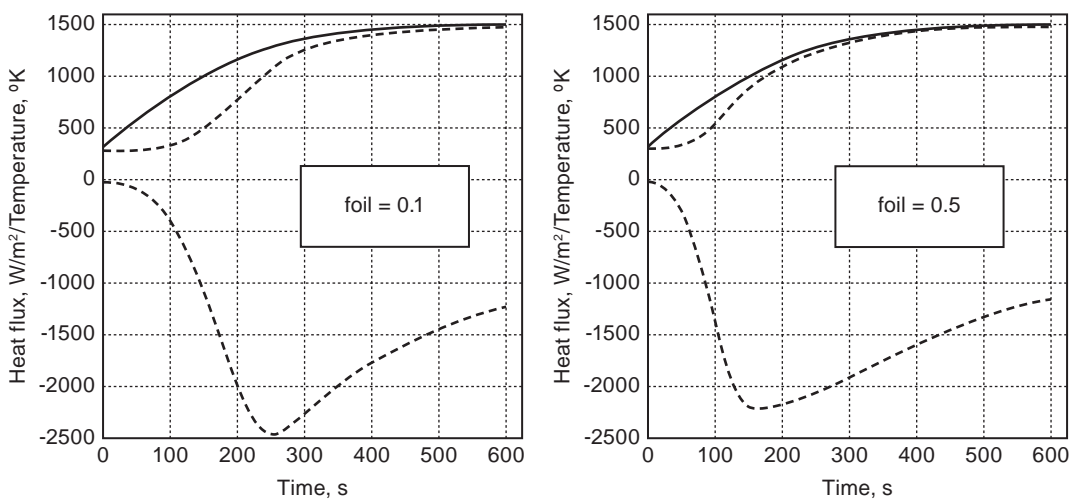


Figure 7.5: Temperature and Heat Flux – wc solid, ins dashed –  $T_{fire} = 1500 \text{ }^\circ\text{K}$



## 7.2 Predicted Component Failure Commencement Times

Table 7.2 shows the estimated times, from the plots in Figures 7.3 – 7.5, for the (outer) steel weather cover surface, the aluminium foil, and the polystyrene foam insulation (hot-side) surface to reach the failure temperatures designated in Table 7.1. Because of the thickness of the aluminium foil (0.3 mm), the temperatures of the foil and the insulation (hot-side) surface were assumed identical for this analysis.

**Table 7.2: Predicted Component Failure Times (seconds)**

Component	$T_{\text{fire}} = 1300 \text{ °K}$		$T_{\text{fire}} = 1400 \text{ °K}$		$T_{\text{fire}} = 1500 \text{ °K}$	
	= 0.1	= 0.5	= 0.1	= 0.5	= 0.1	= 0.5
Weather Cover	170	180	125	125	100	100
Aluminium Foil	330	260	265	180	215	150
Foam Insulation	225	140	190	120	160	95

### 7.2.1 Metal failure

The temperature of the steel outer surface reaches 810 °K, indicating approach to failure, in the range 100 seconds to 180 seconds. The time when the aluminium foil reaches its melting temperature (873 °K) ranges from 150 seconds to 330 seconds. To calculate more accurately the actual response of the system is difficult, requiring assumptions as to the specific behaviour of the system components as they fail (see Section 7.3 for new results). Nevertheless, inclusion of such information for specific failure modes would appear to only increase the rapidity with which the system components would fail.

### 7.2.2 Insulation failure

The polystyrene surface temperature reaches its (assumed) melting point of 510 °K in the range 95 seconds to 225 seconds. Following the time at which the polystyrene foam reaches its melting temperature, the heat flux into the foam insulation maintains an average value ranging from about 1 to about 1.5 kW/m<sup>2</sup> for the balance of the 10 minute period shown. If the temperature of the solid insulation could not rise above its ‘melting point’, the heat flux into the foam surface would be expected to increase because the inner tank cover surface temperature is continuing to rise while the moving melting front remains at (essentially) constant temperature. However, the calculation results presented in JHM HAZMAT 7824 did not provide for modelling any phase changes of the insulation material. Therefore, assuming a continuous heat flux of 1.5 kW/m<sup>2</sup> into the foam surface, which was thought to be conservative for the reason just described, the foam was estimated to melt at a rate (approximately) given by 1.5 kW/m<sup>2</sup> divided by the product of the foam density and its latent heat of fusion. Because of lack of data for polystyrene foam we used the latent heat of fusion for styrene monomer (105 kJ/kg) along with the density of polystyrene foam (26.5 kg/m<sup>3</sup>) to estimate a melting rate of about 3 centimetres per minute. As stated in HAZMAT 7824, we believed that this should be a rough lower limit on the melting rate because the latent heat of polystyrene (mass basis) could be (much) smaller, depending on the molecular weight of the polymerized styrene<sup>4</sup>. Nonetheless, this preliminary analysis indicated that total melting of a polystyrene insulation layer 0.3 m thick could occur less than 10 minutes after it reaches its melting temperature if the foam were subjected to such intense heat exposures as considered here.

### 7.2.3 Insulation combustion

This analysis has not considered the potential for combustion of (poly) styrene vapours mixed with air in the space between the weather cover and the insulation surface. Both the IGC Code and 46 CFR 54 require, in order to take credit for the insulation in PRV sizing, that the insulation on the above deck portion of tanks have approved fire proofing and stability under fire exposure. It is noted that the IGC Code considers the weather-cover an extension of the deck. Polystyrene foam, as currently installed on LNG carriers, does not appear to meet these criteria. Even if the exterior fire were isolated from the foam (by an intact weather cover), ignition of these flammable vapours appears highly likely given the relatively low auto-ignition temperature of styrene monomer (~760 °K) and the fact that only about 1 mm thickness of the insulation would have to vaporise to raise the average vapour concentration in the air space under the weather shield above the lower

<sup>4</sup> See “Update on Issues Remaining”, following.

flammable limit. Given the flue-like configuration formed by the space between the cover and the insulation, the volume of air in that space, and the potential for failure of the steel weather cover that would admit additional air, there is a potential for rapid burning of the insulation material<sup>5</sup> even if the ignition of the vapours prior to the steel weather cover failing did not result in an over-pressure that failed the cover instantly.

## 7.3 Update on Issues Remaining – Appropriate Values of the Environmental Factor $F_1$ to Account for Radiation Shielding by the Tank Cover

As described in the report to the WG and the manuscript accepted for publication by JHM, we compared the equation prescribed for the determination of relieving capacity by the IGC:

$$Q = FGA^{0.82} \quad (1)$$

where

- Q = Relief Valve Required Flow Rate
- F = Fire Factor
- G = Gas Factor
- A = External surface area

with an alternate equation recommended for consideration in a National Academy of Sciences Report to the U.S. Coast Guard<sup>6</sup>:

$$Q_H = qF_1EA \quad (2)$$

where

- $Q_H$  = total heat absorbed by the cargo
- q = heat flux to the outside of the bare container (direct exposure)
- $F_1$  = environmental factor, including insulation and radiation shielding
- E = exposure factor, the fraction of the total tank area (A) exposed to fire
- A = tank surface area

For a Moss sphere LNGC tank (insulated independent tank in hold), the fire factor F in Equation (1) is equal to 0.2, per IGC. The Gas Factor, G, in Equation (1) incorporates the values of heat flux implicitly prescribed in the IGC code as well as combined factors relating to the determination of flow through the relief valve. Equation (1) incorporates the value of only 71 kW/m<sup>2</sup> for heat flux, representing the heat flux to the cargo under conditions of direct (gasoline/kerosene) pool fire exposure to the bare containment. For the present argument, let us call this heat flux  $q^\circ$ , setting aside for the moment the question of the value appropriate for an engulfing LNG fire. Since the 'Gas Factor' in Equation (1) is directly proportional to  $q^\circ$  ( $G = Kq^\circ$ ), Equation (1) becomes

$$Q = Kq^\circ FA^{0.82} \quad (3)$$

Alternatively, using Equation (2) to calculate  $Q$ , where  $Q_H = Q/G = Q/Kq^\circ$ , we have

$$Q = Kq^\circ F_1EA \quad (4)$$

<sup>5</sup> Zicherman, J., Fire Performance of Foam-Plastic Building Insulation, Journal of Architectural Engineering, September 2003.

<sup>6</sup> "Pressure Relieving Systems for Marine Cargo Bulk Liquid Containers," Committee on Hazardous Materials, Division of Chemistry and Chemical Technology, National Research Council, NAS, 1973. It should be noted that members of this committee included representatives from industry and academia, as well as from the insurance industry and regulatory agencies (U. S. Coast Guard).

Since the expression  $Kq^\circ$  is common to Equations (3) and (4), it is the expressions  $FA^{0.82}$  and  $F_1EA$  that should be compared. We believe this is where the problem with the IGC Code equation (Equation (1)) lies. We have studied the history of the development of Equation (1) and point out the following facts, which appear to be of critical importance.

- The factors  $F$  in Equation (1) and  $F_1$  in Equation (2) are not equal:
  - $F$  in Equation (1) accounts for a combination of ‘environmental factors’, which lump together insulation and radiation shielding factors, in the present case protection due to insulation, radiation shielding by the weather cover, and shielding (by the double hull configuration) due to placement of the tank in the hold (below deck level). The factor is empirically assigned, here 0.2, per IGC
  - $F_1$  in Equation (2) accounts for ‘environmental factors’, but here it is clearly intended to account only for the effect of insulation and the radiation shielding afforded by the tank weather cover, it does not account for determination of the fraction of the tank surface that is exposed to fire (or protected by being in the hold). Consequently,  $F_1$  should be set equal to 1 in the absence of both insulation and shielding by the weather cover
- the factor  $E$  in Equation (2) specifies the fraction of the tank surface area exposed to fire. For the Moss sphere, the most critical area is the portion of the tank above main deck – we assume that 40% of the tank area is above deck. The appropriate value of  $E$  in Equation (2) is then 0.4.

Consequently, independent of the value used for the expression  $Kq^\circ$ , the ratio of the relieving capacity indicated by formulas (1) and (2), for a 36 m diameter Moss sphere (Area = 4072 square metres), is:

$$(0.4) (4072) F_1 / 0.2 (4072)^{0.82} = \sim 9 F_1$$

As stated in our report to the WG and in our JHM paper, this means that even if the same heat flux is used (in both formulas), the value of the factor  $F_1$  accounting for insulation and shielding by the weather cover in Equation (4) must not be greater than  $\sim 0.1$  in order that the required relief capacity be as small as indicated by the method currently required by the IGC. Conversely, total loss of insulation and weather cover (radiation) shielding (on the part of the tank exposed to fire, ie, above deck) would result in under-prediction of the required relieving capacity by a factor of  $\sim 9$  (order of magnitude).

To determine the applicable value of  $F_1$  to account for the reduction in heat absorbed by the cargo due to the presence of the steel weather cover alone, without the insulation or its foil covering, steady state calculations were made with COMSOL® of the heat flux to the cargo for the following cases (configurations of the series resistances to heat transfer depicted in Table 1). As these calculations are intended to simulate the heat transfer to the cargo if the steel weather cover surfaces or the tank surface were directly exposed to the fire environment or to the degradation products of the insulation, their respective emissivities were set to 1.0.

1. Case 1 – R6 only. This configuration describes the direct exposure of the fire to the bare LNG tank wall. The appropriate value of  $F_1$  is 1.0.
2. Case 2 – R4 and R5 eliminated. This configuration describes direct exposure of the fire to the weather cover after the PS foam and its aluminium foil covering have melted away and the space occupied by the foam and foil filled with air (no consideration is given here to potential for combustion of the foam products). The appropriate value of  $F_1$  is then the ratio of the resulting heat flux to the cargo (Case 2), to the heat flux to the cargo if components of the insulation system and weather cover are absent, ie direct fire exposure to the LNG tank wall (Case 1).

For fire temperatures of 1300 – 1500 °K, the values of  $F_1$  ranged from 0.4 to 0.42, reflecting the non-linearity of the radiation heat flux boundary condition over the temperature range of interest.

## 7.4 Critical Update on Issues Remaining – Thermal Degradation Properties of Polystyrene Foam: New Results for the Estimated Time for Insulation Failure

There remained in our previous report to the WG important uncertainties about thermal properties of polystyrene foam critical to the estimation of the time to failure, including principally the melting temperature and latent heat of melting/degradation/vaporization. We have recently obtained additional information from the peer-reviewed literature for the thermal degradation properties of expanded polystyrene (EPS) foam used in the expendable pattern casting (EPC) process. Although there are numerous references to the thermal degradation properties of this particular polystyrene foam product and application, all we have found appear to be consistent with the data from Mehta, et. al.<sup>7</sup>, obtained with Differential Scanning Calorimetric (DSC) and Thermal Gravimetric Analysis (TGA) analyses of EPS foam:

<sup>7</sup> Mehta, S., S. Biederman, S. Shivkumar, “Thermal degradation of foamed polystyrene”, Journal of Materials Science, 30, 1995, pp 2944-2949.

Bead collapse temperature	110 -120 °C
Bead melting temperature	160 °C
Molecular weight	300,000 – 500,000
Density	24 kg/m <sup>3</sup>

As the temperature is increased beyond 110 °C the expanded beads begin to collapse and the average bead size decreases substantially. This collapse temperature range compares well with the glass transition temperature of polystyrene, which has been reported to range from 80 to 120 °C.

At 160 °C the beads completely melt to produce a viscous residue.

Volatilisation of the viscous residue begins at 278 °C and the polymer is almost totally volatilised at 460 °C.

DSC analyses yield a small endothermic peak between 90 and 120 °C, thought to correspond to the glass transition within the polymer.

DSC analyses yield a large endothermic peak between 320 to 490 °C. This endothermic peak, representing the heat of degradation, is estimated to be 912 J/g.

The total energy under the endothermic peak between 320 and 490 °C represents the sum of the energy (absorption) effects for vaporization and thermal degradation. The onset temperature of this endotherm is 320 °C, which is 160° above the melting temperature. There was detected no significant melting energy (latent heat of melting or fusion) in these experiments with polystyrene foam, as has been suggested might be anticipated, since most foam materials are amorphous polymers<sup>8</sup>. As the magnitude of the heat of degradation would have only secondary importance in determining the melting rate of the foam if the melted foam material runs off the vertically oriented surface of the insulation, this data indicated further potential for more rapid foam recession (failure) rates than were considered in our preliminary analyses.

Using the value of 912 j/g for the energy required to convert solid polystyrene foam at its melting point (assumed here to be 510 K) to vapour (melting and vaporization), from Mehta, et.al., and utilizing the Moving Mesh Module of COMSOL Multiphysics®, calculations have now been completed which we believe provide reasonable estimates of the times required for the complete failure of 30 cm of polystyrene insulation as currently installed on Moss sphere LNG containments. The new calculations incorporate the following specific changes and extensions of the calculations reported previously:

- The value 912 j/g, representing the energy required to convert the insulation to vapour form
- the melting temperature is assumed to be 510 K. For purposes of the calculation, the phase changes from solid to vapour are assumed to occur at 510 K
- the sensible heat (energy) required to heat the insulation from its initial condition to 510 K has been incorporated, assuming an (average) temperature increase of approximately 320 K to bring the insulation behind the moving front up to 510 K. The heat capacity reported in Table 1 has been used for these calculations.

The total time required to heat the surface of the insulation to 510 K and for the subsequent complete failure (change to vapor form) to a depth of 30 cm for flame temperatures of 1300, 1400, and 1500 °K (radiation heat transfer only) have been recalculated. As the results are sensitive to the emissivity values used, the aluminium foil emissivity was treated parametrically to estimate the potential for complete failure of the insulation in periods of order 10 minutes. The results are shown in Table 7.3.

**Table 7.3: Total Predicted Insulation Failure Times (minutes)**

Foil Emissivity	T <sub>fire</sub> = 1300 °K	T <sub>fire</sub> = 1400 °K	T <sub>fire</sub> = 1500 °K
0.1	28.8	21.8	17
0.3	14.7	11.4	9
0.5	11.6	9	7.2

The calculations indicate that for LNG fire temperatures ranging from 1300 K to 1500 K the insulation is subject to complete failure in time periods ranging from 7.2 minutes to 28.8 minutes, depending on the operative foil emissivity ranging from 0.1 to 0.5, even if the weather cover is undamaged and continues to provide radiation shielding.

We are continuing at the University of Arkansas (USA) and the University of New Brunswick (CA) our independent analyses, using further computational fluid dynamics modelling as well as laboratory experiments, of the dependence of failure rates of polystyrene foam insulation with fire-heat exposure.

<sup>8</sup> Caulk, D. A., 'A foam melting model for lost foam casting of aluminum', International Journal of Heat and Mass Transfer, 49, (2006), p 2124-2136.



# **RESPONSE OF INSULATION MATERIALS TO HEAT**



## 8.1 Thermal Loads on Insulation

If there is an external fire adjacent to an LNG carrier the temperature of the tank cover and the hull structure will rise and eventually expose the insulation surface to thermal radiations and extended temperature.

The inner hull temperature of a membrane carrier in a fire exposure is shown in Figure 8.1.

The expected temperature development of the insulation surface below the weather cover for a Moss carrier is shown in Figure 8.2.

The analysis was based on a one dimensional transient heat transfer model with a fire load of  $150 \text{ kW/m}^2$  and a flame temperature of  $1000^\circ\text{C}$ .

**Figure 8.1: Temperature Rise in the Inner and Outer Hull of a Membrane Carrier (or Below Main Deck of a Moss Carrier).**

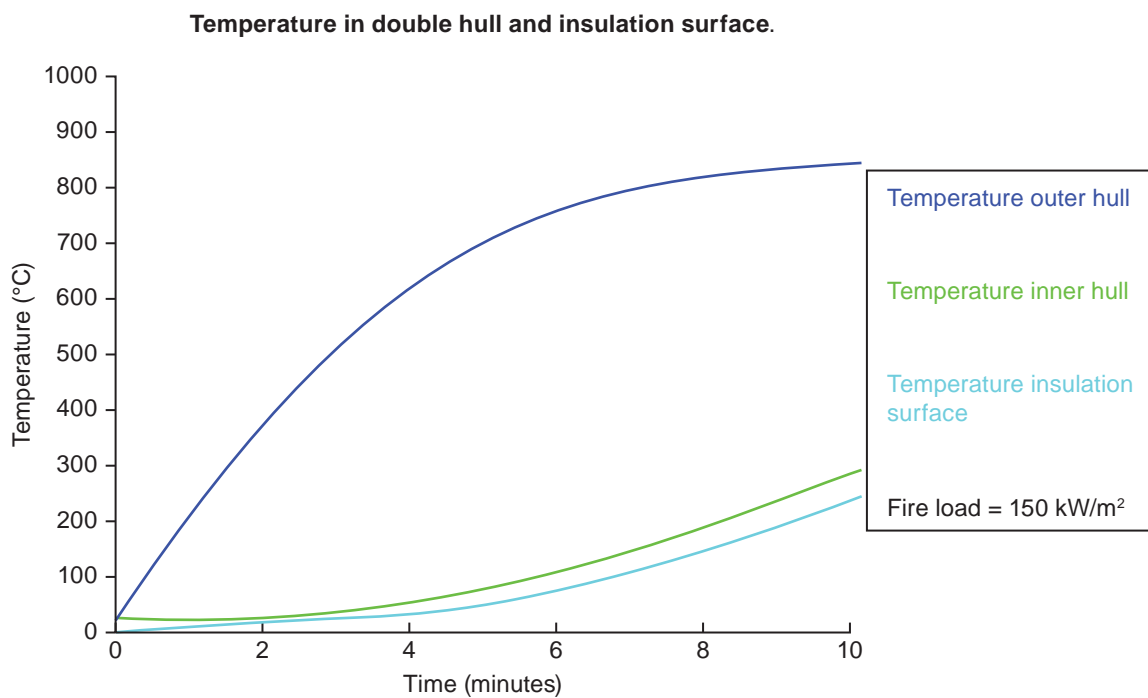
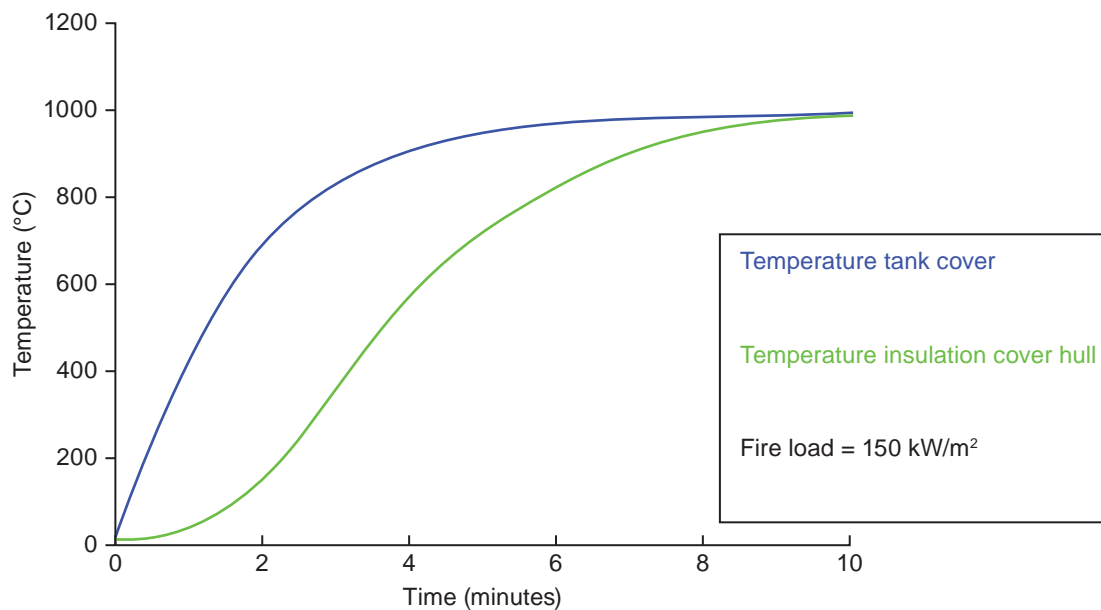


**Figure 8.2: Temperature Rise in the Tank Cover and the Insulation Surface on the Upper Part of a Moss Carrier**  
Temperature in tank cover and insulation top cover



These simple analyses show that the double hull structure for the membrane carriers and the bottom part of the Moss system offer efficient thermal protection of the insulation surface for 10-20 minutes, while insulation surfaces of the upper part of the Moss spheres will reach a temperature above 100 °C after approximately 1-2 minutes.

## 8.2 Thermal Effects on the Insulation

The cargo tank insulation on the majority of LNG carriers is based on expanded plastic foams or plywood boxes filled with perlite. The plastic foams are sensitive to heat while the perlite filled plywood boxes are considered more robust (the main concern would be the integrity of the fixings, not the deterioration of the insulation).

Two basic types of foams are being used:

- Thermopolymers (polystyrene, expanded PVC etc)
- thermosetting polymers (polyurethane foams).

Their responses to high temperatures are fundamentally different

- The thermo-polymers will start melting at a temperature between 100 and 150 °C. Initially a high viscosity liquid will form and the viscosity will reduce as the temperature increases. At significantly higher temperatures a chemical decomposition will start turning the liquid to solid decomposition products
- the thermosetting foams will not melt. At temperatures between 250-500 °C a chemical decomposition will occur. The foam will change to a solid charred layer.

In the tank insulation the foam material is an integral part of the insulation panels. Normally the surface facing the fire load will have an aluminium protection. The panel will be indirectly exposed to the fire load by radiation from the inner hull or the inner side of the weather cover. The effective radiation load on the insulation will be dependent on the temperature of the inner hull/weather cover and the emissivity of the insulation protection.

A progressing damage to the insulation requires that the fire load is transferred deeper and exposes the underlying parts of the foam. This requires that the decomposed parts of foams (melted foam or char) disappear completely and do not restrict the transfer of heat to the undamaged parts of the foam.

If the damaged parts of the foam do not disappear the remains (char or a melted layer) will effectively delay the degradation.

It is anticipated that the metallic foil protection on top of the insulation provides effective protection by:

1. Reflecting a large part of the heat load due to low emissivity.
2. Preventing melted foam or char to escape.

If the decomposed insulation products are not removed, the complete degradation of the insulation will not occur, or will require prolonged fire exposure (>hours).

Partly damaged insulation will provide an effective reduction of the heat transfer to the cargo and limit the amount of boil-off. The steady state heat transfer through a degrading insulation has been estimated as shown in Figure 3.

**Figure 8.3: Steady State (ie max) Transfer into the Cargo Tank as Function of Remaining Insulation Thickness.**

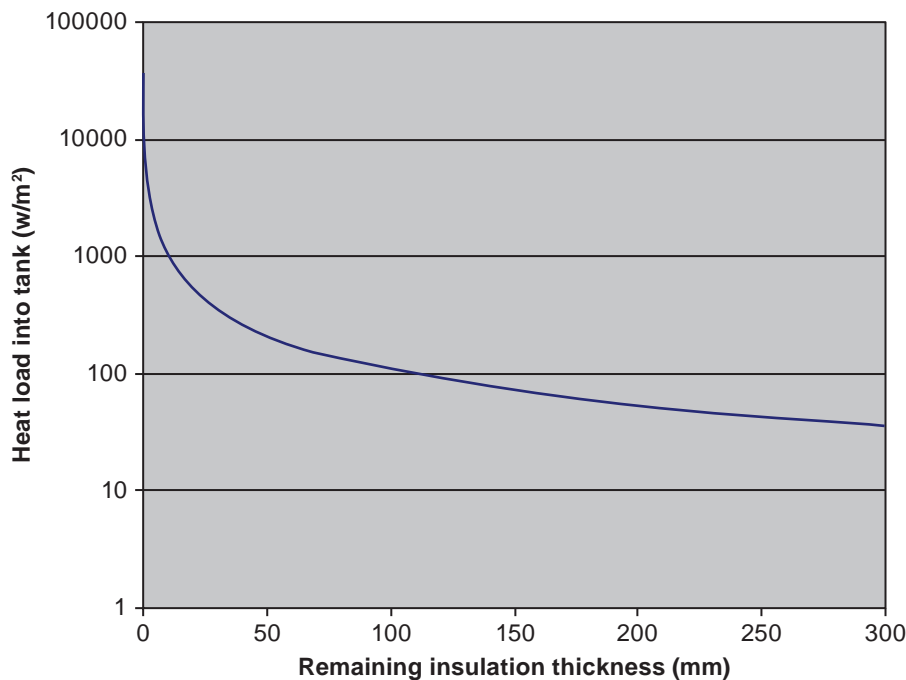


Figure 8.3 shows that any insulation or insulation products will protect the tank.

The key issue will therefore be if the fire load transmitted to the insulation is capable of being totally damaged and remove the insulation and the insulation cover.

We are not aware of a precise analytical model to predict the degradation of insulation material.

The above description of the failure mechanisms is based on results from experimental investigations carried out by DNV in the period 1975-1980.

## 8.3 Outline of DNV Test Programme

DNV conducted a series of tests of insulation material with the objective to determine the thermal damage to plastic foams exposed to high temperatures and radiant heat. The investigation was carried out in two parts.

Part one tested the extent of weight loss on decomposition; this was done by putting test pieces of insulation foams into an oven and the extent of weight loss measured. The procedure was followed for different times and temperatures in both air and inert atmospheres.

Part two tested the behaviour of the insulation foam as part of an insulation panel when exposed to radiation on one side only. In this way one could predict the behaviour of the insulation when a temperature gradient is present. These tests were conducted in conjunction with 'Firetechnical Laboratory', Technical University of Norway, Trondheim.

The first part of the tests demonstrated that the thermo-polymer started to shrink and gradually melted when the temperature was increased 100-150°C. The melted product was a high viscosity fluid and the viscosity reduced when the temperature increased.

The thermosetting foams did not melt. At temperatures above 200-300°C a chemical process started and the foam converted into a solid (but brittle) char.

It was realised that the remaining melted foam or charred parts of the thermosetting form could offer protection to the underlying foam and the objective of the second set of tests was to investigate these protective effects in inhibiting the degradation of insulation panels exposed to radiant heat loads.

The second test programme was performed exposing insulation panels with and without a metallic cover to radiant heat load for prolonged periods of time.

A propane gas heated steel plate (500 × 400 mm) served as radiation source (emissivity 0.8). The temperature of the plate was controlled by regulating the propane and air supply. The tests were carried out with a radiator temperature of up to 800°C, corresponding to a heat load of 75 kW/m<sup>2</sup>.

Each test panel (1400 × 1300 mm) was made up of 100 mm thick insulating material either glued (extruded polystyrene) or foamed in Situ (polyurethane) to a 1 mm thick steel plate. 11 panels were tested, 8 polyurethane and 3 extruded polystyrene. 3 polyurethane panels were tested without shield, 3 with Aluminium shield and 2 with galvanised steel shield. All the extruded polystyrene panels had aluminium shield.

The tests were carried out until a significant temperature increase was observed on the cold side.

The test of unprotected polyurethane with 75kW/m<sup>2</sup> lasted for 1 hour. All tests of panels with metallic surface protection had a typical duration of 3-4 hours before the temperature rise on the cold side was observed.

In all cases the foam thermally decomposed to varying degrees, but ignition did not occur.

It should be pointed out that the Aluminium foil and Galvanised steel plates were very effective in reflecting a large portion of the incident radiant heat. This indicates that the Al. foil/Galv. steel act as good thermal radiation barriers.

When polyurethane foam thermally decomposes char formation is initiated, covering the entire exposed area. This char did not burn and acted as an insulator

Extruded polystyrene behaved in a different way as this material melted and transformed into a rubbery or viscous substance. This substance covered the entire exposed surface, thereby protecting the underlying material.

### 8.3.1 Results

1. Critical temperatures for the polyurethane and polystyrene (expanded and extruded) were around 200°C and 100°C respectively. Below these temperatures no significant deterioration of mechanical or thermal properties occurred.
2. The results are conservative as the effects of cooling from the cargo (and the initial low temperature in the foam) was not included.
3. These tests were conducted in a small scale. The effects of scaling are not known and there might be some questions about what might happen to the reflecting barrier when considered on a bigger scale.
4. One test was conducted where the entire surface was exposed to radiant heat to see if the insulation would fall off under action of its own gravity. The result was positive, ie the insulation did not fall off.
5. Aluminium foil and galvanized steel plates acted as very effective reflecting barrier.
6. Test result part one shows that inert atmospheres do not have any significant effect on weight loss on decomposition. It is, however, likely that inert atmosphere may have positive effects on fire propagation in non self-extinguishing insulation; but the same effect (without inert gas) is obtained when the insulation is self-extinguishing. It is important to note that ignition never occurred in part two of the tests.

## **DISCUSSION**



During the progression of the working group studies it became clear that, for this complex issue of how a large fire scenario may a) emit heat to a high sided vessel and b) affect the internal materials and structure of an LNG carrier, there were many areas of uncertainty. The studies presented capture both steady state and time based calculations, the basis of which rely on knowledge of, or assumptions for, fire scenario conditions.

Given the uncertainty existing within the industry over large pool fire Surface Emissive Powers and how these are likely to impact a carrier structure, it was not possible to gain unanimous agreement in all respects. However, the vast majority came to agree with the conclusions and recommendations made in chapters 10 and 11.

## 9.1 Steady State Conditions

Full agreement was achieved on the steady state conditions, which indicate that in the extreme case of losing the entire insulation layer, then assuming that the factors included in the IGC Code for sizing the relief valves, the valves are capable of relieving the anticipated vapour albeit at raised tank pressures that can be withstood by the cargo tanks. Additionally, this relief valve capability can, as well as loss of insulation, also comfortably accommodate the further extreme case of complete loss of the weather cover of a Moss type LNG carrier.

The above observations include reliance on two elements included in the IGC Code method for deriving pressure relief valve sizing:

- a) That the Fire Factors assumed in the IGC Code are valid, particularly for environmental factors. The full working group agreed that they were valid. An exhaustive search by the working group members revealed no calculated basis for the Fire Factors, but were based on industry experience and determined by the developers of original GC Code, the predecessor of the IGC Code, in the 1970s.
- b) Surface Emissive Power assumed by the IGC Code are valid. Study by the working group revealed that this value (see chapter 2) is used by many similar codes in the wider industry such as CGA and API. However, this value has been challenged for larger LNG fires and large pool fire tests have been commissioned by the USA Department of Energy (DoE). The working group recognised this uncertainty and, despite an extensive examination of previous industry studies, could not conclude that an alternative, definitive value should instead be used and therefore led to the inclusion of Recommendation 1. It was also recognised by the group that considering the inclusion of this value for heat input in many codes and standards in the hydrocarbon process industry, pool fire tests could potentially impact all of these codes.

For steady state conditions, no credit or account has been made for either the pressure relieving capability of the vapour header or the ability to apply the water deluge and fire fighting system onboard an LNG carrier, ensuring that the conclusions of the studies and this report are conservative.

## 9.2 Time Based Conditions

Heat transfer and CFD calculations were performed, a review of previous studies on insulation tests was undertaken and further insulation heat tests were performed. These are set forth in chapters 6, 7 and 8 and in Appendices 2, 3, 5, 6 and 7. A range of times for complete degradation of insulation were indicated through the various studies and tests such that definitive time could not be arrived at due to the conflicting evidence and differing views of the working group members. For this reason, Recommendation 2 is made.

## 9.3 Decisions and Agreement of the Working Group

Despite the studies carried out above and given the recommendations made, unanimous agreement could not be arrived at by the entire working group. However, complete agreement was reached for conclusions 1, 2, 3, 4, 5 and 6. The vast majority agreed with conclusions 7, 8 and 9, leaving only professor Havens not in agreement.

Recommendations 1 and 2 were agreed.

In addition, and although not raised at any working group meeting, the compliance of cargo tank polystyrene insulation materials was challenged due to a lack of fire resistance, although no specific paragraph of the IGC Code could or would be referenced in this respect. It was the opinion of the group that this stood outside of the working group Terms of Reference and that it is the remit of a regulatory body to assess this and that it has done so bearing in mind the historical continued certification of such materials over the past 35+ years. Given that the IGC Code is under review at the time of writing, this can be addressed at this time.

## **CONCLUSIONS**



1. IGC formula and methodology for LNG carrier relief valve sizing compares favourably and is consistent with similar codes such as API, CGA, EN, ISO and NFPA.
2. For the Moss design tank with polystyrene based foam insulation, assuming the worst case scenario of losing the entire insulation effect, the tank pressure will rise to a level that can be accommodated by the tank structure without failure. This is due to the capability of the LNG carrier relief valves to relieve far higher gas flow capacities with rising tank pressure, as indicated by calculations based on the methodology prescribed by the IGC code.
3. Further to 2; due to the capability of the relief valves to accommodate greater gas flows with rising tank pressures and assuming the worst case of cargo tank cover damage and loss of heat shielding due to the possibility of combustion of the insulation and degradation of products causing over-pressures sufficient to fail the tank cover, the relief valve capacity is still sufficient to prevent over-pressure failure of the tank.
4. In addition to conclusions 2 and 3, where even if the entire insulation was lost and the tank cover was completely lost, the capacity of the relief valves can accommodate a further estimated 30% rise in heat flux from a surrounding fire above that contained in the codes referred to in 1.
5. The limit of relief valve capability is the 'choke point' at which no further increase of gas flow can be accommodated through the RV vent system. This is approximately at 4.3 barg.
6. The presence and use of the vapour header will provide further pressure relief via the assumed damaged (holed) cargo tank and the forward vent riser. However, this has not been relied upon for the protection of the cargo tank against over pressure in the points above. The extent to which the vapour header contributes to pressure relief will depend on the fire scenario.
7. The response of the insulation system to heat, with time, is unclear; a detailed understanding of rates of insulation degradation and recession was not available for the structural arrangement of an LNG carrier. One dimensional CFD/heat transfer calculations made by the working group indicated time periods of 10 minutes for a complete degradation to a depth of 30 cm. Conversely, other studies in this report result in a degradation time of up to 29 minutes. Additionally, reports from physical tests carried out in the 1970s indicate time periods of greater than 2 hours, although in these tests, the conditions did not entirely accurately reflect actual LNG carrier dimensions or heat source temperatures.
8. From the behaviour tests of polyurethane foam under heat in an N<sub>2</sub> inerted atmosphere, insulation properties and strength are retained such that the concern for complete failure by degradation under fire conditions is likely to be substantially less for polyurethane based materials.
9. Based on experience from earlier fire incidents and studies included in the report, the tank cover is not likely to collapse under fire loads. It should be noted that the ABS study did not take into account the effect of the water-spray system required under 11.3 of the IGC Code.



## **RECOMMENDATIONS**



1. If large scale LNG fire tests are carried out by Sandia, or others, that show significant conflict with existing values of heat flux used in the IGC Code and other industry codes and standards, the question of the current equations for determining fire-case pressure relief loads merit re-examination by the whole LNG industry and not just the shipping element.
2. Although the working group has determined that current polystyrene foam insulated Moss sphere LNG carriers are equipped with pressure relief valves that provide additional capacity to prevent failure by over-pressure of intact cargo tanks, a better understanding of the foam plastic insulation vulnerability to heating is required to adequately assess the hazards that could result from loss of insulation effectiveness with fire exposure. Given the comparatively short duration of LNG fires as estimated by previous fire scenario studies, a much better understanding of the temporal response of foam plastic insulation materials is necessary to determine the worst case circumstances as referred to in the conclusions above. Further research, which should include physical insulation testing as well as a determination of the potential for additional damage due to combustion of the foam degradation products, is recommended.



## **APPENDIX 1 – MOSS TANK COVER RESPONSE TO HEAT**

## **Appendix 1 – Moss tank cover response to heat**



**TECHNICAL REPORT**

**TR-2007-020**

Coupled Thermal-Stress Analysis on Cover Dome in Moss-Type LNG Carrier

**November 2007**

**American Bureau of Shipping  
Incorporated by Act of Legislature of  
The State of New York 1862**

**Copyright © 2005  
American Bureau of Shipping  
ABS Plaza  
16855 Northchase Drive  
Houston, TX 77060 USA**

**RESTRICTION ON DISTRIBUTION AND DISCLOSURE**

**As noted on the cover, this is a proprietary document of the American Bureau of Shipping. Further distribution of this document in whole or in part, and/or disclosure of the contents thereof, are not to be made without written consent of an authorized representative of the American Bureau of Shipping.**

## Coupled Thermal-Stress Analysis on Cover Dome in Moss-Type LNG Carrier

Note: Unit System in this report is kg, m, s, N, Pa

### Material Properties

#### 1. Conductivity Temp

51.9	20
50.7	100
48.9	200
47.9	300
42	500
30	700
26	900
25	1100
23	1300
21	1500
19	1700
17	1900

#### 2. Density

7800

#### 3. Young's Modulus Poison's Ratio Temp

2.05E+011	0.292	20
1.95E+011	0.292	100
1.85E+011	0.292	200
1.75E+011	0.292	300
1.65E+011	0.292	400
1.55E+011	0.292	500
1.25E+011	0.292	600
5E+010	0.292	700
5E+009	0.292	800
1E+008	0.292	850
100000	0.292	1000
1000	0.292	1200
50	0.292	1400
50	0.292	2000

## 4. Expansion Coefficient

1.38E-005

## 5. Inelastic Heat Fraction

0.98

## 6. Plastic-isotropic

Yield Stress Plastic Strain Temp

3.5E+008	0	20
3.5E+008	0.2	20
3.5E+008	2	20
3E+008	0	200
3E+008	0.2	200
3E+008	2	200
2.5E+008	0	400
2.5E+008	0.2	400
2.5E+008	2	400
2.2E+008	0	600
2.2E+008	0.2	600
2.2E+008	2	600
8E+007	0	800
8E+007	0.2	800
8E+007	2	800
1E+006	0	1000
1E+006	0.2	1000
1E+006	2	1000
10000	0	1200
10000	0.2	1200
10000	2	1200

## 7. Specific Heat Temp

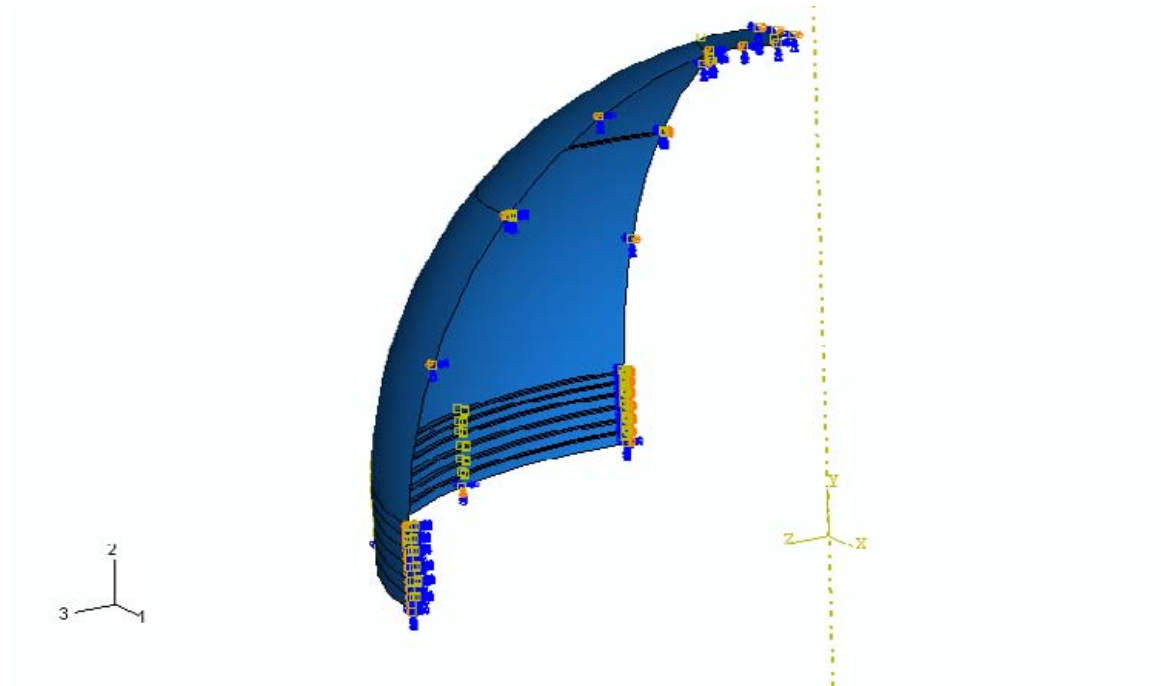
450	20
470	100
510	200
640	500
740	600
830	700
1500	750
820	800
530	900
400	1200

**Boundary Conditions:**

Bottom: Vertical translation and all rotations are constrained

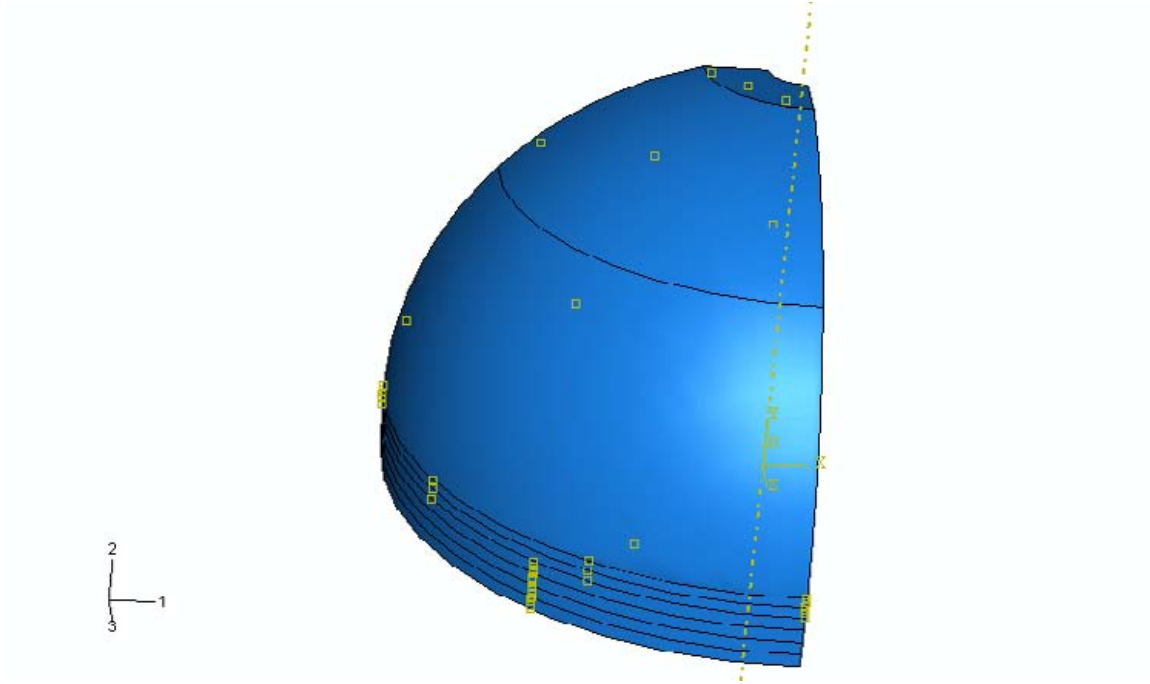
Quarter Model: Two symmetric conditions with respect to 2-3 plane and 1-2 plane, respectively

Initial Temperature: Room (20 C) at all surfaces of components



**Radiation Condition on Outside Surface:**

Outside surface to ambient: Emissivity: 0.8, Ambient Temperature: 20 C



**Loading Conditions:**

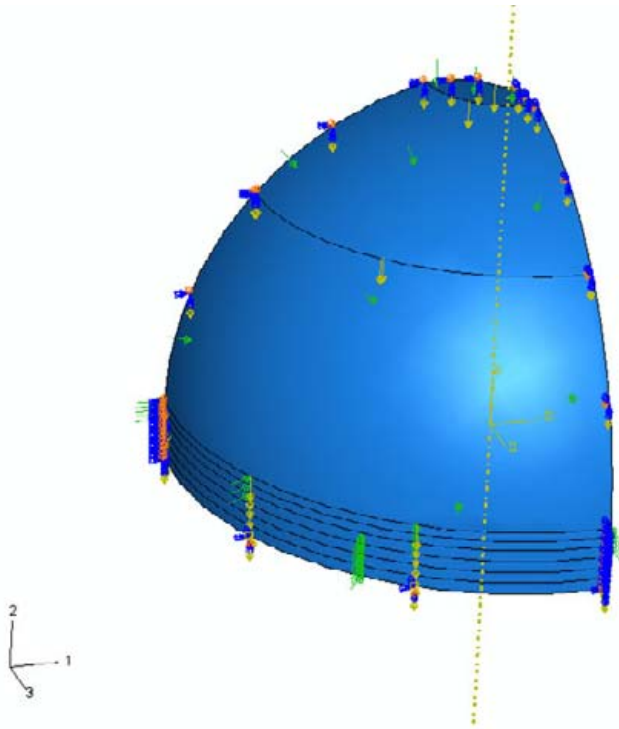
Heat Flux from Outside Surface: Uniformly distributed (200 KW/m<sup>2</sup>, 108 KW/m<sup>2</sup>, and 88 KW/m<sup>2</sup>)

Weight: Uniformly distributed body force (76440 N/m<sup>3</sup>)

**Boundary Condition at Bottom:**

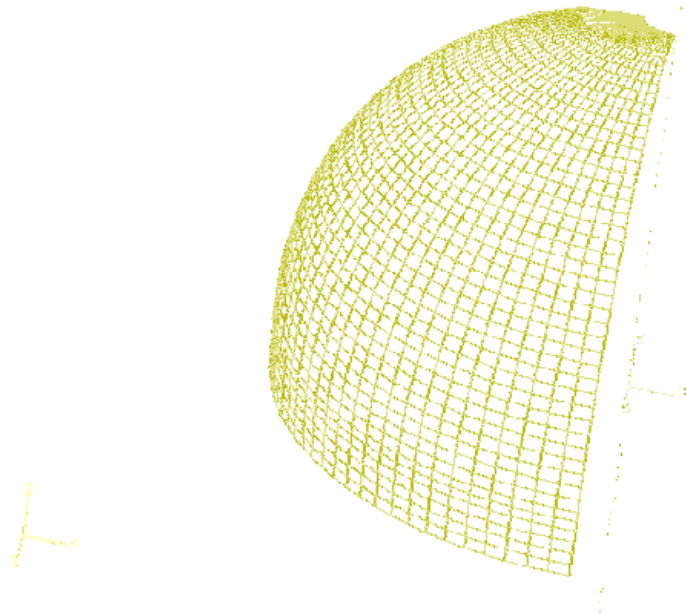
Heat sink (BC temperature at bottom): 100 C

Amplitude time history: 0 C up to 100 C linearly from 0 – 60 s and then get constant at 100 C

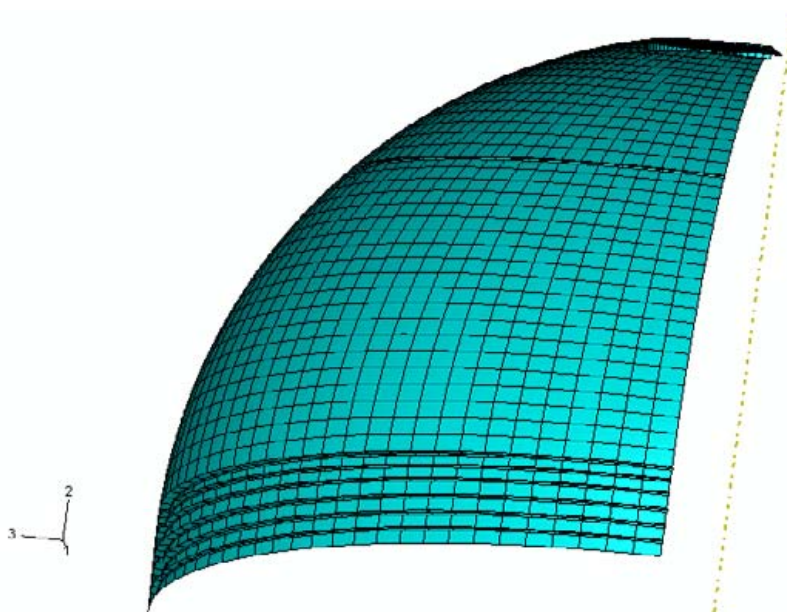


**FE Mesh (Shell Elements):**

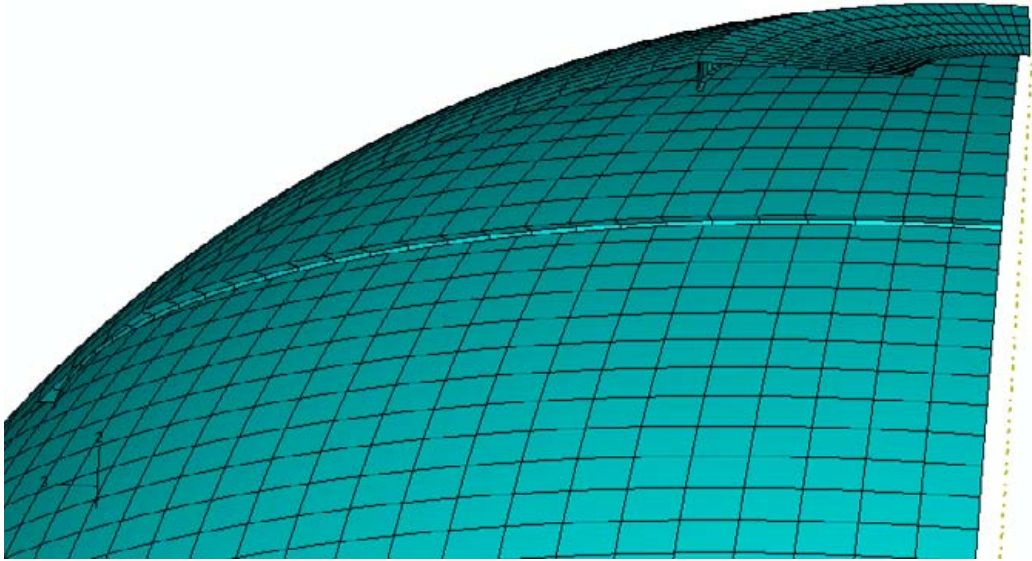
Quarter Model: Cylinder, Partial Sphere, Stiffeners, Opening



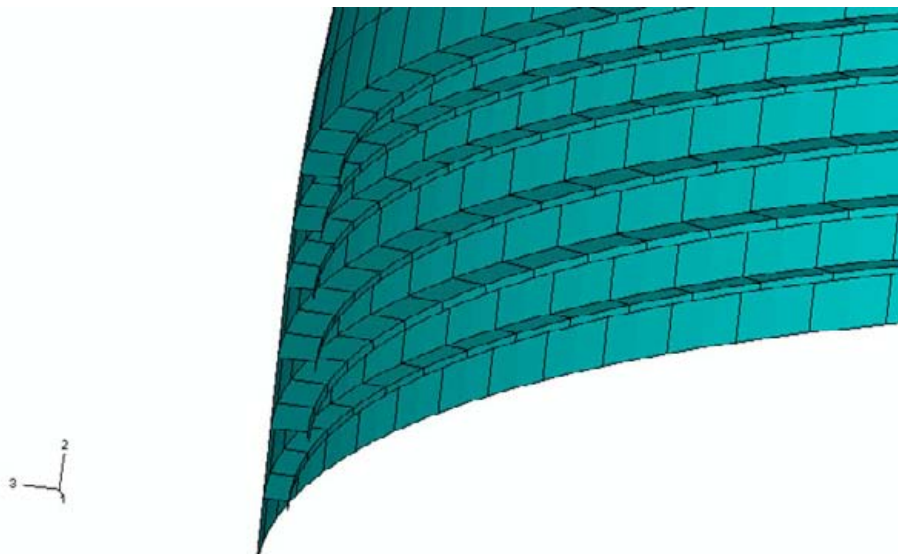
View from outside surface



View from inside surface



Zoom-in on top inside



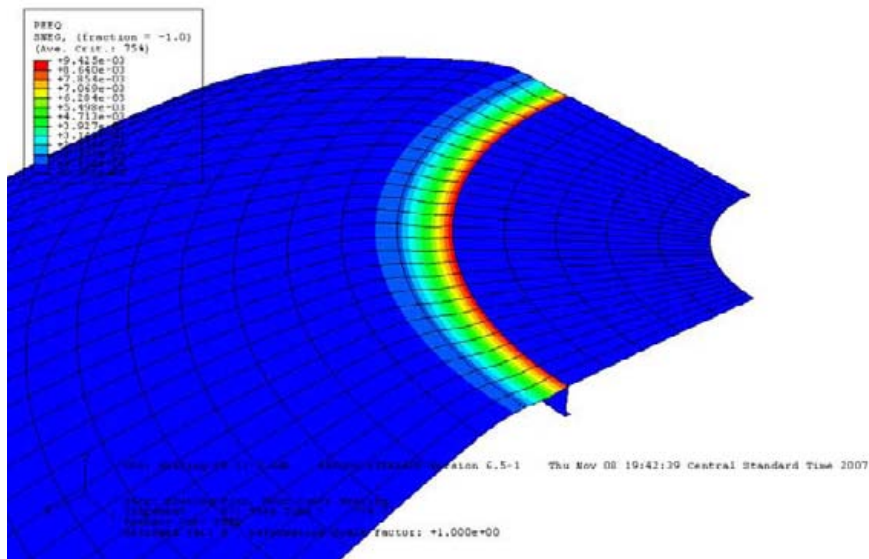
Zoom-in on bottom inside

**FE Results (Fully Coupled Thermal-Stress Analysis) using ABAQUS:**

*The structure collapses around the connection of cover sheet and top platform at 775 s under the heat flux with 88 KW/m<sup>2</sup>, 602 s under the heat flux with 108 KW/m<sup>2</sup>, and 297 s under the heat flux with 200 KW/m<sup>2</sup>, respectively, due to local large deformation caused by the abrupt drop of Young's modulus around 750 C. Hereafter, the structure cannot sustain any more.*

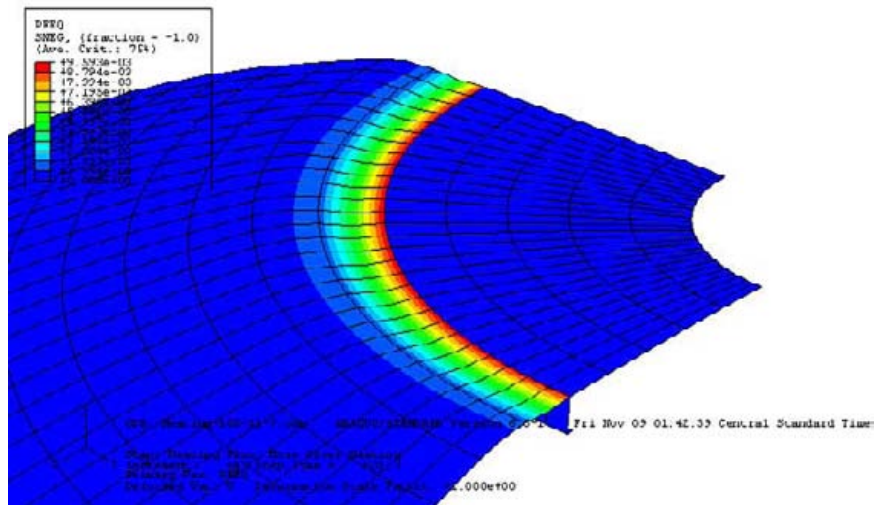
1. Collapse around the connection between cover sheet and top platform

1) In case of 88 kw/m<sup>2</sup>



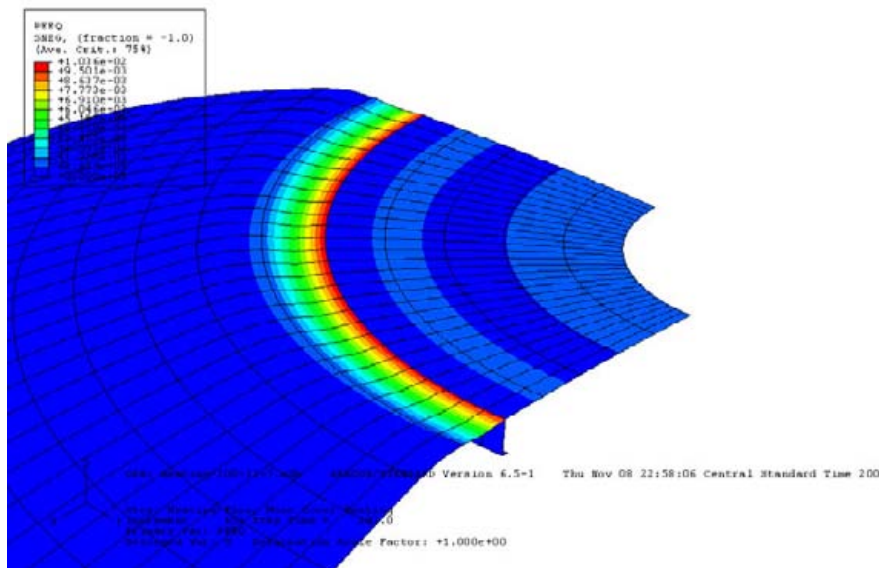
Collapsed at 775 s and plastic strain is 0.94%

2) In case of  $108 \text{ kw/m}^2$



Collapsed at 602 s and plastic strain is 0.96%

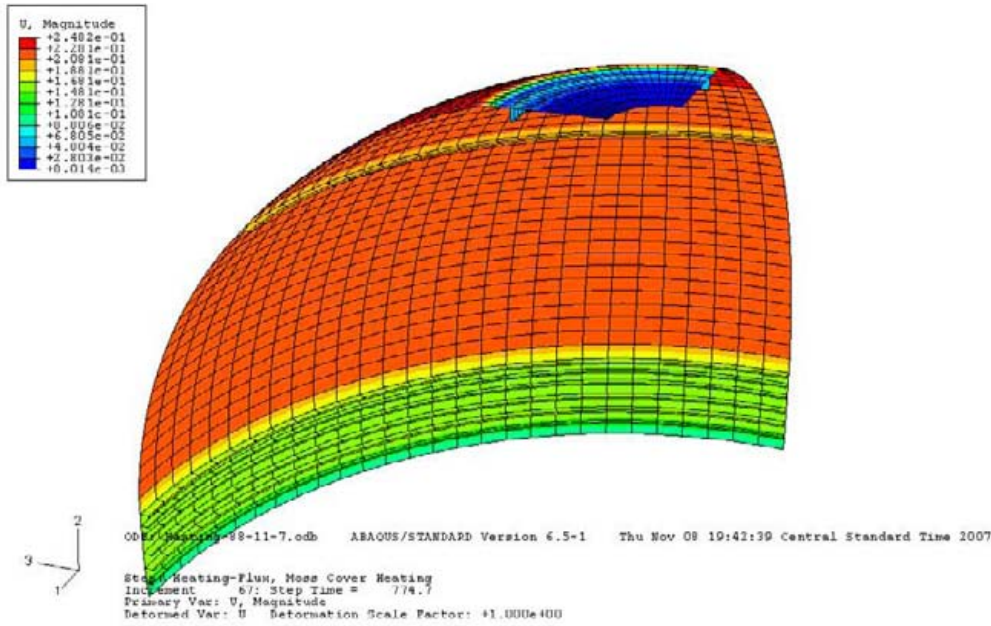
3) In case of  $200 \text{ kw/m}^2$



Collapsed at 297 s and plastic strain is 1.04%

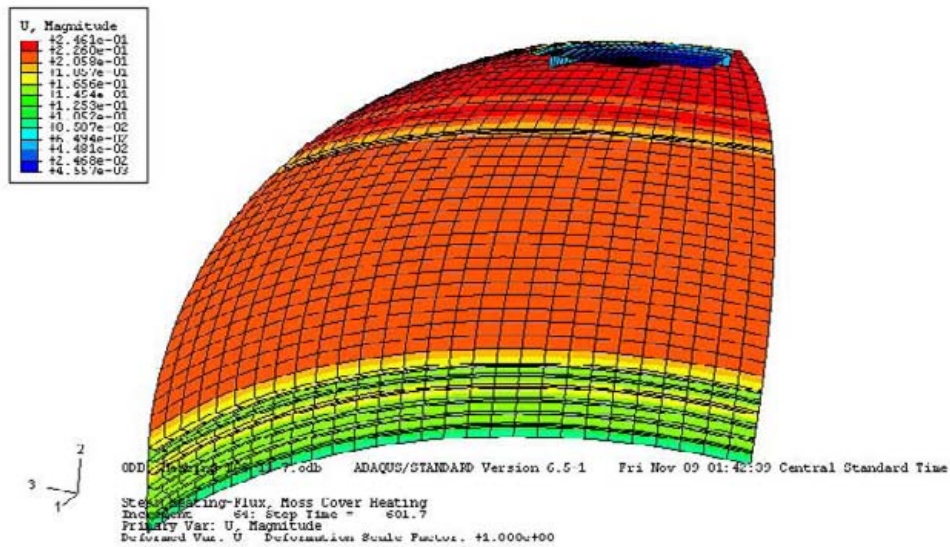
## 2. Deformation at Failure

### 1) In case of 88 kw/m<sup>2</sup>



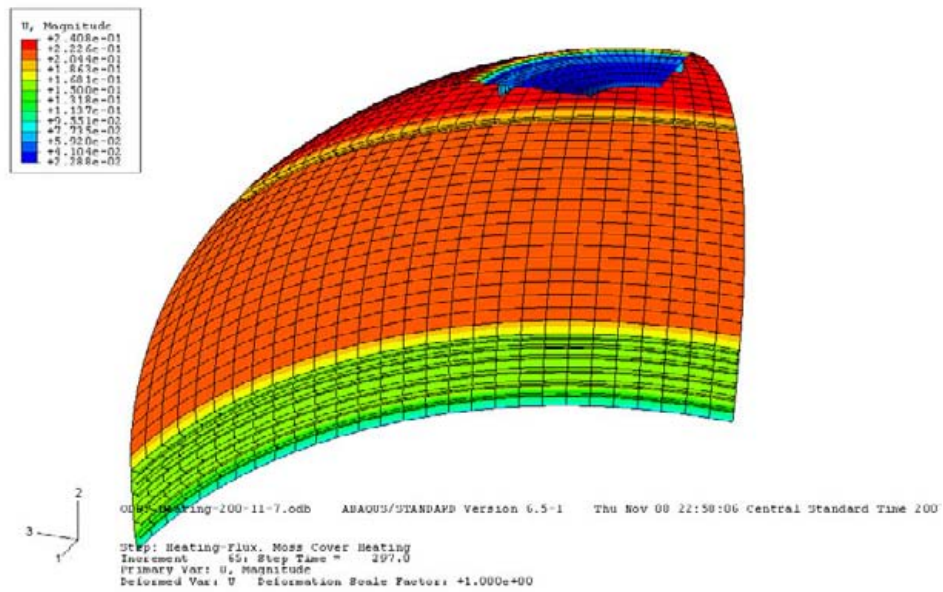
Maximum displacement is 0.25 m at failure

### 2) In case of 108 kw/m<sup>2</sup>



Maximum displacement is 0.25 m at failure

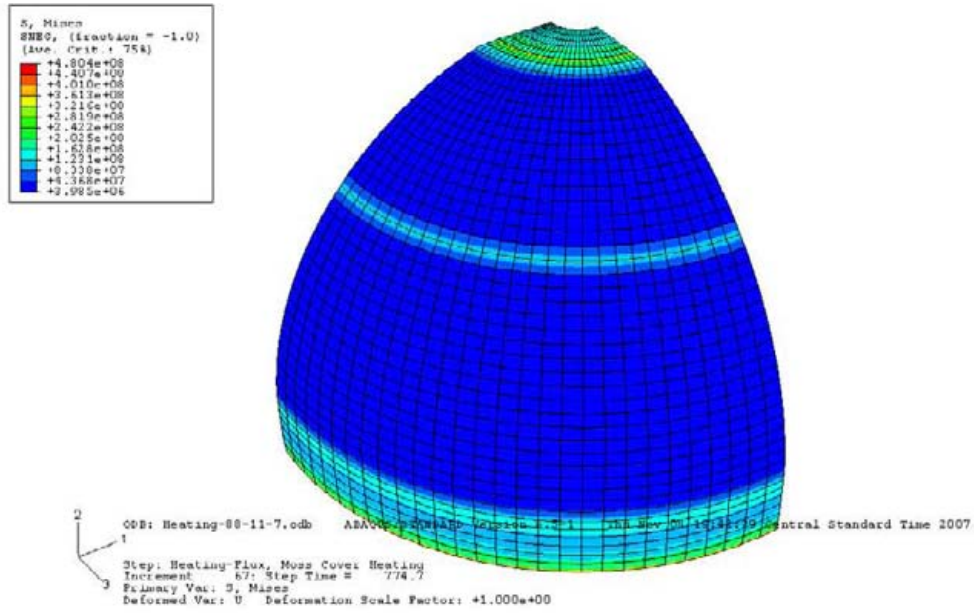
3) In case of 200 kw/m<sup>2</sup>



Maximum displacement is 0.24 m at failure

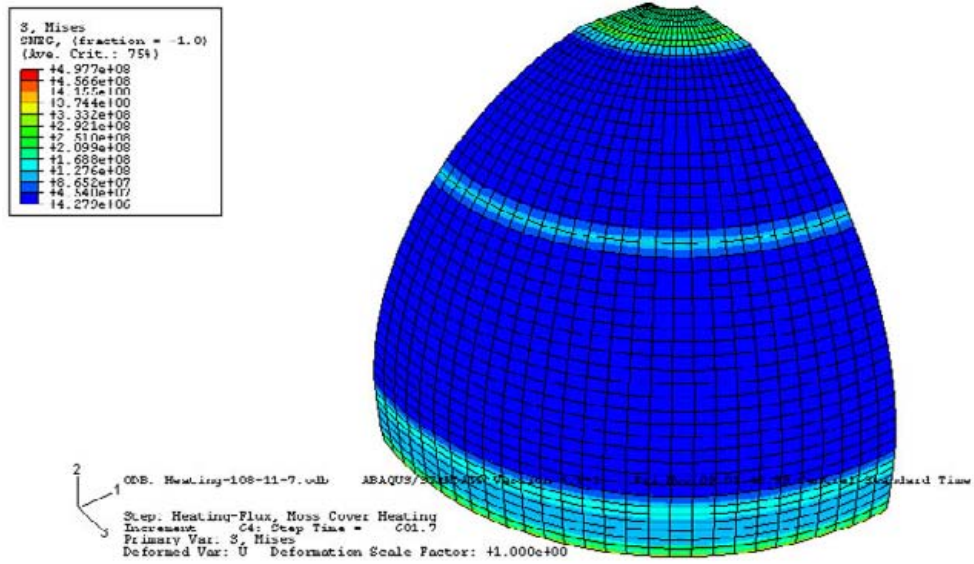
3. von Mises Stress at Failure

1) In case of 88 kw/m<sup>2</sup>



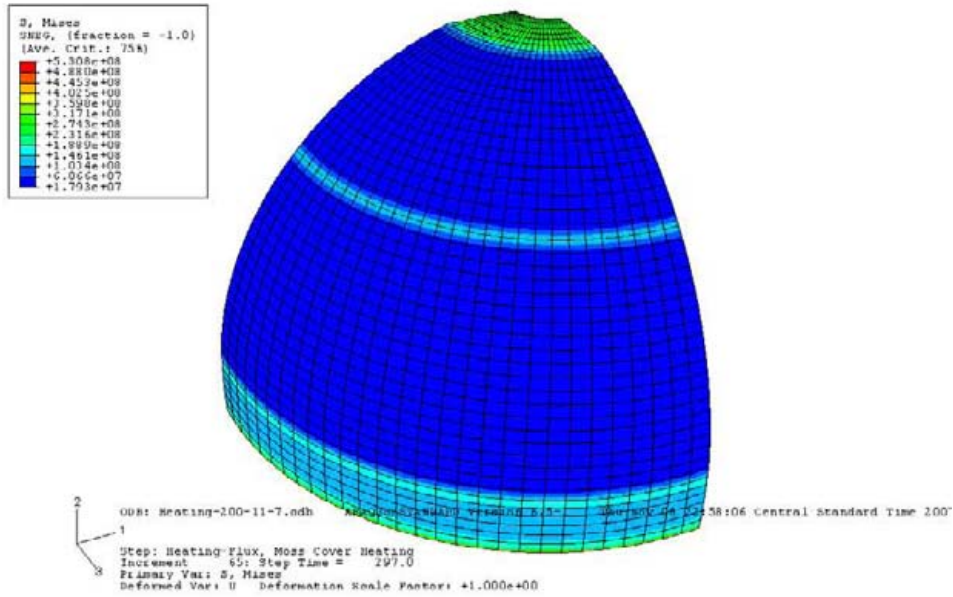
Maximum von Mises stress is 480 MPa at failure

2) In case of 108 kw/m<sup>2</sup>



Maximum von Mises stress is 498 MPa at failure

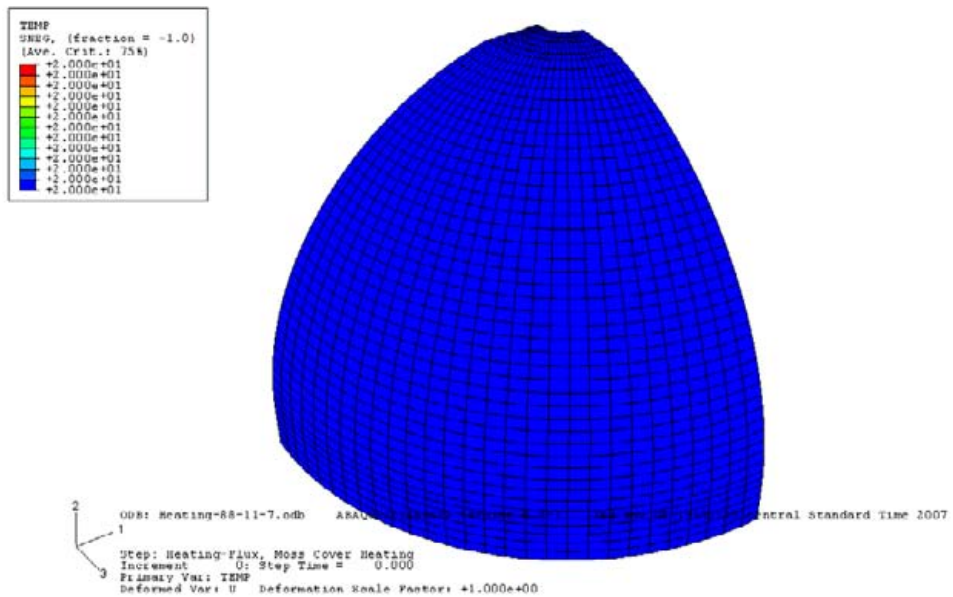
3) In case of 200 kw/m<sup>2</sup>



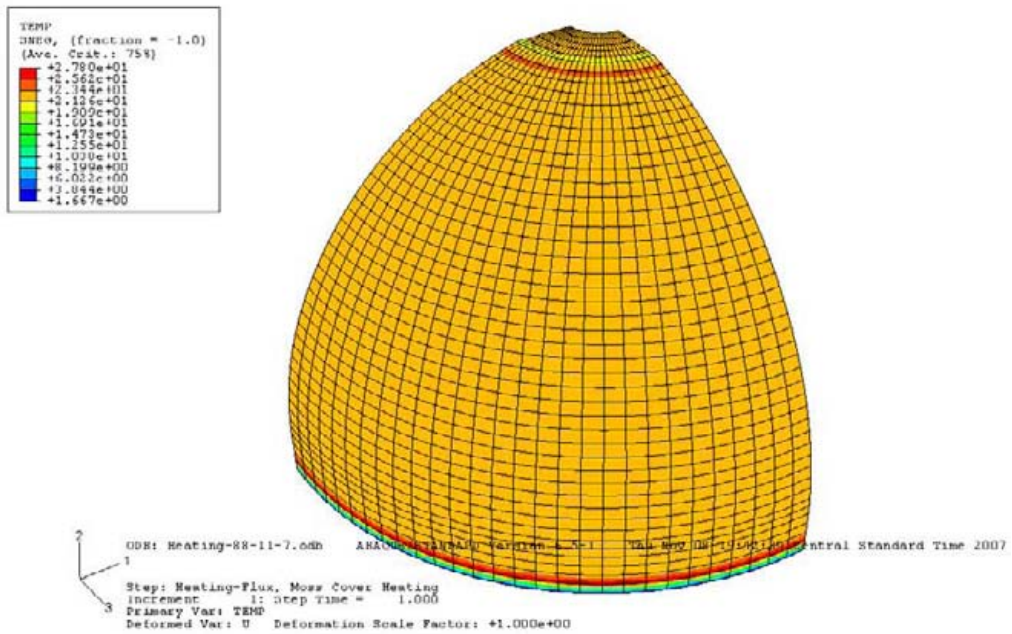
Maximum von Mises stress is 531 MPa at failure

4. Temperature Rising

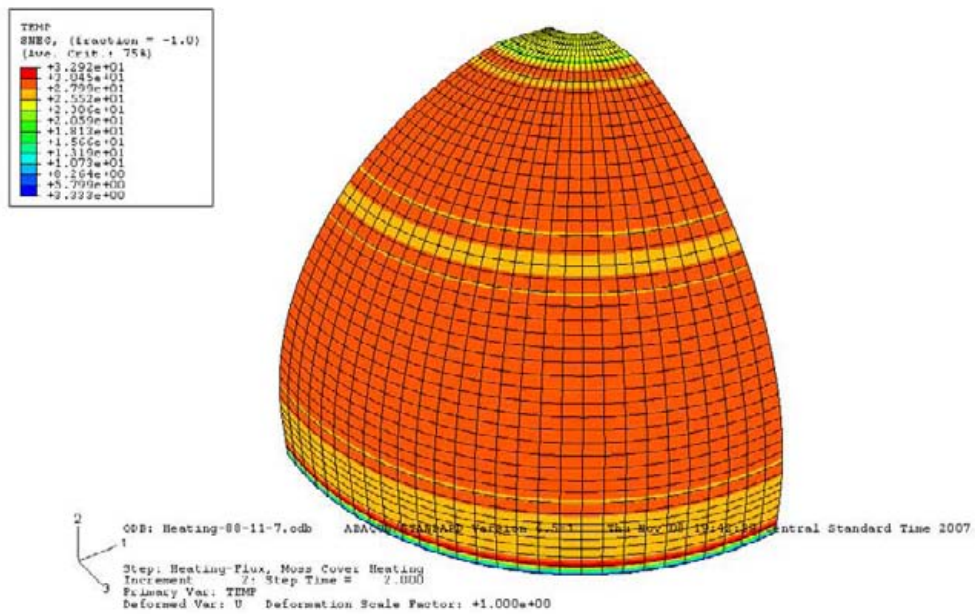
1) In case of 88 kw/m<sup>2</sup>



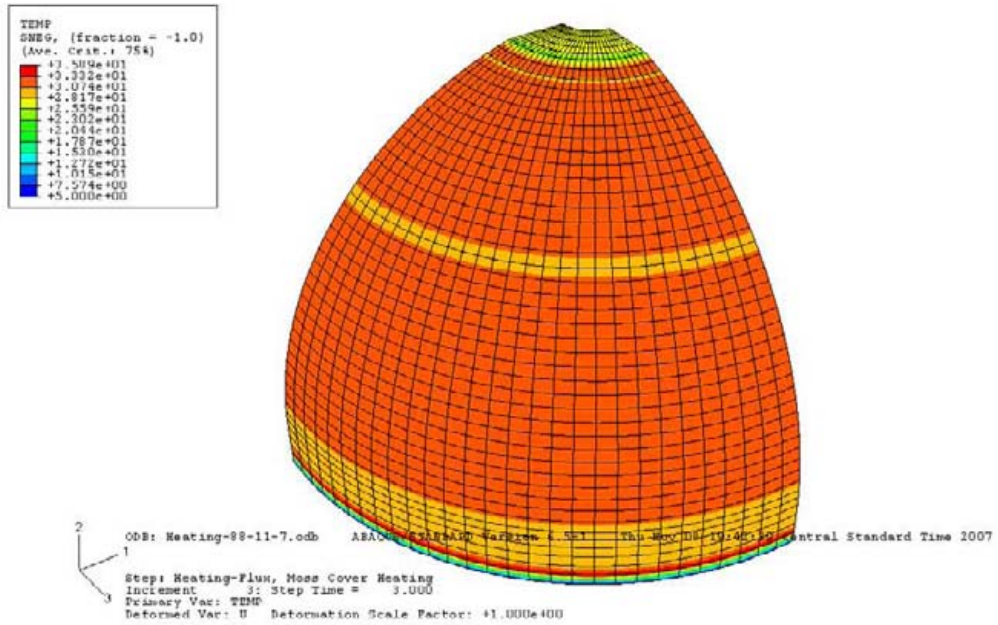
Initial Temperature: 20 C at 0 s



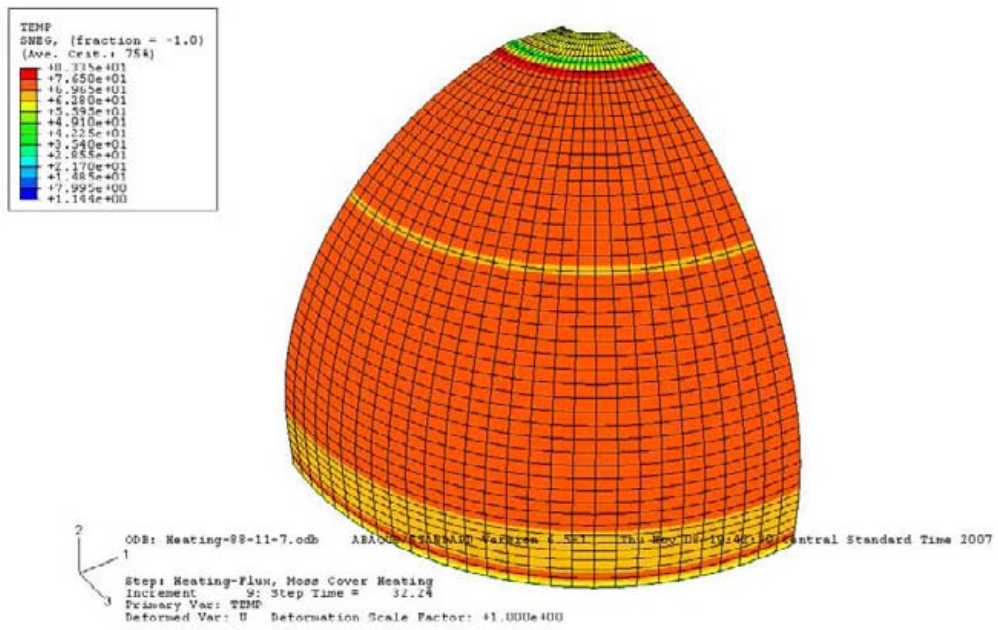
Maximum temperature is 28 C at 1 s



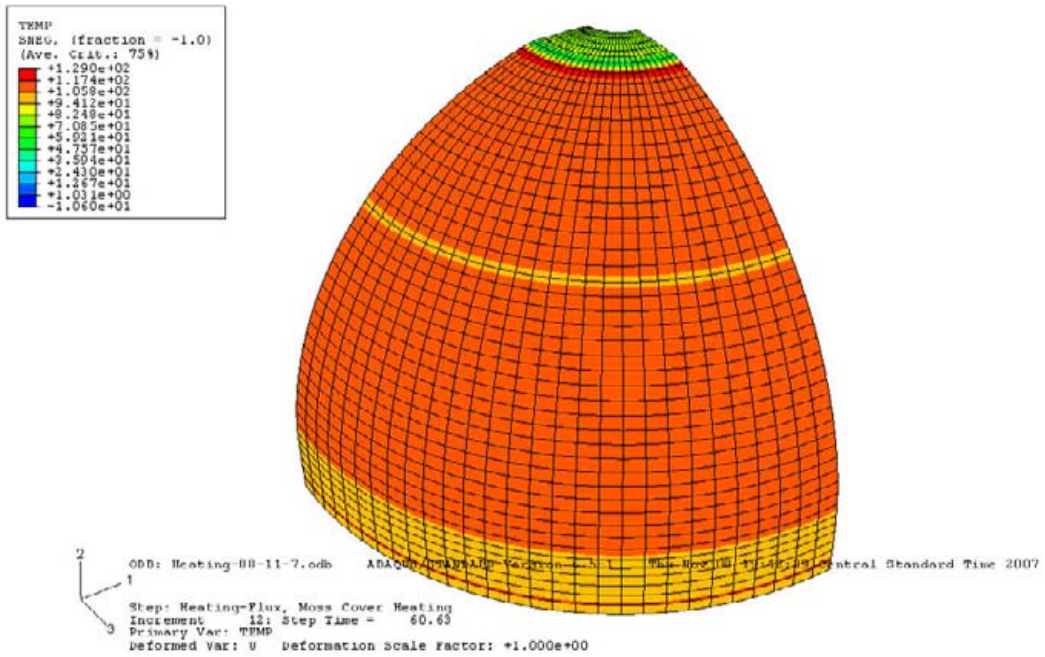
Maximum temperature is 33 C at 2 s



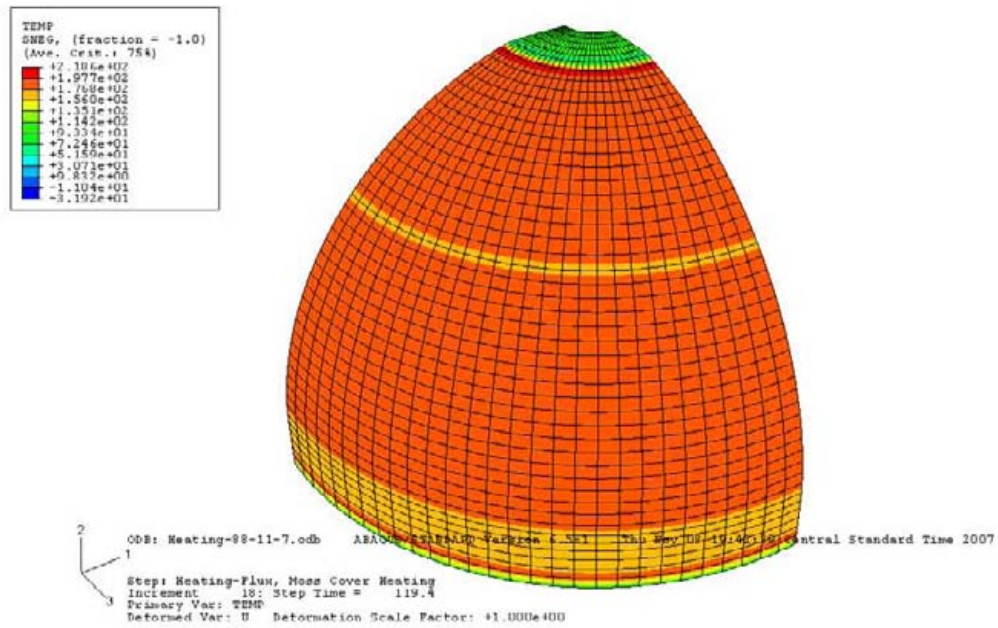
Maximum temperature is 36 C at 3 s



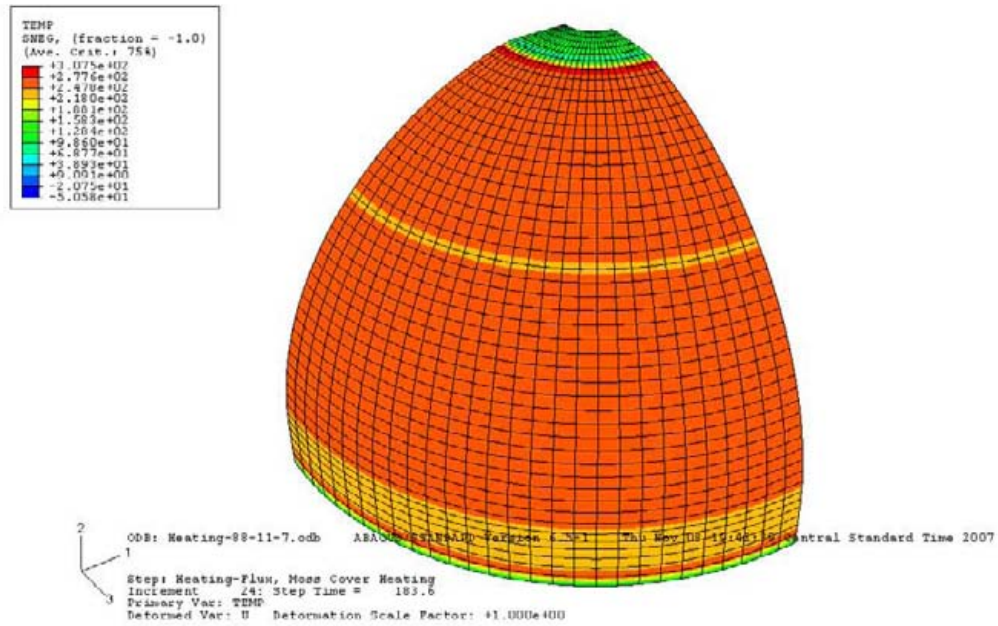
Maximum temperature is 83 C at 32 s



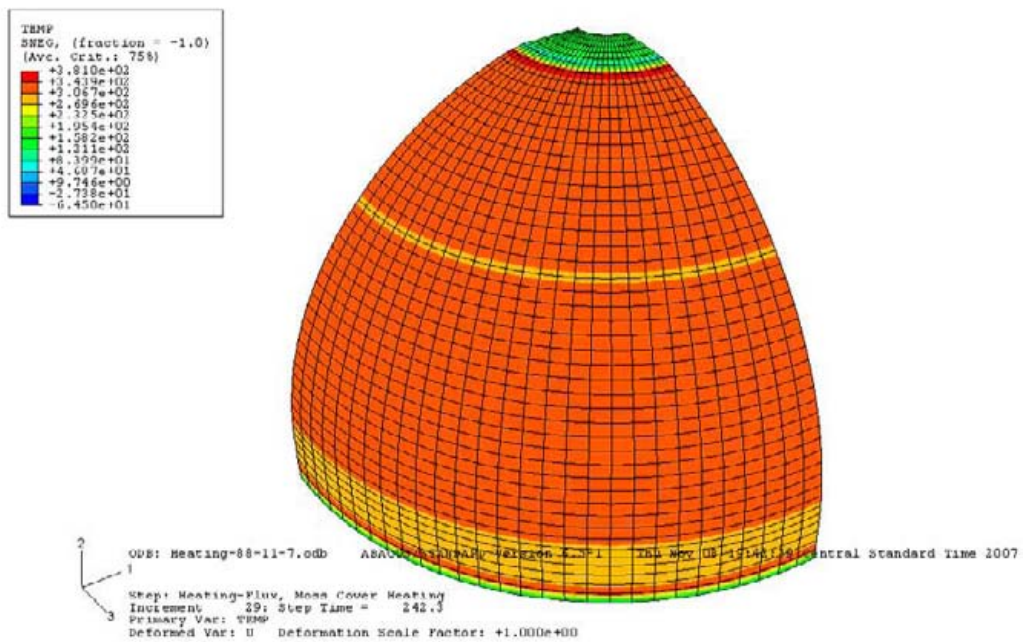
Maximum temperature is 129 C at 61 s



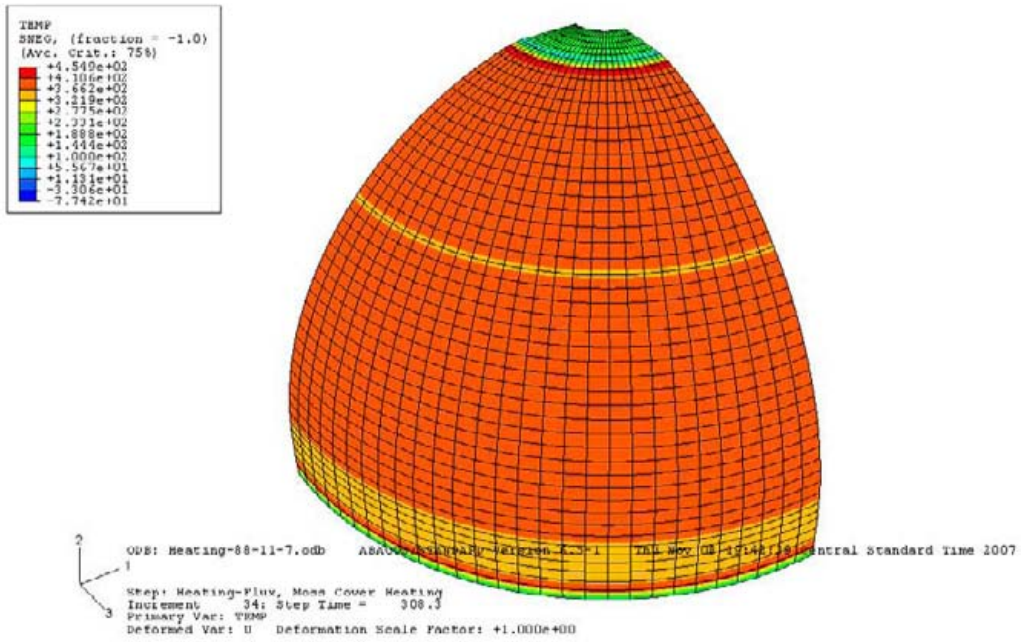
Maximum temperature is 219 C at 119 s



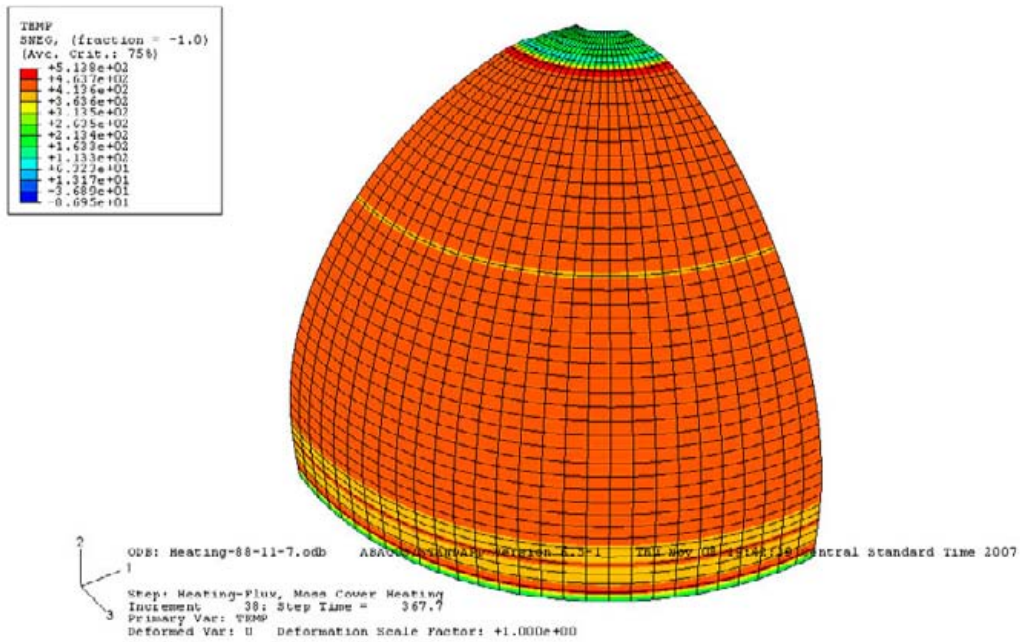
Maximum temperature is 308 C at 184 s



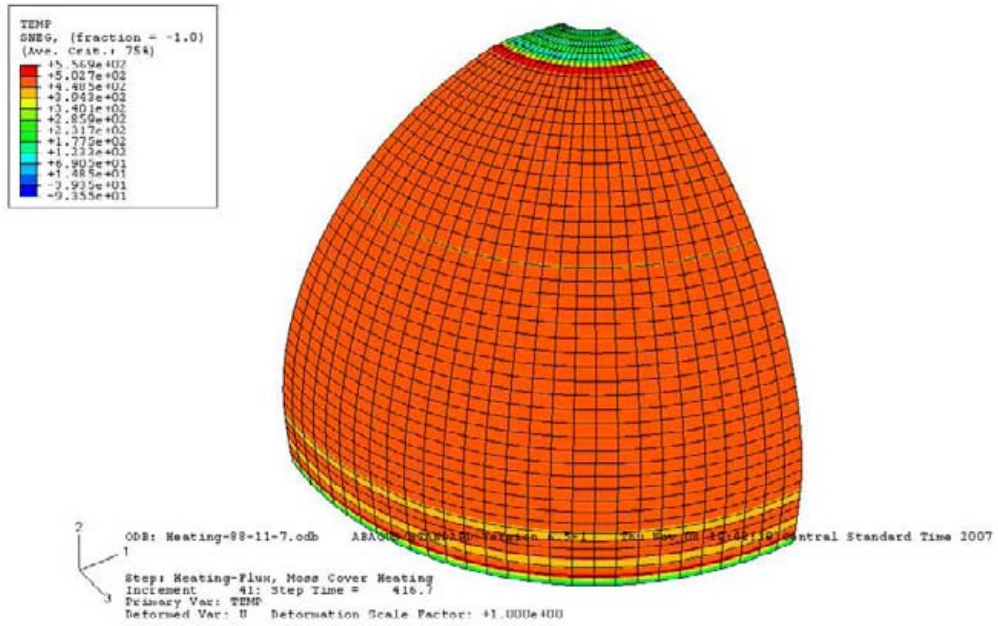
Maximum temperature is 381 C at 242 s



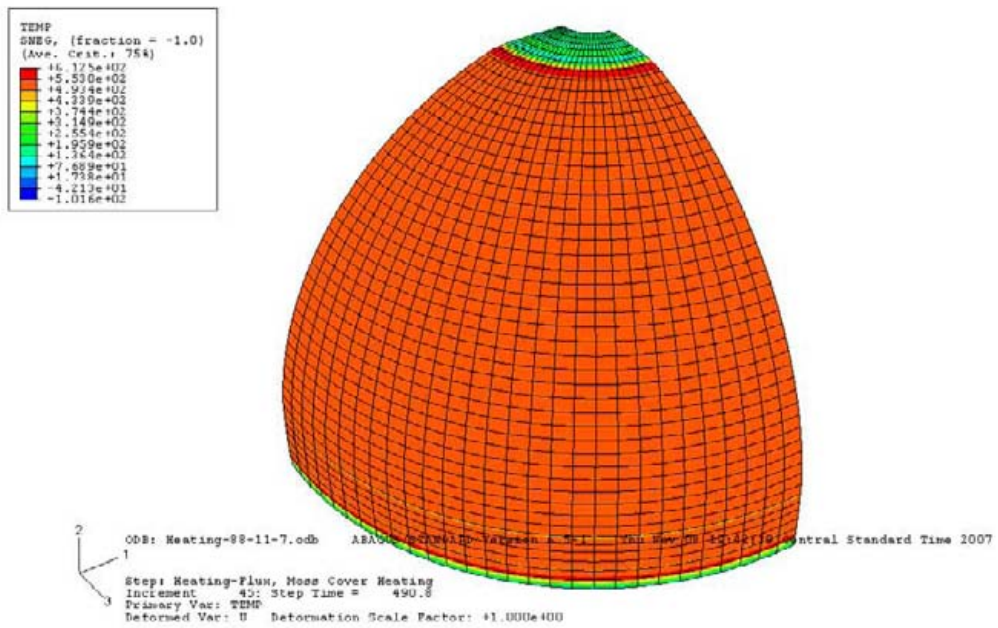
Maximum temperature is 455 C at 308 s



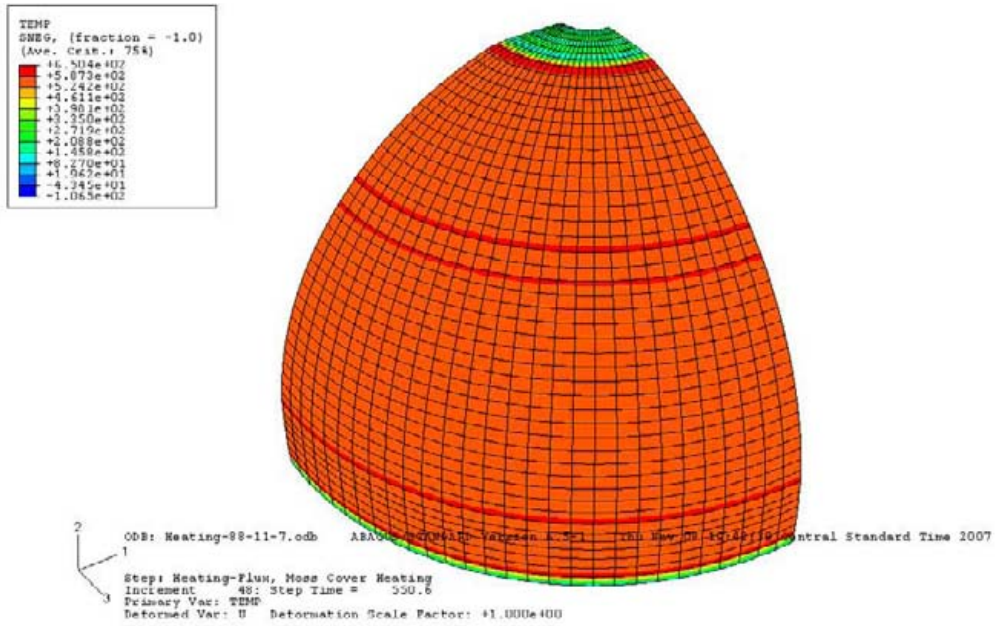
Maximum temperature is 514 C at 368 s



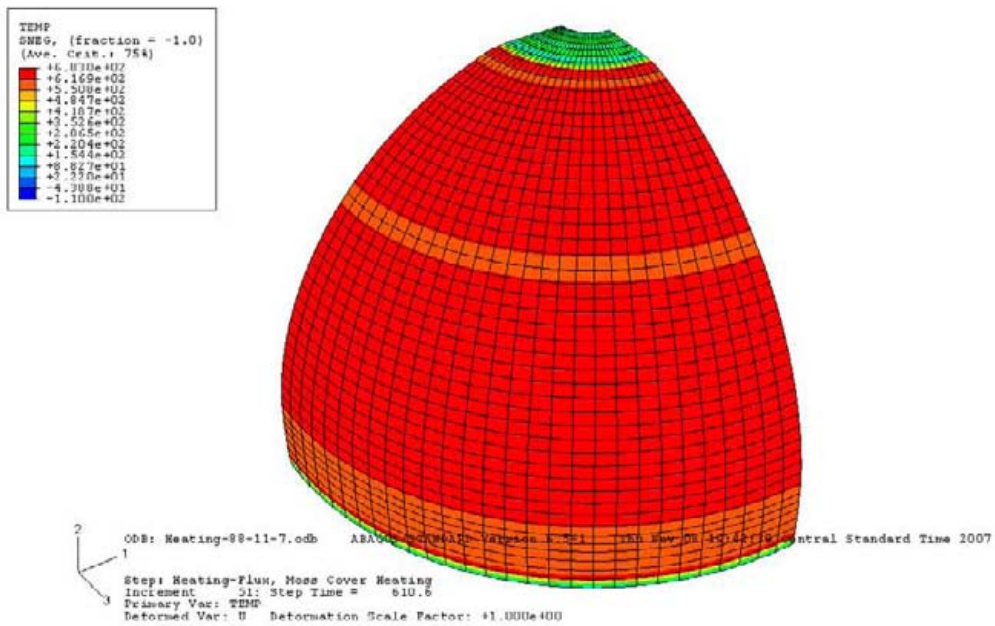
Maximum temperature is 557 C at 417 s



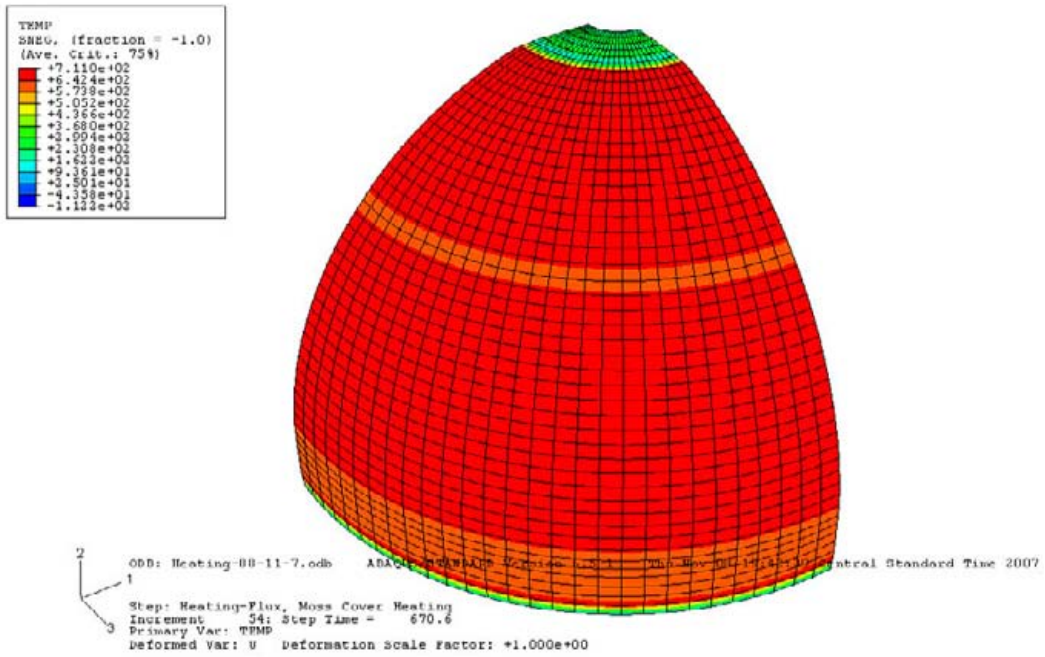
Maximum temperature is 613 C at 491 s



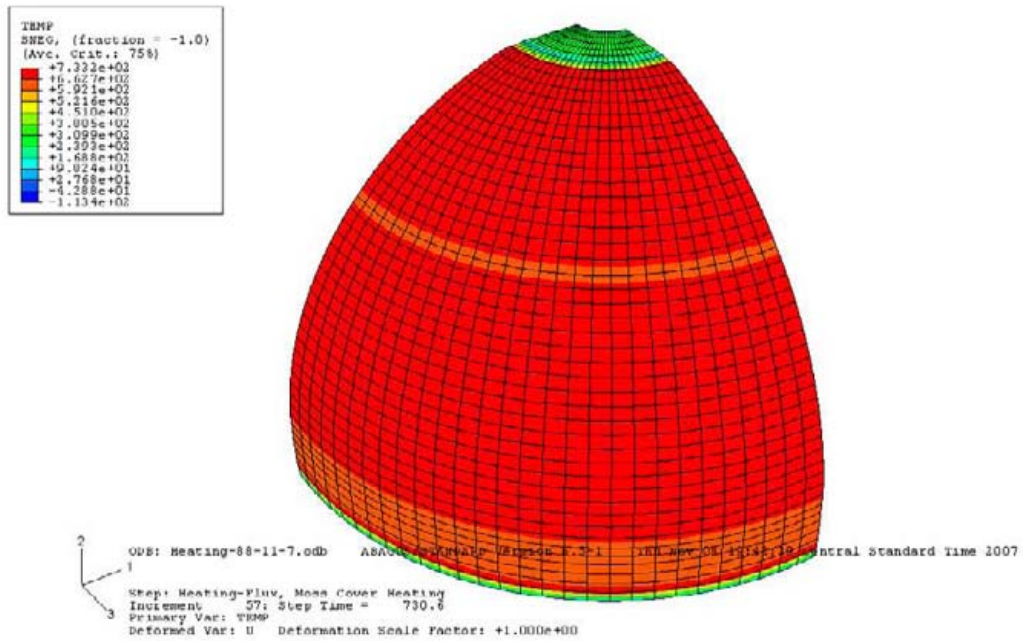
Maximum temperature is 650 C at 551 s



Maximum temperature is 683 C at 611 s

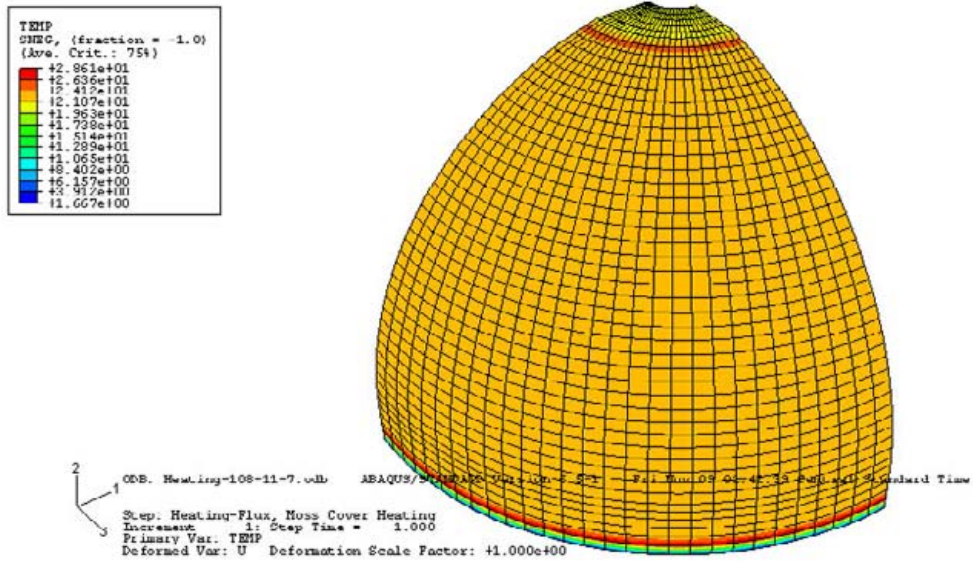


Maximum temperature is 711 C at 671 s

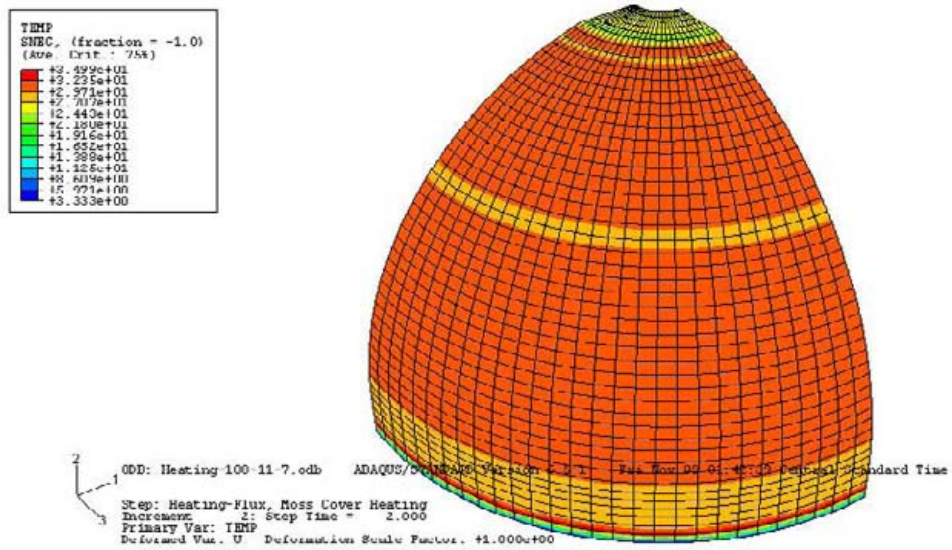


Maximum temperature is 733 C at 731 s



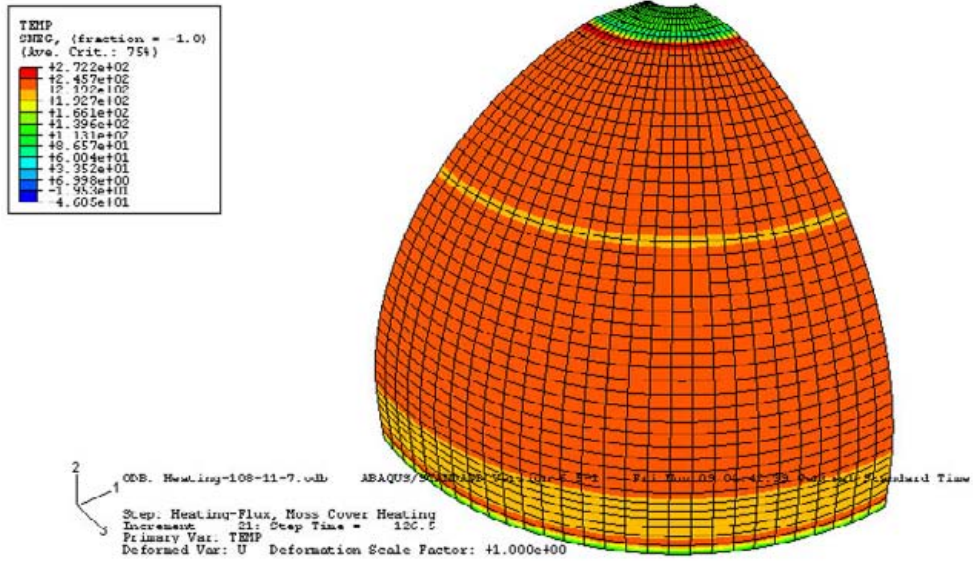


Maximum temperature is 29 C at 1 s

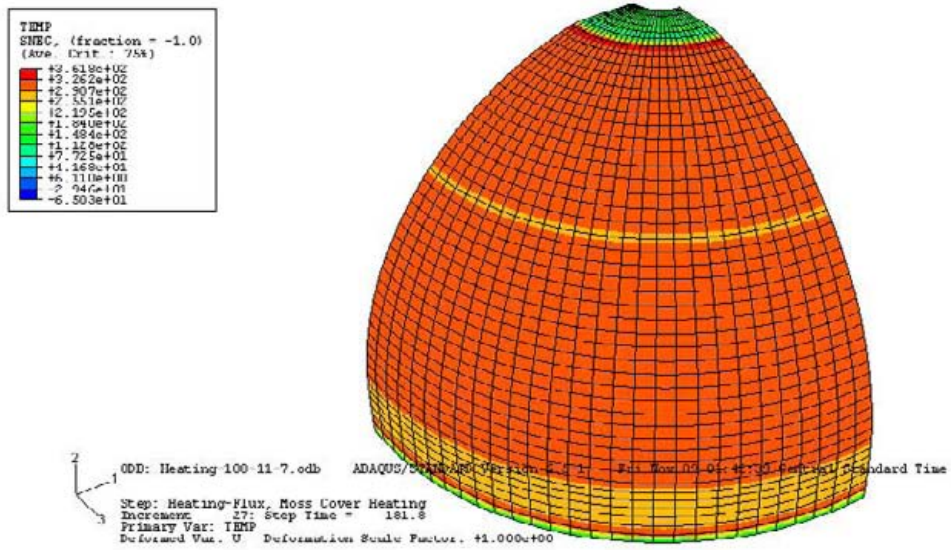


Maximum temperature is 35 C at 2 s

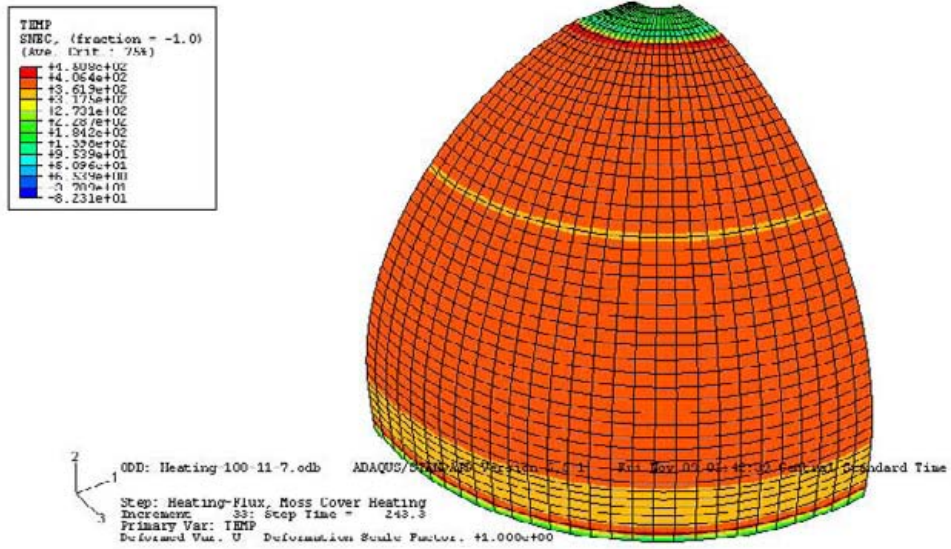




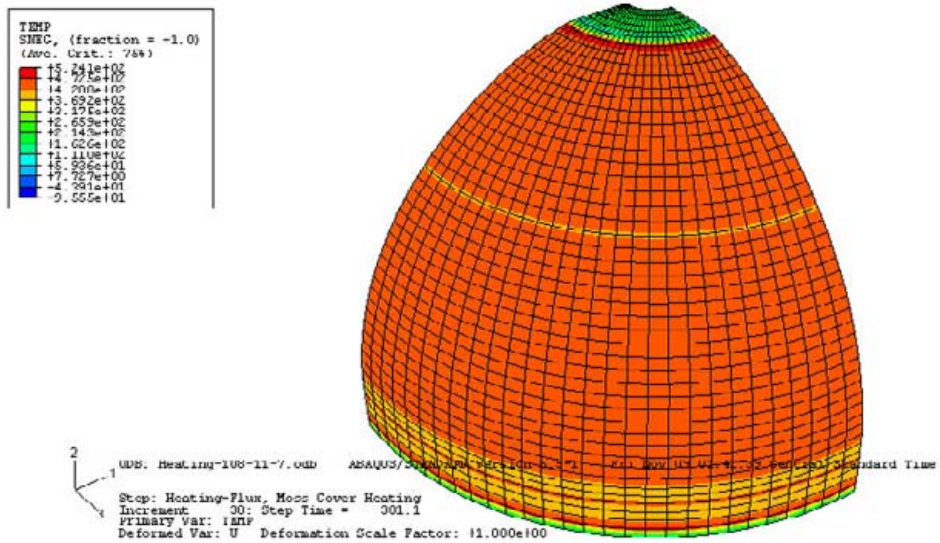
Maximum temperature is 272 C at 127 s



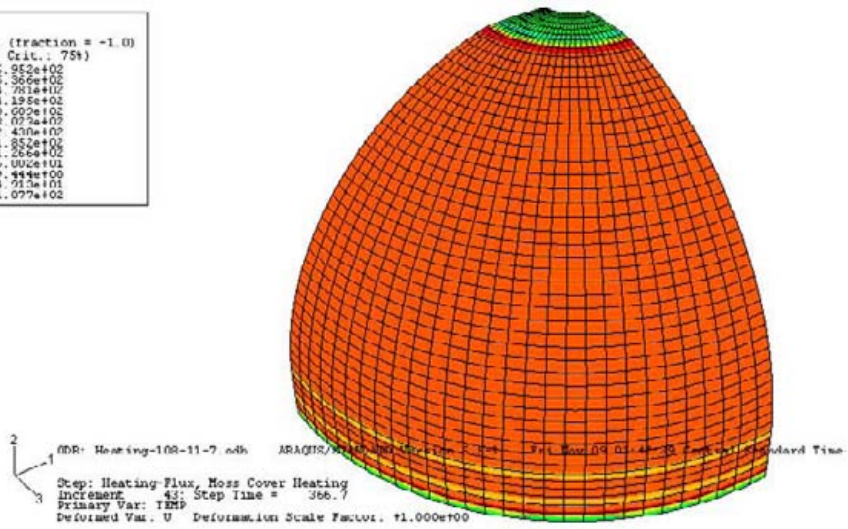
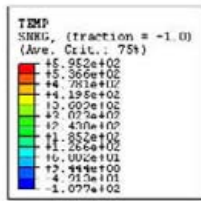
Maximum temperature is 362 C at 182 s



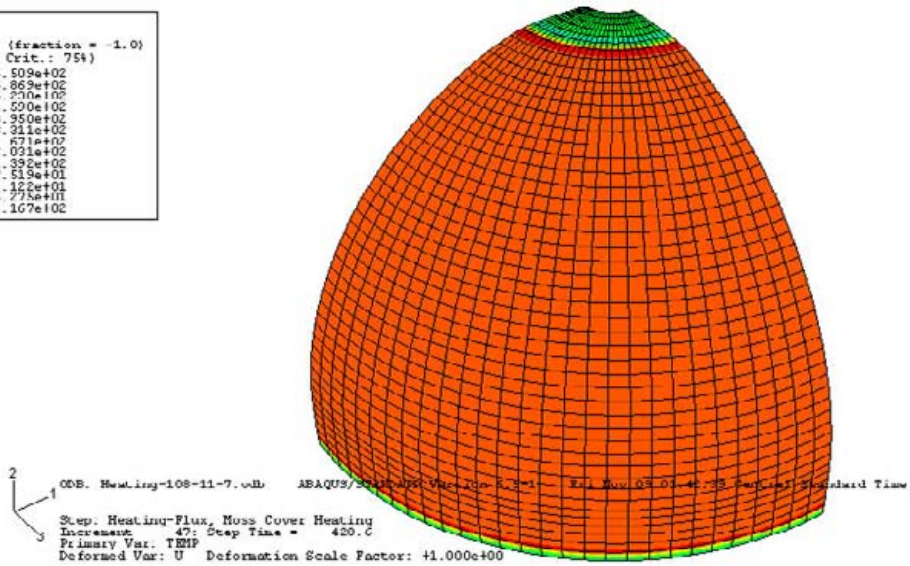
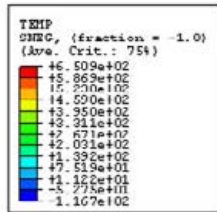
Maximum temperature is 451 C at 243 s



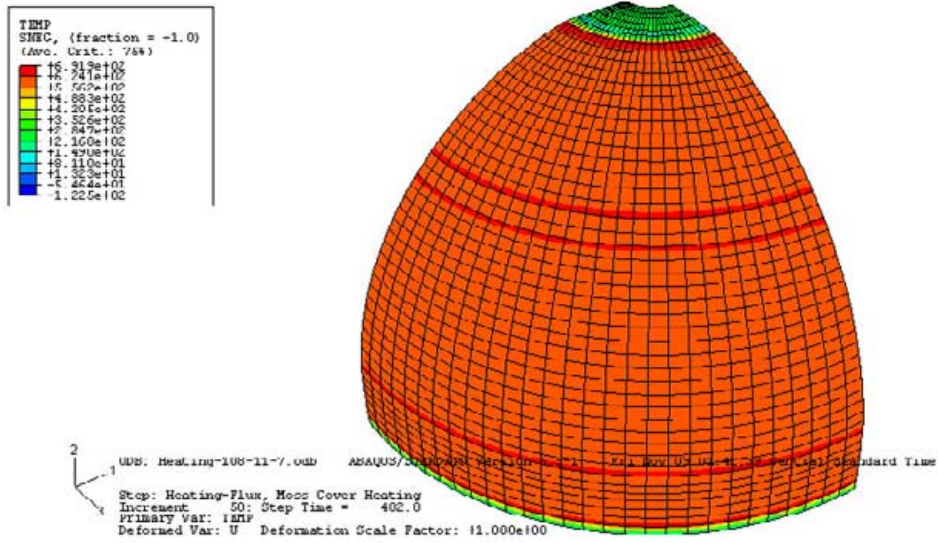
Maximum temperature is 524 C at 301 s



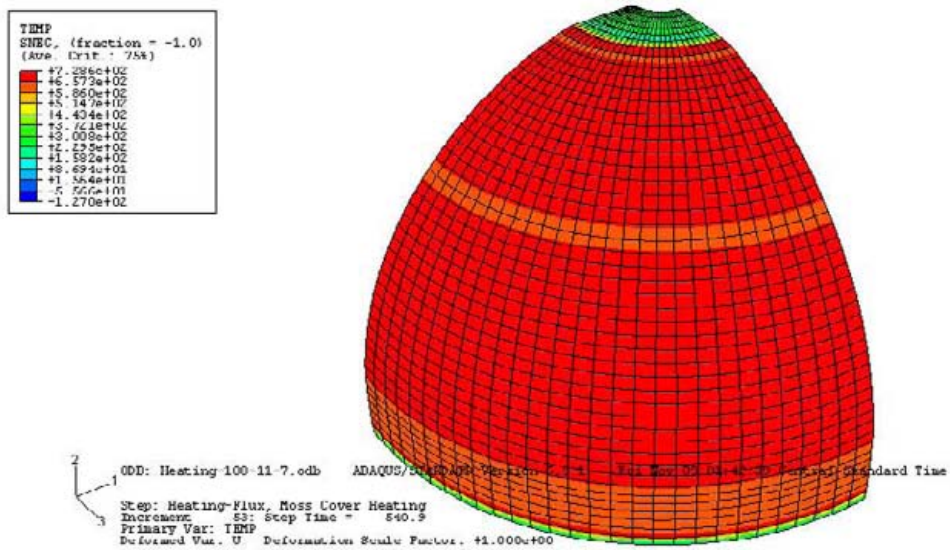
Maximum temperature is 595 C at 367 s



Maximum temperature is 651 C at 429 s

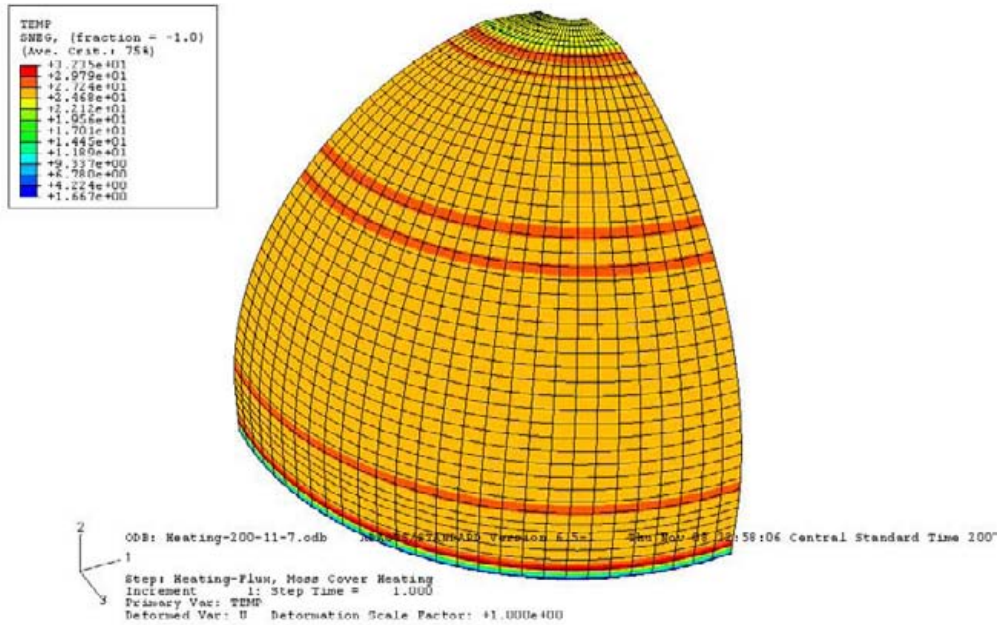


Maximum temperature is 692 C at 483 s

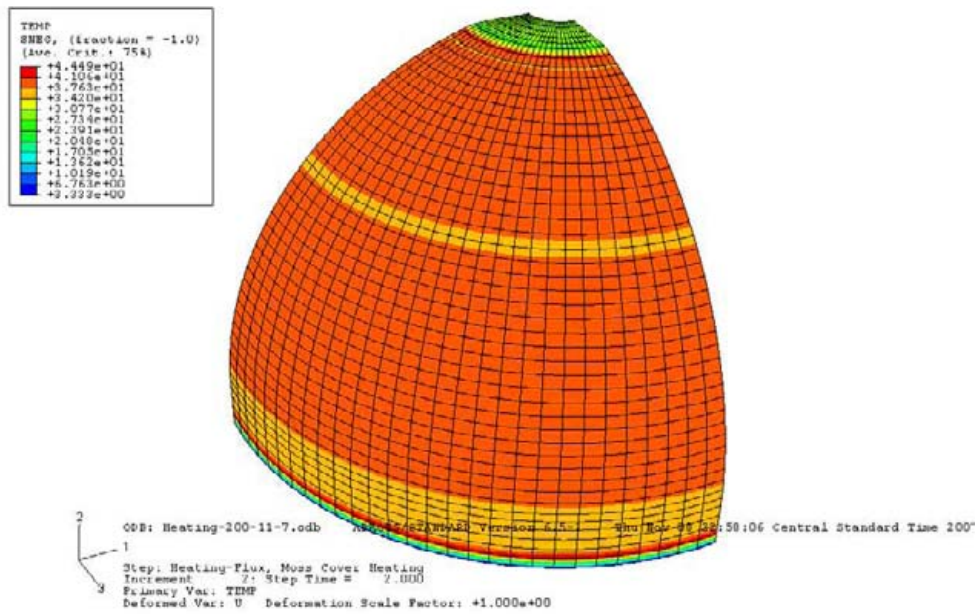


Maximum temperature is 729 C at 541 s

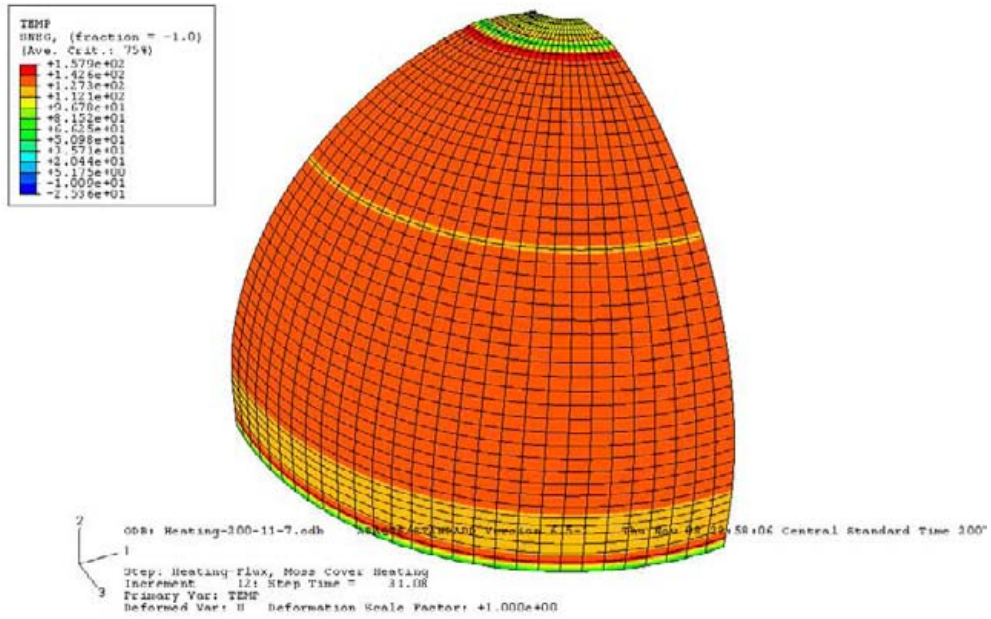




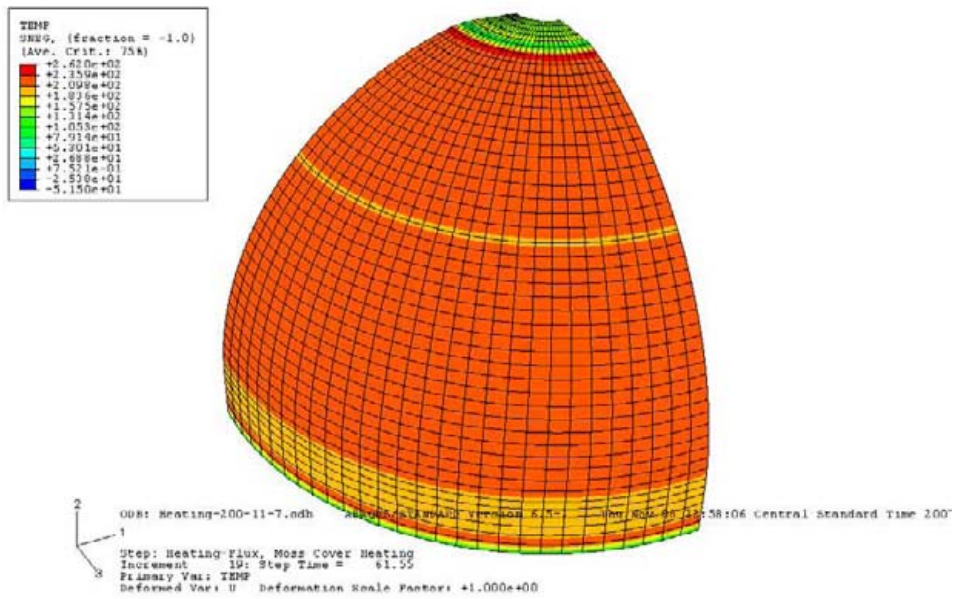
Maximum temperature is 32 C at 1 s



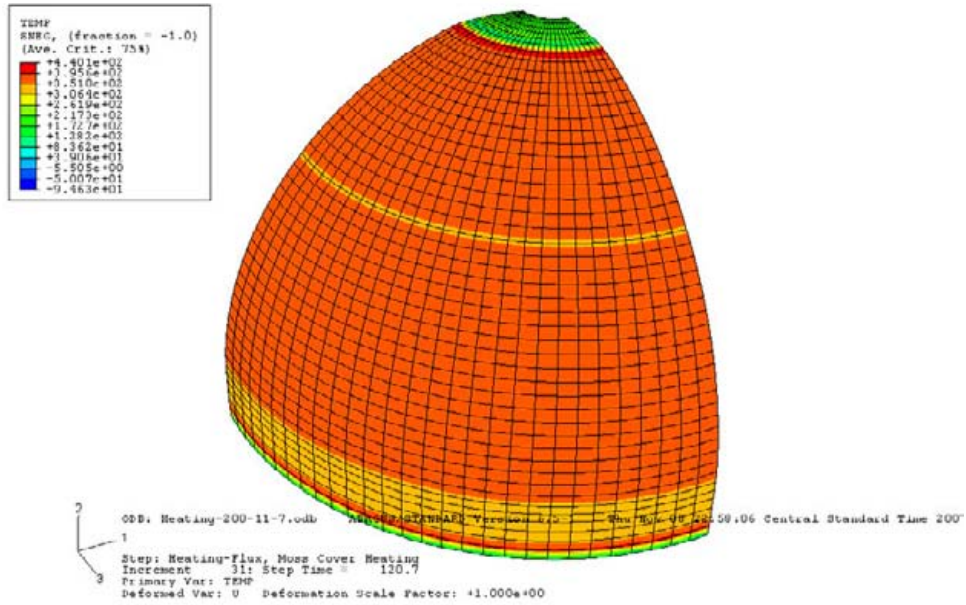
Maximum temperature is 44 C at 2 s



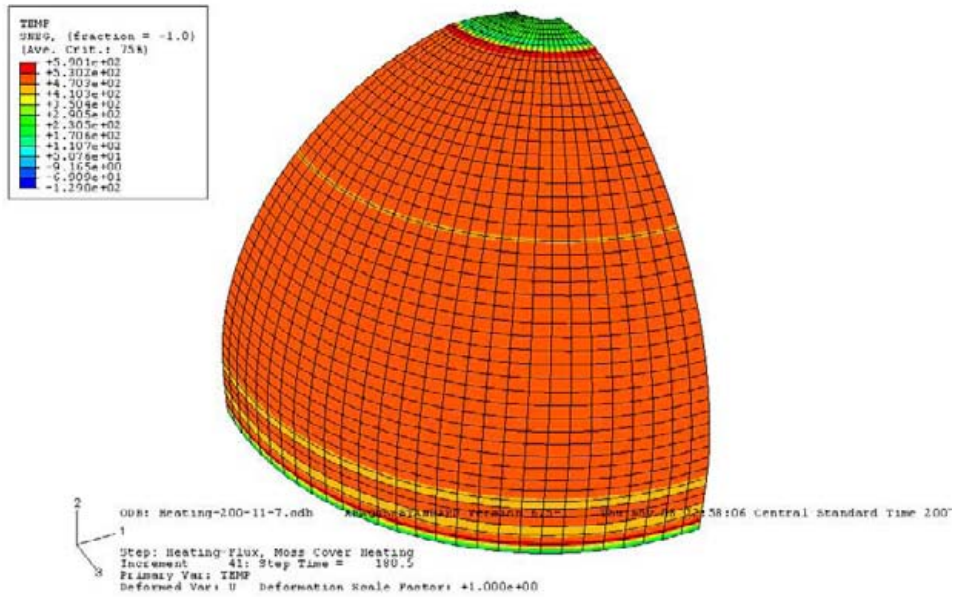
Maximum temperature is 158 C at 31 s



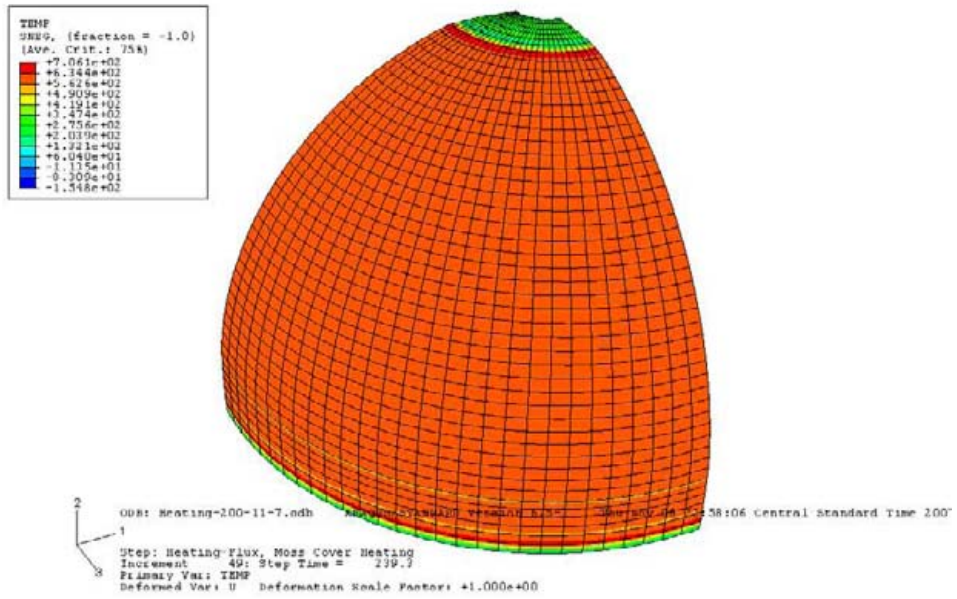
Maximum temperature is 262 C at 62 s



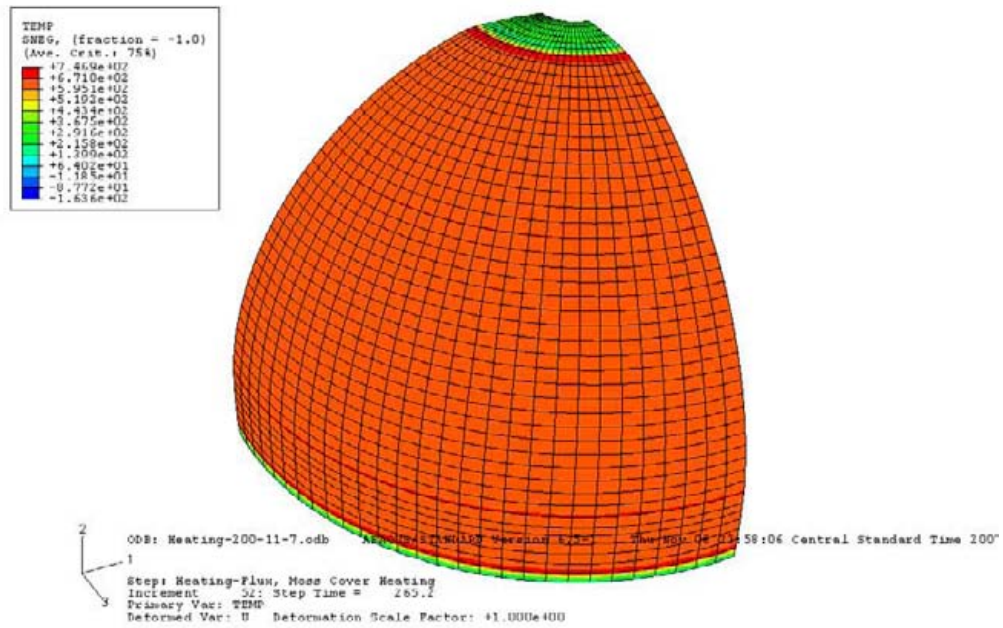
Maximum temperature is 440 C at 121 s



Maximum temperature is 590 C at 181 s



Maximum temperature is 706 C at 239 s



Maximum temperature is 747 C at 265 s



## **APPENDIX 2 – THERMODYNAMIC BOUNDARY CONDITION**



**Prof. Dr.-Ing. Stephan Kabelac**  
**Dr.-Ing. Gerd Würsig (GL)**  
**Dipl.-Ing. Malte Freund**

**SIGTTO Working Group on LNG Fire**

***Thermodynamic Boundary Condition***

**Institut für Thermodynamik - Hamburg 2007**

<b>1</b>	<b>INTRODUCTION.....</b>	<b>4</b>
<b>2</b>	<b>CONCLUSIONS.....</b>	<b>5</b>
2.1	OVERVIEW .....	5
2.2	ANNOTATIONS TO THE CONCLUSIONS .....	6
<b>3</b>	<b>DESCRIPTION OF THE MODEL .....</b>	<b>8</b>
<b>4</b>	<b>METHANE POOL BOILING .....</b>	<b>12</b>
<b>5</b>	<b>HEAT TRANSFER CALCULATIONS.....</b>	<b>14</b>
5.1	1-D HEAT TRANSFER EQUATIONS .....	14
5.2	ESTIMATION OF THE MAXIMUM POSSIBLE HEAT FLUX FROM THE FIRE.....	14
5.3	DIFFERENT PHASES OF THE INCIDENT .....	16
5.4	PHASE 1: COMPLETE INSULATION AND RADIATION SHIELD.....	18
5.5	PHASE 2: DECOMPOSING INSULATION.....	18
5.6	PHASE 3: COMPLETELY REMOVED INSULATION .....	21
<b>6</b>	<b>CFD CALCULATION.....</b>	<b>23</b>
6.1	MODEL DESCRIPTION .....	23
6.2	CFD RESULTS .....	25
<b>7</b>	<b>OUTLOOK.....</b>	<b>27</b>

### ***1 Introduction***

During the meeting in May 2007 in Hamburg of the SIGTTO working group on the effects of large LNG pool fires around a LNG carrier, GL presented some preliminary results of a 1-D thermodynamic calculation of the heat flux into an LNG tank. It was decided that the presented calculations should be validated and the 1-D approach should be evaluated in more detail. The aim of this student study should be the identification and quantification of the limiting factors to the heat flux into the LNG tank. The scope and results of the study are limited by the time available and the nature of the study which was intended to be done as students work.

This report evaluates the heat flux into a liquid-full Moss Sphere LNG tank aboard a ship within an engulfing fire. The calculation consists of 1-D heat transfer calculations and a CFD calculation of the air flow between the weather cover and the tank insulation. The evaluations presented were done in cooperation between the Institute of Thermodynamics at the Helmut-Schmidt University, Hamburg and Germanischer Lloyd.

The assumptions and the 1-D heat transfer calculation are described and the possible maximum heat that can be transferred into the LNG is investigated using pool-boiling data of methane. In the following the different heat transfer calculations are explained and the results are interpreted. A preliminary CFD calculation of the flow field between weather cover and the insulation is presented with its boundary conditions and possible enhancements of the CFD calculations for further investigations.

## 2 Conclusions

### 2.1 Overview

1. The maximum possible emissive power of a LNG fire can be estimated to be only initially  $300 \text{ kW / m}^2$  and decreases as soon as the receiving wall heats up. For a stipulated initial heat flux of  $300 \text{ kW / m}^2$  it decreases to about  $150 \text{ kW / m}^2$  at a wall temperature of  $1000 \text{ }^\circ\text{C}$ , compare Ch. 5.2.
2. The possible heat transfer into the tank strongly depends on the values of the emission coefficient and the rate of deterioration of the insulation material. The heat flux is limited to a very low value until the insulation is deteriorated (compare Ch. 5.4).
3. The maximum heat flux after heating up for the most severe assumptions is limited (see point 1) to  $150 \text{ kW / m}^2$  for the not insulated tank if an initial heat flux of  $300 \text{ kW / m}^2$  is assumed. By assuming an initial heat flux of  $108 \text{ kW / m}^2$  as in the IGC Code, the maximum heat flux is only about  $60 \text{ kW / m}^2$ , see below.
4. The boiling behaviour of the LNG is limiting the maximum possible heat flux to values below the critical heat flux situation of methane. Therefore the heat flux is limited from this side to values below  $300 \text{ kW / m}^2$  before destruction of the inner aluminium tank occurs.
5. There is no possibility of a large burning of insulation material due to the lack of oxygen. The amount of air in the gap only allows for a burning of the top 5 mm of the insulation, therefore the induced heat from the fire is not taken into account and no distinction is made between molten and burned insulation material.
6. The emissivity was first taken to be that of rusted steel,  $\varepsilon = 0.7$ , and changed to the emission of an ideally sooty surface,  $\varepsilon_1 = 1$ . The reality is certainly between these somewhere close to  $\varepsilon_1 = 1$ , therefore the calculations are worst case scenarios.
7. Already the preliminary estimations done with CFD show that there is a heat transfer between the heated area of the tank and the lower part which is protected by the side tanks and the water around the ship. It is assumed that this flow will have a cooling effect and reduce the heat fluxes as calculated in the 1-D calculations given here.

8. For a more detailed examination a detailed CFD calculation should be made. It could clarify quantitatively the cooling effect of the air coming from under the tank as well as the heating up of the tank structure and the development of the temperatures on the insulation surface, if possible including the melting of the PS foam, the convective heat transfer coefficients on the weather cover and the insulation surface, the cooling effect of the air cooling down under the tank and at the ship's bottom, and the heat transfer from the tank wall into the LNG
9. The actual heat flux of a LNG fire is crucial for the calculation, as can be seen from point 1. This can only be determined by a pool fire test. The tests shall supply
  - the actual heat flux of a LNG fire
  - the actual emissivity during the phases of the test
  - the melting rate, melting behaviour, and properties of melting insulation material

## 2.2 Annotations to the Conclusions

To 2. & 6.: The emissivity depends on the different phases, see Ch. 5.3. In the first phase when the fire outside the weather cover starts, the surfaces are in their original condition and therefore the emissivity as well, assuming a rusted steel cover ( $\varepsilon_1 = 0.7$ ) and a shiny radiation shield ( $\varepsilon_2 = 0.07$ ) on the insulation material. These emissivities are considered to be conservative assumptions for the actual emissivities, which are unknown. The radiation shield should be completely shiny, whereas the weather cover in original condition should be painted with an anti-corrosion paint with an unknown emissivity; by taking that of rusted steel, the worst case is taken into account. In phase 2, the surfaces are assumed to be sooty with  $\varepsilon_1 = \varepsilon_2 = 1$ , even though supposedly neither the melting insulation material nor the remnants of the deteriorating radiation shield are ideal black. In phase 3 the complete insulation is molten or burned away, so is the radiation shield. Therefore the surfaces are taken to be sooty with  $\varepsilon_1 = \varepsilon_2 = 1$ , again.

All these scenarios show that there is no heating up of the LNG tank as long as a reasonable amount of insulation is left, which means for about the first 10 minutes of the burning at a deterioration rate of 2 - 3 cm / min as proposed by Havens [according to a preliminary presentation for the SIGTTO WG meeting, Nov. 2007].

To 3.: By combining the maximum possible heat flux of a fire with an initial heat flux of 300 kW / m<sup>2</sup> (compare Fig. 4) with the maximum possible heat flux into the LNG tank with no insulation left (compare Fig. 9), a heat flux of 150 kW / m<sup>2</sup> is obtained at a wall temperature of about 1000 °C. This is plotted in Fig. 1, showing both the emissive power of the LNG fire as well as the possible heat flux into the tank as a function of the receiving outer

wall temperature of the weather cover. The possible heat flux in steady state can be found at the intersection of the two curves, the emissive power and the heat flux into the tank. For lower wall temperatures, the heat flux can not be transferred into the tank and therefore it will heat up the wall until the incoming heat flux equals the heat flux transferred into the tank. When the wall temperature increases above the intersection point, more heat can be transferred into the tank than the wall is receiving, therefore the wall cools down until both heat fluxes are again equalized.

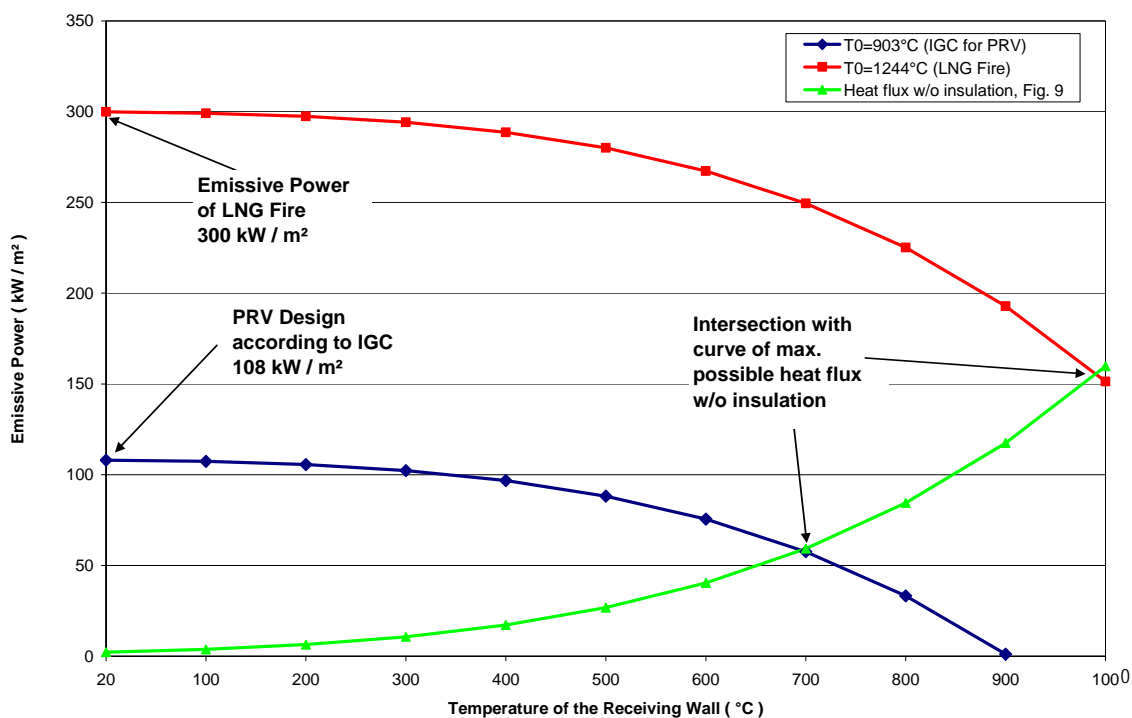


Fig. 1: Maximum emissive power of two fires in combination with maximum heat transfer into the tank without insulation

In case of the design point for pressure release valves (PRV) with an initial heat flux of the flame of  $108 \text{ kW / m}^2$ , the equalization point is reached at a wall temperature of  $700 \text{ }^\circ\text{C}$  and a heat flux of  $60 \text{ kW / m}^2$ .

To 4.: If the boundary condition of an impressed heat flux is applied, film boiling can not occur, as will be shown in Fig. 3. The temperature of the inner aluminium tank will adjust as a result of the equalization of the incoming heat flux from the insulation and the outgoing heat flux into the boiling liquid natural gas (LNG). If this incoming heat flux will rise above  $300 \text{ kW / m}^2$ , the boiling crisis is reached and the aluminium tank wall temperature has to rise dramatically; it will be destroyed before reaching the "new" equilibrium point.

### 3 Description of the Model

The heat transfer calculation has been done with a simplified steady state 1-D model of the LNG tank. The model consists of the weather cover (steel), the air gap between weather cover and insulation, the insulation (PS foam), and the tank wall (aluminium) as shown in Fig. 2. A steady state heat transfer is assumed without the transient process of heating up of the tank structure. The steel temperature  $T_1$  of the weather cover is preset for each calculation; the inner tank wall temperature  $T_4$  is fixed at LNG temperature of  $-162\text{ }^\circ\text{C}$ . For a first calculation, these two temperatures are fixed and a resulting heat flux is calculated, later the heat flux is fixed and the resulting temperatures are calculated. The calculated heat flux is always compared with the maximum possible incoming heat flux from the fire (see Conclusions 1 and 3) and also the maximum outgoing heat flux by pool boiling into the LNG (see Conclusions 4).

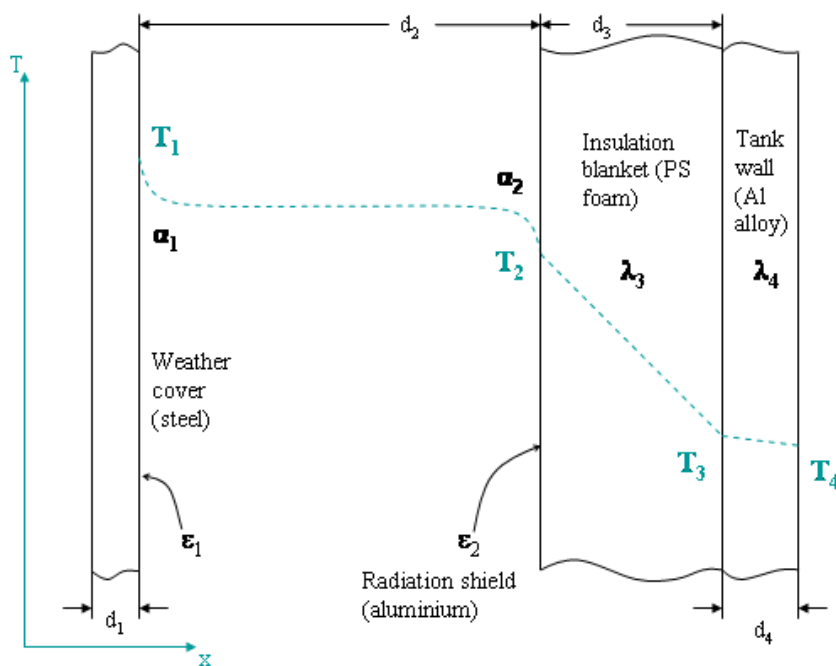


Fig. 2: 1-D model of the LNG tank with its notation

Instead of the spherical wall of a Moss Sphere tank, a simplification is made by using a flat plate model, which is considered a good approximation due to the large radius of the tank and the therefore low curvature. For evaluation of the error of this simplification, both cases are compared. The conductive heat transfer through insulation and tank wall into the spherical tank is calculated using the equation

$$\dot{Q}_{\text{sph}} = 4 \cdot \pi \cdot \left[ \frac{T_4 - T_3}{\frac{1}{\lambda_4} \cdot \left( \frac{1}{R_4} - \frac{1}{R_3} \right) + \frac{1}{\lambda_3} \cdot \left( \frac{1}{R_3} - \frac{1}{R_2} \right)} \right]$$

The conductive heat transfer of a flat plate with the same properties and thicknesses of insulation and tank wall is calculated using the equation

$$\dot{Q}_{\text{plate}} = A_{\text{plate}} \cdot \left[ \frac{T_4 - T_2}{\frac{d_4}{\lambda_4} + \frac{d_3}{\lambda_3}} \right]$$

Here  $A_{\text{plate}}$  is the arithmetic mean of the outer and inner area of the spherical tank and its insulation

$$A_{\text{plate}} = 4 \cdot \pi \cdot \left[ \frac{R_2 + R_4}{2} \right]^2$$

being  $R_4$  the inner tank radius,  $R_3$  the outer radius of the tank wall,  $R_2$  the outer radius of the insulation,  $S_4$  the thickness of the tank wall,  $S_3$  the thickness of the insulation,  $T_4$  the LNG temperature,  $T_2$  the temperature at the outer surface of the insulation, and  $\lambda_4$  the thermal conductivity for aluminium and  $\lambda_3$  the thermal conductivity for the insulation material.

The error of this simplification is calculated to be less than 1‰ and therefore considered negligible in comparison to the uncertainty of the heat transfer coefficients and the emissivities used for this calculation.

The properties of the materials are obtained from data submitted to the SIGTTO working group by Moss Maritime and are shown in Tab. 1.

For the natural circulation of the air in the gap, the convective heat transfer coefficient  $\alpha$  is assumed to be 20 W / m<sup>2</sup>K. For estimation, the convective heat transfer coefficient is calculated for a circular gap according to the Wärmeatlas (see below). For convection in a spherical gap this case is out of range of the correlation of Wright/Douglas [Wright, Douglas, Intl. J. Heat Mass Transfer 29 (1986), pp 725-739]. In the calculation a mean temperature of the air in the gap of 500 K and an outer wall temperature of 1273 K is taken. The Nusselt number is calculated according to the Wärmeatlas [VDI Wärmeatlas, 10<sup>th</sup> Edition, Springer Verlag, pp Fc 1 to Fc 3] using the equation

$$\text{Nu} = 0.2 \cdot \text{Ra}^{0.25} \cdot \left[ \frac{R_1}{R_2} \right]^{0.5}$$

being  $R_1$  the Radius of the outer wall and  $R_2$  of the inner wall, Ra the Rayleigh coefficient

$$Ra = Gr \cdot Pr$$

with the Grashof number  $Gr$  being defined by

$$Gr = \frac{g \cdot s^3}{\nu_m^2} \cdot \left[ \frac{\rho_{inf} - \rho_0}{\rho_{inf}} \right]$$

being  $g$  the gravity,  $\nu_m$  the kinematic viscosity of the air,  $\rho_0$  the density of the air at wall temperature,  $\rho_{inf}$  the density of the bulk air, and  $s$  the characteristic length defined by

$$s = \sqrt{R_1 \cdot R_2} \cdot \ln \left[ \frac{R_1}{R_2} \right]$$

This calculation leads to a convective heat transfer coefficient of

$$\alpha = 1,704 \text{ W / m}^2\text{K}$$

By calculation of the heat transfer based on conservative near-wall temperature in the CFD model (see Ch. 6), the heat transfer coefficient was calculated to be  $\alpha = 1,657 \text{ W / m}^2\text{K}$ . This shows that the value of  $\alpha = 20 \text{ W / m}^2\text{K}$  used for the 1-D calculation is a very conservative assumption.

For the weather cover the emissivity of rusted steel  $\epsilon_1 = 0.7$  is taken, whereas for the radiation shield on the insulation a shiny aluminium surface is assumed with an emissivity  $\epsilon_2 = 0.07$ . After the burning of insulation material and its decomposing, the soot would have blackened both surfaces. Therefore from that moment on both emissivity coefficients are taken to be  $\epsilon_1 = \epsilon_2 = 1$ . This, too, is a conservative assumption

Tab. 1: Overview over the used parameters

parameter	value	unit	
$\alpha_1$	20	W / m <sup>2</sup> ·K	Estimated max. value, s. above
$\alpha_2$	20	W / m <sup>2</sup> ·K	Estimated max. value, s. above
$\epsilon_1$	0.7	-	rusted steel
$\epsilon_1$	1	-	when sooty
$\epsilon_2$	0.07	-	shiny aluminium
$\epsilon_2$	0.7	-	start of Al decomposing
$\epsilon_2$	1	-	after decomp. of Al, when sooty
$\lambda_3$	0.027	W / m·K	at 293.15 K; Src: Moss Maritime
$\lambda_4$	70.8	W / m·K	at 110 K, Src: Moss Maritime
$\sigma$	$5,67 \cdot 10^{-8}$	W / m <sup>2</sup> ·K <sup>4</sup>	Stefan-Boltzmann constant
$\rho_3$	26.5	kg / m <sup>3</sup>	at 293.15 K; Src: Moss Maritime
$\rho_4$	2700	kg / m <sup>3</sup>	Src: Moss Maritime

$d_1$	0.015	m	Src: Moss Maritime
$d_2$	1	m	depth of the air filled space; Src: Moss Maritime
$S_3 = d_3$	0.29	m	Src: Moss Maritime
$S_4 = d_4$	0.02	m	Src: Moss Maritime

#### 4 Methane Pool Boiling

As a second approach, the heat transfer properties of methane in pool boiling are evaluated to estimate the temperature of the inner tank wall. Being the main component of natural gas, methane is expected to represent the properties of natural gas within a reasonable deviation. Pool boiling heat fluxes of methane were measured by Science et al. in 1967 [Science et al., Adv. in Cryog. Eng., Vol. 12, 1967]. Fig. 3 shows the heat fluxes as a function of the wall superheat, the temperature difference ( $T_w - T_{sat}$ ) at different reduced pressures  $P_r$  for nucleate boiling and film boiling. The maximum possible heat flux that can be transferred into the fluid is limited by the critical heat flux, which can lead to the burn out of the heated surface. The critical heat flux is reached when the growing vapor bubbles of the nucleate boiling form a closed film on the heated surface which isolates the surface against the fluid, suddenly decreasing the heat flux and leading to a strong increase in surface temperature for heat-flux controlled systems.

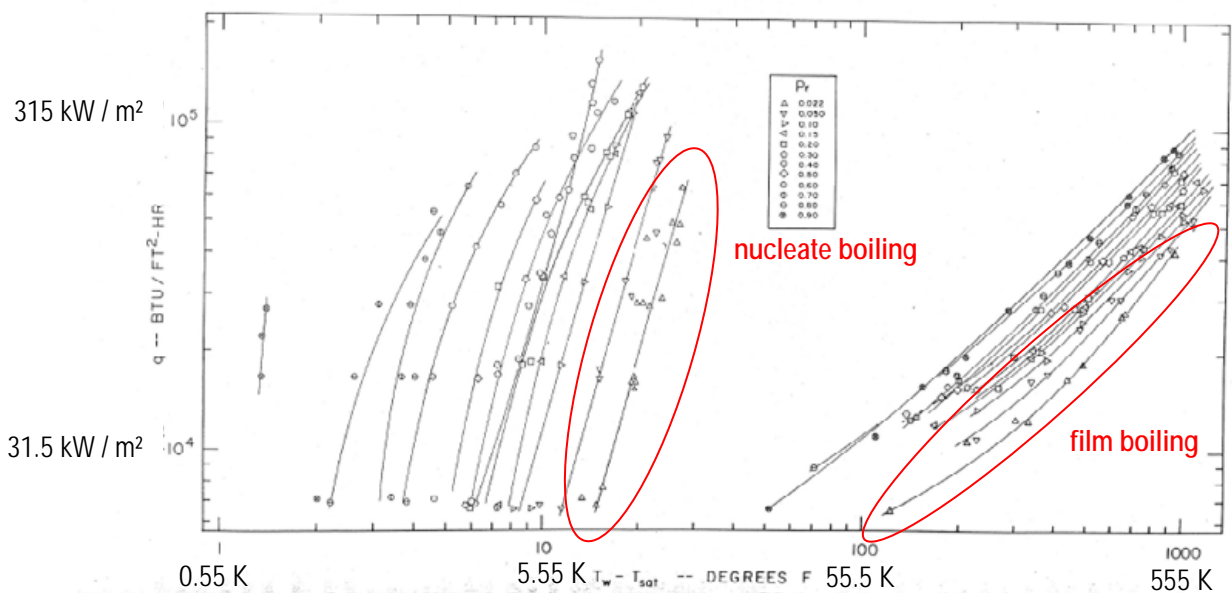


Fig. 3: Boiling curve by Science et al.; heat flux with respect to temperature difference  $T_w - T_{sat}$

In the evaluated LNG tank the LNG is stored at a pressure below the MARVS (Maximum Relief Valve Setting) of 1.25 bar. At MARVS the reduced pressure is  $P_r = 0.027$ , normalized with the critical pressure for methane of  $P_{crit} = 46.1$  bar. At this reduced pressure, the first critical heat flux, the burn out point, was measured by Science with approximately  $300 \text{ kW/m}^2$  at temperature differences ( $T_w - T_{sat}$ ) of about 15 K (27 F). So if the heat flux is

somewhere between  $20 \text{ kW / m}^2$  and  $300 \text{ kW / m}^2$ , the wall temperature will adjust between 7 K and 15 K above saturation temperature of the fluid; if the wall temperature is fixed, the heat flux will be adjusted.

These pool boiling measurements show that the possible heat flux into the LNG tank is limited to less than  $300 \text{ kW / m}^2$ . A higher heat flux would cause the damage of the tank as the wall temperature would jump to  $T_w > 1000\text{K}$ . It should be noted that the measurements of Science were done by use of a heated pipe in a tank filled with liquefied methane. The flow conditions for the bubbles into the liquid are much better compared to the situation at the inner wall of the LNG tank, since, due to the concave shape of the inner tank wall, the bubbles are kept at the tank's inner wall while ascending. This means that the burnout point in our case probably will be reached even at lower heat fluxes.

This leads to the assumption that the critical heat flux will be reached at even lower values than the proposed  $300 \text{ kW / m}^2$  and the incoming heat flux can not be transferred to the fluid anymore. This would lead to an overheating followed by a burnout of the tank wall and therefore a collapse of the whole tank structure. In this case the sizing of the PRVs will not make any difference but the problem will be structural.

## 5 Heat Transfer Calculations

### 5.1 1-D Heat Transfer Equations

The 1-D heat transfer calculation is based on the model as shown in Fig. 2 with the outer steel wall / weather cover, the air filled space in which both convective and radiative heat transfer occurs parallel, the thin radiation shield on the insulation that is modelled only by the use of its emissivity coefficient, the insulation, and the tank wall made of aluminium. The heat flux is calculated by iteration of the insulation thickness  $d_3$ , or in one case the temperature of the insulation surface  $T_2$ , to equalize the heat flux through the air filled space and the heat flux through the insulation and the tank wall. This procedure does not correspond to the real situation, where the insulation material is melting in a certain time, but since we are approximating the different time steps with a steady state calculation this seems reasonable. For the radiation and convection in the air filled space the equation

$$\dot{q} = \sigma \frac{1}{\frac{1}{\varepsilon_1} + \frac{1}{\varepsilon_2} - 1} (T_1^4 - T_2^4) + \frac{\alpha_1 \cdot \alpha_2}{\alpha_1 + \alpha_2} (T_1 - T_2)$$

and for the conduction in the insulation and the tank wall the equation

$$\dot{q} = \frac{\lambda_3 \cdot \lambda_4}{d_3 \lambda_4 + d_4 \lambda_3} (T_2 - T_4)$$

are used.

A maximum value for the temperature  $T_2$  on the surface of the insulation blanket is set for the calculation, as the material cannot be heated above its decomposition temperature. Since the exact decomposition temperature of the used PS foam was not known when performing the calculation, a lower (200 °C) and an upper temperature (300 °C) are taken. The use of a fixed temperature at the insulation surface does not implicate that the insulation thickness has no effects on the heat flux into the cargo as the thickness is calculated based on the heat flux and without a fire this maximum temperature would not be reached.

### 5.2 Estimation of the maximum possible heat flux from the fire

As in the SIGTTO WG discussion already agreed on, the maximum possible emissive power of a LNG fire can be estimated to be about 300 kW / m<sup>2</sup> [Nedelka: Calculation of Radiation Effects from LNG Fires; GdF, 1989] or 290 kW / m<sup>2</sup> [J. Havens: Fire Performance of LNG Carriers Insulated with Polystyrene Foam, 2007], respectively. This emissive power can be taken as the initial heat flux into a cool receiving wall. By assuming ideal emissive coefficients of  $\varepsilon_0 = \varepsilon_1 = 1$  we can calculate the maximum possible emissive power with the equation

$$\dot{q} = \sigma \cdot \Delta T^4 ,$$

being  $\sigma$  the Stefan-Boltzmann constant and  $\Delta T^4 = T_0 - T_1$ . At  $300 \text{ kW} / \text{m}^2$  the theoretical flame temperature can be obtained by assuming the receiving wall at ambient temperature of  $T_1 = 293 \text{ K}$  to be

$$T_0 = \left[ \frac{\dot{q}}{\sigma} + T_1^4 \right]^{1/4} = 1517 \text{ K} .$$

When the receiving wall is heating up, the heat flux will decrease due to the decreasing temperature difference. At a receiving wall temperature of  $1000 \text{ }^\circ\text{C}$ , the heat flux can be calculated to

$$\dot{q} = \sigma \cdot [T_0^4 - T_1^4] = 151 \text{ kW} / \text{m}^2 .$$

The emissive power of a LNG fire based on the initial emissive power of  $300 \text{ kW} / \text{m}^2$  as well as the emissive power of the IGC Code pressure release valve (PRV) design standard fire with a flame temperature of  $903 \text{ }^\circ\text{C}$  can be found in Fig. 4 with regard to the temperature of the receiving wall. For the LNG fire, the heat flux decreases to the value of  $151 \text{ kW} / \text{m}^2$  as described above.

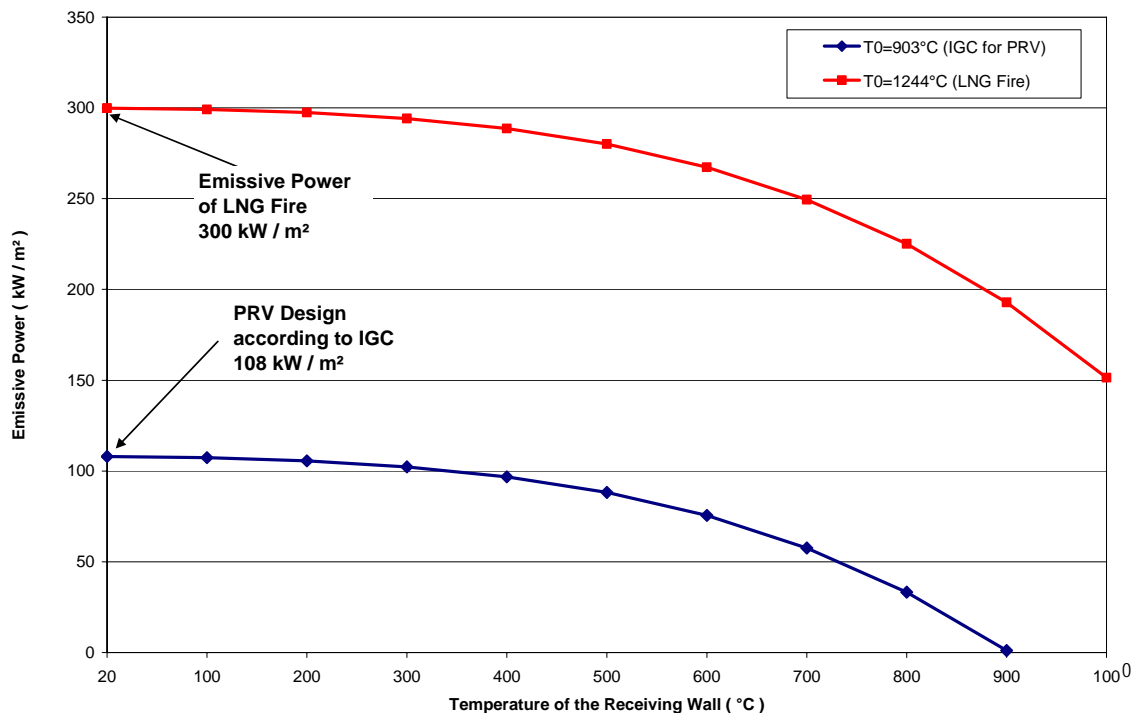


Fig. 4: Emissive power vs. Temperature of the receiving wall for flame temperatures of  $T_0=903^\circ\text{C}$  and  $T_0=1244^\circ\text{C}$

These results show that it is far from reality to assume a heat flux of  $300 \text{ kW} / \text{m}^2$  into a completely heated up outer wall of the LNG tank since the fire can under no circumstance transfer such a high heat flux. Nonetheless,

these results are not incorporated in the following calculations. There are no preconditions but the reader shall have the lower emissive power at high receiver temperature in mind.

### 5.3 *Different Phases of the Incident*

The calculation is split into three different phases of the incident. These three phases represent the heating up of the tank structure and the different stages of deterioration of the radiation shield and the insulation material.

1. The first phase represents the first minutes of the incident, with the radiation shield in good condition and the complete insulation. This is a theoretical case, since neither would the insulation survive higher temperatures than 200 °C / 300 °C, nor the aluminium radiation shield higher temperatures than 660 °C; therefore this is taken up to a steel temperature of 600 °C. The emissivity is taken to be  $\epsilon_1 = 0.07$  for the shiny aluminium and  $\epsilon_2 = 0.7$  for the weather cover.
2. Phase 2 represents the condition after the heating up. The aluminium radiation shield has molten, the surface of the insulation material has shortly burned and the surfaces are sooty. The emissivity is taken to be  $\epsilon_1 = \epsilon_2 = 1$ . The insulation material is melting down depending on the outer wall temperature, leaving a variable insulation thickness. On the surface of the insulation the temperature stays constant because of the melting. In the LNG tank nucleate boiling is assumed. This phase is taken up to a steel temperature of 1000 °C
3. Phase 3 represents the heat transfer after the complete decomposing of the insulation material, leaving only the weather cover and the tank wall with sooty surfaces and therefore the worst-case scenario. The emissivity is taken to be  $\epsilon_1 = \epsilon_2 = 1$ , again.

Even though these calculations are simplified steady state 1-D calculations, they allow for a view into the transient events but without the timeline. Transient calculations done by Havens [according to a preliminary presentation for the SIGTTO WG meeting, Nov. 2007] resulted in the assumption that the insulation material deteriorates with a rate of 2-3 cm / min; the heating up of the outer steel wall to 1000 °C was calculated to take about 5 minutes. In this relatively slow process, we can approximate each time step with a steady state calculation that shows good agreement with the results of the transient calculation.

In Fig. 5 the effect of the use of different emission coefficients can be seen. For each phase the curve of the there used coefficients are marked.

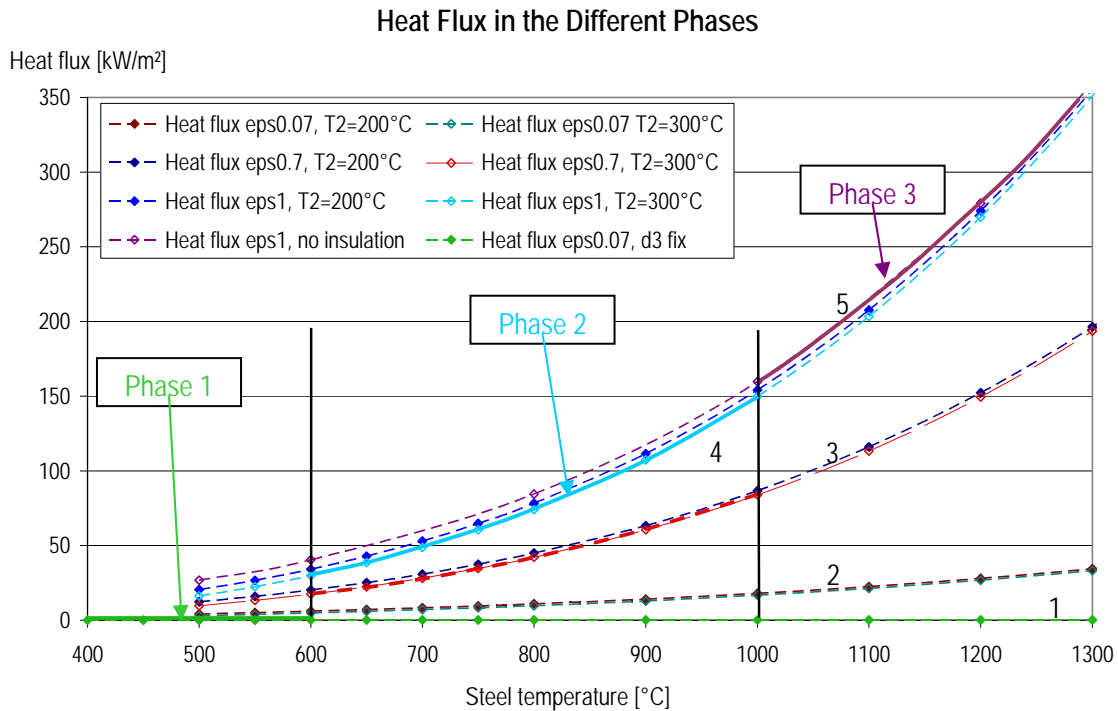


Fig. 5: Heat flux in the different phases of the incident; effects of the emission coefficient

In the first calculation presented in May in Hamburg, the emission coefficients were taken to be  $\epsilon_1 = 0.7$  and  $\epsilon_2 = 0.07$ , therefore they are represented in the graph by the curve 2. By changing the emission coefficient to  $\epsilon_2 = 0.7$  due to the assumed deterioration of the aluminium radiation shield, curve 3 had been obtained, still showing maximum heat fluxes below 200 kW / m<sup>2</sup> at 1300 °C. Heat fluxes higher than 300 kW / m<sup>2</sup> are only obtained when assuming completely sooty surfaces by setting  $\epsilon_1 = \epsilon_2 = 1$ , and at temperatures of the outer steel wall of more than 1200 °C with hardly any (curve 4) or no insulation (curve 5) left. This situation can not be reached as the temperature difference between the fire and the outer wall of the weather cover will be too small to give an input heat flux of more than 150 kW / m<sup>2</sup>, compare Conclusions in Ch. 2.

### 5.4 Phase 1: complete insulation and radiation shield

In phase 1 the LNG tank is considered in original condition. The insulation keeps the heat flux low while the surface temperature of the insulation increases linearly with increasing steel temperature of the weather cover. The results can be seen in Fig. 6, with the heat flux and the insulation surface temperature in dependence on the steel temperature of the weather cover. The heat flux into the LNG tank stays below  $0.2 \text{ kW/m}^2$  even at high temperatures at the outer steel. Since the insulation starts melting between  $200 \text{ }^\circ\text{C}$  and  $300 \text{ }^\circ\text{C}$  and the aluminium radiation shield melts at  $660 \text{ }^\circ\text{C}$ , these values are only theoretical and therefore only valid for lower temperatures and a very short time.

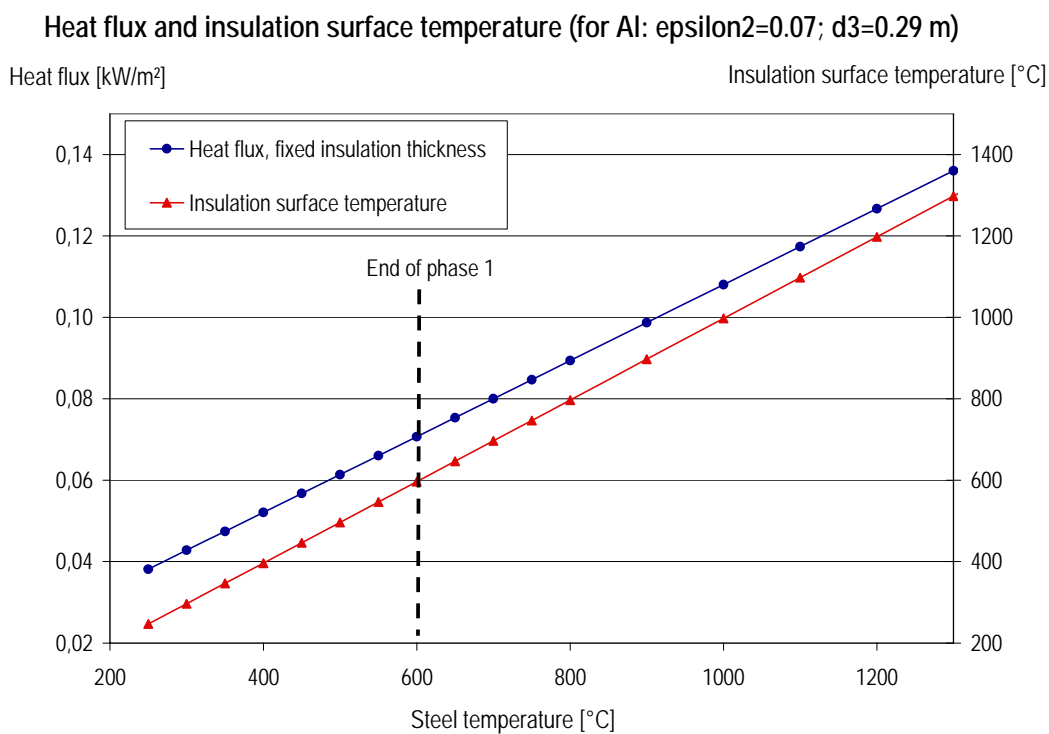


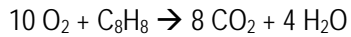
Fig. 6: Heat flux and insulation surface temperature in phase 1

This shows that the incoming heat flux is very low as long as there is a relevant amount of insulation thickness left.

### 5.5 Phase 2: decomposing insulation

In phase 2 the radiation shield is either molten or sooty from the decomposing polystyrene insulation, which can have burned for a short time. For the burning of a relevant amount of the polystyrene more air would be needed than available in the air gap of the tank. The volume of air in the space between weather cover and tank

insulation can be estimated to be about 6000 m<sup>3</sup>. Styrene, the basic molecule from which polystyrene is polymerized, is in chemical formulation C<sub>8</sub>H<sub>8</sub>, with a molecular weight of 104 g / mol. The formulation of the combustion reaction



shows that per mole of styrene 10 mole of oxygen are needed. This leads to a maximum of 21 m<sup>3</sup> of polystyrene that can be burned with the oxygen of the air gap, which is equal to the burning of the top 5 mm of the insulation. For this reason it is concluded that the burning of the insulation material will lead to an increase in the emissivity but will have no relevant effect to the decomposing of the insulation or heat transfer into the tank. The melting of the insulation material leads to a constant temperature at its melting temperature.

The calculated heat transfer and the resulting thickness of the insulation at two melting temperatures of the insulation material are shown in Fig. 7 with regard to the outer steel temperature.

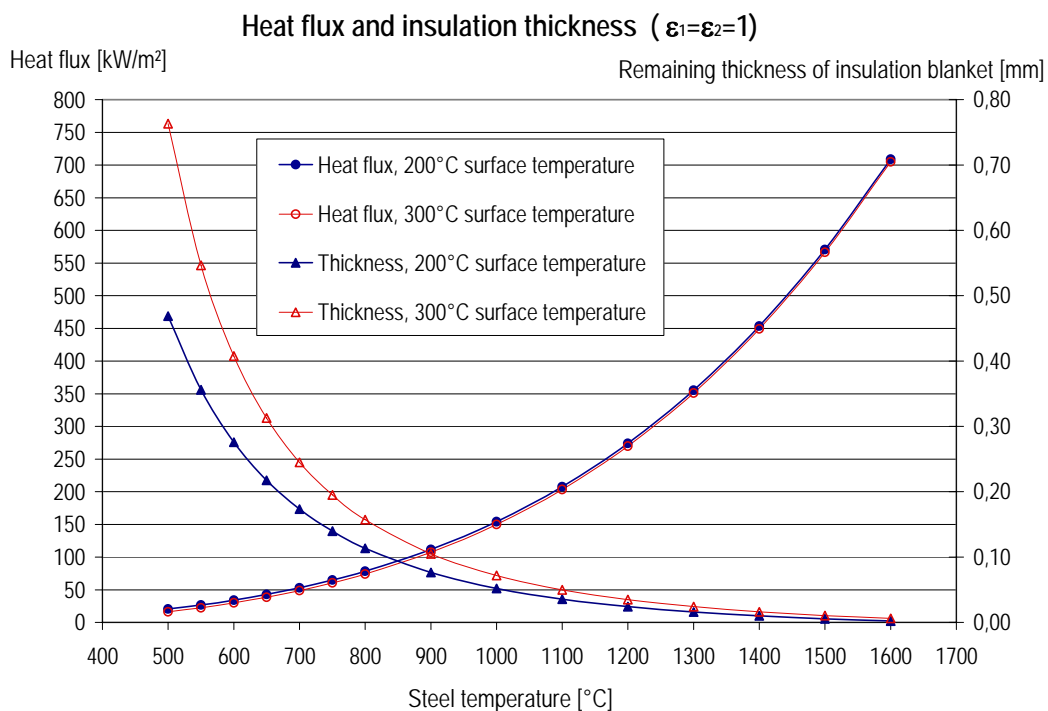


Fig. 7: Heat flux and insulation thickness in phase 2

The emissivity coefficients are taken to be  $\epsilon_1 = \epsilon_2 = 1$ , which means that it is assumed that both surfaces are covered with soot. This leads to a high radiative heat flux resulting in a total heat flux of up to 570 kW / m<sup>2</sup> at

1500 °C. At these heat fluxes, the resulting thickness of the insulation having a temperature  $t < 300$  °C is calculated to be under 0.05 mm.

A second approach is taken by the computation of heat fluxes for a range of fixed values of the insulation thickness  $d_3$ . The calculation is based on the same equations for the heat transfer (see Ch. 5.1) and the same input parameters as the previous calculations; therefore the same results can be found at 200 °C and 300 °C insulation surface temperature as in the graph before. For the emissivity of the insulation surface and the weather cover,  $\epsilon_1 = \epsilon_2 = 1$  was taken again. The insulation thickness  $d_3$  is varied between 0.7 m and 0.025 mm.  $T_2$  is then determined by iteration. The results of this iteration for three steel temperatures are shown in Fig. 8. The variable temperature  $T_2$  at the insulation surface is plotted on the x-axis. For a steel temperature of 1000°C, even at very thin insulation thicknesses the heat flux would still remain below 160 kW/m<sup>2</sup>K. Steel temperatures in the range of 1300 °C are needed to exceed heat flux values of 350 kW/m<sup>2</sup>K. Of course, insulation temperatures of more than 300 °C are only theoretical, but the graph show clearly that the heat flux decreases with increasing insulation surface temperature.

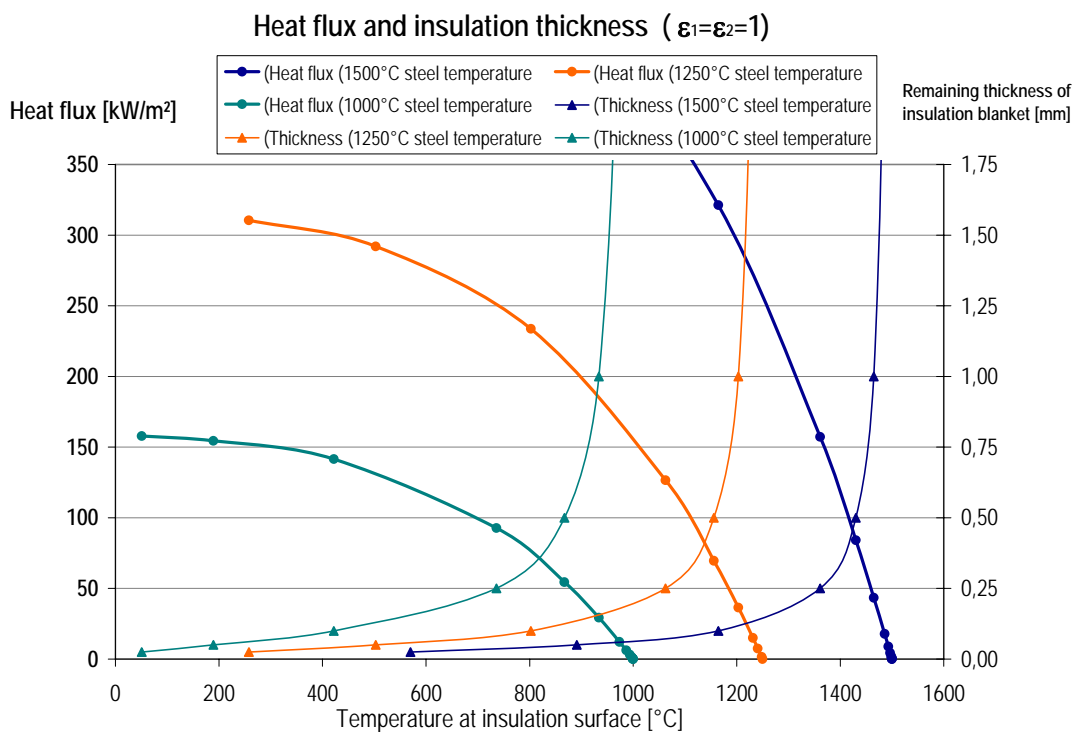


Fig. 8: Heat flux and insulation thickness with respect to insulation surface temperature

### 5.6 Phase 3: completely removed insulation

For phase 3 the heat flux is calculated in the case of the total removal of the insulation blanket. The equation for heat conduction in the tank hull is then reduced with  $T_2$  identical to  $T_3$ . Since the insulation is partly burned, partly molten and pyrolyzed, the surfaces are supposed to be sooty and therefore the emission coefficients are set to  $\epsilon_1 = \epsilon_2 = 1$ . The results of this calculation illustrated in Fig. 9 show that without the thermal resistance of the insulation blanket, a heat flux of 550 kW/m<sup>2</sup>K could be reached at a temperature of the weather cover of 1500 °C, which means melting of the steel.

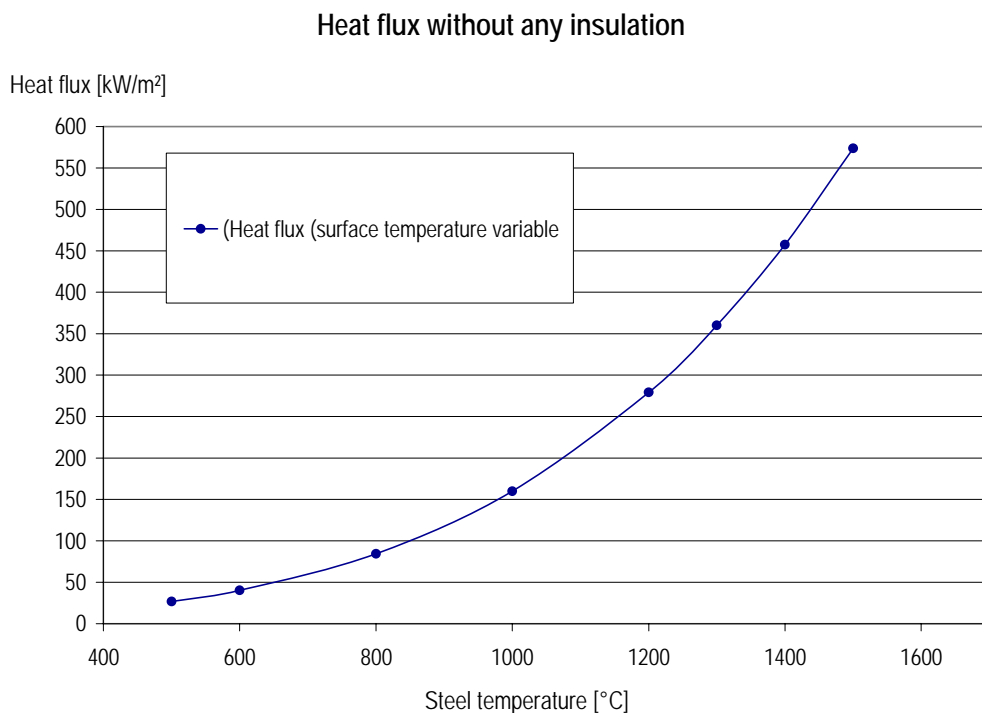


Fig. 9: Heat flux without insulation in phase 3

For a better imagination of the proposed temperatures a look into the incandescence colors of steel is helpful. When assuming a temperature of the outer steel wall of 1000 °C, this means that the complete weather cover will be glowing in bright yellow. By assuming a temperature of 1500 °C the colors increase to bright white incandescence glow and the complete meltdown of the steel. This can be seen in Fig. 10 showing the incandescence colors of steel at different temperatures from 550 °C (dark red) to 1300 °C (bright white).

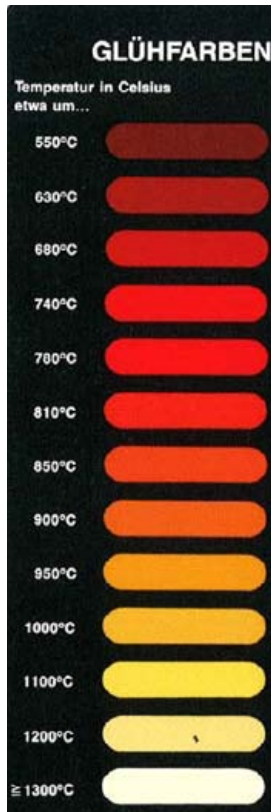


Fig. 10: Incandescence colours of steel at different temperatures

## 6 CFD Calculation

### 6.1 Model Description

For evaluation of the flow field in the air filled space between weather cover and insulation, a preliminary CFD calculation is done. By calculation of the flow field, the overall convective heat transfer coefficients and the cooling effect of the air is estimated.

The CFD model is built according to the data submitted by Moss Maritime. It consists of two air domains, which are separated by the tank skirt (see Fig. 11 and Fig. 13). The upper air is heated up at the hot weather cover and cooled down at the insulation surface of the tank as well as at the ballast tanks and the tank skirt. The ballast tanks are assumed to have a constant temperature of 20 °C, since the seawater cools it from outside. The tank skirt is cooled from the second air domain, which is between the lower part of the tank, the ship's bottom, and the tank skirt at the sides. The ship's bottom is assumed to be adiabatic, which is considered a conservative assumption since it is cooled by the seawater. Due to the limited resources, only the temperatures of the surfaces are set and no heat transfer into the weather cover nor through the insulation and into the tank is modelled. As a surface temperature of the insulation 200 °C are set and for the weather cover 1000 °C. Fig. 12 shows the CFD model, with the insulation surface shown as a green grid.

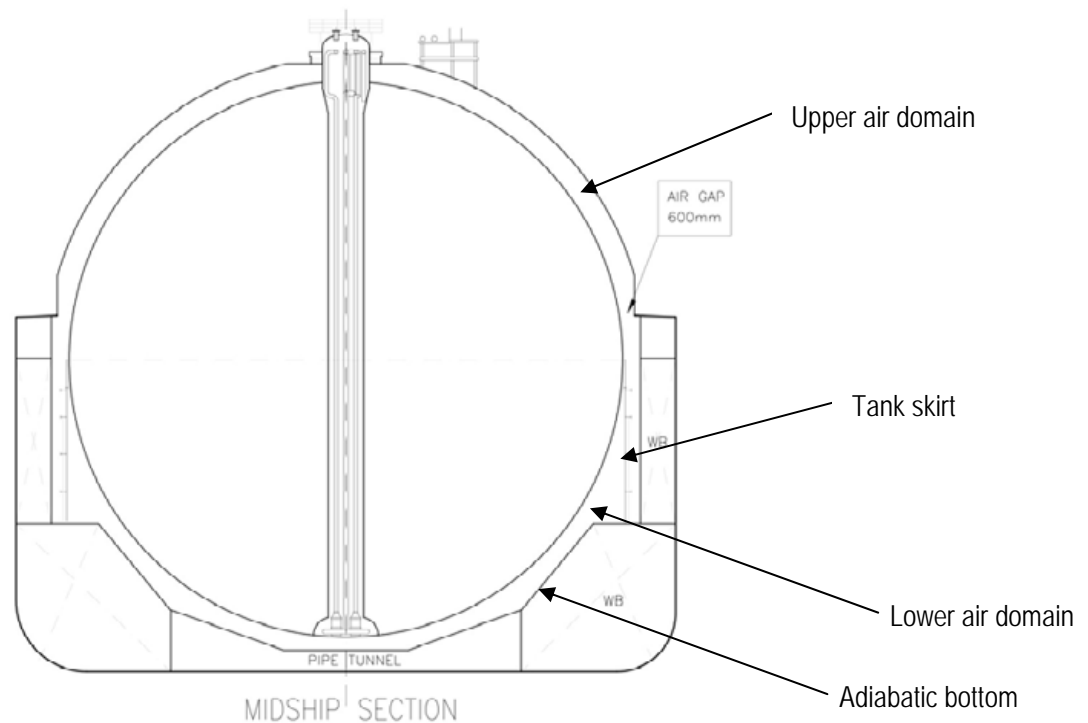


Fig. 11: Cut view of a Moss Sphere LNG tank

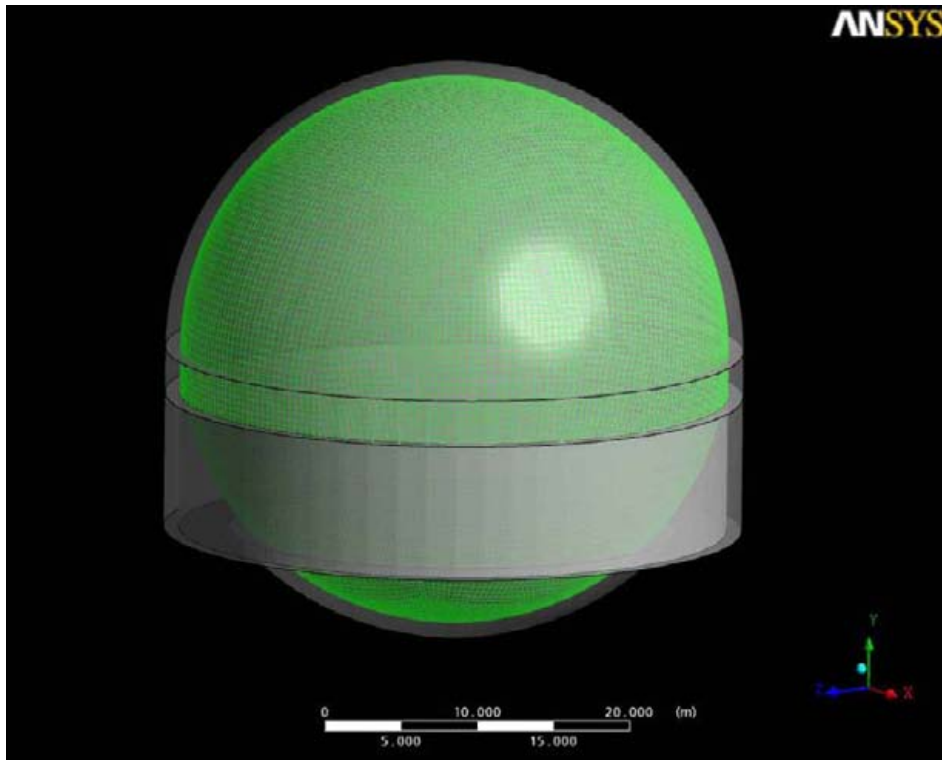


Fig. 12: CFD model of the LNG tank with marked insulation surface

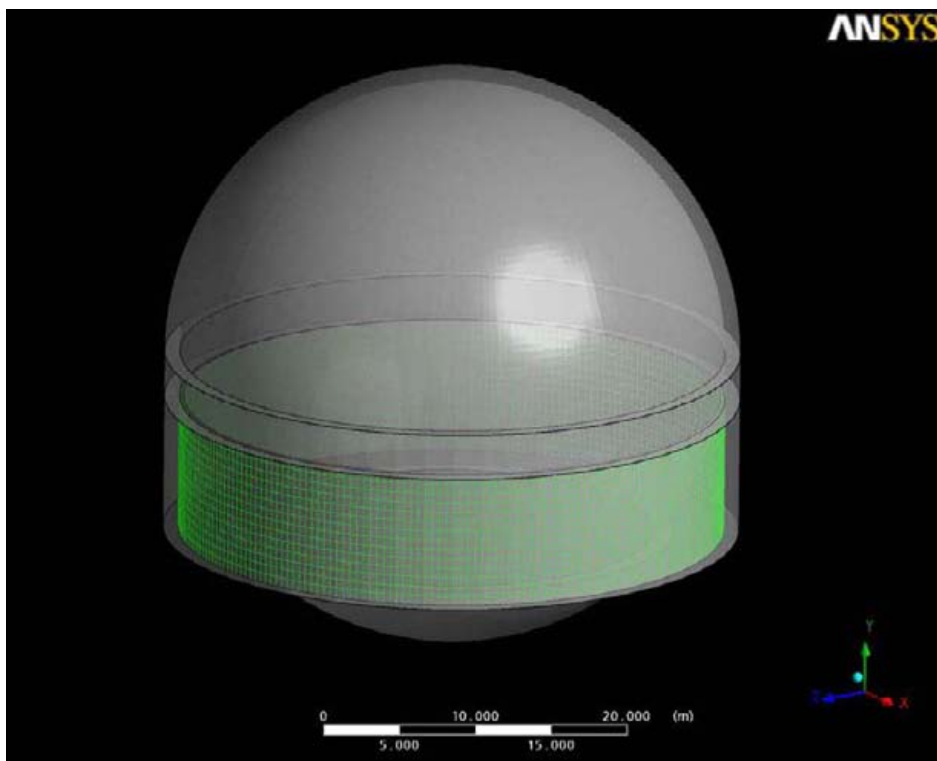


Fig. 13: CFD model of the LNG tank with marked tank skirt

## 6.2 CFD Results

The results of the CFD calculation show an average air temperature in the whole air volume of 574 K, the average temperature in the lower hemisphere is calculated to be 443 K and in the upper, heated hemisphere 668 K. The temperature distribution is shown in Fig. 14. The highest temperatures are obtained at the very top of the sphere, which can be explained by the lowest air velocity due to the air encountering at the top from around the sphere and therefore having the lowest velocity in the middle. The velocity profile in the air gap can be seen in Fig. 15, with the heating up air ascending on the outer wall and the cooling down air descending at the insulation surface. The maximum air velocity is calculated to be less than 2 m / s. The overall convective heat transfer coefficient in the gap was calculated on a plane across the top of the upper hemisphere of the LNG tank. Based on the conservative near-wall temperatures, the coefficient was calculated to be  $\alpha = 1,657 \text{ W / m}^2\text{K}$ .

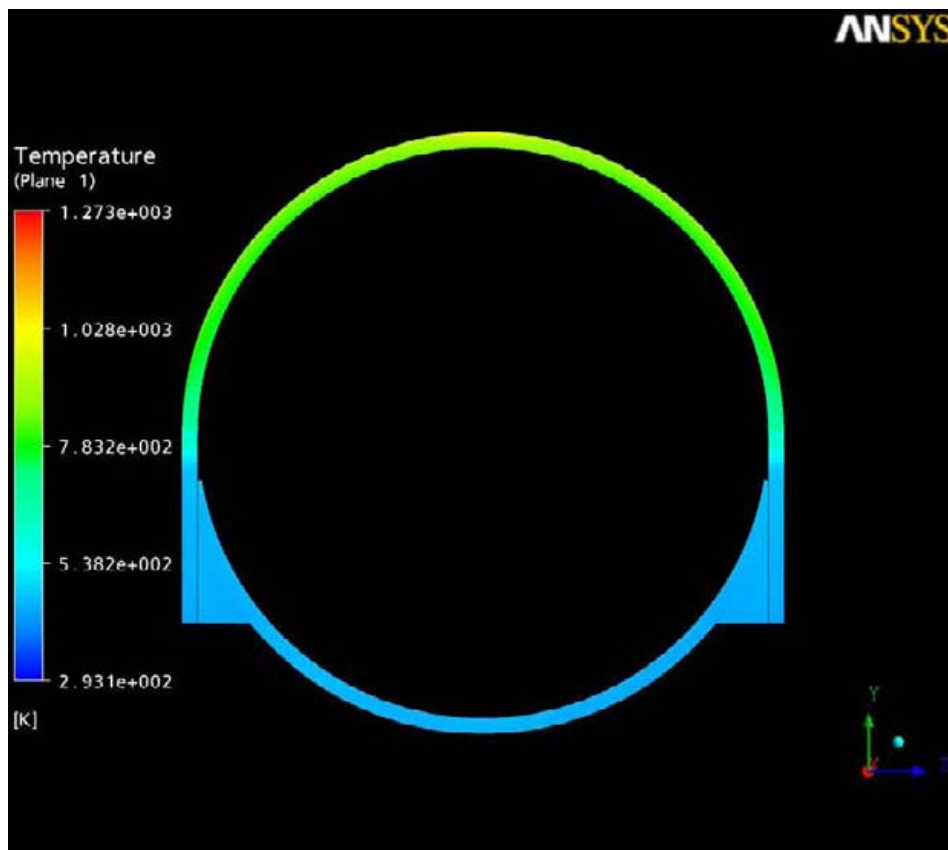


Fig. 14: CFD calculated temperature distribution in the air filled space between weather cover / hull and LNG Tank

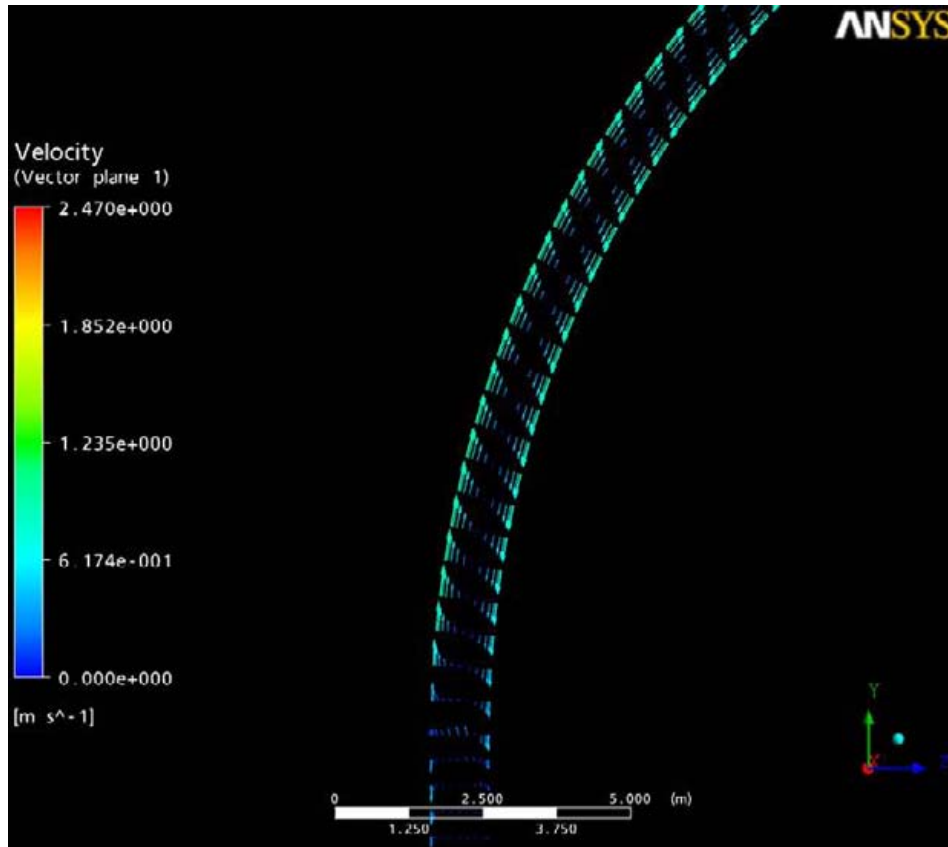


Fig. 15: CFD calculated flow field in the air filled space, upwards on the heated outer steel wall and downwards on the insulation surface

## **7 Outlook**

For a detailed analysis of the heat transfer from an engulfing fire into the LNG tank, a more detailed CFD calculation is necessary. Whereas the already computed CFD calculation aimed only at the flow field in the air space, the next should include the heat transfer through the whole tank with more accurate boundary conditions than the ones that were modelable here. The new calculation based on a CFD program should estimate more precisely

- the heating up of the tank structure and the development of the temperatures on the insulation surface, if possible including the melting of the PS foam
- the convective heat transfer coefficients on the weather cover and the insulation surface
- the cooling effect of the air cooling down under the tank and at the ship's bottom.

In addition to the CFD work, the melting and burning of PS insulation and the boiling heat transfer into the LNG should be analyzed by experiments or material data from the manufacturer.



## **APPENDIX 3 – CFD MODELLING OF THE HEAT INPUT TO AN LNG TANK**



# CFD modelling of the heat input into an onboard LNG-tank

Diploma thesis

Benjamin Scholz

Adviser: Prof. Dr. A. Leder, Dr. Gerd Michael Würsig (GL)

17.07.2008



University of Rostock  
department fluid mechanics



Germanischer Lloyd

## Content



- **Introduction to the topic**
- **Theoretical foundations**
  - Tank design
  - Physical effects of the heat transfer
  - Used Software
- **Preparation of the simulation**
  - Meshing
- **Results**
  - Temperature distribution
  - Heat input
- **Summary**



### Introduction to the topic

- **Substitution of the primary energy sources, petroleum and coal, by natural gas**
  - Trend to mild-carbon fuels, CO<sub>2</sub> reduction,
  - 25 % of the consumed natural gas is transported via gas carrier,
  - Transport in liquid phase, boiling temperature at ambient pressure 111 K , main component: methane,
  - Number of new buildings increased from 26 (2006) to 37 vessels in 2007.
- **The security-relevant aspects of such a transport chain are subject of current discussions.**
- **Classification of a gas carrier according to IGC-Code** (International Code for the Construction and Equipment of Ships Carrying Liquefied Gases in Bulk)
  - Collapse of the structure (tank) is to be avoided in the case of a failure,
  - Worst case scenario is an enveloping fire, nominal value of the heat input is 108 kW m<sup>-2</sup>,
  - Pressure relief valves have to ensure the discharging of an equivalent mass flow to decrease the pressure inside a tank during a failure.



### Introduction to the topic

- **Sandia National Laboratories investigated the potential hazards of spilled LNG in 2004**
  - Potential hazards of a LNG spill over water because of a leakage caused by ship collision or an act of terrorism
  - Burning duration depending on the leak size, 3.4 min (12 m<sup>2</sup>) until 40 min (1 m<sup>2</sup>).
- **A working group of the SIGTTO has been engaged in the investigation / evaluation of possible insufficient dimensioning since 2006** (Society of International Gas Tanker & Terminal Operators Ltd)
  - Decomposition of the insulation as a result of the thermal stress.
- **Goal of this study**
  - Estimation of the heat input into an onboard LNG-tank using CFD-methods.



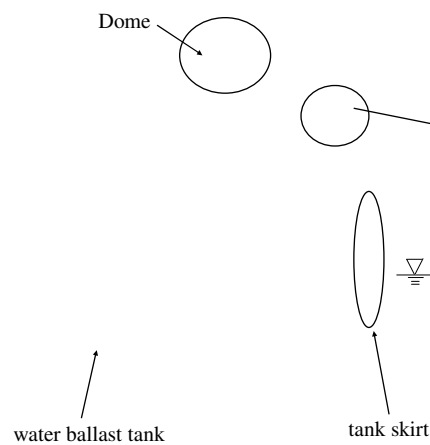
## Content



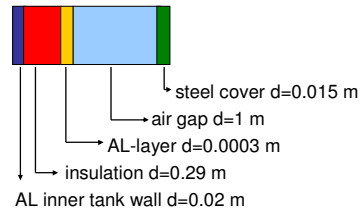
- Introduction to the topic
- **Theoretical foundations**
  - Tank design
  - Physical effects of the heat transfer
  - Used Software
- Preparation of the simulation
  - Meshing
- Results
  - Temperature distribution
  - Heat input
- Summary



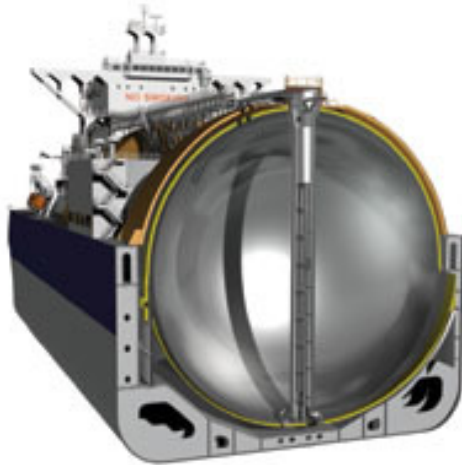
## Moss Design



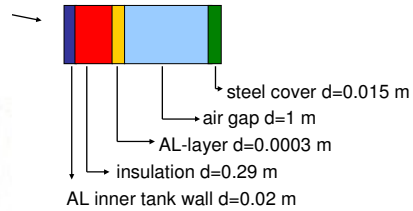
- Spherical Tank; tank support by cylindrical structure (skirt)
- Inner diameter 41.9 m
- Insulation configuration:



## Moss Design (2<sup>nd</sup> picture of the animation)



- Spherical Tank; tank support by cylindrical structure (skirt)
- Inner diameter 41.9 m
- Insulation configuration:



CFD modelling of the heat input into an onboard LNG-tank

17.07.2008

No. 7



Germanischer Lloyd

## Heat flux into the Moss tank

- Heat flux into the tank is caused by the temperature gradient between the inner tank wall and the steel cover

- Heat conduction

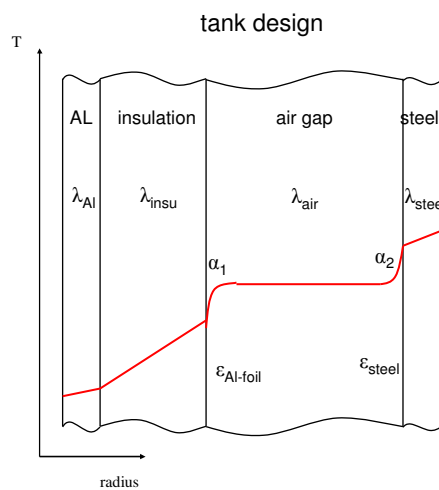
$$\dot{q} = -\lambda \text{grad} \theta$$

- Convective heat flux

$$\dot{q}_w = \alpha(\theta_w - \theta_f)$$

- Thermal radiation

$$\dot{q} = \varepsilon(T)\sigma T^4$$



CFD modelling of the heat input into an onboard LNG-tank

17.07.2008

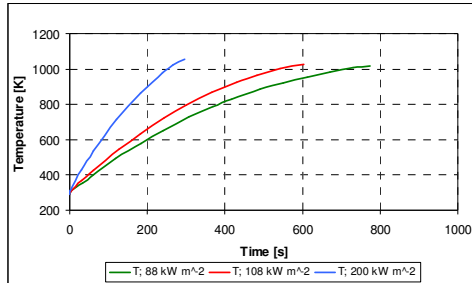
No. 8



Germanischer Lloyd

**FEA-results, American Bureau of Shipping**

Increase in temperature, steel cover



- Thermal collapse of the structure at 1023 K, due to local large deformation caused by the abrupt drop of Young’s modulus
- Connection of cover sheet and top platform
- Impressed heat flux
  - 88 kW m<sup>-2</sup> till 200 kW m<sup>-2</sup>
  - 775 s till 297 s



**Computational Fluid Dynamics, CFX 11.0**

mass conservation: 
$$\frac{d}{dt} \int_V \rho dV + \int_S \rho U_j n_j = 0$$

momentum conservation: 
$$\frac{d}{dt} \int_V \rho U_i dV + \int_S \rho U_j U_i n_j = - \int_S p n_j + \int_S \mu_{eff} \left( \frac{\partial U_i}{\partial x_j} + \frac{\partial U_j}{\partial x_i} \right) n_j + \int_V S_{U_i} dV$$

energy conservation: 
$$\frac{d}{dt} \int_V \rho \phi dV + \int_S \rho U_j \phi n_j = \int_S \Gamma_{eff} \left( \frac{\partial \phi}{\partial x_j} \right) n_j + \int_V S_\phi dV$$

- Spatial discretisation
- Assembling of the conservation equations
- Transfer into a linear system of equations



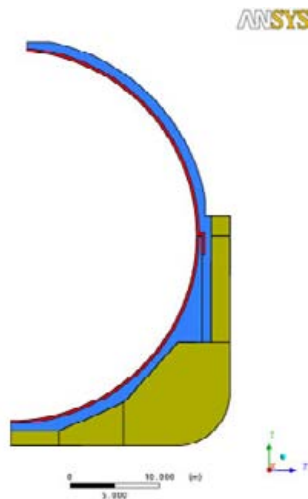
## Content



- Introduction to the topic
- Theoretical foundations
  - Tank design
  - Physical effects of the heat transfer
  - Used Software
- Preparation of the simulation
  - Meshing
- Results
  - Temperature distribution
  - Heat input
- Summary



## Meshing, ICEM

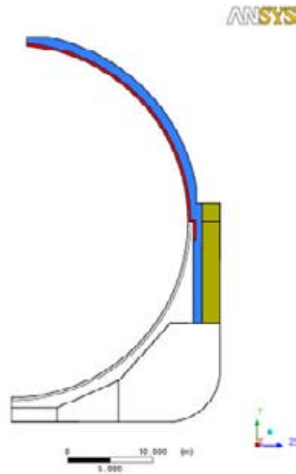


- 2 dimensional model, utilization of the symmetry
- Simplification of the 2 dimensional model for the investigation within the transient calculations
- Finite volume elements

	raw	mid	fine
fluid	30659	61318	153732
insulation	18408	24769	74307



**Meshing, ICEM (2<sup>nd</sup> picture of the animation)**



- 2 dimensional model, utilization of the symmetry
- Simplification of the 2 dimensional model for the investigation within the transient calculations
- Finite volume elements

	raw	mid	fine
fluid	30659	61318	153732
insulation	18408	24769	74307



**Content**

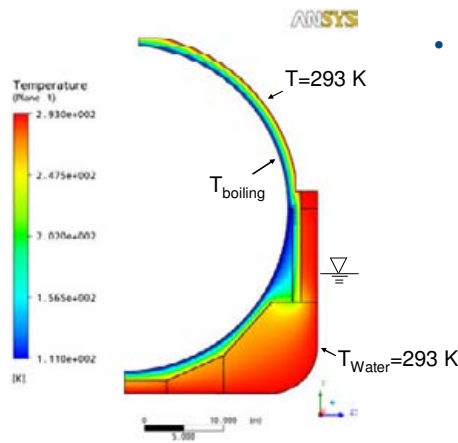


- Introduction to the topic
- Theoretical foundations
  - Tank design
  - Physical effects of the heat transfer
  - Used Software
- Preparation of the simulation
  - Meshing
- Results
  - Temperature distribution
  - Heat input
- Summary



## Results, steady state calculations

### Heat conduction



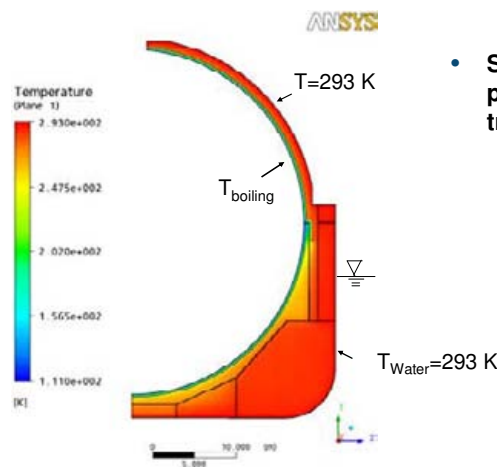
- **Successive consideration of the 3 physical effects of the heat transfer**

- heat conduction,
  - thermal radiation,
    - dominant effect
  - natural convection,
    - moderate convergence
    - transient flow can not be solved
- no significant results



## Results, steady state calculations (2<sup>nd</sup> picture of the animation)

### Heat conduction and thermal radiation



- **Successive consideration of the 3 physical effects of the heat transfer**

- heat conduction,
  - thermal radiation,
    - dominant effect
  - natural convection,
    - moderate convergence
    - transient flow can not be solved
- no significant results



### Transient calculations, 1. simulation series

- **Estimation of the numerical results (simplified model)**
  - Investigations of fluid meshing
  - Investigations of solid meshing
  - Convergence criteria
    - max. residuum  $10^{-3}$  and  $10^{-4}$
    - single / double precision
  - Model criteria
    - thermal radiation Discrete Transfer Model / Monte Carlo Model
    - turbulent natural convection
  - Boundary condition
    - initial heat flux

$$\dot{q} = \sigma (T_{Fire}^4 - T_{Cover}^4)$$

- **Sensitivity studies were performed to achieve results independent from chosen discretisation.**

CFD modelling of the heat input into an onboard LNG-tank

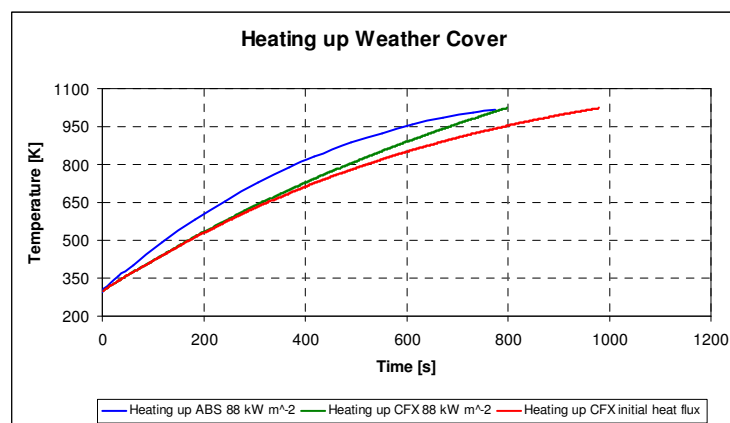
17.07.2008

No. 17



Germanischer Lloyd

### Transient calculations, 1. simulation series (2<sup>nd</sup> picture of the animation)



CFD modelling of the heat input into an onboard LNG-tank

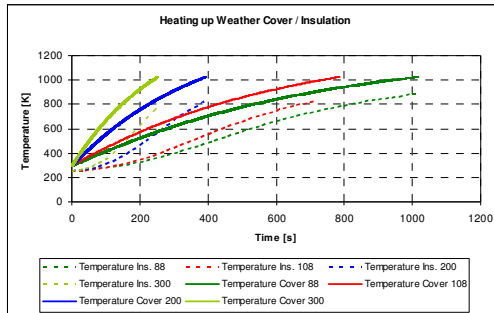
17.07.2008

No. 18



Germanischer Lloyd

## 2. simulation series, heating up cover / insulation

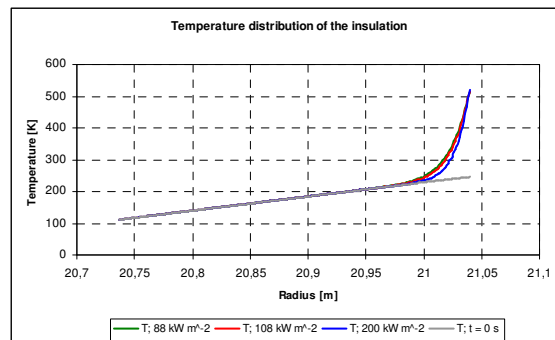


Initial heat flux	473 K	573 K
88 kW m <sup>-2</sup>	390 s	500 s
108 kW m <sup>-2</sup>	335 s	420 s
200 kW m <sup>-2</sup>	210 s	255 s

- Complete heating up, until beginning of the thermal collapse,
- 1. phase, time period until the beginning of melting of the insulation,
- 2. phase (idealized case), time period from the beginning of melting until the thermal collapse of the cover.



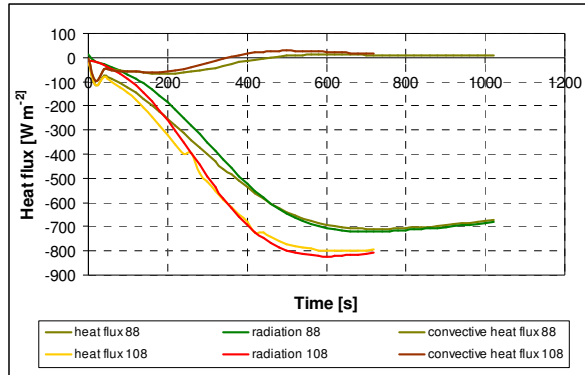
## Temperature distribution in the insulation at $t_{\text{melting}}$



- Graphs refer to three impressed initial heat fluxes,
- Heating up is only recognizable close to the boundary of the insulation,
- Heat conductivity prevent the heat transport from the surface into the insulation,
- No change of the heat input into the tank compared to the operating state.



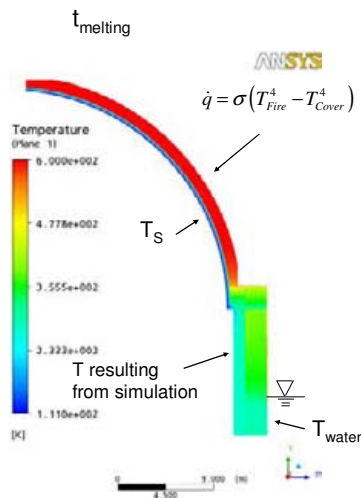
### Heat flux into the insulation



- Splitting up the heat input into the fraction for thermal radiation and convective heat transfer,
- Dominant effect: thermal radiation,
- Small heat input into the insulation compared to the heat flux into the cover.



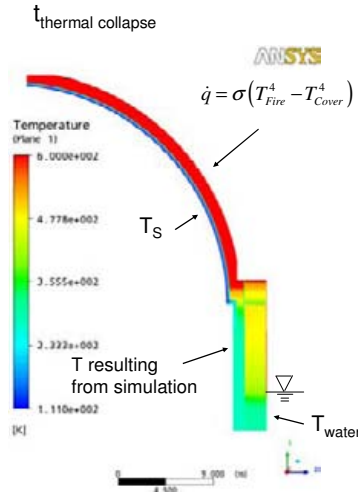
### Temperature distribution $t_{melting}$ and $t_{thermal\ collapse}$



- Temperature layering, highest temperature in the spherical area, critical area regarding the thermal stress
- Dominant effect is the thermal radiation in the spherical area  
→ 2-dimensional calculation sufficient
- Dominant effect is the heat conduction in the area of the skirt  
→ thermal collapse of the skirt don't occur



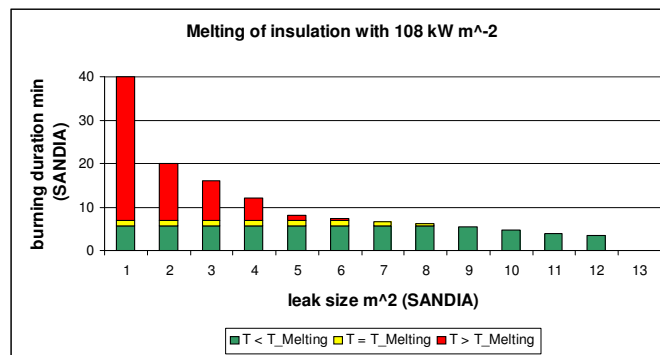
**Temperature distribution  $t_{\text{melting}}$  and  $t_{\text{thermal collapse}}$  (2<sup>nd</sup> picture of the animation)**



- Temperature layering, highest temperature in the spherical area, critical area regarding the thermal stress
- Dominant effect is the thermal radiation in the spherical area  
→ 2-dimensional calculation sufficient
- Dominant effect is the heat conduction in the area of the skirt  
→ thermal collapse of the skirt don't occur



**Coverage case of damage 108 kW m<sup>-2</sup>**



- Via the coloured marked bars the earliest and the latest beginning of melting based on the whole duration of burning is shown,
- Case of damage >6 m<sup>2</sup>, beginning of melting at the end or not during the duration of burning, respectively.



## Content



- **Introduction to the topic**
- **Theoretical foundations**
  - Tank design
  - Physical effects of the heat transfer
  - Used Software
- **Preparation of the simulation**
  - Meshing
- **Results**
  - Temperature distribution
  - Heat input
- **Summary**



## Summary

- **1<sup>st</sup> Simulation series**
  - Investigation of meshing (Fluid / Solid),
  - Estimation of the results regarding different convergence and model criteria.  
→ Sensitivity studies were performed to achieve results independent from chosen discretisation
- **2<sup>nd</sup> Simulation series**
  - Moment for the beginning of melting
  - Moment for the occurrence of thermal collapse (idealized case),
  - Evaluation of the dominant effects of the heat transfer,
  - The heat input into the tank is until the beginning of melting equal of the operation state,
  - The spherical air gap is the area with the highest thermal stress.



**Thank you for your attention!**



## **APPENDIX 4 – JHM PAPER, FIRE PERFORMANCE OF LNG CARRIERS INSULATED WITH POLYSTYRENE FOAM**



Available online at [www.sciencedirect.com](http://www.sciencedirect.com)

Journal of Hazardous Materials xxx (2008) xxx–xxx

**Journal of  
Hazardous  
Materials**
[www.elsevier.com/locate/jhazmat](http://www.elsevier.com/locate/jhazmat)

## Fire performance of LNG carriers insulated with polystyrene foam

 Jerry Havens<sup>a</sup>, James Venart<sup>b,\*</sup>
<sup>a</sup> University of Arkansas, USA<sup>b</sup> University of New Brunswick, Fredericton, NB, Canada

Received 3 August 2007; received in revised form 20 January 2008; accepted 22 January 2008

### Abstract

Analysis of the response of a liquid-full Moss Sphere LNG tank insulated with polystyrene foam to an engulfing LNG fire indicates that current regulatory requirements for pressure relief capacity sufficient to prevent tank rupture are inadequate. The inadequacy of the current requirements stems primarily from two factors. Firstly, the area of the Moss Sphere protruding above what would be the nominal deck on a conventional carrier, which is protected only by a steel weather cover from exposure to heat from a tank-engulfing fire, is being underestimated. Secondly, aluminum foil-covered polystyrene foam insulation applied to the exterior of the LNG tank is protected above the deck only by the steel weather cover under which the insulation could begin to melt in as little as 1–3 min, and could completely liquefy in as few as 10 min. U.S. and International Regulations require that the insulations on the above-deck portion of tanks have approved fire proofing and stability under fire exposure. Polystyrene foam, as currently installed on LNG carriers, does not appear to meet these criteria. As a result of these findings, but giving no consideration to the significant potential for further damage if the polystyrene should burn, the boil-off rate is predicted to be an order-of-magnitude higher than provided for by current PRV sizing requirements.

© 2008 Elsevier B.V. All rights reserved.

*Keywords:* LNG; Polystyrene foam insulation; Pool fire radiation; Pressure relief valve sizing

### 1. Introduction

A recent report by the Government Accountability Office [1] states that both the cold temperature of spilled LNG and the hot temperature of an LNG fire have the potential to significantly damage LNG ship tanks, possibly causing multiple tanks on the ship to fail in sequence. A recent report by Sandia [2] proclaims the credibility of a spill and fire on the sea following a terrorist attack that would have the potential to engulf one or more adjacent tanks on an LNG ship, potentially leading to cascading (successive) failures. As such failures could increase the severity of a catastrophic incident, the report cites as the leading unaddressed research need the determination of the potential for cascading failures of cargo tanks on LNG carriers. This paper first considers the adequacy of present regulatory requirements for pressure relieving systems to prevent over-pressure failure of a current-design, polystyrene foam insulated, liquid-full Moss Sphere exposed to an LNG fire. Then, as the philosophy of

fire protection for such hazardous cargo containment systems is based on provision of protection from fire adequate to prevent failure for a prescribed period of time, the paper describes a one-dimensional transient analysis of the expected response to heat absorption from an LNG fire contacting a single liquid-full, ~36 m diameter (25,000 m<sup>3</sup> volume) Moss Sphere on an LNG carrier.

### 2. Adequacy of regulatory requirements for pressure relief systems on LNG ships

The International Maritime Organization [3] and the U.S. Coast Guard [4] specify similar requirements for pressure relief valve sizing on liquefied gas carriers. The following, quoted from the Coast Guard Regulation, is in all practical respects identical to the requirements of the IGC Code.

“The relief valve discharge for heat input of fire must meet the following formula:

$$Q = FGA^{0.82} \quad (1)$$

where  $Q$  = minimum required rate of discharge in cubic meters per minute of air at standard conditions 0 °C and 1.03 kPa;

\* Corresponding author.

E-mail address: [jvenart@unb.ca](mailto:jvenart@unb.ca) (J. Venart).

$F$  = fire exposure factor for the following tank types— $F = 1.0$  for tanks without insulation located on the open deck,  $F = 0.5$  for tanks on the open deck having insulation that has approved fire proofing, thermal conductance, and stability under fire exposure,  $F = 0.5$  for uninsulated independent tanks installed in holds,  $F = 0.2$  for insulated independent tanks installed in holds,  $F = 0.1$  for insulated independent tanks in inerted holds or for uninsulated independent tanks in inerted, insulated holds,  $F = 0.1$  for membrane and semi-membrane tanks, and

$$G = \text{Gas Factor} = \frac{177}{(LC)} \left( \frac{ZT}{M} \right)^{1/2}$$

where  $L$  = latent heat of the material being vaporized at relieving conditions, kcal/kg,  $C$  = constant based on relation of specific heats (K), Table 54.15–25(c),  $Z$  = compressibility factor of the gas at relieving conditions (if not known  $Z = 1$ );  $T$  = temperature in K at the relieving conditions, (120% of the pressure at which the pressure relief valve is set),  $M$  = molecular weight of the product, and  $A$  = external surface area in  $\text{m}^2$  (for a tank with a body of revolution shape)."

According to the IMO-IGC, for a Moss Sphere (insulated independent) tank installed in a hold, the fire exposure factor is designated to be 0.2. In contrast, Paragraph c-1 of 46 CFR 54.15-25 further states that "For an independent tank that has a portion of the tank protruding above the open deck, the fire exposure factor must be calculated for the surface area above the deck and the surface area below the deck, and this calculation must be specially approved by the Commandant (GMSE)". This added provision of the USCG regulation is important because it indicates the need for careful consideration of the surface area of the tank that could be most severely exposed to heat from a fire, as will be shown below. However, as this provision only affects the value of the fire exposure factor  $F$ , and noting that the Gas factor  $G$  in Eq. (1) can be represented by the product of a heat flux to the cargo multiplied by an appropriate constant  $K$  representing the thermodynamic properties of the cargo, Eq. (1) becomes:

$$Q = F K q A^{0.82} \quad (2)$$

The development of Eq. (2) is described in considerable detail by Heller [5]. This empirical equation is based on fire tests conducted more than fifty years ago; long before the practice of carrying LNG in shipping containers of the size and type considered here. Importantly, the equation precedes current widespread concerns for terrorist attacks on ships that could result in very large LNG fires engulfing the tank. The largest tests for which data were available for the development of Eq. (2) involved tank surface areas of  $568 \text{ ft}^2$  ( $53 \text{ m}^2$ ), nearly 80 times smaller in area and over 600 times smaller in volume than the single LNG Moss Sphere under consideration. Furthermore, Eq. (2) is based on tests in which the liquid wetted area, the total surface area, and the area exposed to fire were all varied, the latter in particular resulting in the  $A^{0.82}$  term. It appears that Heller considered, as we do, that the use of the area ( $A^{0.82}$ ) term in Eq. (2) is inappropriate for application to a catastrophic engulfing pool fire.

In consideration of the much larger fire sizes as well as containment (tank) sizes in use today, it is appropriate to briefly review the current state of knowledge of LNG fire-on-water sizes and durations that might result from an intentional attack on an LNG carrier. The Sandia Report cited earlier [2] analyzed the fire scenario that could follow spillage onto the water of the contents of a single  $1/2$  tank ( $12,500 \text{ m}^3$ ) of LNG, providing analyses for hole size (areas) ranging from  $1$  to  $10 \text{ m}^2$ . The pool size diameter for the nominal hole size of  $5 \text{ m}^2$  was  $330 \text{ m}$  with a burn time of  $8.1 \text{ min}$ . Since the fire diameter would be similar to the pool size, the Sandia Report suggests that with the nominal hole size, the size of the fire (diameter) could be larger than the length of the ship. And while the predicted burn time for the  $5 \text{ m}^2$  hole is only  $8.1 \text{ min}$ , the  $2 \text{ m}^2$  hole size spill is predicted to result in a pool size of  $209 \text{ m}$  diameter with a burn time of  $20 \text{ min}$ , and the  $1 \text{ m}^2$  hole size spill is predicted to give a fire with  $148 \text{ m}$  diameter lasting for  $40 \text{ min}$ . Thus the smallest hole size spill could have a diameter of almost  $500 \text{ ft}$ , or more than half the length of the ship, and might burn for  $40 \text{ min}$ . Finally, assuming the smallest hole size spill and a conservative flame height to flame diameter ratio of  $1/2$ , the flame height could, even for the smallest hole size, considerably exceed the maximum height of the ship above the water line. Given the uncertainties that would attend the actual spreading that would occur as the LNG reaches the water, including wind effects, momentum of the ship, and the presence of objects (including the ship) that could channel the LNG flow, the possibility of complete engulfment of the entire above-deck portion of at least one tank adjacent to the tank ruptured in the attack must be anticipated.

With this background, and to consider the propriety of the current regulatory requirement (based on Eq. (2)) for determination of PRV sizing on LNG carriers in service currently, we reviewed an analysis of PRV system design methods performed for the U.S. Coast Guard by the National Academy of Sciences in 1973 [6].

### 2.1. The National Academy of Sciences Report

The analysis provided in this paper was presented almost four decades ago to the U.S. Coast Guard, at its request, by the U.S. National Academy of Sciences. However, as far as we can tell, there has been no follow-up to the conclusions of the NAS report, despite its suggestion of an urgent need to update the regulatory requirements for pressure relief systems design to accommodate changing practices in the LNG industry. Such a recommendation was particularly apt for the LNG industry in the seventies, as today, as the report was prepared when the LNG industry was just beginning the expansion which has been so much increased recently.

We support the NAS report's statement (applied here to LNG carriers) that the determination of the heat absorbed by an LNG-full Moss Sphere exposed to an engulfing fire can be expressed properly as:

$$Q_H = F_1 q E A \quad (3)$$

where  $Q_H$  = total heat absorbed by the cargo,  $F_1$  = environmental factor, including insulation and radiation shielding,  $q$  = heat flux

Table 1  
Comparison of PRV requirements using Eqs. (2) and (4)

	Area (m <sup>2</sup> )					
	1	10	53	100	1000	4072
Ratio (Eq. (4)/Eq. (2))—IGC Code	2 $F_1$	3 $F_1$	4.1 $F_1$	4.6 $F_1$	6.9 $F_1$	8.9 $F_1$
Ratio (Eq. (4)/Eq. (2))—45 CFR 54	1.3 $F_1$	1.9 $F_1$	2.6 $F_1$	2.9 $F_1$	4.3 $F_1$	5.6 $F_1$

to the outside of the container,  $E$  = exposure factor, the fraction of the total tank area ( $A$ ) exposed to fire, and  $A$  = tank surface area (for full tanks, equal to the wetted area).

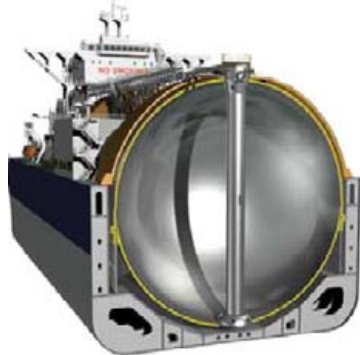
The heat absorbed by the cargo,  $Q_H$ , multiplied by the part of the gas constant  $G$  that accounts for the thermodynamic properties of the cargo ( $K$  in Eq. (2)), gives the relieving capacity:

$$Q = K q F_1 E A \quad (4)$$

where the product ( $EA$ ) represents the area of the outside of the container exposed to fire.

## 2.2. Comparison of Eqs. (2) and (4)

We assumed that 40% of the Moss Sphere protrudes above what would be the nominal deck on a conventional carrier. This area is protected from the heat of an engulfing fire only by the insulation and by the steel weather cover (see illustrations following). With  $E=0.4$ , and a tank-engulfing fire, Table 1 shows the ratio of Eq. (4) to Eq. (2) determined for values of the tank surface area ranging from 1 to 4072 m<sup>2</sup> (the area of a 36 m diameter Moss Sphere), along with the largest value (53 m<sup>2</sup>) from the data base from which the  $A^{0.82}$  term in Eq. (2) was developed, using the requirements for designating the insulation factor  $F$  from the IGC Code and 46 CFR 54 respectively.



Following paragraph (c-1) of the Coast Guard Regulation, the value of  $F$  was determined for the surface area above the deck and the surface area below the deck, assuming the fraction of the tank area above the deck as 0.4, as  $(0.4)(0.5) + (0.6)(0.2) = 0.32$ . We note that this method of determination of the value of the fire exposure factor  $F$  increases the required PRV size by 60%, illustrating the importance of careful handling of the determination of the area of the tank effectively exposed to a fire.

In either case, the extrapolation over tank surface area of the correlation assumed in Eq. (2) (the  $A^{0.82}$  term) by two orders of magnitude is clearly not applicable to the Moss Sphere tank

configurations in use today, particularly in view of the severity of fire exposure that could result from terrorist attack. The highest value of this ratio (using the IGC Code) for a typical Moss Sphere (8.9  $F_1$ ) means that the value of the factor  $F_1$  accounting for insulation (and shielding by the steel weather cover) in Eq. (4) must not be greater than 0.11 in order that the required relief capacity be as small as indicated by Eq. (1). Conversely, total loss of insulation and weather cover (radiation) shielding on the part of the tank exposed to fire, i.e., above the deck, would result in under-prediction of the required relieving capacity by a factor of 9.

Furthermore, we believe that the heat flux implicit in the current regulation may not be appropriate for describing engulfing LNG fire exposure. We note that increasing the heat flux from the currently used value (71–108 kW/m<sup>2</sup>), which is based upon test data for gasoline or kerosene fires only (see Heller [5]), will increase the required vapor relieving capacity by an additional factor proportionally. Whereas local surface emissive heat fluxes have been measured in test LNG fires as high as ~300 kW/m<sup>2</sup>, there is considerable debate regarding the appropriate value for the heat flux applicable to a large engulfing LNG fire. This question is currently being investigated, with large-scale LNG fire tests planned in the United States

for completion in 2008. While it appears clear that with the presently prescribed heat fluxes the relief systems on LNG carriers could be undersized by an order of magnitude; it follows that exposure to an engulfing LNG fire with greater heat fluxes could worsen the under-estimation of the relieving capacity.

As it appears clear then that a Moss Sphere with a pressure relief system designed according to Eq. (1), and for which the PRV system fitted to a specific tank exposed to the fire is required to provide the only pressure relief [7], could be subject to bursting over-pressure if the insulation should fail, it is necessary to determine whether the insulation could withstand

+Model  
HAZMAT-7824; No. of Pages 7

ARTICLE IN PRESS

4

*J. Havens, J. Venart / Journal of Hazardous Materials xxx (2008) xxx–xxx*

Table 2  
Specifications and thermodynamic properties of system components

Zone	Thickness (m)	Density (kg/m <sup>3</sup> )	Heat capacity (J/kg K)	Thermal conductivity (W/mK)	Emissivity	Failure temperature (K)
R2	0.015	7850	475	44.5	0.85	810 <sup>a</sup>
R3	1.0	COMSOL	COMSOL	COMSOL	NA	NA
R4	0.0003	2700	900	70	0.1,0.5	873 <sup>b</sup>
R5	0.30	26.5	1045	0.038	NA	510 <sup>c</sup>
R6	0.02	2700	904	70	NA	873 <sup>b</sup>

<sup>a</sup> Limit temperature for fire exposure, mild carbon steel [8].

<sup>b</sup> Solidus temperature [9].

<sup>c</sup> Melting temperature [10].

such a fire for its duration or until remedial action could be taken.

### 3. One-dimensional transient heat transfer analysis of a Moss Sphere tank section

We utilized COMSOL Multiphysics<sup>®</sup> (formerly MATLAB) to perform a one-dimensional analysis of the thermal response of a unit area section of a Moss Sphere (assumed flat) in which fire (R1) is contacting the steel weather cover (R2), followed by serial resistances representing the air gap (R3) between the cover and the aluminum foil covering the insulation, the aluminum foil (R4) covering the insulation, the insulation (R5), and the inner aluminum tank wall (R6), which is in contact with LNG (R7).

Table 2 specifies the properties of the resistances R2–R6 assumed for the analysis.

The following sections describe the initial conditions assumed for the analysis and the boundary conditions interconnecting the resistances specified in Table 2 as well as the boundary conditions connecting the fire (R1) to the steel cover (R2) and the aluminum tank wall (R6) to the LNG (R7).

#### 3.1. Initial conditions

The initial condition temperature profile for the one-dimensional system was calculated with a steady-state COMSOL analysis assuming an ambient air temperature of 305 K. Fig. 1 shows the temperature profile through the system with aluminum emissivity specified as a parameter, illustrating the sensitivity of the heat transfer calculations to the emissivity of the aluminum foil covering the insulation. Fig. 2 shows the heat flux into the cargo with the foil emissivity as a parameter. For an emissivity of 0.1 (assumed appropriate for a new, clean system) the heat flux into the cargo is approximately 20 W/m<sup>2</sup>. For a 36 m diameter Moss Sphere, this heat flux to the cargo at ambient conditions (305 K) would result in a boil-off rate of ~0.12% of the cargo per day. This result, which is in good agreement with typical specifications for operating Moss-design carriers, provides a useful check on the propriety of the heat transfer calculation methods utilized in the analysis.

#### 3.2. Boundary conditions

We accounted for radiative heat transfer (assuming grey body properties) and convective heat transfer ( $h = 28 \text{ W/m}^2 \text{ K}$  [11])

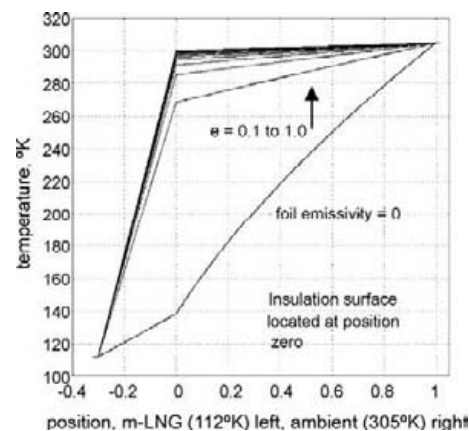


Fig. 1. Initial temperature profile.

from the flame to the weather cover. Radiative heat transfer and conductive heat transfer were accounted for in the air space under the weather cover; convective heat transfer in that space was neglected. The temperature profiles at the interfaces R4/R5, R5/R6, and R6/R7 assumed continuity (infinite heat transfer coefficient assumed from the tank wall to the LNG). Calculations were made for flame temperatures of 1300, 1400, and 1500 K—corresponding to calculated initial (maximum) total (black-body radiative and convection) heat fluxes from flame to

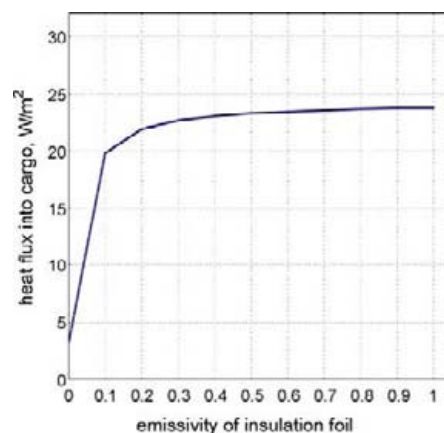
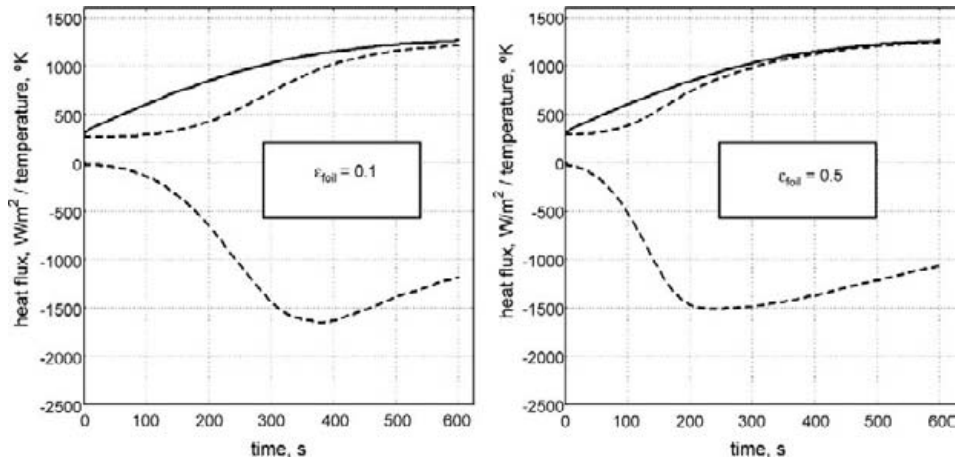


Fig. 2. Operating heat flux into cargo.

Please cite this article in press as: J. Havens, J. Venart, Fire performance of LNG carriers insulated with polystyrene foam, *J. Hazard. Mater.* (2008), doi:10.1016/j.jhazmat.2008.01.094

Fig. 3. Temperature and heat flux—wc solid, ins dashed— $T_{\text{fire}} = 1300$  K.

the steel weather cover (with emissivity = 1.0) of 188, 245, and 315 kW/m<sup>2</sup> respectively.

### 3.3. Results and conclusions

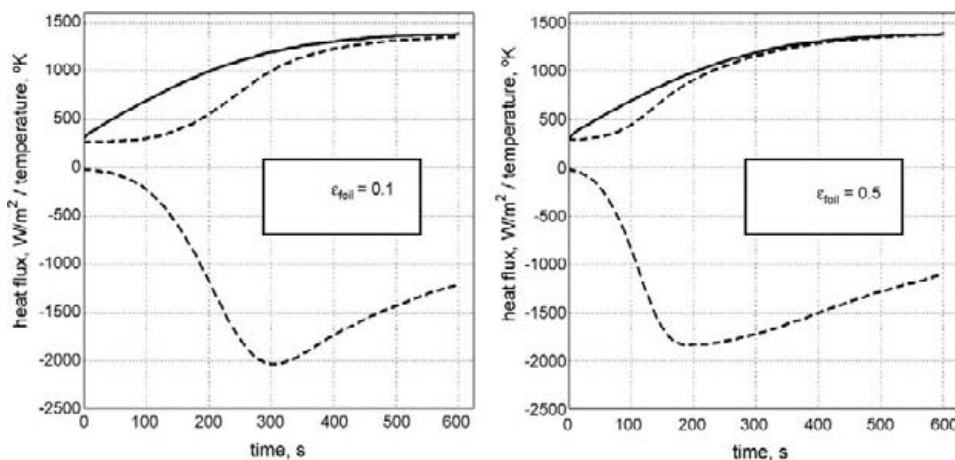
We calculated the time-varying temperatures and heat fluxes throughout the system with properties as specified in Table 2, with flame temperatures of 1300, 1400, and 1500 K, and aluminum foil emissivities of 0.1 and 0.5, the latter representing the range of emissivities that might be expected for new, clean, aluminum foil and dirty, aged aluminum foil respectively. All of our calculations assume that all of the materials (including the insulation) remained in place and functioning with the properties specified above. The purpose of these calculations was to estimate the times at which the components of the tank system would reach temperatures sufficient to cause failure, and further therefrom (using the heat flux at the time of incipient failure) to estimate the time period expected for complete failure of the insulation—the calculation results are not considered applicable for greater times.

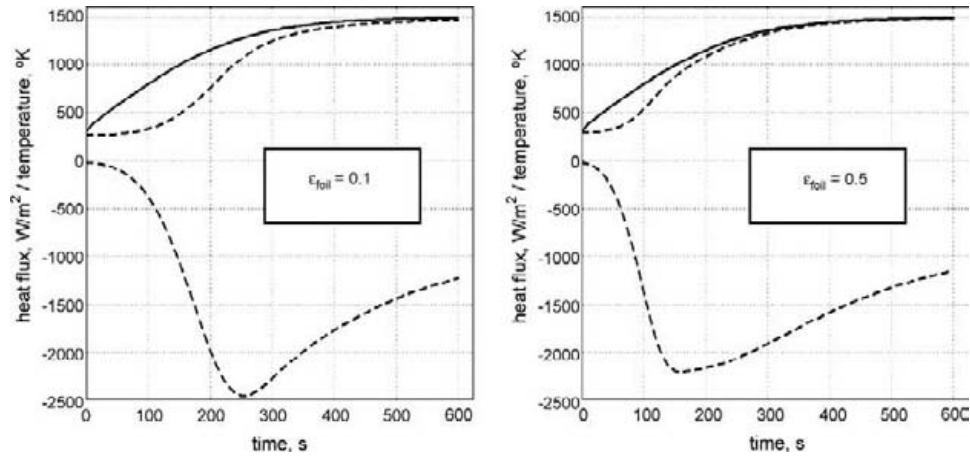
We assumed for purposes of this analysis that failure of the steel and aluminum components of the system would begin upon reaching the designated failure temperature, and we assumed that the minimum rate at which the polystyrene insulation would fail would be determined by its melting rate, which would in turn be determined by the heat flux into the foam at the time at which the foam reached its melting temperature.

Figs. 3–5 show, as a function of time for 600 s of fire exposure, temperatures of the steel weather cover (wc) surface (contacting flame with  $\epsilon = 0.85$ ) and the (hot-side) insulation (ins) surface, as well as the heat flux into the insulation surface, for aluminum foil emissivities of 0.1 and 0.5, for flame temperatures of 1300, 1400, and 1500 K.

### 3.4. Predicted component failure commencement times

Table 3 shows the estimated times from the plots in Figs. 3–5 for the (outer) steel weather cover surface, the aluminum foil, and the polystyrene foam insulation (hot-side) surface to reach the failure temperatures designated in Table 2. Because of the

Fig. 4. Temperature and heat flux—wc solid, ins dashed— $T_{\text{fire}} = 1400$  K.

Fig. 5. Temperature and heat flux—wc solid, ins dashed— $T_{\text{fire}} = 1500$  K.

small thickness of the aluminum foil (0.3 mm), the temperatures of the foil and the insulation (hot-side) surface were assumed identical for this analysis.

#### 3.4.1. Metal failure

The temperature of the steel outer surface reaches 810 K, indicating approach to failure, in the range 100–180 s. The time when the aluminum foil reaches its melting temperature (873 K) ranges from 150 to 330 s. To calculate more accurately the actual response of the system is difficult, requiring assumptions as to the specific behavior of the system components as they fail (and beyond). Nevertheless, inclusion of such information for specific failure modes can do nothing, it appears, but increase the rapidity with which the system components would fail.

#### 3.4.2. Insulation failure

The polystyrene surface temperature reaches its melting point of 510 K in the range 95–225 s. Following the time at which the polystyrene foam reaches its melting temperature, the heat flux into the foam insulation maintains an average value ranging from about 1 to about 1.5 kW/m<sup>2</sup> for the balance of the 10 min period shown. With a continuous heat flux of 1.5 kW/m<sup>2</sup> into the foam surface, the foam would melt at a rate (approximately) given by 1.5 kW/m<sup>2</sup> divided by the product of the foam density and its latent heat of fusion. The latent heat of fusion for styrene monomer is 105 kJ/kg and the density of polystyrene foam is 26.5 kg/m<sup>3</sup>, indicating a melting rate of about 3 cm/min. However, this appears to be a lower limit on the melting rate because the latent heat of polystyrene (mass basis) could be

(much) smaller, depending on the molecular weight of the polymerized styrene. Nonetheless, this analysis indicates that total melting of a polystyrene insulation layer 0.3 m thick could occur in less than 10 min after it reaches its melting temperature if the foam were subjected to the heat exposure considered here.

#### 3.4.3. Insulation combustion

This analysis has not considered the potential for combustion of (poly)styrene vapors mixed with air in the space between the weather cover and the insulation surface. Both the IGC and 46 CFR 54 require, in order to take credit for the insulation in PRV sizing, that the insulation on the above-deck portion of tanks have approved fire proofing and stability under fire exposure. Polystyrene foam, as currently installed on LNG carriers, does not appear to meet these criteria. Even if the exterior fire were isolated from the foam (by an intact weather cover), ignition of these flammable vapors appears highly likely, given the relatively low autoignition temperature of styrene (~760 K), and the fact that only about 1 mm thickness of the insulation would have to vaporize to raise the average vapor concentration in the air space under the weather shield above the lower flammable limit. Given the flue-like configuration formed by the space between the cover and the insulation, the volume of air in that space, and the potential for failure of the steel weather cover that would admit additional air, there is a potential for rapid burning of the insulation material [12], even if the ignition of the vapors prior to the steel weather cover failing did not result in an over-pressure that failed the cover instantly.

We estimated, assuming that all of the foam melts and either burns or runs off, thereby exposing the tank wall to radiation heat transfer from an intact weather cover, that the steady-state heat flux into the cargo (all surface emissivities assigned a value of 1.0 except the steel weather cover, assigned  $\epsilon = 0.85$ ) would range from 80 to 135 kW/m<sup>2</sup> for a flame temperature range of 1300–1500 K. An accurate determination of the potential for failure, and the probable mode, whether overheating of the tank wall in the vapor space or general failure due to over-pressure,

Table 3  
Predicted component failure times (s)

Component	$T_{\text{fire}} = 1300$ K		$T_{\text{fire}} = 1400$ K		$T_{\text{fire}} = 1500$ K	
	$\epsilon = 0.1$	$\epsilon = 0.5$	$\epsilon = 0.1$	$\epsilon = 0.5$	$\epsilon = 0.1$	$\epsilon = 0.5$
Weather cover	170	180	125	125	100	100
Aluminum foil	330	260	265	180	215	150
Foam insulation	225	140	190	120	160	95

is beyond the scope of this paper. Nevertheless, even if potential for failure of the metal components of the system is neglected and no consideration is given to the potential for combustion of the insulation, it appears that a Moss Sphere insulated with non-fire resistant polystyrene foam, protected only from the heat of an engulfing fire by the steel weather shield, could rupture as a result of over-pressure if the weather cover were subjected to an engulfing LNG flame for a time period of order 10 min.

### Acknowledgements

We gratefully acknowledge the assistance of Dr. Alan Schneider, who participated in the preparation of the National Academy of Sciences Report on which we have relied extensively, for his continuing interest in this subject and his willingness to review our thoughts. We are also grateful for assistance in producing the one-dimensional heat transfer analyses to Professor Greg Thoma and his 2007 graduate class in Advanced Chemical Engineering Calculations at the University of Arkansas.

### References

- [1] Public Safety Consequences Of A Terrorist Attack On A Tanker Carrying Liquefied Natural Gas Need Clarification, GAO-07-316, February 2007.
- [2] Sandia National Laboratories, Guidance on Risk Analysis and Safety Implications of a Large Liquefied Natural Gas (LNG) Spill Over Water, 2004.
- [3] International Code for the Construction and Equipment of Ships Carrying Liquefied Gases in Bulk, International Maritime Organization, London, second edition, 1993.
- [4] United States Federal Regulation 46 CFR 54.15-25(c).
- [5] F.J. Heller, Safety relief valve sizing: API versus CGA requirements plus a new concept for tank cars, in: Proceedings of the American Petroleum Institute, vol. 6, 1983, pp. 123–135.
- [6] Pressure Relieving Systems For Marine Cargo Bulk Liquid Containers, Committee on Hazardous Materials, Division of Chemistry and Chemical Technology, National Research Council, NAS, 1973.
- [7] We are informed that all current LNG carriers utilize piping interconnecting all of the LNG tanks on the vessel in order to collect LNG boil-off gas for propulsion and that all valves in said interconnected piping connecting the cargo tanks to additional relief valves are required to be locked open when the ship is in service. As a result, actual relieving capacity may exceed that prescribed by Eq. (1). While this may be true, we believe that the current regulatory practice deserves careful review, since it is not clear whether relief valve capacity placed on external piping (as opposed to the tank itself) is authorized, or whether any such additional piping is designed to allow the boil-off gas flow rates that could occur if the vessel were exposed to severe, even multiple-tank, fire engulfment.
- [8] At 538 °C the maximum permissible design strength (60% of yield) would equal its strength at temperature, SFPE Handbook of Fire Protection Engineering, 1988.
- [9] The range of solidus temperatures, or commencement of melting, for Aluminum alloys is ~510–640 °C.
- [10] Polystyrene foam melts over a temperature range: we assumed for the purposes of this analysis 510 K as a representative value.
- [11] J.R. Welker, C.M. Sliepcevich, Heat transfer by direct flame contact fire tests—Phase I. Prepared for the National Academy of Sciences by University Engineers, Inc., Norman, Oklahoma, 1971.
- [12] J. Zicherman, Fire performance of foam-plastic building insulation, J. Architect. Eng. (September) (2003).



## **APPENDIX 5 – THERMODYNAMIC BOUNDARY CONDITION**



***SIGGTO Working Group on LNG Fire  
Thermodynamic Boundary Conditions  
(Thermodynamic Institute of HSU Hamburg; GL)***

Prof Stephan Kabelac, Dr-Ing Gerd Würsig, Dipl-Ing Malte Freund

2007-11-13



**Germanischer Lloyd**

***Summary of result: Helmut Schmidt  
University and Germanischer Lloyd***

**Report on Thermodynamic Boundary Conditions**

**To SIGTTO WG on LNG fires around LNG Tankers**

**Prof Dr.-Ing Stephan Kabelac, Dr-Ing Gerd Würsig, Dipl-Ing  
Malte Freund**

## 1. Overview

- The maximum possible emissive power of a LNG fire reaches the maximum value (e.g.  $300 \text{ kW / m}^2$ ) only initially and decreases with receiving wall temperature increase.
  - ▶ The maximum heat flux after heating up for the most severe assumptions is limited to  $150 \text{ kW / m}^2$  for the not insulated tank if an initial heat flux of  $300 \text{ kW / m}^2$  is assumed.
  - By assuming an initial heat flux of  $108 \text{ kW / m}^2$  as in the IGC Code, the maximum heat flux is only about  $60 \text{ kW / m}^2$ .
- ▶ The possible heat transfer into the tank strongly depends on the values of the emission coefficient and the rate of deterioration of the insulation material. The heat flux is limited to a very low value until the insulation is deteriorated
- ▶ The boiling behaviour of the LNG is limiting the maximum possible heat flux to values below the critical heat flux situation of methane. Therefore the heat flux is limited from this side to values below  $300 \text{ kW / m}^2$  before destruction of the inner aluminium tank occurs.

## 2. Overview

- There is no possibility of a large burning of insulation material due to the lack of oxygen. The amount of air in the gap only allows for a burning of the top 5 mm of the insulation (p.19).
- The emissivity was first taken to be that of rusted steel (0.7) and changed to the emission of an ideally sooty surface (1). The reality is certainly between these values. Therefore the calculations are worst case scenarios.

### 3. Overview

- The actual heat flux of a LNG fire is crucial for the calculation, as can be seen from point 1. This can only be determined by a pool fire test. The tests shall supply:
  - the actual heat flux of the LNG fire
  - the actual emissivity during the phases of the test
  - the melting rate, melting behaviour, and properties of melting insulation material

### 4. Overview

- Already the preliminary estimations done with CFD show that there is a heat transfer between the heated area of the tank and it's lower. This flow will have a cooling effect and reduce the heat fluxes as calculated in the 1-D calculations.

## 5. Overview

- For a more detailed examination a detailed CFD calculation should be made. It could clarify quantitatively
  - the time dependent heating up of the tank structure
  - the time dependent development of the temperatures on the insulation surface
  - including the melting of the PS foam
  - the convective heat transfer coefficients on the weather cover and the insulation surface
  - the cooling effect of the air cooling from the lower parts of the tank and at the ship's bottom
  - the heat transfer from the tank wall into the LNG

## *GL's proposal for general conclusions of SIGTTO WG from the report results*

- The maximum power transferable to the tank is much less than the nominal heat flux from the fire
- Burning of insulation is not a problem which has to be addressed
- Nearly no heat is transferred into the tank until the complete insulation subjected to the heat flux is gone. No vapour production will occur before this time.
- There is a convection between the lower part of the tank and the upper one which will reduce the energy which can be transferred to the inner tank. This positive effect has not been considered until now.
- It is not possible to endanger the tank by overheating. Only film boiling will endanger the tank and this is not possible



## 1. Maximum emissive power (e.g. 300 kW/m<sup>2</sup>)

- Maximum Temperature from fire: 1517 K

$$T_0 = \left[ \frac{\dot{q}}{\sigma} + T_1^4 \right]^{1/4} = 1517 \text{ K} .$$

When the receiving wall is heating up, the heat flux will decrease due to the decreasing temperature difference.

At a receiving wall temperature of 1000 °C, the heat flux can be calculated to

$$\dot{q} = \sigma \cdot [T_0^4 - T_1^4] = 151 \text{ kW / m}^2 .$$

- Decrease to about 150 kW / m<sup>2</sup> at a wall temperature (weather cover) of 1000 °C

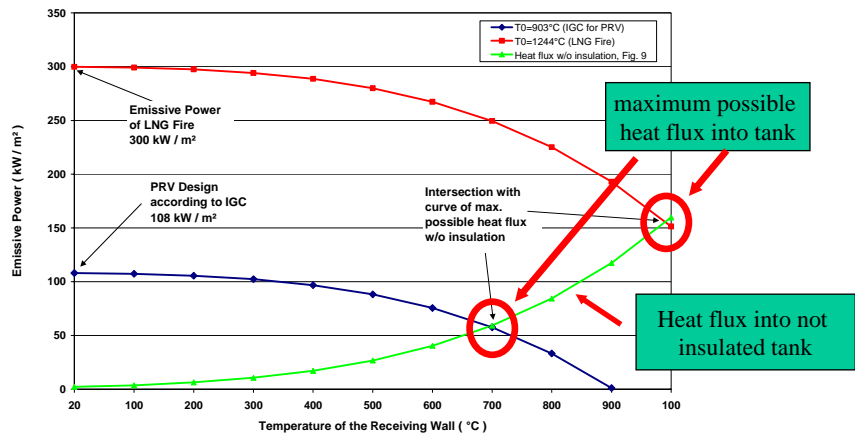
## What does a temperature of 1000°C mean?



The steel colour at 1000°C

Fig. 10. Incandescence colours of steel at different temperatures.

## 2. Maximum emissive power (e.g. 300 kW/m<sup>2</sup>)



Thermodynamic Boundary Conditions

2007-11-13

No. 11

Germanischer Lloyd



Thermodynamic Boundary Conditions

2007-11-13

No. 12

Germanischer Lloyd

## Possible heat transfer

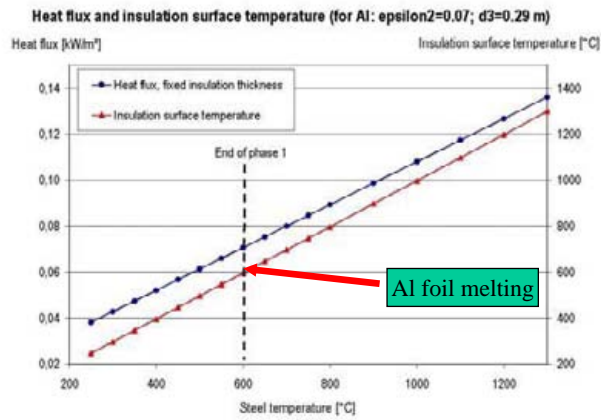
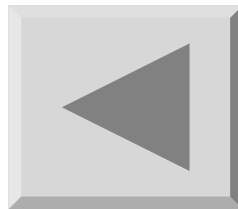


Fig. 6: Heat flux and insulation surface temperature in phase 1

1 Phase: Insulation intact





## 1-D Model

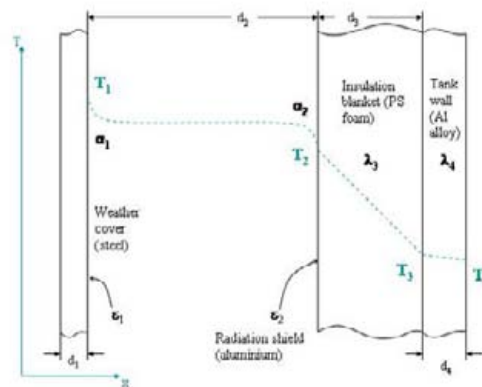


Fig. 2: 1D model of the LNG tank with its notation

Thermodynamic Boundary Conditions

2007-11-13

No. 17

Germanischer Lloyd

## The 3 phases of the incident

1. Phase: represents the first minutes of the incident,
2. Phase: represents the condition after the heating up until the weather cover reaches 1000 °C .
3. Phase: represents the heat transfer after the complete decomposing of the insulation material,

Thermodynamic Boundary Conditions

2007-11-13

No. 18

Germanischer Lloyd

### *1. phase of the incident*

- 1. Phase: represents the first minutes of the incident,
  - the radiation shield is in good condition
  - insulation is complete
  - The emissivity is taken to be  $\epsilon_1 = 0.07$  for the shiny aluminium and  $\epsilon_2 = 0.7$  for the weather cover.

This is a theoretical case, since neither would the insulation survive higher temperatures than 200°C/ 300 °C, nor the aluminium radiation shield higher temperatures than 660 °C; therefore this is taken up to a steel temperature of 600 °C.

### *2. phase of the incident*

- 2. Phase: represents the condition after the heating up until the weather cover reaches 1000 °C .
  - The aluminium radiation shield has molten,
  - the surface of the insulation material has shortly burned and the surfaces are sooty.
  - The emissivity is taken to be  $\epsilon_1 = \epsilon_2 = 1$ .

The insulation material is melting down depending on the outer wall temperature, leaving a variable insulation thickness. On the surface of the insulation the temperature stays constant because of the melting. In the LNG tank nucleate boiling is occurs.

### 3. phase of the incident

- 3. Phase: represents the heat transfer after the complete decomposing of the insulation material,
  - leaving only the weather cover and the tank wall with sooty surfaces
  - this is the worst possible situation
  - the emissivity is taken to be  $\epsilon_1 = \epsilon_2 = 1$ , again.

Thermodynamic Boundary Conditions

2007-11-13

No. 21

Germanischer Lloyd

### Heat flux during the different phases

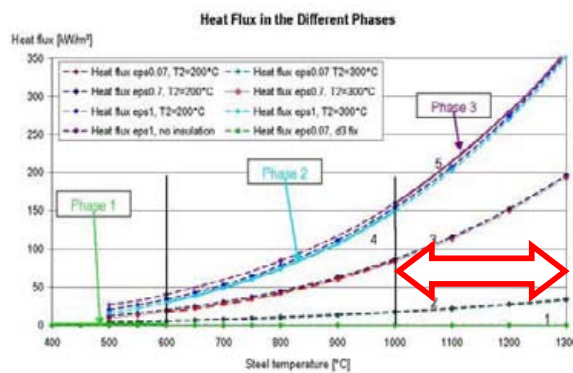


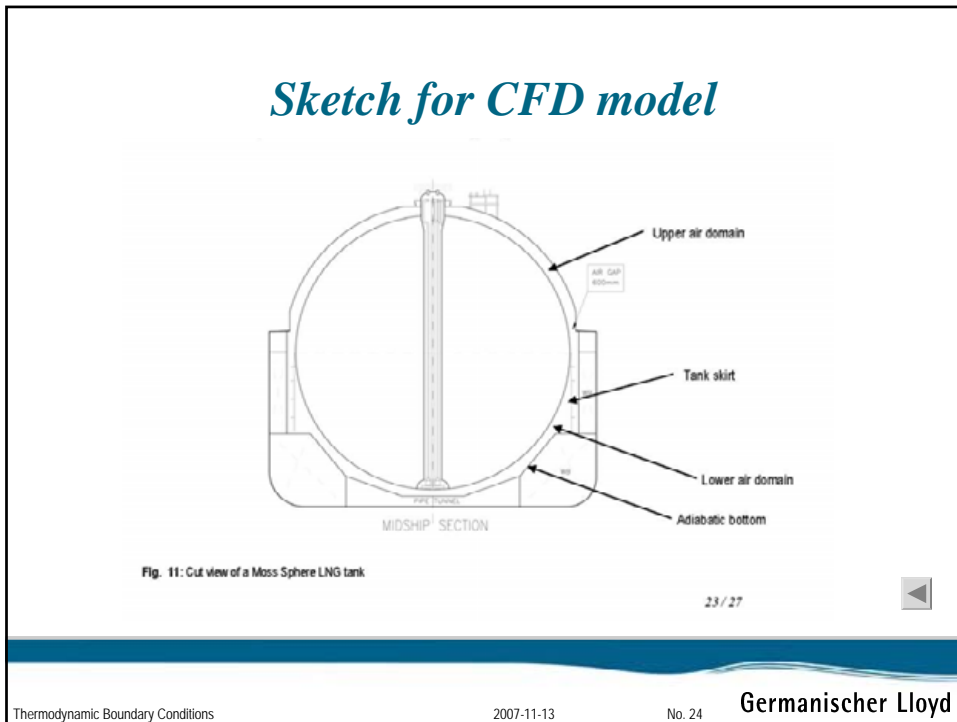
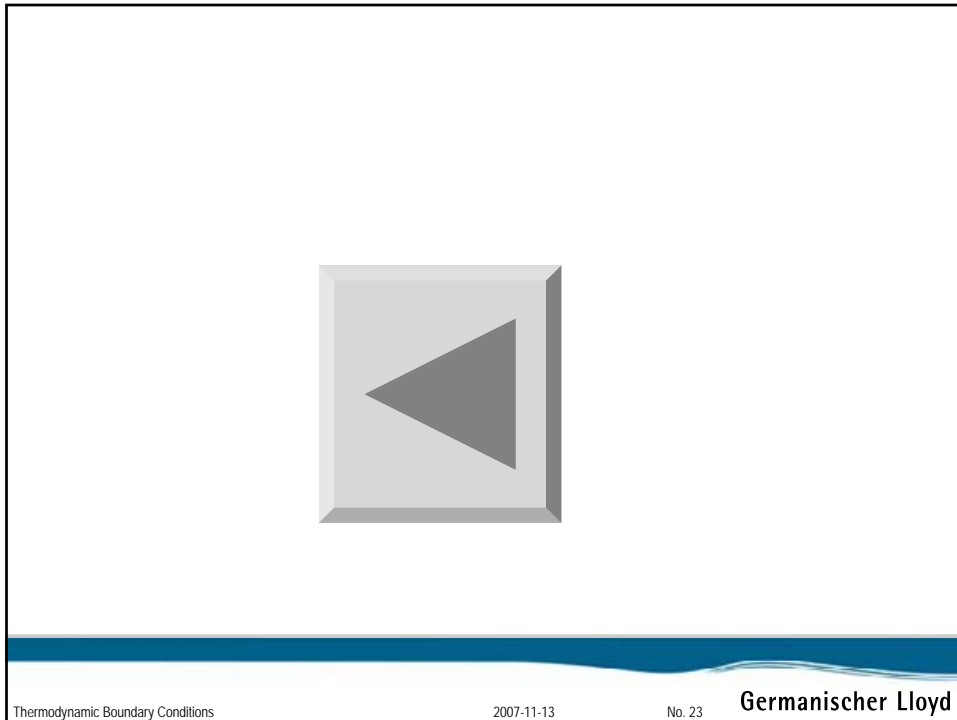
Fig. 5: Heat flux in the different phases of the incident; effects of the emission coefficient

Thermodynamic Boundary Conditions

2007-11-13

No. 22

Germanischer Lloyd



### CFD Model

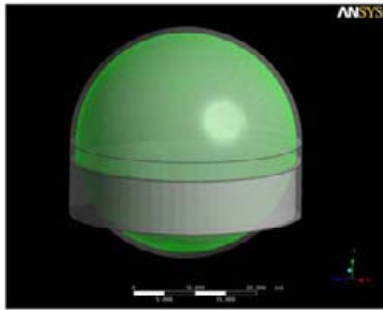


Fig. 12: CFD model of the LNG tank with marked insulation surface

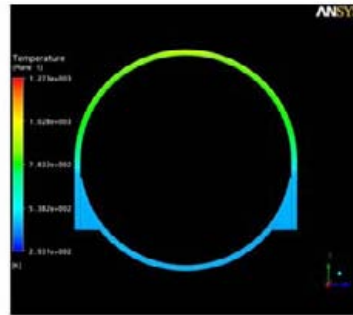
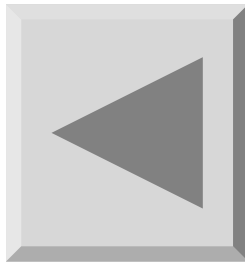


Fig. 14: CFD calculated temperature distribution in the air filled space between weather cover / hull and LNG Tank



*Vielen Dank für Ihre Aufmerksamkeit!*



## **APPENDIX 6 – INSULATION HEATING COMPARISON**



Vergleich Havens  
Aufheizvorgang.xmcd

1

Germanischer Lloyd, Hamburg

**Havens and Venart**  
**Fire performance of LNG carriers insulated**  
**with polysterene foam. J. of Hazardous**  
**Material, Feb 2008**

**Model explanation of GL:**  
**Block of 1 m<sup>3</sup> with a surface of 1**  
**m<sup>2</sup>**

heat flux into the foam:  $q_{\text{point}} := 1500 \frac{\text{W}}{\text{m}^2}$

surface

$$\underline{A} := 1 \text{ m}^2$$

density of polystyrene:  $\rho := 26.5 \frac{\text{kg}}{\text{m}^3}$

volume

$$\underline{V} := 1 \text{ m}^3$$

latent heat of fusion:  $\underline{l} := 105000 \frac{\text{J}}{\text{kg}}$

$$Q_{\text{point}} := q_{\text{point}} \cdot A$$

$$Q_{\text{point}} = 1.5 \times 10^3 \text{ W}$$

$$\text{melting\_rate} := \frac{q_{\text{point}}}{\rho \cdot l}$$

$$Q := V \cdot \rho \cdot l$$

$$\text{melting\_rate} = 5.391 \times 10^{-4} \frac{\text{m}}{\text{s}}$$

$$Q = 2.783 \times 10^6 \text{ J}$$

This corresponds to a melting rate of  
about 3 cm min<sup>-1</sup>.

$$t_{\text{total}} := \frac{Q}{Q_{\text{point}}} \quad t_{\text{total}} = 1.855 \times 10^3 \text{ s}$$

$$t_{\text{melting}} := \frac{0.29 \text{ m}}{\text{melting\_rate}}$$

$$\underline{t} := t_{\text{total}}^{0.29}$$

$$t_{\text{melting}} = 537.95 \text{ s}$$

$$t = 537.95 \text{ s}$$

**Requires energy for heating up of insulation which have not been considered in**  
**Havens and Venart work named above.**

$$c_p := 1045 \frac{\text{J}}{\text{kg} \cdot \text{K}}$$

$$\underline{m} := 0.29 \text{ m}^3 \cdot 26.5 \frac{\text{kg}}{\text{m}^3}$$

$$m = 7.685 \text{ kg}$$

$$T_{\text{average1}} := 111 \text{ K} + \frac{(473 \text{ K} - 111 \text{ K})}{2}$$

$$T_{\text{average1}} = 292 \text{ K}$$

$$T_{\text{average2}} := 111 \text{ K} + \frac{(573 \text{ K} - 111 \text{ K})}{2}$$

$$T_{\text{average2}} = 342 \text{ K}$$

$$\Delta T_1 := 473 \text{ K} - T_{\text{average1}}$$

$$\Delta T_1 = 181 \text{ K}$$

Dr Gerd Würsig, Dip.-Ing Benjamin  
Scholz

Vergleich Havens  
Aufheizvorgang.xmcd

2

Germanischer Lloyd, Hamburg

$$\Delta T_2 := 573\text{K} - T_{\text{average2}}$$

$$\Delta T_2 = 231\text{ K}$$

$$Q_1 := m \cdot c_p \cdot \Delta T_1$$

$$Q_2 := m \cdot c_p \cdot \Delta T_2$$

$$Q_1 = 1.454 \times 10^6 \text{ J}$$

$$Q_2 = 1.855 \times 10^6 \text{ J}$$

$$t_1 := \frac{Q_1}{Q_{\text{point}}}$$

$$t_2 := \frac{Q_2}{Q_{\text{point}}}$$

**Additional time to heat up the insulation to 473 K (t1) or 573 K (t2) melting temperature**

$$t_1 = 969.053 \text{ s}$$

$$t_2 = 1.237 \times 10^3 \text{ s}$$

$$f_1 := \frac{t_1}{t_{\text{melting}}}$$

$$f_2 := \frac{t_2}{t_{\text{melting}}}$$

$$f_1 = 1.801$$

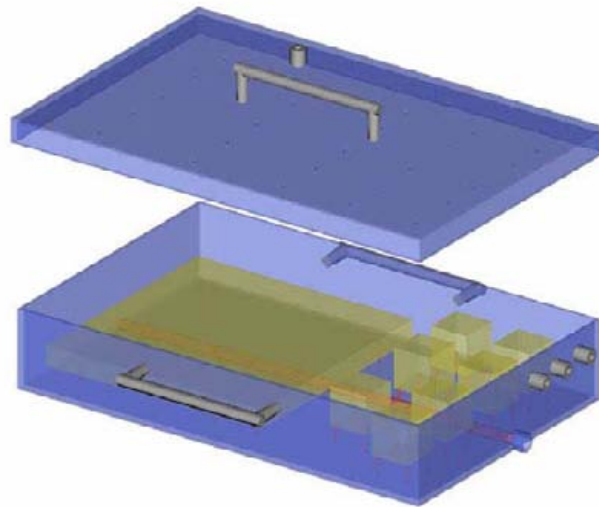
$$f_2 = 2.299$$

## **APPENDIX 7 – POLYURETHANE HEAT TESTS**





## ***Polyurethane Foam Heat Tests***



Gaz de France - Gaztransport & Technigaz



## Test procedure

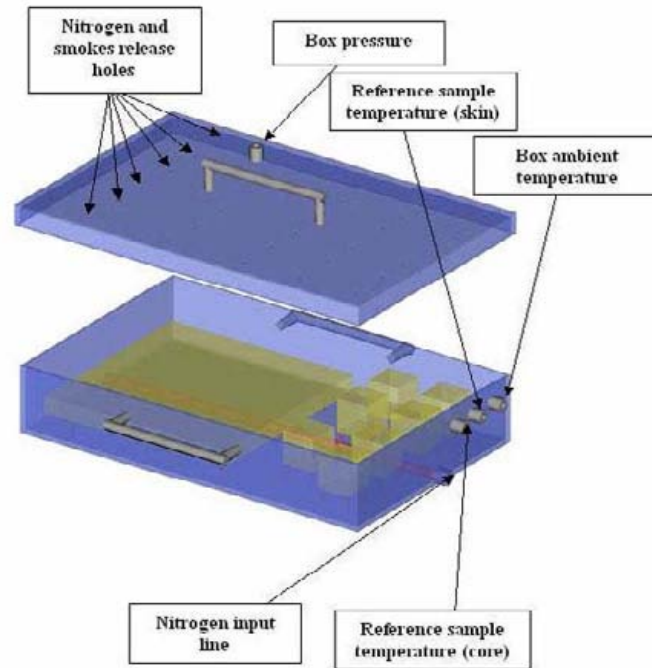


1. Put the samples in place in the dedicated testing box:
    - 5 cubes of 50 x 50 x 50 mm<sup>3</sup> dimension (for compressive tests),
    - 1 piece of 300 x 300 x 25 mm<sup>3</sup> (for thermal conductivity tests),
    - 1 cube of 50x 50 x 50 mm<sup>3</sup> dimension instrumented for reference temperature measurements.
  2. Instrument the box (pressure sensors) and the reference sample (temperature sensor)
  3. Install in the oven and connect with Nitrogen input lines.
  4. Put the box under-pressure with a suitable Nitrogen flux.
  5. Switch on the oven following predefined cycle allowing:
    - A fast temperature rise,
    - A 15-30mn step at given temperature (8 thresholds between 200 and 900°C / 100°C),
    - A « natural » temperature decrease by shutting down the oven.
  6. When the oven temperature decreases below 50°C, stop the nitrogen sweeping and open the oven.
  7. Store the samples referenced by their associated temperature threshold.
- Repeat the procedure for each temperature threshold.

Polyurethane Foam Heat Tests



## Test procedure



Polyurethane Foam Heat Tests



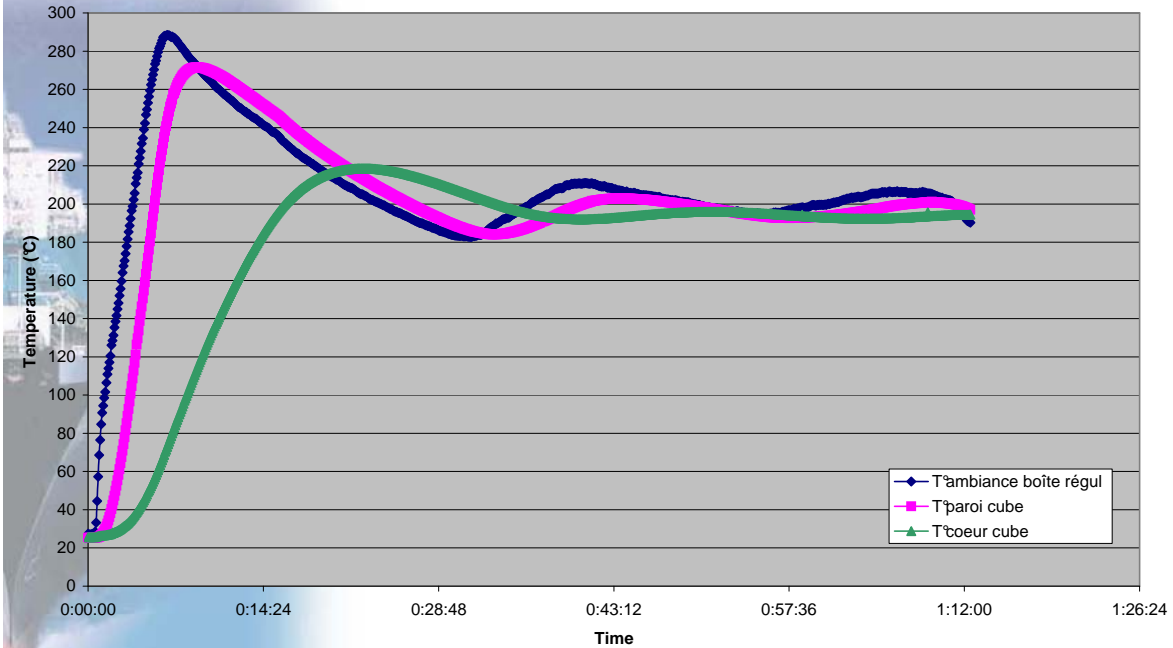
1. Initial state
2.  $T^{\circ}\text{core} = 200^{\circ}\text{C}$
3.  $T^{\circ}\text{core} = 250^{\circ}\text{C}$ , stop heating after 15 min
4.  $T^{\circ}\text{core} = 250^{\circ}\text{C}$ , stop heating 15 min after  $T^{\circ}\text{core}$  reached  $250^{\circ}\text{C}$
5.  $T^{\circ}\text{core} = 250^{\circ}\text{C}$ , stop heating 30 min after stabilization
6.  $T^{\circ}\text{core} = 250^{\circ}\text{C}$  during 3h
7.  $T^{\circ}\text{core} = 300^{\circ}\text{C}$
8.  $T^{\circ}\text{core} = 300^{\circ}\text{C}$  – regulation without overshooting
9.  $T^{\circ}\text{core} = 700^{\circ}\text{C}$

Polyurethane Foam Heat Tests



**Case 2**

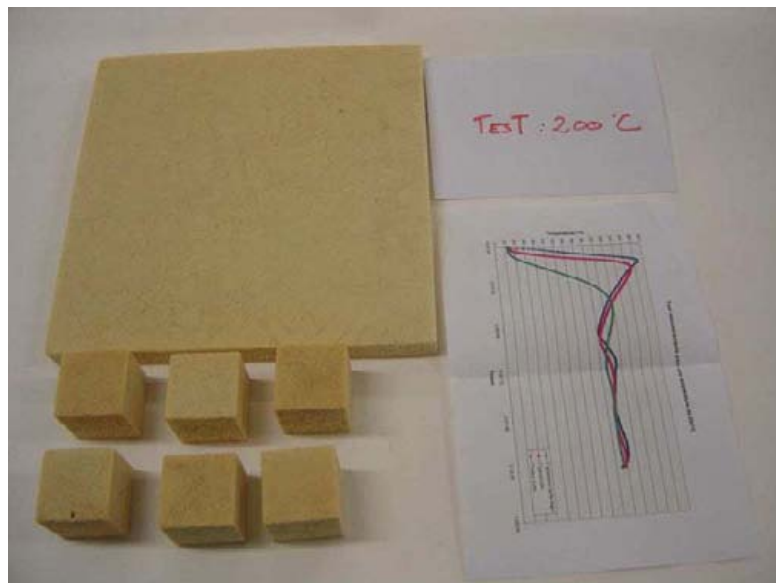
Tests on PU foam - Temp 200°C - 30mn after T°core stabilization



Polyurethane Foam Heat Tests



**Case 2 test results**

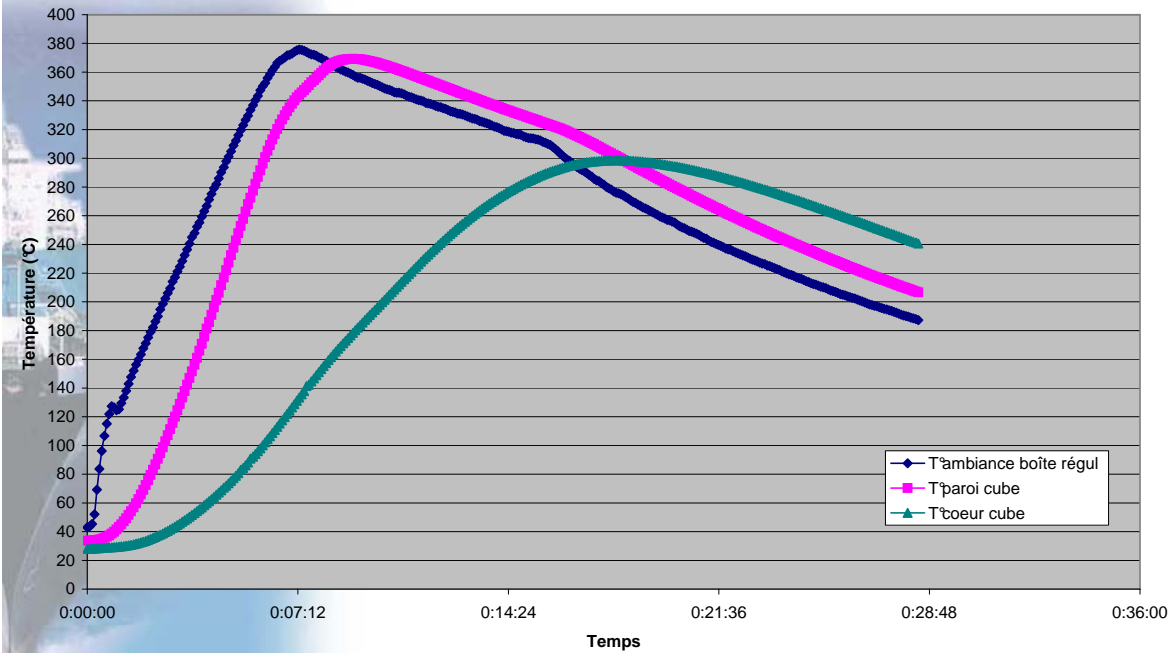


Polyurethane Foam Heat Tests



**Case 3**

Test on PU foam - Temp 250°C - Stop after 15 min heating



Polyurethane Foam Heat Tests



**Case 3 Test results**



Polyurethane Foam Heat Tests



**Case 4**

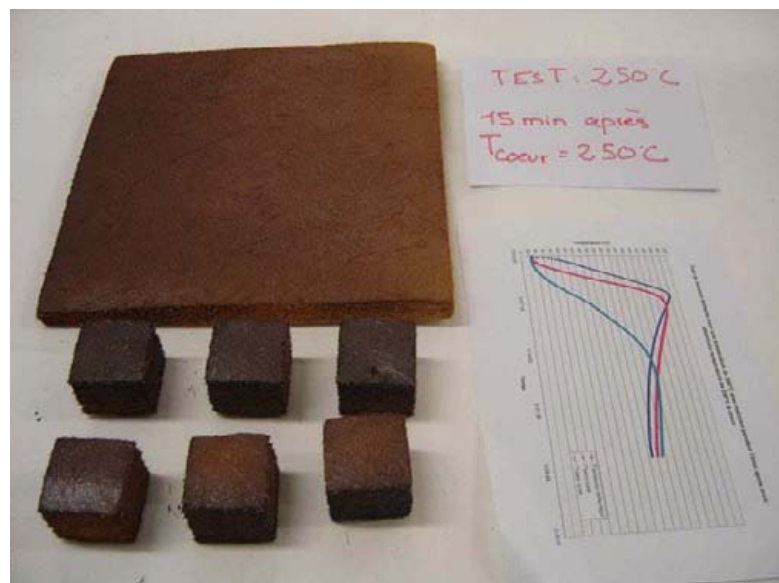
Test on PU foam - Temp 250°C - 15min heating after reaching T°core = 250°C



Polyurethane Foam Heat Tests



**Case 4 Test results**

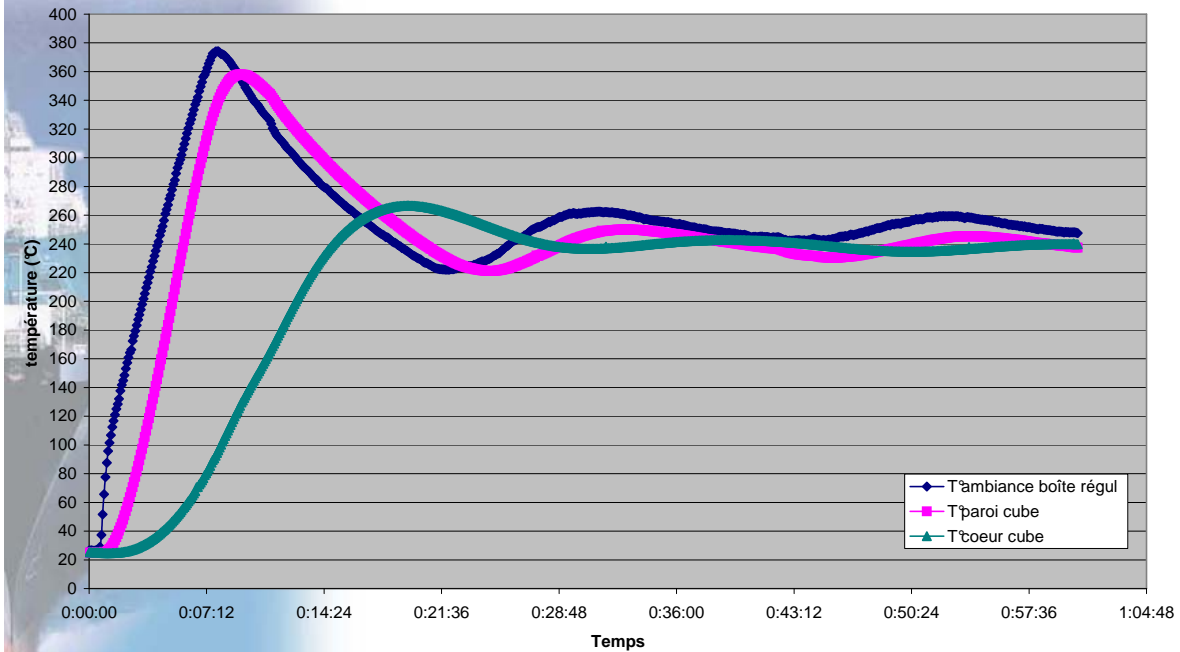


Polyurethane Foam Heat Tests



Case 5

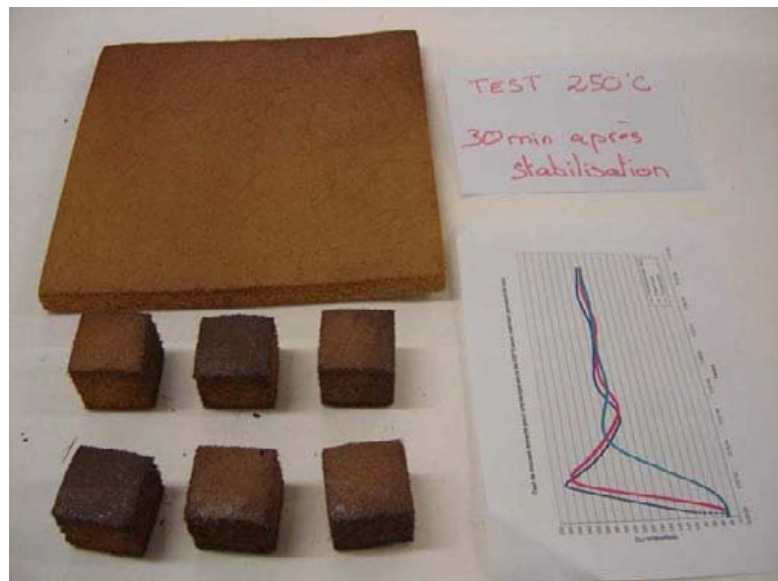
Test on PU foam - Temp 250°C - 30 min after T° core stabilization



Polyurethane Foam Heat Tests



Case 5 Test results

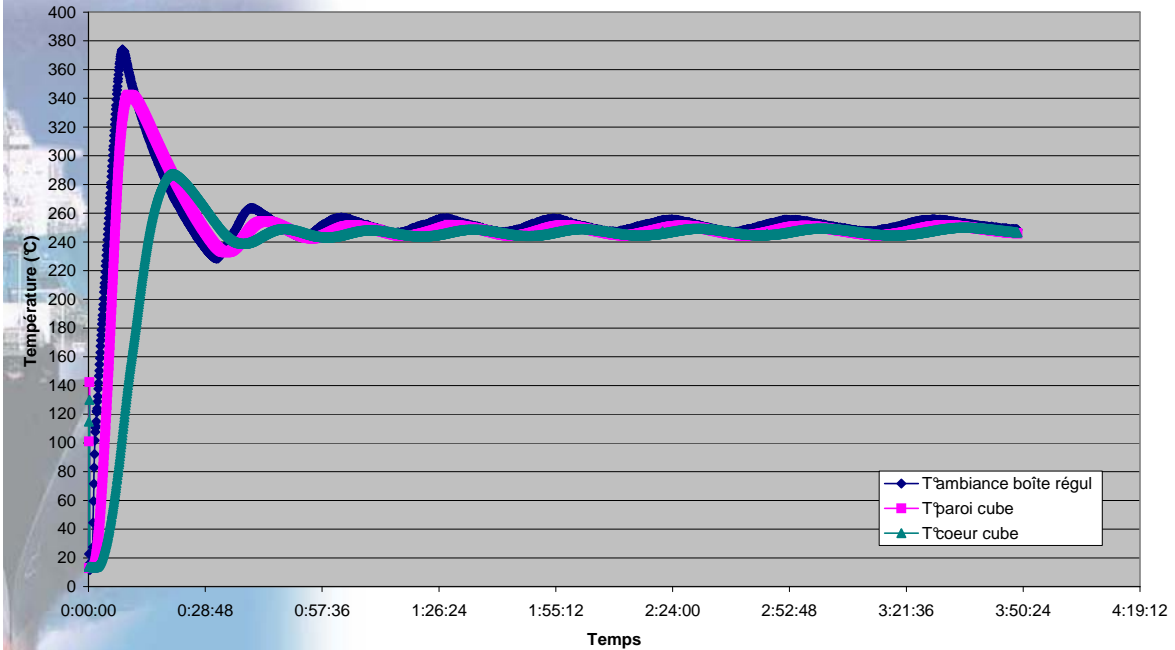


Polyurethane Foam Heat Tests



**Case 6**

Test on PU foam - Temp 250°C - 3h after T° core sta bilization



Polyurethane Foam Heat Tests



**Case 6 Test results**

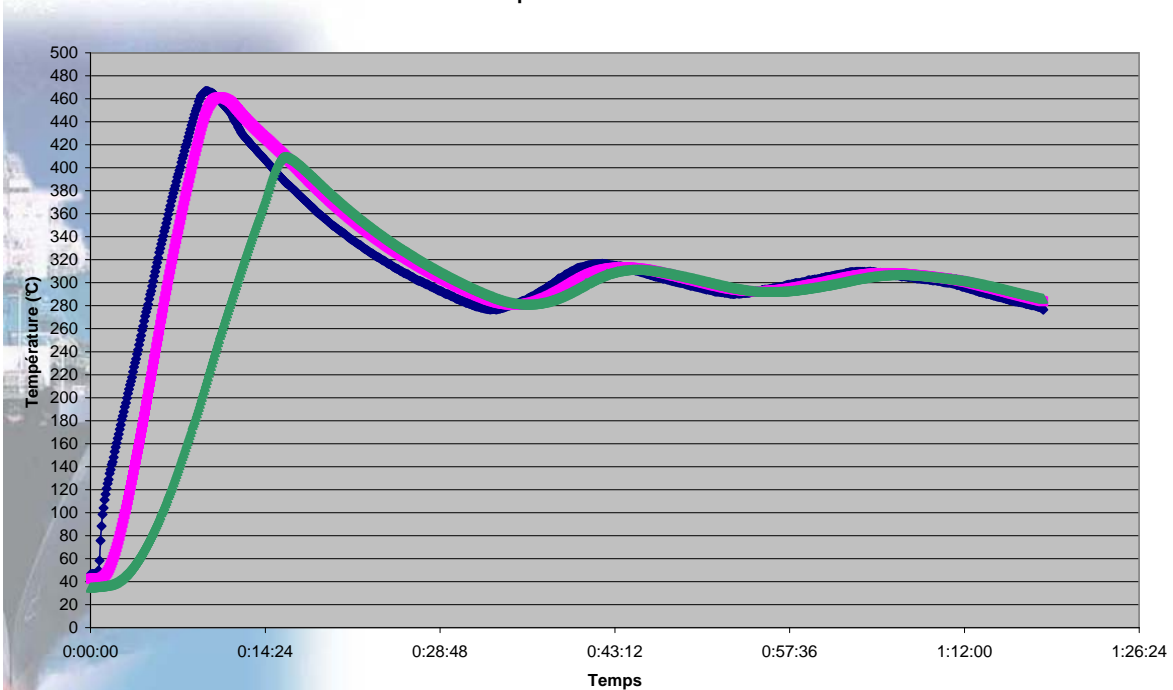


Polyurethane Foam Heat Tests



Case 7

Test on Pu foam - Temp 300°C - 30 min after T° core stabilization



Polyurethane Foam Heat Tests



Case 7 Test results

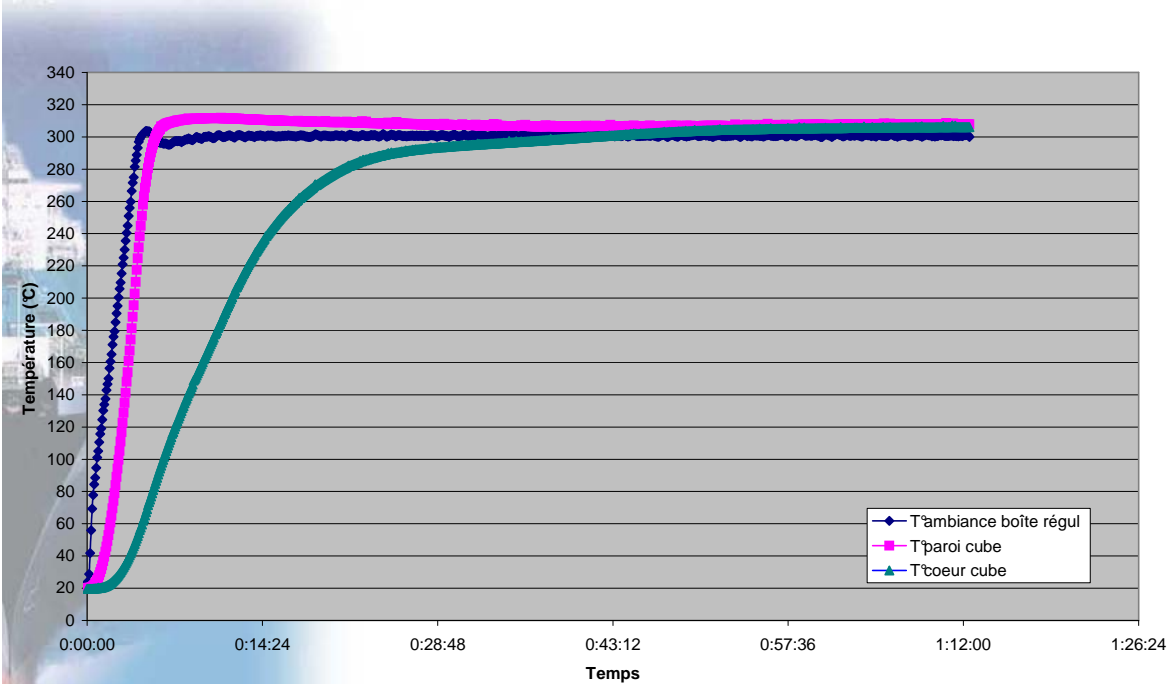


Polyurethane Foam Heat Tests



Case 8

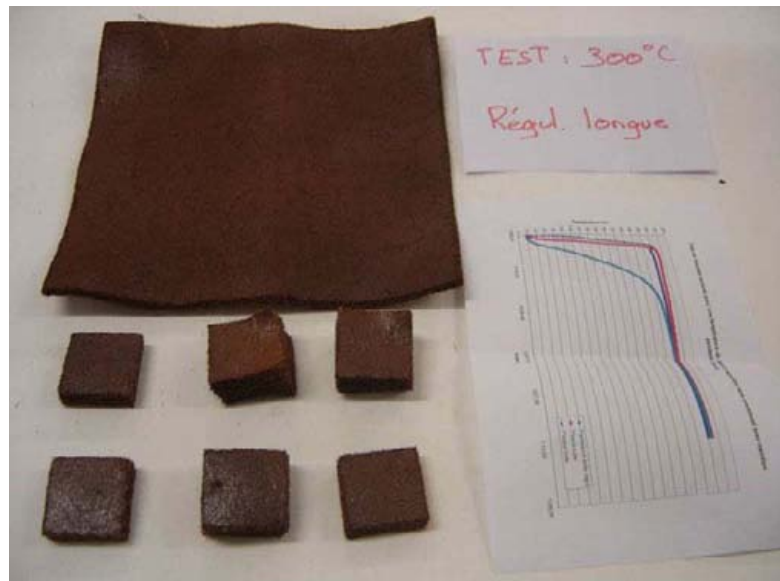
Test on PU foam - Temp 300°C (regulation without overshoot) - 30min after stabilization



Polyurethane Foam Heat Tests



Case 8 Test results

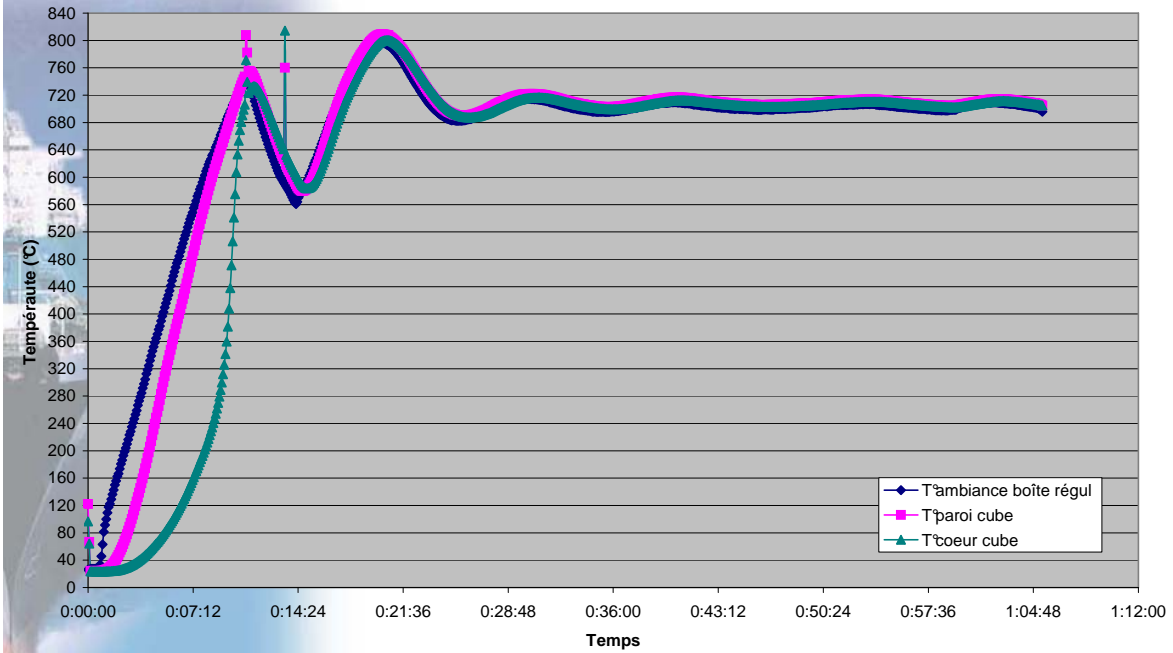


Polyurethane Foam Heat Tests



Case 9

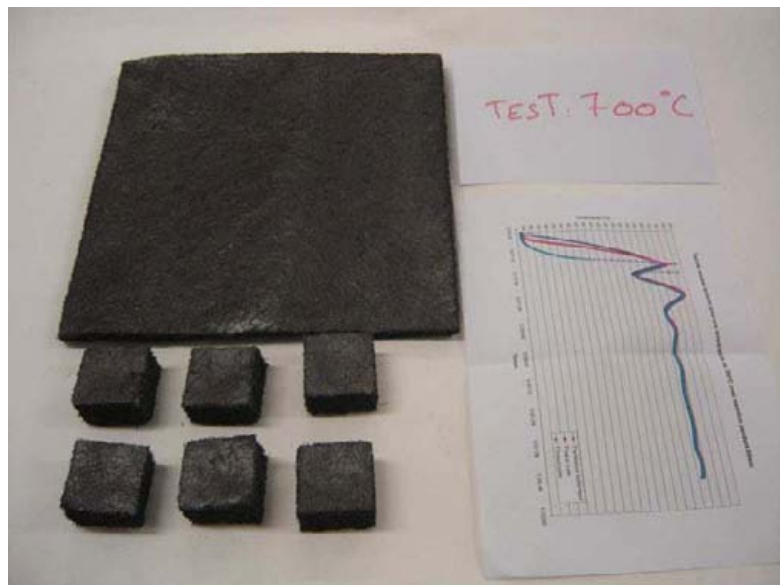
Test on PU foam - Temp 700°C - 30min after T° core stabilization



Polyurethane Foam Heat Tests



Case 9 Test results



Polyurethane Foam Heat Tests



## Test results - Density



Réf	D1	D2	D3	D (kg/m <sup>3</sup> )
<b>1</b>	127.86	128.03	127.78	<b>128</b>
<b>2</b>	124.03	121.51	123.28	<b>123</b>
<b>3</b>	103.37	99.33	97.06	<b>100</b>
<b>4</b>	103.74	103.82	102.96	<b>104</b>
<b>5</b>	108.05	111.32	109.93	<b>110</b>
<b>6</b>	98.47	97.06	96.44	<b>97</b>
<b>7</b>	69.95	74.89	81.55	<b>75</b>
<b>8</b>	141.5	151.21	152.83	<b>149</b>
<b>9</b>	85.2	88.68	82.67	<b>86</b>

Polyurethane Foam Heat Tests



## Test results – resistance to compression



Following ASTM D 1621-2004 procedure

Réf	C1	C2	C3	C (N)
<b>1</b>	3537	3429	3311	<b>3426</b>
<b>2</b>	2869	2946	3106	<b>2974</b>
<b>3</b>	1171	890	931	<b>997</b>
<b>4</b>	1209	1194	1113	<b>1172</b>
<b>5</b>	1243	1123	1198	<b>1188</b>
<b>6</b>	625	327	804	<b>585</b>
<b>7</b>	27	60	74	<b>54</b>
<b>8</b>	98	175	74	<b>116</b>
<b>9</b>	158	107	156	<b>140</b>

Value at which thickness of the sample is reduced by 10%

Polyurethane Foam Heat Tests



## Test results - lambda



Réf	L1	L2	L3	$\lambda$ (W/mK) à 20°C
<b>1</b>	0.033	0.032	0.032	<b>0.033</b>
<b>2</b>	0.036	0.036	0.036	<b>0.036</b>
<b>3</b>				
<b>4</b>				
<b>5</b>				
<b>6</b>				
<b>7</b>				
<b>8</b>				
<b>9</b>	0.045	0.045	0.045	<b>0.045</b>

Polyurethane Foam Heat Tests

